

**HORIZON EUROPE PROGRAMME**  
**TOPIC HORIZON-JTI-CLEANH2-2023-1**  
**GA No. 101137802**

# **ELECTROLIFE**

**Enhance knowledge on comprehensive electrolysers technologies  
degradation through modeling, testing and lifetime prevision,  
toward industrial implementation**



## **Deliverable report**

### **D2.1 – Degradation phenomena compendium**

<b>Deliverable No.</b>	D2.1	
<b>Related WP</b>	2	
<b>Deliverable Title</b>	Degradation phenomena compendium	
<b>Deliverable Date</b>	31.12.2024	
<b>Deliverable Type</b>	REPORT	
<b>Dissemination level</b>	Public	
<b>Author(s)</b>	Alessandro Monteverde	
<b>Checked by</b>	Alessandro Monteverde (POLITO), Domenico Ferrero (POLITO), Massimo Santerelli (POLITO), Maria Chiara Massaro (POLITO), Ignazio Assenza (EGP), Daniele Consoli (EGP), Bastian Etzold (FAU), Akshay Kumar Kandambath Padinjareveetil (FAU), Marina Orlić (TUG), Vanja Subotic (TUG), Anna Freiberg (FZJ), Marc-Alexander Schwarze (1s1 Energy), Daniel Sobek (1s1 Energy)	
<b>Reviewed by (if applicable)</b>	Vanja Subotic (TUG) and Nicola Briguglio (CNR)	
<b>Approved by</b>	Alessandro Monteverde (POLITO)	
<b>Status</b>	Submission	

## Document History

Version	Date	Editing done by	Remarks
01	2024 11 18	POLITO	Draft for
02	2024 12 13	POLITO, ENEL, FAU, Stargate, PF/Hyter, FZJ, 1s1 Energy, TUG, SolidEra, Kerionics	Draft edited considering comments by the partners
03	2024 12 24	POLITO	Draft edited considering comments by the partners for final review
04	2025 01 09	POLITO	Delivered for Submission

## Publishable summary

The ELECTROLIFE D2.1 report, titled "Degradation Phenomena Compendium," is a cornerstone deliverable of the European Union-funded ELECTROLIFE project, which seeks to unravel the complexities of electrolyser degradation. Electrolysers, the backbone of green hydrogen production, are vital for advancing clean energy technologies. However, their durability, reliability, and efficiency are often compromised by various degradation mechanisms. This document delves into these challenges with a comprehensive, multidisciplinary approach, laying the groundwork for innovative solutions.

Electrolysis technologies are categorized into two main types: low-temperature systems, such as Alkaline Electrolysis (AEL), Anion Exchange Membrane Electrolysis (AEMEL), and Proton Exchange Membrane Electrolysis (PEMEL); and high-temperature systems, including Solid Oxide Electrolysis (SOEL) and Proton-Conducting Ceramic Electrolysis (PCCEL). Each technology operates with distinct materials, conditions, and degradation phenomena, making their study both intricate and essential.

At the heart of this compendium is an exploration of degradation mechanisms—chemical, mechanical, and physical—affecting critical electrolyser components like catalysts, membranes, transport layers, interconnectors, and plates. For instance, catalysts face instability due to corrosion, dissolution, and mechanical stress, while membranes degrade under operational stressors such as temperature, water quality, and contaminants. These factors, compounded by operational modes like load fluctuations and on/off cycles, underscore the intricate interplay between system design and environmental conditions.

Drawing insights from industrial applications and EU-funded projects, the report bridges theoretical understanding and real-world challenges. By leveraging advanced characterization techniques, the document provides a granular view of material behaviour under stress. These findings highlight the importance of tailored materials and robust design strategies to extend the lifespan and efficiency of electrolysers.

This report is not merely a technical analysis; it is a call to action to innovate and refine electrolyser technology. By understanding and mitigating degradation, the vision of scalable, cost-effective, and durable hydrogen production can move closer to reality, driving the clean energy transition forward.

## Summary

1	Introduction, main goals, how to use this document and terminology.....	10
1.1	Introduction .....	10
1.2	Electrolysis Technologies Overview .....	10
1.3	Structure and Accessibility of the Document .....	11
1.4	Terminology .....	12
2	Degradation mechanisms.....	15
2.1	Degradation mechanism related to catalyst instability .....	15
2.2	Degradation mechanisms related to the instability of the separator, membranes and ionomers .....	36
2.3	Degradation mechanisms related to the instability of the porous transport layer.....	51
2.4	Degradation mechanisms related to the instability of the bipolar or monopolar plates....	57
2.5	Degradation mechanisms related to the instability of components due to contaminants.	64
2.6	Degradation mechanisms related to electrolyte variables: including composition, concentration and flow configuration.....	71
2.7	Summary of all technologies.....	75
3	Relation between Operational Modes and Degradation .....	76
3.1	Load Fluctuation .....	79
3.2	Partial Load .....	85
3.3	On/Off cycles.....	86
3.4	Synergistic Effects .....	87
3.5	Temperature .....	89
3.6	Pressure .....	91
3.7	Water Flow rate and quality .....	94
3.8	Anomalies stack power supply .....	94
3.9	Environmental conditions, Mechanical stress, seal leakage; BOP.....	95
3.10	Stressors (summarized degradation factor on performance....).....	97
3.11	Impact of Degradation factors on Performance and Reliability .....	99
4	Industrial and partners experience of this topic .....	101
5	EU funded project analysis.....	105
6	Characterization techniques .....	112
7	Exploring Interconnections between Technologies .....	116
8	Conclusions.....	118

GA No. 101137802

9	Risks and interconnections.....	120
10	Reference .....	121
11	Acknowledgement .....	153
12	Appendix A - <<Appendix Title>> .....	154

## List of Figures

Figure 1 Schematic representation of various degradation phenomena. ....	17
Figure 2. Diagrams show the different methods of AEMEL fabrication.....	27
Figure 3 The mechanism of alkaline degradation of alkaline solid polymer electrolyte .....	40
Figure 4. Overview of membrane degradation pathways and transport phenomena in PEMEL systems .....	44
Figure 5: Mechanistic overview of radical attack pathways caused in the chemical degradation of PFSA membranes.....	45
Figure 6. Cyclic reaction pathway of hydroxyl radical attack, demonstrating the unzipping mechanism of the membrane polymer chain.....	46
Figure 7. a) the triple phase boundary of the oxygen evolution reaction (OER); b) Structural depiction of the porous transport layer (PTL), the catalyst layer (CL) and the membrane interfaces .....	54
Figure 8. Cross-sectional view of PEM electrolyzer anode, depicting the flow channels of the stainless steel bipolar plate (BPP) and the interactions at the catalyst layer interface. ....	60
Figure 9. Schematic visualisation of hydrogen trap sites in a metallic lattice.....	61
Figure 10. Degradation factors, Degradation mechanisms and degradation effects .....	76

## List of Tables

Table 1. Features of most common electrolyzers. ....	11
Table 2 Mechanisms for Ir degradation. ....	28
Table 3. Summary of all technologies .....	75
Table 4. Stressors for AEL, AEMEL and PEMEL .....	98
Table 5. Stressors for SOEL and PCCEL.....	99
Table 6. Impact of Operational Modes and Degradation Factors on Electrolyser Technologies.....	100
Table 7. Electrolife partners degradation phenomena observed .....	103
Table 8. Summary of EU project funded related to degradation studies .....	109
Table 9. Characterization techniques for AEL .....	112
Table 10. Characterization techniques for AEMEL.....	113
Table 11. Characterization techniques for PEMEL .....	114
Table 12. Caracterization techniques for SOEL .....	114
Table 13. Caracterization techniques for PCCEL .....	115

## Abbreviations & Definitions

Abbreviation	Explanation
ADT	Accelerated Durability Test
AEI	Anion exchange ionomers
AEL	Alkaline Electrolysis
AEMEL	Anion Exchange Membrane Electrolysis
BCZY	Barium Cerium Zirconate Yttrium
BOP	Balance of Plant
CCM	Catalyst coated membrane
CCS	Catalyst coated substrate
CL	Catalyst layer
Co	Cobalt
Co-ns	Cobalt hydroxide nanosheets
CNN-LSTM	Network-long short-term memory
CV	Cyclic voltammetry
DRT	Distribution of relaxation times
EIS	Electrochemical Impedance Spectroscopy
Fe	Iron
Fe-nr	$\beta$ -FeOOH nanorods
HFR	High-frequency resistance
HTO	Hydrogen-to-oxygen impurity content
HER	Hydrogen Evolution Reaction
H NMR	Proton Nuclear Magnetic Resonance
ICP-MS	Inductively coupled plasma-mass spectrometry
IHP	Inner Helmholtz Plane
Ir	Iridium
MEA	Membrane electrode assembly
MILP	Mixed integer linear programming
Ni	Nickel
OCP	Open Circuit Potential
OER	Oxygen Evolution Reaction
PBR	Pilling-Bedworth Ratio
PCCEL	Proton-Conducting Ceramic Electrolysis
PEI	Polyethyleneimine
PEMEL	Proton Exchange Membrane Electrolysis
PPS	Polyphenylene sulfide
PSU	Polysulfone
PTL	Porous transport layer
PV	Photovoltaic
QA	Quaternary ammonium groups
RHE	Reversible Hydrogen Electrode
Ru	Ruthenium

GA No. 101137802

SEC	Specific energy consumption
SOEL	Solid Oxide Electrolysis
SPRDE	Stationary probe rotating disk electrode
TPB	Triple-phase boundary
Tg	Glass Transition Temperature
XPS	X-ray photoelectron spectroscopy
YSZ	Yttria-Stabilized Zirconia





# 1 Introduction, main goals, how to use this document and terminology

## 1.1 Introduction

The ELECTROLIFE consortium aims to compile a comprehensive dataset on the degradation of electrochemical systems by gathering extensive information from existing literature, project findings, and data available from electrolysers manufacturers. To accomplish this, the consortium intends to leverage the expertise and experiences of its members, as well as access data through the Joint Research Centre (JRC) of EU-funded projects relevant to this topic. The objective is to ensure thorough data collection and to leverage existing knowledge within the consortium.

## 1.2 Electrolysis Technologies Overview

Electrolysis is an electrochemical process that utilizes electrical current to decompose water into hydrogen and oxygen. This process is fundamental for clean hydrogen production and involves a range of technologies operating at different temperatures and employing various components. Electrolysis technologies can be broadly classified into two categories: low-temperature and high-temperature systems.

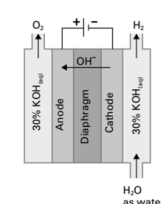
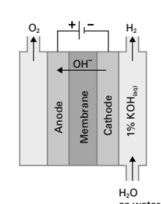
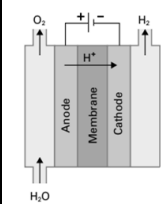
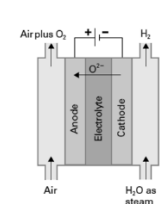
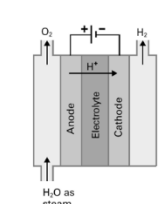
### 1. Low-Temperature Electrolysis Technologies:

- Alkaline Electrolysis (AEL): Uses a liquid alkaline solution (e.g., KOH) as the electrolyte.
- Anion Exchange Membrane Electrolysis (AEMEL): Employs an anion-conducting membrane as the electrolyte.
- Proton Exchange Membrane Electrolysis (PEMEL): Utilizes a proton-conducting fluoropolymer membrane, such as Nafion.

### 2. High-Temperature Electrolysis Technologies:

- Solid Oxide Electrolysis (SOEL): Operates at elevated temperatures using a solid oxide ceramic electrolyte.
- Proton-Conducting Ceramic Electrolysis (PCCEL): Utilizes proton-conducting ceramic electrolytes and also operates at high temperatures.

Each of these technologies has unique components, operating conditions, and performance characteristics, as summarized in Table 1 below.

Parameter		AEL	AEMEL	PEMEL	SOEL	PCCEL
						
Electrode material	Cathode	Ni, Co or Fe coated on stainless steel	Ni/Ni alloys	Pt/Pd	Ni/YSZ (Nickel-Yttria Stabilized Zirconia)	Ni/BCZY (Nickel-based ceramic)

	Anode	Ni coated on stainless steel	Fe, Ni, Co oxides	IrO <sub>2</sub> , RuO <sub>2</sub>	Lanthanum Strontium Manganite (LSM) or lanthanum strontium cobaltite ferrite (LSCF)	BCZY-based perovskite materials
	Electrolyte	Lye: 25-30% Potassium Hydroxide solution in water	Anion Exchange ionomer (e.g. AS-4)	Fluoropolymer ionomer (eg Nafion, a DuPont)	Solid oxide (ceramic) electrolyte such as YSZ (Yttria Stabilized Zirconia)	Proton-conducting ceramic electrolyte (e.g., BaCeO <sub>3</sub> doped with Zr and Y, BCZY)
	Energy Source	100% electrical power	100% electrical power	100% electrical power	Electrical power with optional thermal energy input for efficiency	Electrical power with optional thermal energy input for efficiency
	Current density	Up to 0.5 A/cm <sup>2</sup>	0.8* – 1,5** - 2*** A/cm <sup>2</sup>	Up to 3 A/cm <sup>2</sup>	Typically 0.3 – 0.5 A/cm <sup>2</sup>	Typically 0.3 – 0.5**** A/cm <sup>2</sup>
	Product	Hydrogen and Oxygen	Hydrogen and Oxygen	Hydrogen and Oxygen	Hydrogen and Oxygen	Hydrogen and Oxygen
	Gas outlet pressure	Up to 40 bar	Up to 35 bar H <sub>2</sub> , 1 bar O <sub>2</sub>	Up to 100 bar	Typically near atmospheric (1 bar), higher possible with pressurization stages	Typically near atmospheric (1 bar), higher possible with pressurization stages
	Cell temperature	~80 °C	~60 °C	~60 °C	~700-1,000 °C	~500-700 °C

Table 1. Features of most common electrolyzers. In the table: \*0.8 A/cm<sup>2</sup> is referred to non PGM catalyst with 1.8 V cell voltage; \*\*1.5 A/cm<sup>2</sup> is referred to PGM catalyst with 1.8 V of cell voltage; \*\*\*AEMEL activity up to 2 A/cm<sup>2</sup> with PGM as catalyst and 2 V cell voltage at ambient pressure. \*\*\*\* Low TRL

### 1.3 Structure and Accessibility of the Document

The D2.1: "Degradation Phenomena Compendium" provide a detailed analysis of degradation phenomena across various electrolyser technologies, including AEL, AEMEL, PEMEL, SOEL, and PCCEL. Each section delves into technology-specific degradation mechanisms, and is structured as follows:

- Degradation Mechanism (Section 2): Analysis of how individual components degrade and their impact on system performance.
- Relation between Operational Modes and Degradation (Section 3): Examination of degradation phenomena influenced by different operational modes.
- Industrial and Partners' Experience (Section 4): Insights from industrial applications and partner contributions on degradation-related challenges.

GA No. 101137802

- EU-Funded Project Analysis (Section 5): Overview of findings and data from EU-funded projects relevant to electrolyser or fuel cell degradation.
- Characterization Techniques (Section 6): Identification of the techniques used to characterize and assess degradation.
- Exploring Interconnections Between Technologies (Section 7): Investigation of commonalities and differences in degradation phenomena across the various electrolyser technologies.

Each section provides a technology-specific perspective, enhancing the understanding of degradation processes and potential mitigation strategies.

## 1.4 Terminology

### **Cold standby state**

Standby state requiring warm up before a demand to operate can be met [1].

### **Cold start**

Transition from cold standby to hydrogen production.

### **Cold start ramp time**

Time from cold standby state to the nominal value considered [1].

### **Constant current operation**

Operational mode when the electrolyser is operated at a constant current (galvanostatic mode) [2].

### **Degradation mechanisms**

Degradation mechanisms encompass all the phenomena (chemical, mechanical, physical, etc.) that occur within the components of an electrolyser (cell or stack), contributing to a reduction in performance, reliability, durability, and/or useful life of the electrolyser.

### **Degradation factors**

Degradation factors refers to all those factors, events, states that cause/activate degradation mechanisms (and therefore degradation) on the electrolyser.

Degradation factors are also named “stress factors” or “stressors”.

### **Emergency shutdown**

Control system actions, based on process parameters or manually activated, designed to stop the system and all its reactions immediately to prevent equipment damage and/or personnel hazards [1].

### **Emergency stop**

Operating procedure or action intended to stop as rapidly as possible but in a controlled manner the operation of a device or system which has become dangerous or possess a hazard [1].

### **Hot idle ramp time**

Time from hot standby state to the nominal value considered (specifying the ramp of current) [1].

GA No. 101137802

### **Hot standby state**

Standby state providing immediate operation upon demand [1].

### **Hot start**

Transition from hot standby state to hydrogen production.

### **Nominal operation mode**

Operation of the device using the parameter setting defined to obtain the nominal performances as defined in the technical specifications [1].

### **Operational mode**

Operational modes refers to any combination of operating conditions [1].

A list of main operational modes is:

- Partial load operation:
  - Hydrogen production at steady state / constant load (minimum, intermediate, nominal load or overload)
- Load fluctuation
  - Hydrogen production at variable load
- Start-Stop cycles (On Off)
  - Cold standby state
  - Warm standby state
  - Hot standby state
  - Cold start
  - Hot start
  - Shutdown
  - Emergency shutdown

### **Operative strategy**

An operative strategy is a combination of several “operational modes” (and to reach specific scenario).  
Source: this definition is provided in this document only for the purposes of ELECTROLIFE project.

### **Overload capability**

Overload capability is the ability of the electrolysis system to operate beyond the nominal operating (i.e voltage higher than critical value) and design point for a limited period of time, typically in the range of a few minutes to less than 1 hour. The overload capability is mainly used to provide greater flexibility in different grid-service applications (e.g. secondary control reserve) [1].

### **Regulation profile**

Variable power profile such as the grid power profile resulting from energy injection and withdrawal. This can be affected by renewable energy sources, energy fluctuations and network disturbances [1].

GA No. 101137802

### **Steady state**

State of a physical system in which the relevant characteristics/operating parameters remain constant over time [1].

### **Shutdown**

Sequence of operations, specified by the manufacturer, that occurs to stop the system and all its reactions in a safe and controlled manner [1].

- **Cold shutdown:** transition to cold standby state
- **Hot shutdown:** transition to hot standby state

### **Warm standby state**

Operating state of equipment powered and warmed up at a temperature that allows a fast restart of the system [1].

### **Standby state**

Normally idle or idling piece of equipment that is capable of immediate automatic or manual start-up and continuous operation [1]

### **Regulation mode**

Mode of operation where the device is working using a variable power, i.e. provided by the network to compensate for grid imbalances.

## 2 Degradation mechanisms

The section 2 explores key degradation phenomena across five main electrolyser technologies: AEL, AEMEL, PEMEL, SOEL, and PCCEL. Each technology's unique characteristics and challenges are examined to uncover the underlying mechanisms driving performance degradation.

Central to this analysis is the examination of catalyst instability, which significantly impacts the durability of both anode and cathode. Corrosion, dissolution, surface poisoning, and structural changes are highlighted as critical issues that impair catalytic activity. Furthermore, the membranes and ionomers, essential for maintaining ionic conductivity and gas separation, are analysed for chemical and mechanical vulnerabilities under operational stresses.

The porous transport layers (PTL) and bipolar and monopolar plates also come under scrutiny, as these components are integral to reactant delivery, current distribution, and overall system architecture. Mechanical wear, contamination, and electrochemical stresses on these elements are explored in detail. Additionally, the impact of contaminants—whether introduced via feedstock or as byproducts of operation—is assessed for their role in accelerating material degradation and reducing efficiency. The section also addresses the influence of concentration, flow configuration, and quality, which often exacerbate component degradation. By identifying these stressors or degradation factors, the analysis offers valuable insights into their contribution to system instability and degradation.

### 2.1 Degradation mechanism related to catalyst instability

#### 2.1.1 AEL

The catalyst (cathode and anode) plays a vital role in the electrolysis process and its durability significantly affects the lifetime and overall operational expenses of AEL systems[3–5]. Although a mature technology, focusing solely on catalytic activity may be insufficient for commercialization, and hence attention needs to be directed towards degradation phenomena that could potentially affect the durability of electrocatalysts[6–10]. These include catalyst deactivation[11], gas crossover[12], bubble removal effects[13], corrosion[14,15], surface blockage, hydrogen induced blistering[16], tribocorrosion[17], that can severely hamper the overall efficiency of systems. Further, these factors become prominent at high current densities, and focus must be placed on local pH changes, corrosion, and mass transfer to ensure successful integration into a high-power industrial electrolyser. Overall, understanding the mechanism behind degradation of both cathode and anode is vital from an economic perspective and for the immediate commercialization.

##### 2.1.1.1 Cathode

The half-reduction reaction of water electrolysis for generating hydrogen via hydrogen evolution reaction (HER) occurs at the cathode[4,5,18] and is expressed by:



The choice of catalyst for carrying out reaction is vital and ranges from noble metals such as Platinum (Pt) and Iridium (Ir)[19–21], to transition metals like Nickel (Ni), Iron (Fe), and Cobalt (Co)[22], as well as bimetallic catalysts such as Iron–Nickel Phosphide ( $Fe_{2x}Ni_{2(1-x)}P$ )[23,24], carbon based Co onto nitrogen-doped graphene (Co-NG)[25,26], self-supporting catalysts as Mn(II)-containing MOF[27,28], metal oxides (manganese oxide),[29,30] composite materials (Ni based)[31,32], cathode electrode (Ni-

GA No. 101137802

Fe electrocatalyst)[33]. Further, the exploration of new electrocatalysts that could prevent degradation and/or self-repair under abrupt on/off cycling conditions is a current research topic.

The major degradation phenomena for the cathode include a) corrosion, b) dissolution, c) deactivation, d) passivation, e) mechanical degradation and gas bubbles, f) degradation associated with intermittent operation, and g) shunt current. These phenomena are explained in the paragraphs below.

- a. **Corrosion:** Corrosion is an oxidation and thus normally critical at the anode[34,35]. Interestingly, under shutdown conditions[11,36], the cathode may serve as anode (anodic corrosion), with reverse current accelerating degradation (see **subsection G** for details). Nevertheless, corrosion can also occur at normal operation at the cathode as described below. Cathodic corrosion is a typical phenomenon in electrodes, particularly metallic ones, accounting for the combined effect of highly corrosive alkali metal hydroxide electrolyte (typically KOH) and an extra driving force (cathodic polarization)[8,10,37,38]. The corrosion can either be normal (uniform corrosion; Figure 1) or local. The gradual thinning of material, resulting from a uniform electrochemical reaction, falls to the normal anodic corrosion and does not occur at the cathode during normal operation. While, corrosion due to the environment variability and the protective layer breakdown can aid in local corrosion. Among localized corrosion, cathodic **pitting corrosion** (Figure 1) is known for cathodes in alkaline media, resulting in smaller pits or holes on metal electrocatalyst surface[11]. Multiple studies have further detailed that the pitting is anticipated to occur on passivated (oxide covered) cathode surfaces when exposed to aggressive environments, such as in presence of chloride ions[36], under normal electrolyte conditions (30% potassium hydroxide (KOH) and 1% lithium hydroxide (LiOH)),[37] or due to pitting from hydrogen gas bubbles at higher potential[11]. Formation of corrosion products at/under hydrogen bubble and their reduction to metal upon detachment is detailed in the following reference[38]. Interesting overview on the passivity breakdown and pitting corrosion in binary alloys is also available in literature[39]. Overall, the process begins at defective sites in the oxide layer of cathodes due to mechanical damages/chemical species attack. These sites serve as large cathodic area, while the exposed metal acts as small anodic site. During corrosion, metals dissolve and become anode ( $M \rightarrow M^{n+} + ne^-$ ) with its surrounding serving as cathode e.g. through minor amount of dissolved oxygen ( $O_2 + 2H_2O + 4e^- \rightarrow 4OH^-$ ). Also, some interesting findings were put forward by Yanson et al., on cathodic corrosion[40]. The electrode is reported to corrode, upon cathodic treatment at high negative potentials in alkaline solutions and no major changes are evident in acidic solutions. However, corrosion is triggered with addition of alkali salts, showcasing the effect of destabilization phenomenon of protective layer in alkali environment.



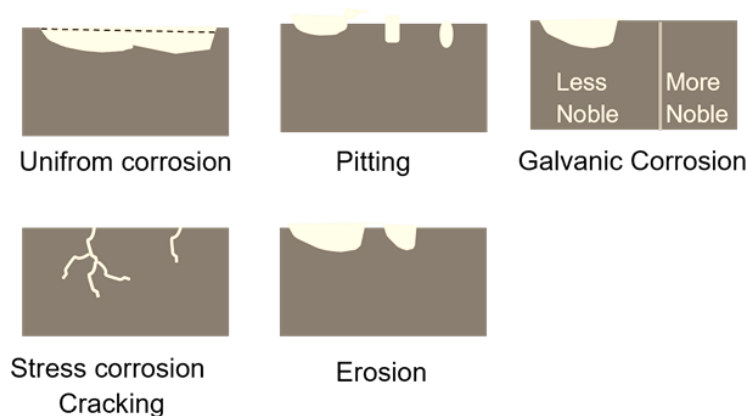


Figure 1 Schematic representation of various degradation phenomena.

- b. Major critical factors affecting the cathodic corrosion rate involve electrode materials employed, polarization potential, and electrolyte composition. As tracking the corrosion during polarization remain a task, measurement at open circuit potential (OCP) is found to be an interesting method[41,42]. The OCP of electrode showcases its pristine electrochemical state, indicating the voltage developed when the electrode is not connected to an external circuit. Measuring OCP values of metals intended to study would further serve as indicator in describing the metal in its pristine state (without any external influences) and this would help to track the corrosion behavior with time. The corrosion/degradation rate of electrocatalyst under free state (under OCP) would face a slower degradation (due to natural factors such as temperature, moisture, etc.) when compared to its subjection to polarization (due to controlled potential). In line with the following discussion, in a study by Wang et al., different coatings (CrMnFeCoNi and CrFeCoNi) were evaluated under OCP and polarized conditions using electrochemical impedance spectroscopy (EIS) Nyquist plots[43]. They found that corrosion behavior varied significantly based on whether the electrodes were freely corroding or under polarization. Interestingly, deviation in the corrosion rate between electrochemical methods, such as polarization resistance and Tafel extrapolation, and analytical technique (weighing before and after experiment) was put forward by Prazak et al., suggesting introduction of correction factor to the electrochemical data[40]. In parallel, significant difference in the corrosion rate of metal (Fe, Cr, Co, Mn, steels, etc) was observed in another study, upon comparing electrochemical corrosion rate with analytical results, concluding the analytical measurement was independent of applied potential, delivering an abnormal dissolution behavior[44,45]. Chemical dissolution is thus considered to be main reason for cathodic degradation under cathodic polarization ( $M + nH_2O \rightarrow Mn^+ + nOH^- + n/2H_2$ )[46], and the hydrogen produced in the course of reaction are from both water reduction and chemical dissolution of cathode material (less contribution from HER). Some suggestions on improving the Wagner-Traud Diagram were suggested by Kolotykin, considering both chemical and electrochemical reactions influencing corrosion[44]. Unfortunately, the electrochemical determination of cathodic corrosion rate is complex, as the predominant current during the process is from HER, nullifying the assessment of isolating current contribution from dissolution and/or deposition. More details on the dissolution process and mechanisms associated are detailed in the following sub section.

Temperature, pH and experimental conditions (mechanical, chemical etc.) are critical parameters that accelerate corrosion[47]. Quick corrosion of catalysts is the result of increased reaction rates at high temperature. For instance, cathodic corrosion of Fe in KOH electrolyte solutions was reported where in the corrosion products below 60 °C were traces of  $Fe(OH)_2$ , [46] while above 60 °C  $Fe(OH)_2$  and  $Fe_3O_4$  are present, and magnetite is the only observed product

above 200 °C. In another interesting work, carbon steel was subjected to temperature variation study (70-80 °C) in 8 M KOH for 7 days[47]. Prolonged exposure to high temperatures showed increased chances of corrosion. In principle, temperature plays a vital role in accelerating both the corrosion rate and type of corrosion. Also, there are reports on corrosion decline in open systems with temperature > 80 °C, due to decline in solubility of oxygen in water, while in a closed system, the corrosion rate would increase[47]. Pourbaix diagrams (potential-pH diagrams) illustrate the thermodynamic stability of various species of a specific metal in relation to pH (x axis) and electrochemical potential (y axis)[10,47]. In another words, corrosion of specific metal and/or corrosion potential can be predicted using the following method, aiding the researchers to understand the catalysts longevity at specific conditions. For instance, in Fe-H<sub>2</sub>O systems, Fe can passivate by forming stable oxides like Fe<sub>2</sub>O<sub>3</sub> at high pH, while ionic species such as HFeO<sub>2</sub><sup>-</sup> dominate at low pH, enhancing corrosion. Turbulence is reported to destroy the protective oxide coating layers over the catalyst surface (cathode), potentially enhancing the possibilities for corrosion. The effect of turbulence is reported to be less for Ni catalysts over carbon steel[48]. Further, hydrogen cracking is another phenomenon aiding corrosion of catalysts, accounting for the penetration of hydrogen atoms from corrosion reactions or cathodic polarizations in to the catalyst interstitial structure. Researchers consider the combined effect of turbulence-assisted hydrogen cracking to be a lethal combination in enhancing corrosion[47].

- b) **Dissolution:** As for corrosion, dissolution is an anode-related problem and is not common at the cathode. But due to secondary effects or specific conditions, dissolution can take place also at the cathode. It is highly likely that dissolution process at cathode could be assisted by cathodic corrosion, as reported in the article by Liu et al[49]. Also, this phenomenon can occur at cathode during electrochemical reactions, by a complex ion formation or reduction of cathode material[50,51]. Dissolution into the electrolyte would severely alter the innate properties of the electrolyte such as pH variation, concentration, and in parallel, loss of active material from catalysts would alter its morphological structure and/or electronic structure. The dissolution is common in highly alkaline solution, wherein the cathode gains electrons or form complexes resulting complex ions. For example, anionic species is found to be the product of dissolution of transition metal such as Fe, Ni with the reaction:  $2\text{Fe} + 4\text{OH}^- \rightleftharpoons 2\text{HFeO}_2^- + 2\text{e}^- + \text{H}_2$  [10,51]. Further, the dissolution reactions may vary for the same system, post passivation and formation of stoichiometric components. Importantly, solubility of a given metal (catalyst) in a compound (electrolyte) relies on its chemical composition. Selective dissolution is another phenomenon witnessed in alloys, wherein major changes to electrocatalyst structures occur accounting for dissolution of one or more components from alloy[52]. This main process proceeding towards catalyst degradation involves initial particle growth, followed by coarsening of metal particles, and eventual detachment of metal particles from support to electrolyte, with time. Interestingly, deterioration tracking in alloy would be interesting, as majority degradation reported is on single-metal electrodes. With two metals present in the catalyst structures, degradation will be influenced by electronic interactions of both metals (variation in degradation rates of metal with respect to one another), spatial arrangement of the atoms, microstructure (grain boundaries or phases within alloy are susceptible to corrosion such as pitting), etc. In a reported study on using Fe-Ni alloy for HER in AEL, it was observed that the alloys with high Fe content caused pitting corrosion during HER, while the activity increased up to 90 wt.% Fe[11]. The corrosion products were mainly iron oxides. Further, employing cathodic polarization of 60Ni-Fe alloy for a day,

showcased a degradation of catalysts, further evaluated via XPS analysis. Oxide and hydroxide of Fe ( $\text{Fe}_3\text{O}_4$ ,  $\text{Fe}_2\text{O}_3$ ,  $\text{FeOOH}$ , and  $\text{FeO}$ ) were evident that enhanced degradation, while a weak peak of Ni ( $\text{NiO}$ ) accounted for its low contribution to the corrosion.

- c) **Deactivation:** The declining ability of cathode to facilitate the reduction reaction could be termed as cathodic deactivation, which is attributed to electrode poisoning, surface morphology changes and/or loss of active sites. Ni electrocatalysts for AEL are well known, yet they face degradation after prolonged operational hours. Low HER activity, due to factors such as chemical state of electrode surface, oxide formation, hydride absorption, etc, is the major limitation of this set of catalysts. Low HER activity of Ni electrode could be due to cathode poisoning mechanism accounting to the diffusion of hydrogen atoms into the nickel electrode. The process can be divided into: a) hydrogen absorption, b) electrode deactivation, and c) changes in the reaction pathway. Broadly speaking, the hydrogen produced at the cathodic end interacts with nickel electrode at high hydrogen gas pressure or cathodic current density, resulting in a Ni-H bond[53]. This is expected to vary the electronic structure of nickel, lowering its metallic nature (unfilled d orbital) and delivering sp configuration which is less catalytically active. The altered structure would aid electrode deactivation, increasing the negative potential for hydrogen production. Studies have also reported that the HER would be limited by the desorption step due to Ni-H formation and increasing the Tafel slope from 200 to 1000 mV/dec. A possible solution to mitigate this issue would be the use of protective coatings (such as Fe)[54], that would serve as barrier, preventing hydrogen atoms from diffusing into the Ni electrode.
- d) **Passivation:** Catalyst surfaces, especially metals, possess a protective layer of deposited oxide, hydroxide, or oxyhydroxide, accounting for the interaction between the electrolyte ions ( $\text{OH}^-$ ) and the existing ionic species[10]. They hamper the degradation of catalysts by reducing the reactivity of metal surfaces by minimizing the free energy of the system. pH, electrode potential, temperature, and electrolyte species, including cations in the electrolyte, influence the process. Catalysts with denser and less porous structures prevent degradation to an extent, accounting for their ability to restrict the penetration of corrosive ions into interior of catalysts and preventing deposition of corrosive or reduced species at catalysts pores. For instance,  $\text{NiO}$  forms a denser and effective protective layer,[55] while  $\text{Fe}_3\text{O}_4$  is known to reduce to Fe under cathodic polarization in alkaline solutions resulting in dissolution and deposition[56]. Upon exposure to air and/or alkaline solutions (disagreements continue on type of hydroxide) Ni develops a bilayer of  $(\text{Ni}(\text{OH})_2)$  at surface, and non-stoichiometric Ni Oxide layers beneath it ( $\text{Ni}/\text{NiOx}/\alpha\text{-Ni}(\text{OH})_2$ )[57]. Reduction of oxide and hydroxide to metallic  $\text{Ni}^0$  is possible at negative potential, but a complete residual removal/conversion of hydroxide is not possible, leaving behind detectable hydroxides post HER experiments as well. Evaluation of XPS results post HER, showcased that the samples observed two peaks with binding energies assigned to  $\alpha\text{-Ni}(\text{OH})_2$  and other two intense peaks, ( $\text{Ni}^0$ ) and no hydrides. Further, determining the Pilling-Bedworth Ratio (PBR) would provide an understanding of the composition of oxide layers, thereby limiting the degradation of catalysts to an extent.

$$PBR = \frac{V_{oxide}}{V_{metal}} = \frac{M_{oxide}\rho_{oxide}}{nM_{metal}\rho_{metal}} \quad (2)$$

where V, n, M, and  $\rho$  stand for molar volume, the number of atoms of metal per molecule of the oxide, atomic or molecular mass, and density, respectively[58]. Poor protection is identified as

PBR <1 and PBR>2, while  $1 < \text{PBR} < 2$  indicate ideal protection[59]. Parallely, although the Ni(oxy)hydroxide is expected to protect the cathode due to its passivating properties, yet frequent reduction/oxidation cycles prevent it from stabilizing over catalyst surface and aid towards undesirable species[58,60]. Interestingly, in a study by Bode et al., four phases of Ni (oxy)hydroxide were known to electrochemically form two hydroxides and two oxyhydroxides, including  $\alpha\text{-Ni(OH)}_2$ ,  $\beta\text{-Ni(OH)}_2$ ,  $\gamma\text{-NiOOH}$ , and  $\beta\text{-NiOOH}$ [61].

**Mechanical degradation and gas bubbles:** Mechanical degradation is another important factor in AEL systems, occurring via detachment or breakdown of materials due to mechanical stress, which results in structural changes, defects and distortion of catalyst surfaces. Hydrogen bubble dynamics is a crucial phenomenon, wherein the hydrogen bubbles generated as part of cathodic polarization lead to exert mechanical force on substrate eventually leading to degradation[10,62]. As size of the bubble increases, the catalysts particles may detach from electrode surface aiding to material loss and catalyst modifications. This effect enhances when catalysts are subjected to longer working hours. The hydrogen molecules can also nucleate at surfaces leading to an increase in the pit size of electrode, subjected to bubble evolution. Current density, electrode material, and electrolyte composition are also vital parameters that influence mechanical degradation such as the contact glow discharge phenomenon. During cathodic charging and at high current density, the electrical discharge at the interface between the electrode and the electrolyte causes localized heating and ionization events resulting in particle ejection from the surface, aiding to change to surface morphology and material properties.

- **Hydrogen source-hydrogen uptake:**  $\text{H}_2$  can degrade the catalyst's structure post entering, wherein the sources could be either from previous manufacturing processes or environmental  $\text{H}_2$  generated through aqueous corrosion or cathodic polarization[10,63]. The  $\text{H}_2$  adsorption route on catalyst surfaces can be either via physical (at ambient temperatures) or chemical (at higher temperatures) route. The physically adsorbed  $\text{H}_2$  transforms to chemically adsorbed  $\text{H}_2$  prior to being absorbed into the electrocatalysts. The HER mechanism can be illustration as follows[64,65]:



In studies evaluating the impact of cathodic polarization, Flis et al. reported that tracking the  $\text{H}_2$  uptake rate in a system revealed an initial increase (increased surface hydrogen coverage and weak bonds of  $\text{H}_{\text{ads}}$ ), followed by a decrease (surface saturation and formation of various oxygen-containing species)[66]. Interestingly, the passive oxide layers on the surface would serve as a barrier to  $\text{H}_2$  adsorption, limiting its entry into catalysts structure. Dissolution of passive layer would enhance degradation, due to enhanced  $\text{H}_2$  uptake by metal surfaces.

- **Hydrogen-induced damage:** Adsorption of  $\text{H}_2$  on the HER cathode surface can result in two major damage modes, such as hydrogen embrittlement and crack initiation from hydride formation[16]. Hydrogen embrittlement refers to the condition where the cathode is softened and becomes more brittle due to  $\text{H}_2$  accumulation at high stress regions or at

defect sites in material, resulting in delayed fracture and/or reduced load bearing capacity. The  $H_2$  sources could be either from manufacturing processes (corrosion reactions, metal plating, etc.), or upon exposure to  $H_2$  environment. This is common to metal such as Ni, titanium, aluminum alloys, etc. The mechanism of embrittlement[67,68] post  $H_2$  adsorption involves a series of steps such as:

- *Hydrogen Enhanced Decohesion*:  $H_2$  weakens the interatomic bonds between the catalyst metal atoms, reducing the cohesive force between metal atoms and eventually affecting the metal distribution. The  $H_2$  accumulates at interface or grain boundaries.
  - *Hydrogen Enhanced Localized Plasticity*:  $H_2$  increases dislocation mobility, resulting in localized deformation and crack propagation.
  - *Hydrogen-induced phase transformations*: In this step, the  $H_2$  can combine with the metal atoms to form brittle hydride phases, initiating cracks and followed by degradation of catalyst materials.
- **Hydrogen-Induced Blistering**: This phenomenon is evident in more ductile materials, wherein the accumulation of H atoms at trap sites (microcavities, grain boundaries, dislocations) and their combination cause pressure build up in cavities, which eventually resulting as blisters on catalysts surface[16,68]. They appear as raised areas on the metal catalyst surface and the area beneath the blister is often thinned due to the plastic deformation.
  - **Stress corrosion cracking and Tribocorrosion**: Mechanical and local degradation in alkaline pressurized electrolysers often encounter stress corrosion cracking and  $H_2$  formation at crack tips is one of the main reasons of this phenomena[68]. Interestingly, Ni-clad steels[69] are known to deliver strength and corrosion resistivity for operation in pressurized systems upon exposure to high-pressure stress and temperature conditions due to the passive NiO. Meanwhile, tribocorrosion accounts to the interdependence of electrochemical and mechanical degradation[10,17]. In electrolysers, the electrodes are exposed to both corrosive environments and mechanical stresses (Figure 1). Corrosion enhances the surface roughness, thereby enhancing the weaker surfaces susceptible for quick mechanical degradation and also the mechanical process can also remove the protective oxide layers enhancing corrosion. Further, the particles during the polarization act as abrasive agents, enhancing the mechanical detachment. Among tribocorrosion, the flow accelerated corrosion is relevant as they occur in a system where the solution (electrolyte) interacts with the material surface (catalyst).

Overall degradation rate can never be considered as a sum total of electrochemical and mechanical degradation, due to synergetic effect. In principle, accounting to a complex combination of electrochemical reactions, mechanical stresses, and fluid flow, degradation from single entity alone cannot be traced in such systems.

- f. **Degradation associated with Intermittent operation - Reverse Current**: The electrocatalysts are also expected to withstand intermittent conditions which can arise upon integration with renewable energy sources, or in situations of forceful shut down as part of the maintenance, replacements or malfunction rectification[70,71]. In general, during normal operation of electrolysers, oxidation and reduction occur at anode and cathode respectively. However, during

the shutdown conditions, the current flow does not damp completely, rather flows in opposite direction, termed as the reverse current. So, during this phenomenon, multiple events occur such as depletion of remaining electrode capacity, hydrogen absorption, formation of hydride compounds, and potential gas crossover through the diaphragm, which can result in adsorption on opposite electrodes or even explosion[70–73]. Also, reports confirm that this results in oxidation at cathode and reduction at anode, thereby affecting the innate role of the electrocatalysts employed. The reverse current flow from anode to cathode in a bipolar configuration of AEL system delivers a condition similar to a galvanic cell, where spontaneous redox reactions can occur accounting for a high potential difference between the cathode and anode. For instance, in a recent study, strategies of cathode protection against reverse current in zero gap electrolyzers were reported by a group of researchers. Initially, the effect of shut down and reverse current effect was studied by comparing the OCP between two pure Ni electrodes, after being cathodically polarized at  $-300$  mV in 1 M KOH[73]. A decrease of  $-0.9$  V was observed in a time span of 60 min, confirming the reverse current and self-discharge post shutdown. Formation of O-containing products with lower conductivity relative to metallic Ni, and secondary element dissolution are expected to result in lower cathode performance, calling for significant attention to be put on the oxidation state of Ni. Overall, the surface of the Ni electrode changed gradually and irreversibly from a metallic Ni or  $\alpha$ -Ni(OH)<sub>2</sub> to hydroxide or oxide phases, such as  $\beta$ -Ni(OH)<sub>2</sub> or NiO, during the repetitive positive-going potential scan above 0.6 V versus RHE. XPS and CV analysis revealed that irreversible hydroxide and oxide phases were formed on the cathode Ni electrode during the self-discharge process due to the reverse-current, resulting in a degradation phenomenon after the shut-down process. Meanwhile, the XPS results of anode did not show any major deviation in its elemental states. Meanwhile, in another case, Ni electrodes subjected to reverse current, post HER showcased some interesting results as well. CV experiments were carried out on Ni mesh after polarization at  $-100$  mA cm<sup>-2</sup> in 1 M NaOH at room temperature[74]. Three distinct regions were evident: a) reversible  $\alpha$ -Ni(OH)<sub>2</sub> phase during anodic scan (to Ni<sup>0</sup>), b) irreversible  $\beta$ -Ni(OH)<sub>2</sub> phase and c) NiOOH formed via oxidation of either  $\alpha$ - or  $\beta$ -hydroxide. The reverse current can significantly affect/alter the cathode surface periodically accounting for the increase in the potential even in shutdown conditions. Various oxygenated species are formed on the cathode catalyst surface such as the  $\alpha$ -Ni(OH)<sub>2</sub> and  $\beta$ -Ni(OH)<sub>2</sub> phases, and upon restart condition most of the oxygenated species can return back to metallic Ni state, while  $\beta$ -Ni(OH)<sub>2</sub> formed does not revert back to metallic nickel, reducing the cathode efficiency. Hence, with time the catalysts would severely degrade calling for replacements. Some studies have also suggested solutions post evaluating the trend in catalyst degradation in term of the potential window and scan rate. For instance, experiment at low potential is advised ( $E < -0.4$  V vs. RHE), and at slow scan rate of 0.1 mV/s[75]. Such strategies are expected to enhance the durability of cathodes and minimize the stress on the electrode material and mechanical failures over time.

Switching to effect of intermittent operations on alloys, an interesting study was reported by Flis-Kabulska et al[11]. Precisely, mechanism of increasing pitting corrosion of Ni-Fe cathodes during cathodic polarization were detailed and performance of FeNi alloy was evaluated with pure Fe and Ni in 25wt% KOH at 80 °C under intermittent conditions. Two experiments conducted were a) turning off cathodic polarization b) applying anodic polarization after cathodic polarization. In first case, cathodic polarization was switched off after a particular time interval and OCP was observed to shift to positive direction (more noble direction). It was found

that the Fe-Ni alloy tended to stabilize at the potential associated with nickel iron oxide ( $\text{NiFe}_2\text{O}_4$ )[76] concluding this oxide would aid towards better stability against degradation, while pure Fe showcased stability potentials related to dissolved species like  $\text{Fe}(\text{OH})_4^{2-}$ , [77] which are having high chances of degradation. Meanwhile, in the second case, three peaks were identified showcasing some interesting observation of the catalyst. The anodic peak at  $-0.85$  V vs.  $\text{Hg}|\text{HgO}$  indicates oxidation reactions where metallic Fe converts to dissolved  $\text{Fe}(\text{OH})_4^{2-}$  and hydrogen desorbs as  $\text{H}^+$  ions. While the anodic Peak at  $-0.70$  V vs.  $\text{Hg}|\text{HgO}$  is related to the oxidation of either Fe or Ni or surface corrosion products. The cathodic peak upon reversal concluded the reduction of  $\text{NiFe}_2\text{O}_4$  back to metallic iron and nickel, and a significant increase in current that was absent before the anodic step. It is noted that most corrosion products are reduced back to metallic forms during the cathodic reduction, which were formed during the anodic state previously. However, incomplete reduction or stay back of these remain are possible leading to enhanced corrosion with time. Strategies such as electrodeposition process in the preparation of FeNi alloy can play a vital role, as anomalous deposition can aid to less deposition of Fe, resulting in corrosion at later stages.

Among Ni alloy, Raney Ni, and NiMo are interesting catalyst materials notable for their reliable activity and stability, yet at intermittent operation they are known to show sign of dealloying[78]. For instance, dealloying of Zn and Al for Raney Ni, while Mo in NiMo alloy, results in degradation of Ni based catalysts for AEL. Interestingly, the precursor material is shown to play a vital role in catalyst stability, where the difference in it showcases two different degradation effect[79]. For instance, Raney Ni electrode procured from Ni-Zn alloy degrade at 30 wt% KOH at  $90^\circ\text{C}$ , while from sulphide nickel operated for more than 3000 h without any major degradation. Herein, the reaction of Ni with water was found to be key degradation process during shutdown condition (or depolarized condition)[80]. In an experiment with Raney Ni cathode, it was found that during shut off conditions, Raney Ni would severe as anode, resulting the electrons to flow from Raney Ni to the other electrode causing depletion of the adsorbed  $\text{H}_2$  on Raney nickel surface (Oxidation occurs:  $\text{H}_{(\text{ads})} \rightarrow \text{H}^+ + \text{e}^-$ ). Due to this oxidized effect, a potential shift to more positive (noble) values is evident in Raney nickel electrodes with time, accounting to surface structure variation, oxides/hydroxide formation and deviation from inherent performance. It is evident from the experiments that sudden rise to  $+200$  mV vs. RHE followed by stabilization indicates that the most critical period for electrode damage is anticipated to be during the initial moments of shutdown[10].

In an effective strategy to mitigate the following issues, a cathodic protection system was designed, connecting a sacrificial anode (lead (Pb), zinc (Zn), tin (Sn), and aluminum (Al)) to the Ni cathode. These sacrificial anode are more readily oxidizable metal than Ni, that dissolves instead of the Ni cathode oxidizing, preventing cathode deactivation[73]. Chronopotentiometry (CP) at  $0.1$  mA  $\text{cm}^{-2}$  for 30 minutes in 1 M KOH was employed for assessments. Ni with Pb, Zn, Al, and Sn maintained potential below irreversible phase formation, effectively preventing Ni deactivation, while, Cd, Fe, and Mg aided no protection. Pb was found to be the most promising candidate due to its cost-effectiveness and chemical stability in alkaline media, while Zn is preferred for further experimentation accounting to its limited hazardous nature. Effect of the Zn cathodic protection system on the performance of an AEL stack during repeated start-up/shut-down was carried out, and degradation of 13.8% was identified in the absence of cathodic protection. In principle, the accelerated durability tests (ADT) under simulated reverse-current conditions demonstrated the effectiveness of the design in preventing cathode degradation.

- g. **Shunt current:** A common event often seen in AEL electrolysers (bipolar electrolyser configuration) is the shunt current, also referred to as leakage, bypass, or parasitic current, due to the stacked multiple cells configuration and short circuits (low-resistance paths) created by ionic conduction through the electrolyte[79,81]. Here, the current flows through unintended pathway, thereby bypassing the current to the electrodes, leading to severe energy loss and non-uniform current distribution. The electrical connection between cells can create leak circuit and area near the terminal electrodes may experience high current densities, when compared to edges of bipolar plates, resulting increased overpotential and localized corrosion (at high current density region) and shifted local potential. Also, long and wide flow channels, near terminal electrodes, and electrolyte inlet and outlet ports, manifolds are possible regions where shunt current can originate. In terms of cathode, this shift in potential would accelerate the degradation process, accounting for the unexpected oxidation reaction. Prolonged exposure to shunt current can aid to degradation process. Solutions to mitigate the issue include improvement of sealing, optimization of flow field designs delivering reduced resistance pathway, and electronic compensation techniques.

#### 2.1.1.2 Anode

Another vital component of electrolyser is the anode, where  $\text{OH}^-$  is oxidized to form  $\text{O}_2$ , which bubbles up to the gas collector, releasing electrons that close the current circuit[71,72]. The half reaction at the anodic end, called oxygen evolution reaction (OER), is given by the following equation:



Durability of anode is hampered by degradation phenomena such as oxidative metal dissolution, surface reconstruction, agglomeration, passivation etc., as detailed subsequently.

- a) **Corrosion/Dissolution:** Oxidative metal dissolution and/or metal oxide corrosion is a common corrosion event affecting the anode in AELs. The electrocatalysts (especially anode) undergo various redox reactions, causing the M-M bond to weaken and form M-O bond in basic and high potential electrolytes. The destabilization of M-M bond, accounts to the interaction of active oxygen species ( $\text{OH}^*$  radicals,  $\text{O}^{2-}$  anions) on catalysts surface with water molecules or adsorbed intermediates ( $\text{OH}^-$ ,  $\text{OOH}^*$ ,  $\text{O}^*$ ), followed by partial electron transfers from metal surface to reaction intermediates result in formation of M-O bond and eventually the gradual dissolution of metal in to electrolyte occurs during OER accounting to high potentials and reactive species generated[82]. Intermediates like metal oxyhydroxides are formed during dissolution, which can further inhibit the overall catalytic activity. An interesting discussion on the mechanism of degradation of metal oxide anodes during OER has been reported by researchers involving processes of dissolution, oxidation, and structural changes at the electrode-electrolyte interface. Also, Liu et al.'s, work provided some interesting insights on the Ni anode corrosion. The Ni anode (99.95% Ni and 0.05% impurities) tested for 4 weeks in KOH solution showcased veinlet-like corrosion textures and tiny pits[83]. Sediments of various morphologies were evident on the anode surface and EDS analysis confirmed the polyhedron particle to be Pb and agglomerated particle to be a mixture of Pb, Ni, O, K, Sn and C. Further, the potential map on Ni anode from the localized electrochemical tests confirmed the coexistence of negative and positive potentials at anode (corroded continuously) resulting in a galvanic cell. The galvanic corrosion (Figure 1) (application of anodic potential) causes dissolution of anode impurities (Pb and Sn) and its precipitation occurs at cathode, limiting the HER. XPS spectra of cathode confirmed the



precipitation of impurities as well. Overall, the sedimentation was influenced by both anode material exfoliation and ion precipitation, aiding towards degradation of components and lowered efficiency. An over dimensioned large cathode can enhance corrosion. Further, in an interesting work on evaluating pitting corrosion on high-strength high carbon steel wire in high alkaline deaerated chloride electrolyte, observations were made that pitting can be induced in the controlled anodic potential range and without  $O_2$ , even with significant amount of chloride concentration (1 M)[47]. Overall, pitting corrosion occurs when anodic potential is applied beyond the safety margin and, with continued application, can lead to crevice corrosion.

- b) **Surface reconstruction:** The protonation of catalyst surface due to the interaction of protons generated during the OER and metal oxide electrocatalysts can aid in corrosion (continuous erosion of the catalyst surface), dissolution, and/or undergoing amorphization of catalysts from its crystalline phase[84]. The amorphous phases of catalysts would be enhanced with the quick and uncontrolled growth of metal oxide or hydroxide species in OER conditions, leading to high degree of structural defects. Further, these disordered atomic arrangements and their composition would aid in enhancing the dissolution of electrocatalysts periodically. Also, the reactive intermediates such as metal oxyhydroxide species can enhance dissolution and further oxidation as well. *Self-Healing Catalysts*, are considered as regenerative catalysts that can repair themselves and prevent degradation. They are activated upon application of an external electrical bias, that would aid in movement of electrons and ions for self-repair. They would be further influenced by higher electrolyte concentration providing higher degree of ions to repair, high temperature conditions, applied current and potential and ensuring good mass transport conditions for efficient movement of reactants and products. In a study by, Kuroda et al., interesting insights on the self-repairing anode catalyst (hybrid cobalt hydroxide nanosheets (Co-ns) modified tripodal ligand serving as catalysts layer over anode) was reported to self-repair, making them ideal for operational under fluctuating electricity from renewable sources[85].<sup>85</sup> The Co-ns not only delivers high OER activity, but also ensure the longevity of Ni anodes, enabling self-repair under cycled potential and don't interfere with the AEL cathode as well. Further, in a very recent report, colloidal composite self-repairing catalyst of Co-ns with  $\beta$ -FeOOH nanorods (Fe-nr) over Ni anode was fabricated and evaluated. The composite catalyst delivered high activity and durability under an accelerated durability test (ADT)[86]. Further engineering of such catalyst's structures could aid in preventing the degradation of catalysts for an enhanced time frame.
- c) **Deactivation (Surface blockage and Nanostructuring):** Hinderance at the catalytic sites by unwanted species such as reactive oxygen species ( $O^*$ ,  $OOH^*$ ), and metal oxide species ( $MO^*$ ,  $M-OH^*$ ) can significantly hinder the catalytic activity of catalysts and can aid in catalyst deactivation[87]. This could either be a physical blockage, and/or due to chemical interaction. Employing strategies such as surface modification via tailoring functionalities over catalyst surface, electrochemical cleaning is some of the mitigation strategies suggested. Often the internal surface of catalysts does not participate in catalytic reactions and most reaction are from the unsaturated surface atoms. Interestingly, nanostructuring is an important technique to enhance the catalytic sites and intrinsic activity of each site[88]. For ideal performance it is vital to ensure that the distance between two active centers should be less than the van der Waals radii of  $O_2$ .

- d) **Passivation:** Oxide layer formation during the OER reactions in harsh electrolyte conditions, results in catalyst surfaces are often covered with semi- or nonconductive oxide layer impeding current flow, accounting to the lowered contract area between catalyst and electrolyte.<sup>82</sup> This would call for the increased voltage facility, to achieve same geometric activity, but would enhance the catalyst deactivation rate. Overall, the chemical oxidation of metal during OER enhances the metal dissolution rate and decline stability. The transition metal subjected to OER reactions are expected to undergo variation in electronic structure and valence states, enhancing the chances of dissolution of respective metal catalysts. Despite the dissolution behavior, Ni, Fe, Co shows better durability over noble metal and precious metals such as Ru and Ir. Further, in an investigation on assessing the activity-stability factor for monometallic 3d transition metals (M-O<sub>x</sub>H<sub>y</sub>; M=Fe, Co, and Ni) in KOH electrolyte was conducted, where they were stabilized over a Pt surface with controlled reactive site coverage and high roughness factor[89]. The O<sub>2</sub> production and metal dissolution were analyzed using a stationary probe rotating disk electrode (SPRDE) coupled to an ICP-MS spectrometer. The results revealed that the Ni catalysts showcased long term stability with minimal degradation due to slow dissolution rate from the polarization and steady-state analysis.
- e) **Gas Bubbles:** The gas bubbles formed during the reaction can affect the kinetics and degradation of catalyst[90–92]. Nucleation, growth, coalescence, and detachment can be considered as the four major processes in life cycle of gas bubbles, wherein the accumulation of bubbles can aid blocking active sites, minimize electrolyte contact, alter the mass transfer rates, prevent electrolyte diffusion, passivate, enhance ohmic resistance, thereby creating dead zones over catalysts surfaces. Aerophobic electrodes are reported to mitigate the following dead zones, caused due to bubble accumulation[93]. The porous nature facilitates short diffusion channels for reactants and products enhancing mass transfer property, delivering efficient gas desorption, and enhancing water absorption (hydrophilic electrode nature) needed for OER. Electrodes of this type ensure enhanced durability and combining the electrode with other catalyst modification techniques such as doping would further enhance the performance and stability of AEL electrocatalyst. Porous Ni/Ni-Fe-Mo-Ox nanoplates[94] and FeCoNiP@C[95] catalysts are some of the examples.

### 2.1.2 AEMEL

In AEMEL systems, catalysts are selected based on similar principles to those used in AEL, particularly to enhance electrochemical activity and stability (refer to section 2.1.1). The electrochemical activity of Ni and steel plate electrodes have been improved by surface modification via electroplating or plasma-coating of various alloys[96]. Raney-type alloys of Ni are favoured at the cathode for the HER in alkaline conditions[97], whereas alloys of NiFe are highly active OER catalysts due to partial-charge transfer between Ni and Fe, increasing the activity of the OER on Ni centers. In case nanoparticle catalysts adhere loosely to a substrate via physical binding, an ionomer may be necessary to prevent delamination. The substrate for CL deposition can either be a membrane, forming a catalyst coated membrane (CCM) or a porous transport layer (PTL), referred to as a catalyst coated substrate (CCS) or a porous transport electrode (PTE). Differences are depicted in Figure 2. Catalyst coated substrates are frequently used to allow for ex situ characterization of novel catalysts. A downside of the CCS approach is that when assembled into a electrolysis cell, an ionic interface between the membrane and the ionomer in the CL must be formed. If the ionomer possesses a glass transition temperature (e.g., 130

GA No. 101137802

°C for Nafion), hot pressing above the  $T_g$  is required to reduce interfacial resistance[98]. For example, Park, Sung et al. showed much improved AEMEL performances by hot-pressing a CCS containing a FAA-3 AEI (anion-exchange ionomer), although this was further improved using a CCM[99].

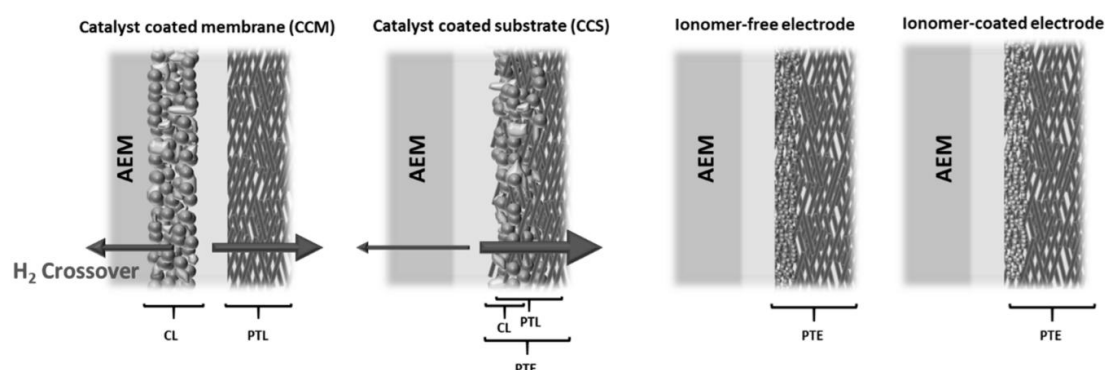


Figure 2. Diagrams show the different methods of AEMEL fabrication, adapted from [100].

CCMs are sometimes favoured to hot-pressed CCS whereby the solvent in the ink partially solvates the membrane, allowing for a percolating ionic network between the membrane and ionomer, which reduces interfacial ionic resistances. An additional benefit is that CL deposition can be controlled to a higher degree, unlike coating onto porous substrates where penetration depth and catalyst distribution are both difficult to control and to quantify[101].

#### Catalyst delamination

A thin CL close to the membrane also enables a low ionic resistance through the CL. However, with a CL distinct from the PTL, specific challenges arise, including a higher propensity for catalyst delamination, reduced porosity between catalyst particles, and a loss of electrical conductivity through isolation of catalysts when the ionomer content is too high[102]. More recent work by Park showed that the macroporosity of CCS configurations can decrease mass transport resistances while electrical conductivity is improved, in comparison to a CCM[103]. Chen, Holdcroft et al. recently showed substantial differences in  $H_2$  crossover through the AEMEL when a CCM or CCS fabrication method is used[104]. Reduced porosity in the CCM might cause a localized buildup of  $H_2$  at the CL/AEM interface, leading to an increased gas crossover.

#### Adsorption of quaternary ammonium (QA) groups on the cathode catalyst

For the HER process, the positively charged QA moiety induces specific adsorption and electrostatic effects. As a result, the  $H_2O$  HER reactants within the IHP (Inner Helmholtz Plane) experience a lower effective potential in the presence of anion exchange ionomers (AEI) compared to Nafion, inhibiting the electrocatalyst activity, as reported by Bates et al.[105]. Moreover, as further reported by Bates et al., the ammonium functionalities of QA have been shown to affect the formation of HER intermediates at Pt and NiMo surfaces.

#### Adsorption of phenyl groups on the anode catalyst

Aside from the adsorption of QA groups at the cathode, adsorption of phenyl groups on the anode catalyst has also been reported to inhibit OER, with a strong dependence on the ionomer used[106]. Li, Kim et al. used  $^1H$  NMR to show the presence of phenol groups in a CL originally containing a quaternized biphenyl AEI after 100 h of electrolysis[107]. The acidity of phenolic groups localized at the ionomer-catalyst interface is purported to be the main cause of a decrease in the OER activity. In addition to inhibiting the reaction kinetics, oxidation of phenyl groups of a PiperION membrane was observed by the Boettcher group[108], indicating that there is also concern for the oxidative stability

of ionomers at the anode. Krivina, Boettcher et al. examined the stability of three commercial, ether-free polyphenylene AEIs (Sustainion, PiperION and Aemion) cast onto Au/Ti or Pt/Ti quartz crystals[109]. XPS was used to examine the degradation of each ionomer in a variety of supporting electrolytes. The Aemion AEI was shown to degrade in a  $K_2CO_3/KHCO_3$  buffer solution (pH = 10) but less so in 1 M KOH (pH = 14) and in 1 M borate buffer (pH = 8). A higher carbonate ion conductivity in Sustainion appears to mitigate differences in ionomer stability between KOH and  $K_2CO_3/KHCO_3$  buffer. The Boettcher group also reported that the extent of ionomer degradation depends on the electrical conductivity of the catalyst, where more significant oxidation of TP-85 (Versogen) ionomer was observed on  $IrO_2$  catalysts, as opposed to a variety of Ni/Co/Fe oxides which have lower electrical conductivity[110]. Lower electrical conductivity is suggested to limit ionomer oxidation to regions close to the metallic PTL instead of throughout the entire CL.

### 2.1.3 PEMEL

The (electro-)chemical instability of the anode and cathode catalysts is dominated by the potential the catalyst is experiencing during operation and secondary modes, as shut-down and start-up. As known from extensive PEMFC literature, several degradation mechanisms have to be considered for PGM-based materials. The dominant irreversible mechanisms are dissolution, detachment, agglomeration and Ostwald ripening. Secondary degradation mechanisms related to the support (if used) have to be considered, additionally.

The most common anode catalysts used in PEMELs are Ir-based catalysts due to their remarkable electrochemical activity and stability towards the oxygen evolution reaction (OER). Iridium undergoes several oxidation state changes in the operating voltage regime of a PEMEL. Metallic iridium converts into (different) amorphous suboxide and oxy-hydroxide phases (generalized as  $IrO_x$ ) before restructuring into a rutile  $IrO_2$  phase. On the other hand, rutile  $IrO_2$  can be reduced to lower oxidation states by permeating hydrogen during idle times of the PEMEL. Such phase transformations inherently trigger iridium dissolution.

Equation	Half-cell voltage
$Ir + 2H_2O = IrO_2 + 4H^+ + 4e^-$ (7)	$E=0.926+0.0591 \cdot pH$
$IrO_2 + H_2O = IrO_2^*OH + H^+ + e^-$ (8)	$E=1.21-1.50 V$
$2IrO_2^*OH = 2HIrO_2 + O_2$ (9)	$E=1.3-1.60$
$HIrO_2 + 3H^+ = Ir^{3+} + 2H_2O$ (10)	$E=1.3-1.60$
$HIrO_2 = IrO_2 + H^+ + e^-$ (11)	$E=1.3-1.60 V$
$IrO_2^*OH = IrO_3 + H^+ + e^-$ (12)	$E \geq 1.6 V$
$2IrO_3 = 2IrO_3 + O_2$ (13)	$E \geq 1.6 V$
$IrO_3 + H_2O = IrO_4^{2-} + H^+$ (14)	$E \geq 1.6 V$

Table 2 Mechanisms for Ir degradation.

**Catalyst Dissolution:** Above certain threshold anodic potentials during operation, the Ir-catalyst experiences increasing amounts of oxidative stress caused by the OER. Through this exposure, iridium dissolves and forms various oxidized complexes via several reaction pathways, as listed in Table 2

GA No. 101137802

[111,112]. Now in solution, these intermediate ionic forms can undergo multiple reactions as they freely move and tend to migrate into the membrane, where they cluster together to form localized, concentrated zones or *bands* of deposited iridium or IrOx nanoparticles[113]. These bands are observed to add to the membrane degradation mechanisms by compromising its structural integrity[114]. The extent of these effects is influenced by hydrogen activity across the membrane, which strongly depends on cathode operation pressure, cathode structure and current density. Additionally, these Ir-ions are transported through the membrane to the cathode by the electromagnetic field, where through re-precipitation, they interact with and consequently deactivate cathodic catalytic sites[111,112,114]. According to Becker et al., based on the total dissolved migrated iridium observed in their work, 46% was found in the cathode, with a further 28% settled in the membrane[114].

The anode catalyst stability during PEMEL operation is significantly affected by the starting material chosen to fabricate the catalyst layer. It is important to point out that there is no agreement in the literature for the exact dissolution mechanism(s) of the Ir based catalysts, not even for liquid electrolyte model systems commonly employed in electrocatalyst research. Most of the studies showed that the OER and dissolution of Ir oxide share the same intermediates e.g. IrO<sub>2</sub>OH and HIrO<sub>2</sub>, as is seen in equation (7-14) (Table 2). Kasian et al.[115] reported that the Ir-based catalysts experience different degradation mechanisms at different potentials. The authors found that the formation of IrO<sub>3</sub> (equation 12-14) at higher anodic potentials (above 1.6 V vs RHE), contributes to the overall Ir dissolution, and results in lower OER activity.

Iridium degradation rates by dissolution are further exacerbated by chlorine ion contaminants[112,114] (refer to section 2.5 for more details), by prolonged exposure at high anodic overpotential operation, frequent dynamic load cycling, and low Ir-loadings (observed to be significant at low loadings of  $\leq 0.4 \text{ mg Ir cm}^{-2}$ , and even further pronounced at ultra-low loadings of  $0.8 \text{ mg Ir cm}^{-2}$ ) [111,112]. While failure modes in commercial MEAs with high PGM loading in their catalyst layers ( $1\text{-}3 \text{ mg PGM cm}^{-2}$ ) have been studied and reported[116–118], very few studies focus on the degradation mechanisms at high current densities in MEAs with low catalyst loadings in the anodes[113,119]. Rozain et al.[120] showed that the degradation of the anodes with low Ir loading (less than  $1 \text{ mg cm}^{-2}$ ) in the catalyst layer is more significant than that of anodes with high catalyst loadings. In addition, Siracusano et al.[119] reported that the performance loss in the MEAs with low catalyst loading is caused by changes in the catalyst's oxidation state.

Dissolution processes are inherently dependent on the ion concentration of the surrounding environment as charge neutrality has to be considered for net material loss in the form of ions. Liquid model systems will therefore lead to different net dissolution rates compared to what we expect to see as PGM ion leaving the anode in the exhaust water (low counter ion concentration) of a PEMEL. The polymer electrolyte in the catalyst layer and the membrane on the other hand will offer a material loss path that can significantly enhance local dissolution and that will lead to secondary degradation modes due to the mobility of those ions through the PEMEL (see later discussion).

Changes in Catalyst Morphology: In addition to dissolution, particle coarsening and coalescence contribute to changes in the anode's surface morphology, reshaping and restructuring it at the cost of system efficiency and stability. This change is predominantly instigated by the growth of the anodic catalyst particles and is largely driven by the redeposition of smaller dissolved ionic Ir and Ir-oxide species through Ostwald ripening and/or agglomeration, thereby reducing the number of available active sites for the OER[111,112]. Over time, these morphological changes can propagate into and

GA No. 101137802

affect the bulk of the catalyst layer, leading to both physical and functional degradation of the CCM as a whole.

Changes in the surface structure can further be caused by physical factors induced by internal titanium impurities (e.g., emanating from porous transport layer corrosion) that can block and neutralize the catalyst active sites (more in Section 2.5). Additionally, mechanical stress from gas bubbles accumulating in the catalyst-ionomer matrix (particularly in cavities), can cause the catalyst to separate from its support[112,121].

Both modes of degradation involve the loss and/or displacement of Ir-material of the anode that can be accelerated by the presence of contaminants (see section 2.5 for more details), leading to [111,112,114]:

- A thinner, less accessible catalyst layer, which translates into a reduced electrochemically active surface area (ECSA), hindering reaction efficiency and stability,
- Irregular interfacing and a loss of contact between catalyst layer and ionomer, which increases contact and mass transport resistance while simultaneously hindering proton conductivity and electron transport, and
- Overall lower performance issues due to the higher overpotential requirements to overcome these inefficiencies.

Finally, only few studies examine anode catalyst aging for supported catalyst materials. In such cases, degradation of the support and its impact on cell performance and lifetime has to be considered, additionally. Passivation of the catalyst support can be caused by formation of poorly conductive oxide shell on the surface of the support material, which results in increased ohmic resistance. Audichon et al.[122] suggested that RuO<sub>2</sub> supported Ir catalyst tends to be passivated as the potential increases, which results in lowering the OER activity.

### Cathode Catalyst Degradation

Platinum is widely used as the standard cathode catalyst for PEM electrolyzers due to its high affinity towards the hydrogen evolution reaction (HER), its excellent electrical conductivity and its durability under harsh acidic conditions. However, like its anodic counterpart, platinum-based catalysts remain susceptible to degradation mechanisms that over time reduce their efficiency and performance, underlining the need to better understand these phenomena to improve system longevity.

Degradation of Pt-based catalysts is driven by the potential the catalyst experiences and generally follows the same mechanisms known from PEMFC (v.s.).

Redox Cycling and Catalyst Dissolution: Platinum dissolution occurs under high current densities and frequent load cycling (intermittent start-stop cycles), whereby Pt particles enter solution from the catalyst surface and tend to diffuse into and across the membrane. Much like the anodic degradation of its iridium counterpart, although to a lesser extent, this process leads to precipitate formation and accumulation in the membrane as well as at the anode, reducing active surface area and accelerating the mechanical degradation of the membrane[114,123,124].

Dynamic load cycling and voltage fluctuations aggravate catalyst degradation through the repeated oxidation-reduction cycles between PtO, metallic Pt and Pt-ions. During standard operation, the cathode sits close to 0 V<sub>RHE</sub>, i.e., there is no significant degradation to be expected electrochemically. However, during cycles of start-up and shutdown, the chemical surface potential of the Pt can exceed 0.8 V<sub>RHE</sub>, which leads to surface oxidation. Upon subsequent operation, the catalyst is reduced again,

GA No. 101137802

which will trigger the  $\text{Pt}^{2+}$  dissolution and redeposition pathways. In addition to the formation of a Pt-band, analogous to that observed for anodic iridium, mixed Pt-Ir clusters can form when iridium ions are simultaneously present. On a macro scale, this means that these cycles impose chemical stress on the catalyst, which over time leads to cumulative weakening of the catalyst layer and eventual material losses[112,114,119,125,126].

Surface Coarsening: Furthermore, these cycles induce surface morphology changes through particle coarsening, largely attributed to the Ostwald ripening effect, which was analogously seen at the anode. Particularly at higher temperatures (around 80 °C), particle growth is observed, even under steady-state operating conditions: smaller Pt particles dissolve and redeposit onto larger ones, contributing to a loss of catalytic active sites and lower reaction efficiency[112,119,124,127].

Delamination: At high current densities, degradation is exacerbated by localized hydrogen buildup at the cathodic catalyst layer. This phenomenon is linked to mass transfer limitations of hydrogen, where the increased rate of  $\text{H}^+$  to  $\text{H}_2$  formation outpaces the rate at which the bubbles can diffuse away from the catalyst layer. This bottleneck leads to an accumulation of hydrogen bubbles at the ionomer/cathode interface[111,112,123,127]. Their presence generates additional mechanical stress, increasing the likelihood of Pt-particles physically detaching from the carbon support (*delamination*). Detached particles not only reduce the active catalyst area through material loss but can also contribute to surface morphology changes by agglomeration, leading to larger, less active clusters that degrade the overall catalyst efficiency[112,113,124]. Thinner membranes compound this issue by enabling higher rates of hydrogen crossover. The increased crossover accelerates  $\text{H}_2$ -induced degradation, such as Pt dissolution, migration and redeposition, ultimately resulting in reduced voltage efficiency and current density[111,114,124].

It has been reported that a reduction of the Pt loading in the cathode does not have significant impact on the MEA performance due to the extremely fast kinetics of the HER on Pt catalyst. However, for the development of Pt cathode catalyst layer, durability is important in the context of reducing the Pt loading.

It should be noted that contaminants, especially halogen anions as  $\text{Cl}^-$  will further enhance the PGM dissolution of the catalyst layers, as well as general corrosion and pitting of the catalyst layer structures[128]. Especially the oxidation state of the iridium-based anode catalyst might play a crucial role in the resilience of the anode toward such contaminant effects.

### **Carbon Catalyst Support Degradation**

Carbon is vital as a support at the cathode of catalyst-coated membranes (CCMs) due to its high electrical conductivity and highly porous surface, which facilitate catalyst activity and efficiently stabilize the dispersal of catalyst particles, respectively. Like active catalyst materials, carbon suffers from degradation over time under the harsh conditions of PEM electrolyzer operation. The major degradation pathways include chemical breakdown and catalyst detachment.

Carbon support materials exposed to hydroxyl radicals undergo significant degradation, leading to the breakdown of their structural integrity and functionality. The hydroxyl radicals are formed through the decomposition of hydrogen peroxide, which itself arises from precursor reactions at potentials between 0.682 to 0.695 V in the presence of protons and oxygen species. This effect is particularly pronounced at weak points within the carbon or graphite structure, such as edges or defects, and can be a function of the inherent carbon material quality[111,112,125,129].

Comparable to the active material, physical stresses also impact the carbon catalyst support layer. Damage induced by mechanical forces like pressure differentials or clamping stresses during assembly can disrupt the structural integrity of the carbon support layer, leading to *delamination* or detachment from the membrane. This disruption introduces non-uniformity in contact points between components, raising component resistance and reducing overall system efficiency[112,113,126].

### **Fabrication-Linked Degradation (1)**

Fabrication techniques can also influence the stability and durability of the catalyst-coated membrane (CCMs) as a whole. Flaws and imperfections in the catalyst layer, such as cracks or spots referred to as missing catalyst layer defects (MCLDs), often originate during the fabrication processes like decal transfer and spray coating. These defects, formed at the catalyst-membrane interface, can propagate under operational stresses, including non-uniform membrane swelling (Section 2.2) and mechanical loads, which lead to delamination of the catalyst layer and reduce the overall structural integrity[119].

In decal transfer, hot pressing is a critical step in CCM fabrication to bond the catalyst layer to the membrane. However, the temperatures operated during this process are crucial to the CCM performance and lifetime. Higher temperatures closer to the 200 °C mark have been observed to lead to membrane thinning and poorer adhesion between the catalyst layer and membrane when compared to more optimized, lower temperatures (around 180 °C)[119]. Additionally, spray coating techniques offer an alternative and more scalable fabrication process, but suffer from non-uniform deposition, requiring more precise and optimal control to minimize defects[119].

#### **2.1.4 SOEL**

The degradation mechanisms associated with solid oxide electrolysis (SOE) are extensively reviewed in the work of Professor Vanja Subotić [130]. This section highlights the key findings from her comprehensive literature analysis and experimental research.

Nickel, in combination with yttria-stabilized zirconia (YSZ), is the most widely used catalyst for both solid oxide fuel cell (SOFC) and solid oxide electrolysis cell (SOEL) modes. Despite its efficiency, Ni is susceptible to various degradation mechanisms that undermine the long-term performance and stability of SOC systems. This section explores two critical phenomena affecting Ni-based electrodes: **Ni reoxidation** and **Ni agglomeration**.

##### *2.1.4.1 Ni reoxidation*

**Ni reoxidation** poses a significant threat to the structural and functional stability of fuel electrodes, as it prevents the electrode from maintaining its initial performance and morphology. Two primary causes of Ni reoxidation include:

1. **Redox cycling** – Repeated reduction and oxidation processes at the fuel electrode.
2. **Excess oxidizing species** – Steam or air diffusion resulting from leakage, high fuel utilization in SOFC mode, or low steam utilization in SOEC mode.

Research on Ni reoxidation under SOE conditions is limited. Schefold et al. [131] observed minor performance losses after 66 hours of operation at a low current density of 0.18 A/cm<sup>2</sup>, attributing the degradation to Ni reoxidation at the fuel electrode's rim. However, this effect was absent at higher current densities, emphasizing the importance of operating conditions in mitigating reoxidation.



GA No. 101137802

In another study [133], localized reoxidation of Ni sites occurred during steam electrolysis with an  $H_2/H_2O$  ratio of 20/80. After 80 hours at  $600 \text{ mA/cm}^2$ , approximately 50% of the Ni surface was oxidized. Increasing the current density to  $1,200 \text{ mA/cm}^2$  significantly reduced the oxidation. Importantly, neither the electrode porosity nor the electrochemical performance was adversely affected.

More severe reoxidation was reported under high steam concentration conditions. Operating with an  $H_2O/H_2$  ratio of 90/10 or greater led to significant Ni reoxidation, even at elevated current densities and a voltage limit of 1.35 V [134]. These findings underscore the critical role of steam content and the need for carefully optimized operating parameters to minimize degradation.

#### 2.1.4.2 Ni agglomeration

**Ni agglomeration**, also known as Ni coarsening, is an irreversible degradation mechanism that becomes more pronounced over prolonged operational periods. This process results from material instability and is influenced by factors such as temperature, steam concentration, and fuel composition [135]. Introducing ionic conductors into the fuel electrode can reduce agglomeration at high temperatures [136].

The adverse effects of Ni agglomeration include a reduction in the active triple-phase boundary (TPB) surface area, which is vital for cell efficiency [137–139]. Additionally, agglomeration leads to the formation of inactive Ni/YSZ regions, further diminishing performance. This phenomenon is not restricted to specific operational modes and can occur even under open circuit voltage (OCV) conditions [140]. Zou et al. [141,142] reported significant degradation of the Ni/YSZ interface after only 20 hours under OCV due to Ni particle coarsening.

Steam partial pressure has a significant impact on Ni agglomeration. High steam concentrations accelerate the process, particularly during electrolysis operation [134,143–146]. For instance, The et al. [146] analyzed SOEL microstructures after 6,100 and 9,000 hours and observed that humid environments significantly enhanced Ni coarsening. They identified a direct relationship between nickel growth rates and the  $H_2/H_2O$  ratio.

Holzer et al. [143] conducted a comparative study of Ni growth under dry ( $H_2/N_2 = 3/97$ ) and humidified (60%  $H_2O$ ) conditions. They found that, in humid environments, Ni growth rates were initially high—140% per 100 hours during the first 200 hours of operation. After 1,000 hours, however, the growth rate dropped to nearly zero. In contrast, under dry conditions, Ni degradation was much slower at approximately 1% per 100 hours, remaining constant over 2,000 hours.

Simulations by Hubert et al. [137] revealed slightly lower Ni coarsening rates in electrolysis mode (25%) compared to SOFC mode (30%) at  $850^\circ\text{C}$  over 1,000–2,000 hours. These findings highlight the nuanced relationship between operational parameters and degradation rates, emphasizing the need for tailored strategies to mitigate agglomeration.

### 2.1.5 PCCEL

#### Air electrode

The limited OER activity is a significant bottleneck in the performance of Protonic Ceramic Electrolysis Cells (PCCEs), particularly at lower temperatures [147–149].

He et al. [150] investigated a composite air electrode made of  $\text{Sm}_{0.5}\text{Sr}_{0.5}\text{CoO}_{3-\delta}$  (SSC) and  $\text{BaZr}_{0.3}\text{Ce}_{0.5}\text{Y}_{0.2}\text{O}_{3-\delta}$  (BZCY35), proposing a mechanism that involves surface dissociative adsorption of water, charge transfer, and proton migration to the triple-phase boundary (TPB), where gas, electrode,

and electrolyte meet. Electrochemical impedance spectroscopy (EIS) measurements highlighted that water ionization and proton transfer to the electrolyte are the rate-limiting steps. Conversely, Tian et al.[151] proposed a bulk-surface hybrid mechanism for  $\text{Pr}_{1.75}\text{Ba}_{0.25}\text{NiO}_{4+\delta}$ , a triple-conducting material (conducting  $\text{H}^+$ ,  $\text{O}^{2-}$ , and  $\text{e}^-$ ). They observed that while water dissociation and proton incorporation are fast, the reduction of surface  $\text{O}^-$  is the rate-limiting step due to its slower catalytic capability.

Unlike oxygen ion-conducting SOECs, water in PCCEs participates in hydration, proton transport, and OER[149]. High proton conductivity in air electrodes shifts OER activity from the TPB to the electrode surface, significantly enhancing overall performance.

To address the challenges of water oxidation and OER in air electrodes, research has emphasized designing materials with high electronic conductivity in oxidizing environments, superior ionic conductivity, and catalytic activity[148,149,152,153]. Key considerations include high water tolerance, phase stability, and chemical compatibility with electrolytes. Conventional SOEC air electrodes use mixed oxygen ion and electron conductors (MIECs), while PCCEs employ triple ionic-electronic conductors (TIECs), which simultaneously transport protons, oxygen ions, and holes, optimizing TPB area utilization[152]. TIECs typically exhibit perovskite ( $\text{ABO}_3$ ), double-perovskite ( $\text{AA}'\text{B}_2\text{O}_{5+\delta}$ ), or Ruddlesden–Popper (RP) structures ( $\text{A}_{n+1}\text{B}_n\text{O}_{3n+1}$ ). Large alkaline- earth or rare- earth metal (eg, Ba, La, Sr, and Pr) is partially substituted into A- site to increase electronic conductivity[149,152]. Small tri- or tetravalent transition metal ions occupied in the B- site.  $\text{BaCo}_{0.4}\text{Fe}_{0.4}\text{Zr}_{0.1}\text{Y}_{0.1}\text{O}_{3-\delta}$  (BCFZY) is a representative perovskite-based TIEC, that has demonstrated high proton conductivity and low polarization resistance, achieving a notable current density of  $1 \text{ A cm}^{-2}$  at  $600^\circ\text{C}$ [154]. Other materials like double-perovskite oxide PBSCF and layered nickelates such as  $\text{La}_{1.2}\text{Sr}_{0.8}\text{NiO}_{4-\delta}$  have also demonstrated excellent performance in steam electrolysis due to their unique structural and conductive properties[155,156]. In particular, The layered  $\text{Ln}_2\text{NiO}_{4+\delta}$  ( $\text{Ln} = \text{La}, \text{Nd}, \text{and Pr}$ ) nickelates with RP structure have gained more interest as air electrodes in PCCEs due to their triple- conducting properties and high oxygen diffusion[157].

### *Degradation mechanisms*

The primary challenge for air electrodes in PCCEs is maintaining chemical stability in highly humidified conditions.

Degradation mechanisms include: 1) phase changes, 2) thermo-mechanical incompatibility, and 3) cation interdiffusion[149,157,158].

#### *1) Phase changes*

Alkaline-earth cations in the A-site of air electrodes perovskites may destabilize phases in the presence of  $\text{H}_2\text{O}$  and  $\text{CO}_2$ . Research has shown that hydrothermal conditions can lead to phase instability, as seen experimentally with BCFZY air electrodes [154]. Similarly, the double-perovskite BGLC air electrode, even exhibiting an excellent performance at high steam concentration, formed a secondary phase in the presence of steam[159]. Also, nickelate electrodes like  $\text{Pr}_2\text{NiO}_{4+\delta}$  are prone to decomposition under oxidizing conditions[157].

#### *2) Thermo-mechanical incompatibility*

Most of the air electrodes in PCCEs are cobalt- based oxides because of their high electronic conductivity and OER activity. These electrodes, despite their high OER activity, suffer from thermal-mechanical mismatches (i.e. differences in thermal expansion coefficient with electrolytes), which generate strains that might cause cracking and delamination at the electrode/electrolyte interface.

#### *3) Cation interdiffusion*

GA No. 101137802

Cation interdiffusion was found between conventional MIECs and proton conductors, leading to poor chemical and structural stability. For instance, experimental works highlighted the phenomenon for LSM/BCY[160], LSCF- BZY20[161], LSM-BCZYZnO [162].

### *Improvement Strategies*

Various strategies have been explored to enhance the performance and stability of air electrodes. Cation doping in the A-site can improve hydration, oxygen vacancy concentration, and phase stability. For instance, replacing La with Ba in strontium cobalt ferrite reduces strontium segregation[149], while Ca substitution in PBSCF enhances stability[163]. Introducing fluorine into the oxygen sublattice has also been shown to improve ionic conductivity and structural stability[164]. Alternatively, eliminating alkaline-earth elements altogether, as seen in the work of Ding et al.[165] on PNC ( $\text{PrNi}_{0.5}\text{Co}_{0.5}\text{O}_{3-\delta}$ ) electrodes, improves chemical stability. Finally, tailoring the microstructure of the oxygen electrode has been proposed as an effective way to avoid the gas diffusion limitation, decrease the steam starvation limitation, and reduce the partial pressure of the oxygen at the electrode/electrolyte interface. Using 3D hollow-fiber designs[165] or applying functional layers[155] between electrodes and electrolytes has proven effective in enhancing reaction areas and long-term stability. The exsolution process, which stabilizes active particles on the host support, further boosts electrode durability[163].

## **Fuel electrode**

### *SOA and Degradation*

Nickel-based cermet materials, commonly used in SOELs and PCFCs, remain the standard for PCCELS, offering both electronic conductivity and catalytic activity. To achieve a highly stable fuel electrode in PCCELS, strategies used for the anode of PCFCs, such as doping, infiltration/impregnation, in situ exsolution, and incorporating a functional layer between the fuel electrodes and electrolytes, can be directly applied. Most of the investigated electrodes are Ni-BZY, Ni-BZCY and Ni-BZCYb. The main degradation phenomena that occur in fuel electrodes of PCCEL are the ones described for the Ni-based electrodes of SOECs, such as nickel migration and agglomeration during operation that can compromise performance (readers are referred to the section dedicated to SOEC for further details on these mechanisms). An example of Ni migration documented for PCCEL consisted in the diffusion of Ni from electrode to electrolyte during the co-sintering of Ni-BZCYb/BZCYb[166]. In general, the fuel electrode in PCCEL is always operating under a reducing atmosphere, as the electrode is not exposed to high steam concentrations such as in SOEL, thus it is relatively stable during long-term electrolysis operation. In reversible operation modes, redox cycling can cause volume changes in fuel electrodes, leading to degradation.

Strategies such as reducing the thickness of fuel electrodes[167] or employing exsolved nanoparticles[154] to enhance metal-support interaction have been implemented to mitigate these issues. Metal-supported PCCELS offer improved mechanical stability and resistance to thermal cycling, further advancing the durability of fuel electrodes[168].

## 2.2 Degradation mechanisms related to the instability of the separator, membranes and ionomers

### 2.2.1 AEL

Ionic transport is achieved by using high concentration (10–30 wt %) KOH/NaOH, with maximum specific conductivity values of  $950 \text{ mS cm}^{-1}$  for KOH (50 °C, 30 wt %) and  $650 \text{ mS cm}^{-1}$  for NaOH (50 °C, 20 wt %)[37]. In order to prevent mixing of the gases, a diaphragm separator is required. Originally composed of asbestos, modern diaphragms are now fabricated from hydrophilic composites and/or polymeric materials that ensure enough porosity and wettability for efficient ionic transport between the electrodes, but not so high a porosity to allow significant gas crossover, especially if the bubble point differential pressure is exceeded[38]. Therefore, in addition to ensuring ample stability, diaphragm separators have typical thicknesses of 200–500  $\mu\text{m}$ , adding to the ohmic overpotential. Broadly speaking, In AEL system, porous diaphragms are often used for the separation of anodic and cathodic compartments, and are susceptible to several degradation effects such as mechanical degradation, chemical degradation, and thermal effects[169]. Earlier, asbestos was employed as diaphragm, but it was banned at later stages due to health risks and corrosion in alkaline environments, prompting the search for alternatives[170,171]. Initial alternatives were materials based on polysulfone and polyphenylene sulfide[172], but their low hydrophilic nature has called for better options. For instance, chemical degradation in polyphenylene sulfide (PPS) diaphragms is reported, wherein they absorb KOH rapidly into the pores. Although this enhances conductivity, it also leads to structural weakening and aids towards corrosive nature of diaphragm. A solution was a hybrid material consisting of a PPS woven felt layer for mechanical stability, coated with a composite of inorganic particles and poly-sulfone polymer. This design allows liquid to be soaked for ionic conductivity, but gives high gas transport resistance. Further, inorganic materials such as  $\text{ZrO}_2$ ,  $\text{CeO}_2$ ,  $\text{TiO}_2$ , yttria-stabilized zirconia, and  $\text{BaSO}_4$  have also been reported to be employed as inorganic particles accounting for enhanced hydrophilicity and electrolyte soaking.

Advanced diaphragms such as Zirfon PERL UTP500 and Zirfon Perl UTP220 are commonly employed in AEL and build on this principle, accounting for their ability of overcoming the aforementioned limitations along with merits such as high ionic conductivity, efficient gas separation and minimization of gas contamination, corrosion resistance and high chemical stability[173]. These diaphragms are made of zirconia ( $\text{ZrO}_2$ ) nanoparticles (85%) bonded with a polymeric binder, typically polysulfone, resulting in enhanced hydrophilic nature, that is vital for systems that evolve  $\text{H}_2$  and  $\text{O}_2$ . The membrane is stable in electrolyte conditions of 30 wt% KOH and at 90 °C (that are common in AEL). As alternative the RX-200 membrane was recently reported, and shows high ionic conductivity comparable to Zirfon PERL 500[174]. Other merits are permeation anisotropy and first stability of over 900 h.

- a. **Thermal and Chemical degradation:** Zirfon is subjected to degradation usually at extreme experimental conditions (experiments above 110 °C)[175]. Operating beyond this temperature would cause the degradation of polysulfone polymer and also can create failure in electrolyser stack due to its loss of structural integrity, molecular weight and functionality. Since AELs are mostly operating at 90 °C and higher temperatures, it could also lead to general corrosion issues for other metal parts. Thermal degradation of the membrane is only a matter of fault process operation and not during normal operation.
- b. **Mechanical stress, leaching and gas crossover:** Experiments conducted at high current density demonstrated mechanical wear or erosion causing thinning of diaphragm, resulting in gas

crossover and reduced overall efficiency. Further, pressure fluctuations can result in mechanical stress on the diaphragm, thus degrading the material. As the diaphragm degrades, it can aid in the gas crossover, leading to reduced efficiency.

c. **Degradation Studies reported:**

- The most commonly known porous separator is AGFA's Zirfon, which is a porous composite membrane of polysulfone (PSU) and  $ZrO_2$  particles, reinforced with PPS fibers. The study by Li. Hongjing et al[39]. investigates the chemical stability of a poly(oxindole biphenylene)/ $ZrO_2$  (POBP/ $ZrO_2$ ) porous separator in AEL and provides insights into the degradation mechanism of the widely used Zirfon separator under similar conditions. Zirfon, composed of polysulfone reinforced with zirconia, experiences degradation primarily due to high pH and elevated temperatures, typical in AEL environments. The degradation of Zirfon occurs through several mechanisms: chemical attack on polysulfone, increased gas crossover, and zirconia particle leaching. Under alkaline conditions, the polysulfone matrix undergoes hydrolytic cleavage, breaking down its polymeric structure. This process is accelerated by high temperatures and strong alkaline solutions (e.g., 6 M KOH and  $80^\circ C$ ), compromising mechanical integrity and increasing gas permeability. This breakdown creates a more porous membrane structure, allowing more gas to cross between the anode and cathode compartments, reducing hydrogen purity and impacting the electrolyser's efficiency and safety. Additionally, in prolonged high-pH conditions, zirconia particles in Zirfon may gradually leach out, further weakening the separator's structure and increasing ionic resistance over time. In contrast, the POBP/ $ZrO_2$  separator, particularly with 60% zirconia content, demonstrated high chemical stability, retaining low area resistance and effective hydrogen isolation, making it a more durable alternative to Zirfon for long-term AEL applications.
- Teledyne Brown Engineering has conducted degradation assessments of Zirfon™ diaphragm within their electrolyser modules with a special focus on its chemical stability, gas permeation resistance, and electrical resistance. The separator was soaked in 25% KOH solution at  $90^\circ C$  for several weeks. No major visible degradations were observed, showcasing the strong chemical resilience behavior for long term experiments. Evaluation of the separator performance in KOH electrolyser revealed excellent resistance to hydrogen permeation. Additionally, its electrical resistance yielded voltage drop lower than 5% when compared to conventional separators. Employing shims aids in mitigated external leaks with separator of 0.5 mm thickness. Further, the Deutsche Forschungsanstalt für Luft- und Raumfahrt confirmed excellent electrochemical performance and gas purity (purities higher than 99.9% at current densities ranging from 100 to  $400 \text{ mA cm}^{-2}$ ) upon using these separators for a zero-gap electrolysis laboratory cell[176]. Long term testing application of using the separator for 2800 h revealed its long-term usability for commercial applications. The Zirfon™ separator also showcased improved electrolyte retention and better wetting of the electrodes. Results from SORAPECs showcased that it is best separator for Ni- $H_2$  space batteries. VITO investigated two different types of separators where Type 2 separator's ability resulted in a higher energy density ( $110 \text{ mAh g}^{-1}$ ) over Type 1[176].

- In another study[177], different diaphragm materials were evaluated for AEL, including Zirfon™ Perl UTP 500 (Zirfon Ref), Zirfon™ pre-commercial called Zirfon Eco, Zirfon™ pre-commercial called Zirfon Thin, Chloromethylated block copolymer of styrene-ethylene-butylene styrene; 1,4-Diazabicyclo octane functional groups (PSEBS-CM-DBC)[178], Polysulfone and polyvinylpyrrolidone blend membrane (PSU-PVP)[179]. The analysis was integrated with physical and electrochemical characterization. **Physical characterization** results revealed that Zirfon Ref has a thickness comparable to that of Zirfon™ Eco, while all other membranes were much thinner, with concerns about degradation accounting for the structural integrity (Zirfon™ Thin), the mechanical stability (PSEBS-CM-DBC) the variability in thickness and swelling (PSU-PVP), and eventually leading to degradation during long-term experiments. Zirfon materials showcased a higher density over other set of materials, wherein low porosity would aid affect the permeability and performance. The bubble point analysis, that accounts for the effectiveness of separator in maximizing flow through pores, revealed that the Zirfon™ Ref and Thin provide robust pore structures, while the Eco showed a lower bubble point. The pore size distribution results revealed that PSEBS-CM-DBC showed no flow-through the pores, while PSU-PVP was not compatible with measurement methods, and Zirfon™ Eco and Zirfon™ Thin are in this range of Zirfon Ref material. **Electrochemical results** showed that Zirfon Thin caused lower ohmic resistances compared to its thicker counterparts (Zirfon Ref and Zirfon Eco), while the gas purity was increased by using thinner diaphragm. Thus, thinner diaphragms are expected to be favorable if operating at higher current densities, while thicker diaphragms will be ideal for operating at lower current densities or if the gas purity is of utmost importance. Thicker diaphragms might be advantageous for operation at intermittent conditions as well. Interestingly, there are reports showing no significant degradation of the Zirfon tested in the range of 80-95 °C and in electrolyte concentration of 40 wt% KOH[180]. The catalysts showed no major signs of degradation for several days under the aforementioned experimental conditions and the manufacturers claim the lifespan of these diaphragms to be around 5 years[181]. Visual inspection of these diaphragms showed some color variations which are possibly accounted for the electrode-electrolyte interactions[169]. Further analysis revealed that the results for ohmic cell resistance and gas impurity were within acceptable ranges, and no significant swelling was observed. Degradation of cathodes could be accelerated due to the physical adsorption of species (such as OH<sup>-</sup>, organic or metallic impurities), that can poison the catalyst surface and block its active sites.

## 2.2.2 AEMEL

AEMEL development dates back to the 1960's when they were first used in electrodialysis for water desalination[182]. The majority of anion exchange membranes (AEMs) are based on polymeric structures functionalized with quaternary ammonium (QA) groups. Significant chemical degradation of the typically used QA group occurs through the Hofmann elimination reaction, unless the stability of β-H is induced by using heterocyclic QAs with geometric constraints on the elimination reaction[183] or using alternative cationic groups such as imidazolium which does not possess β-H[184]. As it is known that main chain segments are also susceptible to degradation, for example, the poly(aryl ether

GA No. 101137802

sulfone)[185], polymer backbone structures must also be considered for hydroxide ion stability. Concurrent with the increase in membrane stability in alkaline media, there has also been a significant increase in membrane conductivity, enabling the commercialization of a wide variety of AEMs such as Fumasep FAA-3 (Fumatech), A201 (Tokuyama), Aemion (Ionomr Innovations), Sustainion (Dioxide Materials), Orion TM1 (Orion Polymer), and PiperION (Versogen)[108,186].

#### 2.2.2.1 Conductivity reduction

In their review on AEMEL durability, Li, Kim et al. estimated the effective conductivity of a hexamethyl trimethylammonium functionalized Diels–Alder poly-(phenylene) (HTMA-DAPP) AEI to be in the range of 1.2–3.7 mS cm<sup>-1</sup>, depending on the concentration of KOH (ranging from 0 to 1 M), whereas the effective conductivity of 1 M KOH is 27 mS cm<sup>-1</sup> at 50 °C[187]. The effective conductivity within a CL is inversely proportional to the square of tortuosity. Thus, when aiming to reduce ionic overpotential within the CL, the connectivity of the ion-conducting network becomes more important than the inherent conductivity of the ionomer material.

#### 2.2.2.2 Ionomer swelling

Ionomer swelling is greatly dependent on the concentration of the supporting electrolyte if one is used. Ions absorb into the ionomer when the concentration (i.e., chemical potential) of ions in the supporting electrolyte exceeds the chemical potential within the hydrophilic channels of the polymer, resulting in a reduction of the water activity and deswelling[188]. The transition concentration where water uptake starts to decrease has been used to ascertain the activity coefficients of the counterions in real systems and examine the degree of ion condensation within a variety of ion-conducting polymers, aiding the development of more ionically conductive materials[189,190]. In relation to ionomer stability, a reduction in swelling when using an electrolyte can significantly improve the adhesion of the CL[191]. With an emphasis on anode performance and stability, a technical objective is to develop ionically conductive polymers with low dimensional swelling. Ionomeric materials swell because of the internal pressure of water in the hydrophilic domains, which is balanced by the elastic force of the polymer, as determined by factors such as chain entanglement and cohesivity[192]. Therefore, aside from changing the amount of water uptake, the elastic modulus of the polymer may be increased to resist changes in dimension. Several strategies have been employed to increase the elastic modulus of the ionomeric membranes. These include use of non-ionic reinforcements[193] and covalent cross-linking[194–196].

Kohl and co-workers also explored epoxy adhesives to improve the mechanical stability of CLs but they noted that adhesion of the cross-linked ionomer to the catalyst needs improvement[197]. Improved CL stability was achieved by increasing the adhesion of the AEI to the epoxy resin, which serves as an intermediary binder. Initially, the use of a triamine cross-linker was explored, which reacts with an oxirane group of an epoxy adhesive. The best stability improvements were instead found for a terpolymer possessing -(CH<sub>2</sub>)<sub>2</sub>COOH functional group, favoured over others due to greater mobility for covalent bonding to the epoxy adhesive. This “self-adhesive” ionomer was studied for its effect on stabilization of both the cathode[198] and anode[199]. Ionomer processability was found to be particularly important, wherein amination after casting the catalyst ink ensured ionomer solubility and improved the final ionomer distribution within the CLs. In complementary work, Mayerhöfer, Peach et al. improved the adhesion of CuCoO<sub>x</sub>-containing CLs incorporating an Aemion (HMT-PMBI) AEI by heat treatment at 220 °C[200]. Heat treatment was shown to significantly increase the elastic modulus and

GA No. 101137802

reduce volumetric swelling of HMT-PMBI, resulting in greater mechanical stability of CLs operating with 0.1 M KOH supplied to both sides of the cell[201].

### 2.2.2.3 Alkaline degradation

Rising temperatures enhance the performance of the cell, but this comes at a cost—higher temperatures also accelerate membrane degradation, especially in alkaline environments. Alkaline degradation becomes a critical concern as the membrane's cationic groups are increasingly damaged by the harsh conditions, which limit the membrane's durability and force cells to operate at lower temperatures to prevent rapid deterioration. Various mechanisms can be identified through which the alkaline environment can damage the cationic groups of the membranes, with the main ones shown in Figure 3.

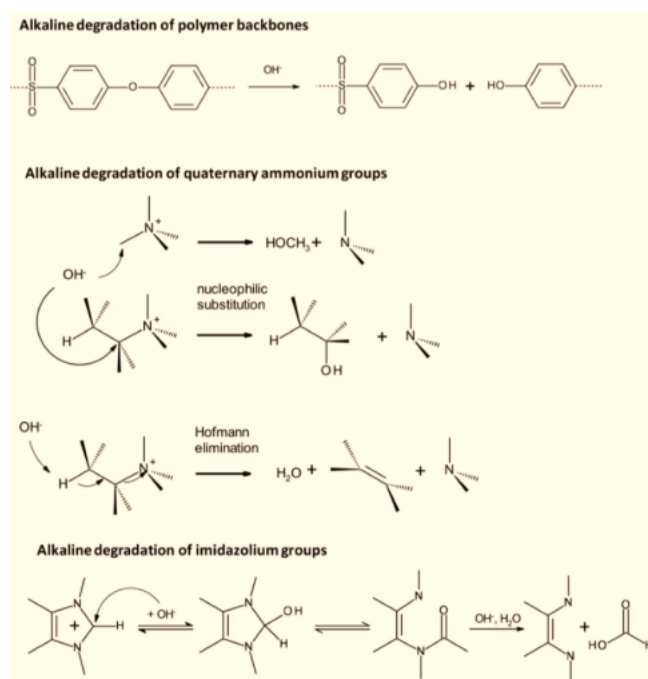


Figure 3. The mechanism of alkaline degradation of alkaline solid polymer electrolyte[202]

### 2.2.2.4 Oxidative stability of ionomers

In addition to considering the ionic connectivity afforded by the ionomer and its influence on the electrochemical surface area (ECSA) of the electrocatalysts, we must also understand the impact of the ionomer on the intrinsic activity. By considering that an alkaline environment within AEMELs is provided by the fixed cationic functional groups, it is thought that an AEI with a high IEC might induce a localized environment with a higher pH and thus influence electrode kinetics. To test the effect of ionomer IEC (ion exchange capacity) on the local pH environment, Mayerhofer, Thiele et al. coated a Pt RDE with a Nafion proton-exchange ionomer (PEI) or an Aemion AEI and monitored changes to the HOR/HER reversible potential in different electrolyte solutions[203]. Under these conditions, the pH of the electrode was primarily dependent on the external solution, less than the expected pH within the ionomer coating. The pH of the local environment is also defined by the local rate of  $\text{OH}^-$  consumption (anode) or production (cathode) from the faradaic reactions. Cao, Holdcroft et al.[204] reported that when the pH in Aemion AEM was monitored by doping with thymolphthalein, no colour change was observed at the anode, where  $\text{OH}^-$  is consumed, even once maximum conductivity was reached. Local pH changes were utilized to control the microenvironment during  $\text{CO}_2$  reduction. Kim,



GA No. 101137802

Bell et al. showed improvements in the faradaic efficiency of CO<sub>2</sub> reduction on a Cu electrode when coated with a Nafion PEI, as opposed to a Sustainion AEI[205]. They reported that the likely explanation for the improved faradaic efficiency is the trapping of produced OH<sup>-</sup> ions due to Donnan exclusion through the PEI, which is known to suppress the competing HER. However, ion migration must match the rate of reaction, and so a suppression of OH<sup>-</sup> transport might only be met with changes in overpotential. Electrochemical ionomer–catalyst interactions must also be considered, as demonstrated by Bates, Mukerjee et al., who showed clear inhibition of the HER on a Pt catalyst in the presence of an AEI with QA functional groups, attributed to specific adsorption on Pt(111) surface sites[105]. However, on a composite Ni–Cr/C catalyst, the ionomer is reported to enhance HER activity, highlighting that such effects are equally dependent on the catalyst, as well as the ionomer’s functional group. Similar to HER inhibition on Pt, Faid, Sunde et al. reported lower charge transfer resistances and higher activity for the HER (Ni/C) and OER (NiO) when using a Nafion PEI instead of a Fumion AEI[206]. They attributed the decreased activity with Fumion, primarily at the cathode, to adsorption of the QA headgroups and, as a result, showed the highest activities with reduced ionomer contents (~10wt%).

## 2.2.3 PEMEL

### 2.2.3.1 Membrane

The membrane in a PEMEL is a key component for efficient and safe production of hydrogen. It has to conduct protons at low overpotential and separate the anode and cathode compartment with respect to electric insulation and separation of the product gases.

The instability of the perfluorosulfonic acid membrane at the severe operating electrolysis conditions (including high cell voltage, high current density, high temperature, high H<sub>2</sub> output pressure, and low pH) is another source of MEA degradation. That is the reason why much thicker membranes are currently used in the MEAs for the commercialized PEMELs compared to the membranes used in the MEAs for PEM fuel cells. In addition, the industrial PEMELs operate at 30 bar differential hydrogen pressure, which results in increased hydrogen crossover (H<sub>2</sub> molecules diffuse from the cathode compartment through the membrane and reach the anode compartment). The differential pressure is the main driving factor for increased H<sub>2</sub> crossover. Since the lower flammability limit of H<sub>2</sub> in O<sub>2</sub> is about 4 vol.%, the hydrogen crossover can easily cause safety hazards. The safety limit for industrial electrolyzers is considered to be 50% of the lower flammability limit (LFL). Aside of safety concerns, crossover of the product gases will also necessarily lead to an efficiency loss with respect to the net hydrogen flux being available in the cathode exhaust.

Membrane degradation can follow different modes: Cation contaminations can lead to a loss of proton conductivity through the PFSA due to blockage of the anionic polymer head groups (see ionomer part for deeper discussion). The functionalities of the membrane can further be irreversibly lost by mechanical and chemical degradation. Due to the rough surface of the PTL structures used, local compression can be high causing imprints of the membrane that lead to local thinning[207]. Such thinned out regions will be hot-spots for gas crossover and could in the extreme case lead to electric shorts and/or pinhole formation.

Aside of mechanical stressors, the chemical degradation of PEMEL has to be considered. Radical formation upon chemical recombination of hydrogen and oxygen at the cathode can occur, which is known to lead to severe membrane thinning from PEMFC literature. In PEMEL membrane thinning was mainly observed to originate from the cathode where hydrogen peroxide is preferably formed by the chemical recombination of crossover oxygen and the hydrogen present[208]. Such radical formation

GA No. 101137802

has also been observed for recombination layers added into the PEMEL membrane, trying to prevent hydrogen crossover from resulting in safety concerns at the anode[209].

### 2.2.3.2 Ionomer

Just as for the membrane, different failure modes for the ionomer can be differentiated. Catalyst-ionomer adhesion depends on how ionomer materials change in the hydrated environment of an electrolyser. In PEMEL development excessive ionomer swelling has been noted to cause delamination of CLs, which is an irreversible mechanical degradation. The same chemical degradation mechanisms as for the membrane have to be considered for the ionomer, additionally. Contamination of the persulfonic acid groups with foreign cations can occur especially upon impure water supply to the PEM or contamination of the feedwater upon corrosion processes in the plant or cell components. Cations as  $\text{Na}^+$  and  $\text{Ca}^{2+}$  (common tap water impurities) are known to significantly reduce proton conductivity of PEMs but as shown by Padgett et al.[210], they can be removed again upon subsequent rinsing cycles using clean DI water supply. Transition metal cations as  $\text{Fe}^{3+}$ , however, are known to lead to irreversible ionomer and PEM degradation, i.e., rinsing cycles are only able to recover a small portion of the original PEM conductivity. Such contaminations commonly originate from corrosion processes, but they could also form in the cell upon contamination with debris (and subsequent “in-situ” corrosion caused by the environment at the anode) from pumps or e.g. scratched passive BOP components. Impacts on proton conductivity of cations has been observed for contamination levels of the feedwater of <10 ppm[211].

In PEM electrolyzer (PEMEL) systems, the membrane and ionomers play central roles in ensuring efficient and safe operation. The membrane, typically made of perfluorosulfonic acid (PFSA) ionomer, serves both as a physical barrier to prevent gas mixing and as a medium for proton conduction at low overpotential. It also electrically insulates and separates the anode and cathode compartments, ensuring separation of product gases. Similarly, ionomers within the catalyst layers enable local proton transport between catalyst active sites and the membrane. Together, these components form the catalyst-coated membrane (CCM), the reactive core of the membrane-electrode assembly (MEA).

The membrane and ionomer remain susceptible to various failure modes, which include chemical degradation from radical attack, mechanical stress induced by dynamic and cyclical operation, and, relatedly, physical wear linked to swelling and shrinking, which are attributed to changes in hydration levels. Research on (chemical) degradation in PEM has been widely studied in fuel cells and has shown to lead to severe membrane thinning. Findings from PEMFC literature can be partially applied to PEMEL systems, where unique conditions, such as higher operating voltages, introduce additional or intensified degradation pathways. The acidic environment, characteristically high current densities, elevated operating temperatures and hydrogen output pressures are all contributing factors in the instability of PFSA membranes in the context of PEMEL. As a result, much thicker membranes are currently employed in commercial PEMEL systems compared to those in PEMFCs to enhance durability and to mitigate degradation mechanisms caused by these operational factors. This remains an area of ongoing research as thinner membranes can enable improved system performance and economics. Understanding these degradation mechanisms is key as they directly impact the membrane’s conductivity and structural integrity, ultimately affecting the system’s lifetime and performance[111,112,125,129,212,213].

### Radical-Induced Chemical Degradation

One of the most significant pathways that compromises the membrane's stability is via the formation of reactive oxygen species (ROS)[213]. These aggressive radicals are induced by various conditions, and once formed, actively attack both the membrane's structural and functional groups[125,212–215].

Anodic Pathway: High Voltage H<sub>2</sub>O<sub>2</sub> Formation and Radical Generation: While the primary reaction at the anode in electrolyzer systems is the oxygen evolution reaction (OER), driven by the oxidation and decomposition of water, under sufficiently elevated operating voltages, a competing reaction pathway is triggered[111,112,129]. Specifically, according to Rui et al.'s work, as the system potential approaches ca. 1.8 V, hydrogen peroxide (H<sub>2</sub>O<sub>2</sub>) begins to form as a by-product at the anode via the following reaction[129]:



At higher voltages, the rate of hydrogen peroxide formation increases. However, this process competes with the OER and is eventually constrained by mass transfer limitations arising from the oxygen buildup on the anode. The low pH of the acidic environment, combined with high temperatures, promotes the self-decomposition of hydrogen peroxide various free radicals, collectively referred to as reactive oxygen species (ROS), with the hydroxyl radical (OH•) being the most commonly formed.

This degradation is further exacerbated by contaminant metal ions (such as Fe<sup>2+</sup> or Cu<sup>2+</sup>) that catalyze radical formation via Fenton-like reactions (see Section 2.5 for details). These ROS are highly reactive and aggressively attack the perfluorosulfonic acid (PFSA) membrane structure, releasing fluoride species in the process – an indicator of membrane degradation, which will be explored further below. Elevated temperatures can accelerate this process, doubling the fluoride release rate (FRR) with every 10 °C increase observed[111,112,125,129].

The anodic pathway, involving the generation of these radicals due to the formation and subsequent breakdown of H<sub>2</sub>O<sub>2</sub>, has not been as widely studied compared to its cathodic counterpart, and remains an emerging mechanism and area of further study to focus continued efforts on, as highlighted by the work done by Rui et al.[129].

Cathodic Pathway: Oxygen Crossover and H<sub>2</sub>O<sub>2</sub> Formation: On the cathode side, these ROS are also generated as a result of the hydrogen peroxide formation, but via a different pathway. Here, the prevailing understanding and accepted precursor conditions for degradation are based on anodic oxygen that crosses over and reacts (or recombines) with hydrogen through a Pt-catalyzed reduction pathway at the cathode catalyst layer[129,208]:



Where, once formed, it tends to decompose thermo-catalytically into the aggressive, highly reactive radicals that attack the membrane structure. While increased temperatures apply to the accelerated

GA No. 101137802

degradation at the cathode as well, this side is uniquely influenced by higher anodic oxygen partial pressures that contribute to the larger oxygen flux rates across the membrane and eventually the yield of hydrogen peroxide[125,129,212–214].

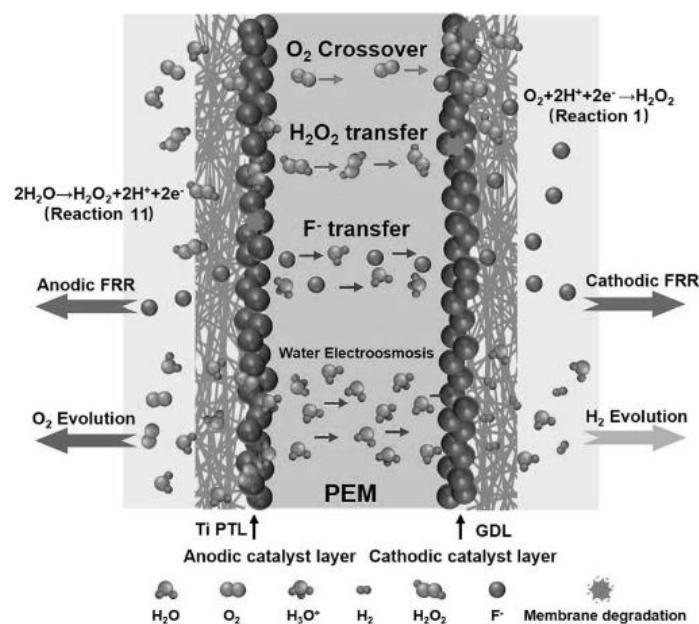


Figure 4. Overview of membrane degradation pathways and transport phenomena in PEMEL systems[215]

**Interpretation and Implications** - It follows that operating conditions that enhance this situation by increasing the oxygen concentration gradient between half-cells - such as spikes in gas formation caused during start-up and shutdown cycles or under dynamic operation - should be minimized, if not avoided altogether, to mitigate the formation of ROS. While this should be part of possible mitigation strategies, the interplay of these mechanisms and transport phenomena of the different species involved at the membrane-catalyst interface, as shown in Figure 4, highlights the complexity and interdependence of these pathways. Further understanding is essential to optimize membrane stability and performance in PEMEL systems.

**Mechanism Overview:** The formed radicals locally attack vulnerable sites within the PFSA membrane, targeting its structural and functional groups such as the carboxyl end groups of the ionomer backbone, ether bonds within side chains and the ionically active sites of sulfonic acid groups as depicted in the overview of Figure 5. This radical attack results in molecular disintegration and decreases the membrane's ion exchange capacity, leading to conductivity loss and mass loss through fluoride release, ultimately contributing to membrane thinning[213].

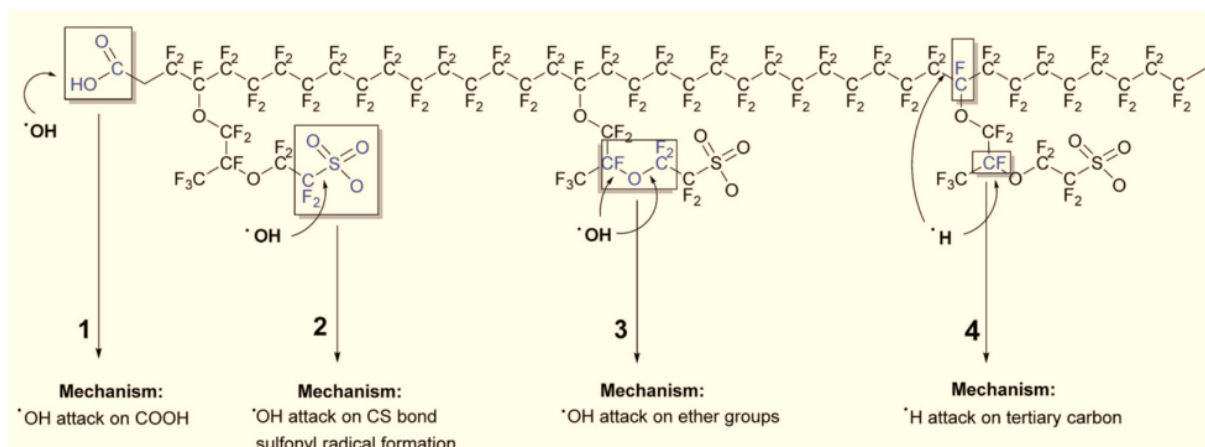
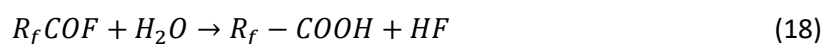
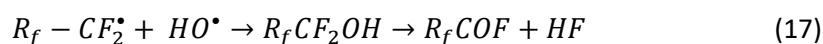
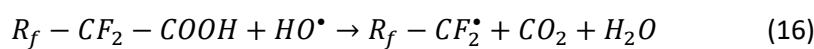


Figure 5: Mechanistic overview of radical attack pathways caused in the chemical degradation of PFSA membranes, adapted from [125].

**Radical Attack at Carboxyl Groups.** The primary and initiating step to membrane degradation occurs at the terminal carboxylic acid groups ( $\text{R}-\text{CF}_2-\text{COOH}$ ) of the PFSA polymer chain – the structural backbone. Under radical attack, these carboxyl groups are considered to be amongst the most vulnerable sites in the membrane and are first targeted and oxidized, releasing  $\text{CO}_2$  and forming a fluorinated radical ( $\text{R}_f-\text{CF}_2\cdot$ ) (Reaction 16). This radical undergoes subsequent reactions to form other fluorinated intermediates, such as fluorinated alcohols ( $\text{R}_f-\text{CF}_2\text{OH}$ ) or acyl fluorides ( $\text{R}_f-\text{COF}$ ) (Reaction 17) [129,212,213]:



Through a final hydrolysis step, these intermediates react with water to regenerate the carboxyl group (Reaction 18). With the starting point of the degradation sequence once again restored, the cycle can restart. In this way, the degradation pathway can propagate indefinitely, continuously removing  $\text{CF}_2$  units along the polymer chain, causing the membrane to unravel or *unzip* as is commonly referred to in literature (Fig 6). As this *unzipping* mechanism results in mass loss and the release of HF and  $\text{CO}_2$  as degradation by-products, the membrane's functionality and structural integrity are directly impacted, contributing to pinholes and cracks forming as well as overall thinning of the membrane. In extreme cases, this eventual breakdown can compromise the safe operation of PEMEL systems, posing short circuiting and/or explosion hazards [112,129,212,213].

**Attack on Side Chains and Functional Groups.** The ROS radicals also target the side chains of the PFSA membrane, particularly at weak C-S bond sites of the active sulfonic acid groups or the ether (C-O-C) bonds of the side chains. These sites are favored by radicals due to their relatively low bond dissociation energy and a destabilizing effect of the functional acid groups' acidity [111,212,213]. As integral parts that connect the functional side chain to the backbone of the membrane, a radical attack at these points results in chain cleavage, causing fragmentation, reducing proton conductivity, and compromising water retention [212,214]. Experimental studies conducted by Zaton et al. have identified sulfur-containing by-products, such as  $\text{SO}_2$ , as evidence of the C-S bond cleavage [216].

GA No. 101137802

Similarly, fluorinated alcohols and sulfur oxides released during degradation were observed in spectroscopic analyses and confirm the breakdown of the ether bonds within the side chains[212,214]. These vulnerabilities are further exacerbated by high oxidative stress, higher operating temperatures and dry or cyclical hydration conditions[111,212,214,215].

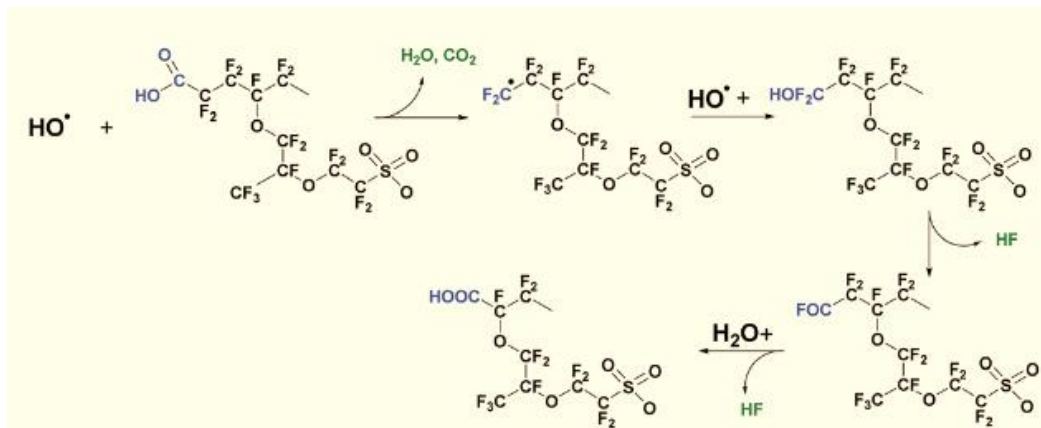


Figure 6. Cyclic reaction pathway of hydroxyl radical attack, demonstrating the unzipping mechanism of the membrane polymer chain[213]

### Mechanical Degradation Pathways

Dynamic operating conditions, temperature fluctuations, mechanical pressure differentials between half-cells and the variation in hydration levels of the PFSA membrane all induce a significant amount of mechanical stress in PEMEL systems. Over time, these various stressors detrimentally alter the membrane's mechanical and chemical properties for optimal functionality and compromise its structural integrity, deforming its surface characteristics, creating defects such as pinholes and cracks, and even causing a separation of the ionomer layers (*delamination*)[112,212,214,215]. In a vicious cycle, these structural changes expose new surfaces of the membrane, offering further points of attack for chemical degradation pathways, accelerating overall material deterioration and reduced system performance and safety[111,125,212,217].

Hygrothermal Aging: Degradation by means of hygrothermal aging is a function of moisture absorption, thermal load and time. This means that either under prolonged or even intense cyclical exposure of the membrane to humidity and temperature variations, this form of aging sets in. Over time, aging is expressed as morphological changes to the membrane's structure and introduces surface defects and stresses such as micro-cracks and pinholes. These defects weaken the membrane's mechanical stability and increase gas crossover as a result.

As previously highlighted, the rise in gas flux rates across membrane causes an increase in chemical degradation by hydrogen peroxide formation and subsequent ROS generation. This effect is further compounded by pressure differentials across the membrane, whereby product gases are forced through weakened zones of the membrane structure, accelerating the propagation and growth of defect areas. To counteract these effects, next-generation membranes are designed with structural reinforcements (in the form of polymer supports) and have demonstrated improved resistance by distributing mechanical loads more evenly and reducing the defect propagation[125,212,214,215].

**Hydration-Induced Stress:** The uptake and release of water during hydration-dehydration cycles causes physical swelling and shrinking of the ionomer and membrane, generating an internal stress within their structures. When unevenly spread, localized stress points form and can induce mechanical fatigue, material cracking and pinhole formation. As with hygrothermal aging, pressure differentials between the half-cells can apply additional forces to the already strained areas, contributing to complete deformation of the membrane structure. In the context of catalyst-ionomer adhesion, irreversible delamination of the catalyst layer occurs under excessive ionomer swelling, which significantly reduces the CCM's durability and functionality. Membranes designed with cross-linked reinforcements have shown to mitigate these stresses by restricting molecular movement, thereby providing better stability and improving the lifetime of the membrane and stack as a whole[112,125,212].

**Chemical-Mechanical Feedback Loop:** The membrane is subjected to physical forces such as pressure fluctuations, clamping stresses, and mechanical vibrations, which exacerbate mechanical failure modes like cracks, delamination, and pinholes. For instance, over compression or uneven pressure distribution of the rough PTL surface onto the membrane can lead to imprints, resulting in local membrane thinning[207]. Once the membrane is compromised, these forces accelerate defect growth and propagation, converting these thinned out regions into hotspots for uncontrollable gas crossover, initiating a self-reinforcing cycle in which chemical and mechanical degradation pathways interact and continually intensify one another. This feedback loop significantly shortens the membrane's lifespan, degrades system performance, and in extreme cases, can lead to electrical short-circuiting[112,212,214,215,218].

**Implications** - Membrane thinning under these conditions poses a significant safety risk, especially in industrial PEMEL systems that typically operate at differential pressures of up to 30 bar<sub>g</sub>. This elevated pressure gradient drives increased H<sub>2</sub> crossover (from cathode to anode), increasing the likelihood of flammable gas mixtures. With a lower flammability limit (LFL) of hydrogen in oxygen of approximately 4 vol.%, hydrogen crossover presents a serious hazard with minimal safety margins. Consequently, operational shutdown thresholds in industrial settings are set at 25% of the LFL. Beyond of safety concerns, gas crossover reduces system efficiency by decreasing the net hydrogen flux available in the cathode exhaust.

To mitigate these risks, approaches such as incorporating recombination layers into PEMEL membranes have been explored to address radical formation and the safety concerns posed by hydrogen crossover at the anode[209].

### **Fabrication-Linked Degradation (2)**

As explored in Section 2.1, PEMEL – *Fabrication-Linked Degradation (1)*, non-uniform catalyst layer deposition, where certain areas of the membrane are exposed to higher catalyst loadings, may have a compounding deterioration effect and exacerbate localized degradation mechanisms. It follows that areas with increased catalyst loading may experience elevated hydrogen production rates due to increased electrochemical activity and an associated increase in heat generation. These localized effects may amplify stress and promote the formation of reactive oxygen species (ROS), increasing the likelihood of membrane rupture and pinhole formation and reducing overall system durability. While further study is required to quantitatively validate these relationships, the importance of precise catalyst layer fabrication to minimize non-uniformities is well supported in the literature[119].

## 2.2.4 SOEL

SOELs rely on advanced electrolyte materials to achieve high efficiency and long-term stability under extreme operating conditions. Among the candidates for SOEL electrolytes, zirconia-based, ceria-based, and lanthanum gallate-based oxides have been extensively studied, each presenting unique advantages and challenges. [219–222]

Doped ceria, such as Gd<sub>2</sub>O<sub>3</sub>-doped cerium oxide (GDC), offers superior oxygen ion conductivity compared to YSZ (yttria-stabilized zirconia). However, its application in SOELs is limited due to the partial reduction of Ce<sup>4+</sup> to Ce<sup>3+</sup> under electrolysis conditions, which compromises ionic transference and leads to material degradation. Eguchi et al. [223] demonstrated that high applied voltages accelerate ceria reduction, making pure ceria electrolytes unsuitable for long-term SOEL operation. Similarly, lanthanum gallate-based oxides, such as LSGM (doped with strontium and magnesium), exhibit high ionic transference and conductivity. However, issues like thermal expansion mismatch and reactions with nickel-based electrodes (e.g., forming LaNiO<sub>3</sub>) limit their practical application. [219]

Zirconia-based materials, particularly yttria-stabilized zirconia (YSZ), are widely adopted due to their chemical stability under extreme reducing and oxidizing conditions and their superior ionic conductivity at high temperatures. Despite these advantages, YSZ is vulnerable to structural degradation, especially in the corrosive environments typical of electrolysis. Long-term operation often leads to pore formation along grain boundaries, increasing ohmic resistance and reducing cell efficiency [219,222].

Degradation in SOELs predominantly occurs at the electrolyte-electrode interface. Tietz et al. [224] demonstrated that prolonged operation at 1 A/cm<sup>2</sup> and 780°C results in intergranular fractures, void formation along grain boundaries, and compositional changes within YSZ electrolytes. These structural modifications increase ohmic resistance and reduce the mechanical integrity of the cell.

Knibbe et al. [225] and Laguna-Bercero et al. [226] identified the formation of 30 nm pore-like structures along grain boundaries near the oxygen electrode. These pores result from the nucleation and growth of oxygen clusters due to high anodic polarization potentials, which block ion transport and increase resistance. Prolonged exposure to high voltages (>1.8 V) exacerbates this process, leading to void expansion and grain boundary degradation [221].

The reduction of thin YSZ electrolytes, particularly under high steam conversion rates, induces irreversible damage. SEM analyses revealed void formation at grain boundaries and delamination at the electrode-electrolyte interface, highlighting the vulnerability of YSZ to long-term structural weakening. Additionally, thick YSZ electrolytes are particularly prone to internal pore expansion, which further compromises their mechanical and ionic properties [220,221]

Strategies to mitigate SOEL degradation focus on enhancing the stability of electrolyte materials and their interfaces. The use of GDC interlayers between LSCF oxygen electrodes and YSZ electrolytes prevents adverse chemical interactions and reduces interfacial resistance. However, the stability of GDC interlayers depends on sintering conditions and operational currents. Kim and Choi demonstrated that co-sintering cells at optimized temperatures (e.g., 1400°C) enhances interlayer performance. Electrochemical modelling suggests that controlled electronic conduction through the electrolyte can stabilize the cell by mitigating oxygen gas accumulation at the electrode interface. However, this comes at the expense of reduced electrical efficiency. The inclusion of composite layers, such as Ce<sub>0.43</sub>Zr<sub>0.43</sub>Gd<sub>0.1</sub>Y<sub>0.04</sub>O<sub>2-δ</sub>, has been shown to decrease strontium diffusion into the YSZ interface, improving the durability of GDC interlayers and reducing long-term degradation [219–221]



## 2.2.5 PCCEL

Ceramic proton conductors employed for PCCEL mostly consist of  $ABO_3$ -type perovskites, such as barium cerate ( $BaCeO_3$ ) and barium zirconate ( $BaZrO_3$ ). In perovskite oxide proton conductors, as a general mechanisms (valid both in electrolysis and fuel cell modes) the mechanism of generation of protons inside the electrolyte consists in a hydration process under humid and reducing conditions, which is affected by temperature, partial pressure of water, concentration of oxygen vacancies and lattice oxygen. The state-of-the-art  $BaCeO_3$  and  $BaZrO_3$  demonstrate high proton conductivity and significant proton charge carrier concentrations due to their excellent hydration properties. Generally,  $BaZrO_3$  offers superior thermodynamic stability, while  $BaCeO_3$  is characterized by enhanced proton conductivity, reduced parasitic electronic conductivity, and better sinterability. As a result, many proton conductors are developed as solid solutions combining these materials. To further enhance hydration levels and proton conductivity, acceptor dopants (e.g., Y, Yb) can partially replace the B-site ions, creating oxygen vacancies. Consequently, materials such as  $BaZr_{1-x}Y_xO_{3-\delta}$  (BZY),  $BaZr_{1-x-y}Ce_yY_xO_{3-\delta}$  (BZCY), and  $BaZr_{1-x-y-z}Ce_yY_xYb_zO_{3-\delta}$  (BZCYYb) have emerged as the most extensively studied electrolytes for PCCELS.

However, these electrolyte materials are affected by several degradation mechanisms[228].

Barium-containing proton conductors are prone to instability in the presence of  $CO_2$  and steam. This instability arises from unfavorable reactions between the A-site cation and the process gases, which lead to the formation of carbonates and hydroxides. Under high steam concentrations, the proton bond  $OH\cdot O$  is converted into an ionic bond, forming hydroxyl groups ( $OH^-$ ). This transformation ultimately causes the proton conductors to decompose. As highlighted by Traversa and Fabbri[229] in early studies on Barium cerates and zirconates for fuel cell applications: “Barium cerate can be stable in the presence of steam at temperatures above  $\sim 600^\circ C$ , but the damage caused by barium cerate decomposition in water is expected to be cumulative since the reverse reaction would require heating up to temperatures above  $1500^\circ C$ ”. In the work of Liu et al.[230] is shown the equilibrium products of the reactions of  $BaCeO_3$  and  $BaZrO_3$  with  $CO_2$  and  $H_2O$  as function of the temperature, which indicate that both perovskites are thermodynamically unstable at lower temperatures.

Concerning the operation in relevant conditions for PCCEL operation,  $BaCeO_3$  is more prone to decompose by chemical reaction with steam. For example, Yang et al.[231] experimentally investigated at button cell level the operation of a PCCEL featuring a  $\sim 15\text{-}\mu m$ -thick Ce-rich  $BaCe_{0.8}Zr_{0.2}O_{3-\delta}$  electrolyte (doped with Indium) under humidified hydrogen (3 vol%  $H_2O$ ) and moist air (20 vol%  $H_2O$ ) at the electrodes from 600 to  $700^\circ C$ . The electrolyte experienced a  $\sim 9\%$  reduction in current density during a 10-hour operation at 1.1 V.

By contrast,  $BaZrO_3$  demonstrates relatively better stability under typical PCCEL operating conditions due to its slower reaction kinetics with  $CO_2$  and  $H_2O$ [149], even if its poor sinterability leads to the presence of a large, poorly conductive grain boundary density, resulting in quite low total proton conductivity. For example, the stability of barium zirconate is supported by evidence showing no phase change in Zr-rich  $BaZr_{0.8}Y_{0.2}O_{3-\delta}$  (BZY20) films after exposure to boiling water or steam at  $600^\circ C$ [232]. Hydration of proton conductors not only triggers phase transitions but also causes lattice expansion. The degree of chemical expansion depends on the oxide's basicity and the level of acceptor doping[158]. Significant expansion can generate mechanical stress, reducing conductivity and impairing the interface between the electrolyte and electrode. For example, in the work of Bi and

GA No. 101137802

Traversa, the ohmic resistance of a chemically stable BZY20 electrolyte increased after 80 hours of operation at 1.3 V and 600°C[233].

In addition to chemical instability and expansion, other factors such as BaO evaporation and redistribution of acceptor dopants between A-site and B-site during high-temperature operation influence oxygen vacancy concentrations and, consequently, proton conductivity[158]. To address these issues, sintering aids are often employed to lower the sintering temperature and enhance the grain size of BaZrO<sub>3</sub>-based electrolytes. However, certain sintering aids, such as NiO, can induce mechanical degradation of BZY due to the reduction of NiO at grain boundaries[234].

Several strategies have been studied to avoid or mitigate electrolyte degradation in PCCEL. Su and Hu[235] recently described in detail the material improvements studied for PCCEL electrolytes. In their work, they identified three types of improvements.

### 2.2.5.1 Modification of Chemical Composition

Adjusting the chemical composition of Ba-based proton conductors is a primary strategy to achieve a balance between chemical stability and conductivity. Ytterbium, Hafnium and Gadolinium, among others, have been used to replace zirconium and improve the stability of the electrolyte. Electrolytes with BZCYyb4411 composition, with a Zr:Ce ratio of 4:4, demonstrated enhanced stability in environments containing CO<sub>2</sub> and H<sub>2</sub>O, while minimizing conductivity and sinterability deterioration compared to Ce-rich compositions[236,237].

Murphy et al. substituted zirconium in BZCYyb with hafnium (Hf) to increase stability, and synthesized BaHf<sub>x</sub>Ce<sub>0.8-x</sub>Y<sub>0.1</sub>Yb<sub>0.1</sub>O<sub>3-δ</sub> (BHCYYb)[238]. XRD analysis revealed no significant phase changes in BHCYYb after 500 hours of conductivity testing in a 25% CO<sub>2</sub>, 25% H<sub>2</sub>O, and 50% H<sub>2</sub> environment at 700°C. Moreover, a PCCEL utilizing BHCYYb3511 as the electrolyte and PBSCF as the air electrode exhibited stable performance over 1000 hours at 1 A cm<sup>-2</sup> and 600°C.

Enhancing the chemical stability of perovskite oxides can also be achieved by optimizing the tolerance factor closer to 1 toward an energetically favorable cubic structure[152]. Partial substitution of B-site ions with acceptor dopants reduces oxide basicity, improving the tolerance factor and stability.

For example, Rajendran et al. developed a tri-doped BaCeO<sub>3</sub>-BaZrO<sub>3</sub> electrolyte by substituting Zr with Y, Yb, and gadolinium (Gd) to form BCZYybGd[239]. XRD results demonstrated the stability of this material for over 200 hours in a 50 vol% steam/argon atmosphere at 600°C. This stability is attributed to Gd's higher electronegativity (1.20) compared to Ce (1.12), which enhances the crystal structure and reduces dopant-hydroxyl interactions. Consequently, a BCZYybGd-based PCCEL experienced only 1.7% degradation after 200 hours at 1.3 V, 600°C, and 20% moisture.

The incorporation of transition metals in Ba-based proton conductors has also been shown to significantly improve stability and sinterability. For instance, introducing Cu<sup>2+</sup> into BZCYyb1711 at interstitial positions forms BCZYyC2, which exhibits high chemical stability under high-temperature and high-humidity conditions[240]. BCZYyC2 showed no degradation during a 60-hour reversible operation, with its ohmic resistance remaining stable.

Similarly, Iron-doped BZCY17 remained stable for 25 hours in 100% H<sub>2</sub>O at 400°C[230], while the undoped BZCY17 decomposed within 5 hours. The improved stability was attributed to the thermodynamically stable BaFeO<sub>3</sub> phase. A-site deficiencies have also been effective in reducing carbonate formation[241]. For example, Kim et al. reported that a Dy(Disprosium)-doped BaCeO<sub>3</sub>

GA No. 101137802

pellet exposed to water at 90°C rapidly collapsed, while a 5%-Ba-deficient Dy-doped BaCeO<sub>3</sub> pellet remained stable [242]. This improvement was attributed to reduced basicity, which suppressed intergranular amorphous phase formation.

#### 2.2.5.2 Protection from H<sub>2</sub>O and CO<sub>2</sub>

Another strategy consists in physically shielding the electrolyte from H<sub>2</sub>O and CO<sub>2</sub> through protective layers at the electrolyte/electrode interface. Li et al. demonstrated this by applying a ~10-μm-thick La<sub>2</sub>Ce<sub>2</sub>O<sub>7</sub> layer onto the BZCYYb1711 electrolyte to form a bilayer structure. La<sub>2</sub>Ce<sub>2</sub>O<sub>7</sub> offers moderate proton conductivity and greater water resistance [48]. The bilayer cell maintained a stable electrolyzing potential of 1.13 V under an applied current density of 0.4 A cm<sup>-2</sup> in 60 vol% humidified air for 102 hours. By contrast, an uncoated electrolyte experienced a sharp drop in potential from 1.29 V to 1.07 V within 10 hours under similar conditions.

#### 2.2.5.3 Morphology modification

Stability can also be enhanced through morphological adjustments. For instance, dense pellets of Ce-rich BZCYYb1711 displayed high resistance to H<sub>2</sub>O and CO<sub>2</sub>, whereas BZCYYb1711 powders were susceptible to phase changes due to their larger surface area exposed to gases[154].

## 2.3 Degradation mechanisms related to the instability of the porous transport layer

### 2.3.1 AEL

In principle, the expanded metal (Ni) sheet or metal mesh coated with a catalyst layer are common electrocatalyst material used in AEL. Since they are surrounded by liquid electrolyte, no classical PTL exists. However, if less stable metal or alloys coated with Ni are used instead of bulk Ni at anodic end, then it could result in pitting corrosion at the electrode and eventual degradation.

### 2.3.2 AEMEL

The paper by N.U. Hassan and et al[243]. investigates the impact of porous transport layer (PTL) properties on the performance and durability of AEMELs for efficient hydrogen production. PTLs play a crucial role in the OER electrode by facilitating water transport, supporting the catalyst, and aiding in oxygen removal. However, designing PTLs that balance high performance with long-term durability is challenging. The study compares nickel-alloy (such as Hastelloy) and stainless steel PTLs, finding that nickel-alloy PTLs generally achieve lower operating voltages due to reduced contact resistance and potentially more active sites for the OER. Optimal PTL performance and durability require a precise balance of porosity and density. Higher porosity aids in oxygen and water transport but can lead to higher contact resistance and reduced adhesion of the catalyst layer, which, in turn, raises operating voltage. The authors identified an ideal density range (about 62-65%), providing an efficient compromise between gas bubble removal and stable catalyst support. To further improve

GA No. 101137802

performance, some PTLs were compressed to create smoother surfaces, reducing contact resistance and enhancing stability by maintaining consistent contact between the catalyst layer and membrane. However, durability issues arose with certain PTL configurations. High-density PTLs tended to trap gas bubbles, leading to gradual increase in cell voltage, while overly porous PTLs sometimes caused short circuits, as membrane penetration occurred under stress. Ultimately, the findings highlight the importance of careful PTL engineering. The study provides key insights into how material choice, porosity, and surface properties can be fine-tuned to enhance both the performance and longevity of AEMELs.

The cell operates with components immersed in a liquid electrolyte, but it produces gas-phase molecules that are not sufficiently soluble in the liquid. This leads to the formation of bubbles at the electrodes, which, if not properly evacuated through the cell structure, can reduce the active surface area available for the electrocatalytic reaction. A structure with insufficiently open porosity that traps bubbles can significantly hinder performance. In contrast, the presence of interconnected mesopores and micropores promotes bubble detachment. The hydrophilicity of the catalyst/GDL (gas diffusion layer) can aid in bubble detachment, while operating at high pressures stabilizes smaller, more numerous bubbles. A high current density, resulting in the production of large amounts of gas, can exacerbate the problem. Similarly, an increase in potential enlarges the bubbles and increases their adhesion to the substrate. The formation of bubbles can also have irreversible effects by damaging catalyst particles or worsening structural stresses within the cell. Additionally, the PTL must be properly engineered to release bubbles efficiently and quickly. Finally, the presence of bubbles results in a higher local current density and an increase in local temperature, as the insulating air prevents proper cooling of the membrane.

A PTL with varying porosity—smaller porosity on the membrane side and larger porosity on the bipolar side—could facilitate faster and more effective bubble evacuation, improving overall cell performance[244].

### 2.3.3 PEMEL

Porous transport layers (PTLs) play a crucial role in the MEAs degradation process. Due to the high potentials and (local) low pH, titanium is the material of choice for the PTL in PEMEL. A stable oxide skin is formed at the surface of the titanium, which in the pristine state already leads to a significant contact resistance. Interestingly, the beneficial effect of a conductive gold coating applied to the PTL on the overall overpotential at begin-of-life is strongly dependent on the anode catalyst material[245]. However, the oxide layer is known to grow over prolonged PEMEL operation[246,247], which leads to the general necessity to add a protective layer onto the PTL, commonly done by sputter coating with gold[248,249], platinum or iridium[250–252]. Rakousky et al[253]. successfully reduced the cell degradation rate by 89% and decreased the ohmic resistance by using a Pt-coated PTL.

During long term MEA operation, Ti in the PTL can corrode and cause contamination of the anode catalyst layer, leading to a decrease in the anodic exchange current density[254]. Corrosion of the PTL will be aggravated by anionic contaminants in the water as fluoride ions, which can be formed upon membrane and ionomer decomposition via hydroxyl radicals.

The porous transport layer (PTL) in PEM electrolyzers is generally designed to be highly wettable and robust to facilitate water delivery to and gas bubble shedding from the reactive zones of the stack, the membrane-electrode-assembly (MEA). Failure modes of the PTL include chemical degradation,

GA No. 101137802

pore blockage associated with changes in surface morphology and mechanical stresses during operation[255,256].

**Corrosion and Passivation:** Cutting-edge materials for the PTL are based on titanium and titanium-alloy substrates, often coated with platinum to enhance durability and resist corrosion. These substrates are engineered into various geometrical forms ranging from meshes, foams and powders to optimize gas and liquid flow. Though the Pt coating serves to shield the titanium base from direct exposure to the harsh acidic environment and high potentials in the system, achieving complete coverage of these intricate geometries can be challenging during fabrication and preparation, which may leave some titanium exposed. This exposure allows localized corrosion to occur, altering the PTL's surface profile through electrochemical degradation. The corrosion process releases metal ions (such as  $Ti^{2+}$  and/or species from different alloy types) as inherent system contaminants (more details in section 2.5), weakening the PTL's mechanical structure through erosion and compromising the performance of downstream components such as the catalyst layers, leading to a decrease in the anodic exchange current density [112,255,257].

Additionally, due to the oxidative stresses introduced at the anode during operation, particularly at these high overpotentials, passivation of the titanium surface into titanium dioxide ( $TiO_2$ ) can occur. The passivation process helps prevent further depletion of PTL material through corrosion, acting as a protective barrier, but causes a significant rise in ohmic resistance as it is electrically insulating. This subsequently translates into overall higher system energy requirements through voltage losses and reduced efficiency[112,255]. According to Yuan et al., this passivation mechanism accounts for up to 78% of the observed degradation[255].

As this oxide layer grows over prolonged PEMEL operation[246,247], the resulting increase in ohmic resistance presents yet another critical reason to apply a protective conductive coating, commonly achieved through sputter coating with gold[245,248], platinum or iridium[250,251]. Interestingly, the beneficial effect of a gold coating applied to the PTL on the overall overpotential at begin-of-life is strongly dependent on the anode catalyst material[245]. Rakousky et al.[117] successfully reduced the cell degradation rate by 89% and decreased the ohmic resistance by using a Pt-coated PTL.

**Water Management and Surface Morphology Changes:** Effective water management on the anode side is crucial for proper PTL functionality, with both Yuan et al. and Zhao et al. suggesting that hydrophilic properties in advanced PTL designs significantly enhance water transport[255,256]. However, the combined effects of corrosion and oxidation phenomena lead to increased surface roughness and coarsening.

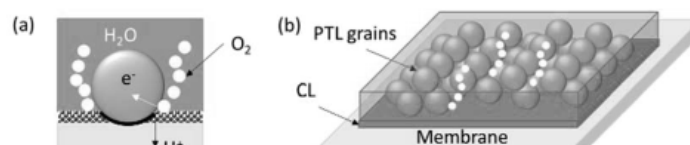


Figure 7. The triple phase boundary of the oxygen evolution reaction (OER); b) Structural depiction of the porous transport layer (PTL), the catalyst layer (CL) and the membrane interface[255]

These changes fundamentally alter the PTL's material properties, resulting in reduced wettability, longer and varying water diffusion paths, and local confinement effects at the PTL/catalyst layer interface (Fig. 7), further contributing to poor water distribution and inefficient gas removal. These factors create localized areas of poor mass transport due to pore blockage (water and gas bubble accumulation), ultimately hindering reaction efficiency at the anode catalyst layer (see Fig. 7)[112,127,255,256].

**Mechanical Degradation:** Various modes of material fatigue and repeated wear introduced by pressure gradients, overpressures, temperature fluctuations and mechanical vibrations can lead to elastic and plastic deformation of the PTL structure. Through emerging surface cracks, separation of the PTL coating or dissolution of the oxide layer, corrosion can be amplified, exposing and over time penetrating the underlying bulk material. Non-uniformly exerted contact pressure across the stack when sealed can further intensify and accelerate the degree of the PTL's structural degradation, resulting in pore deformation that constricts water and gas transport pathways. This further adds to mass transport loss sources and significantly reduces the PTL's ability, and by extension, the system's overall efficiency and stability[112,255].

### 2.3.4 SOEL

The performance and longevity of solid oxide cells heavily depend on the integrity of their electrodes, which play a critical role in the electrochemical processes. Protecting the electrodes from degradation is essential to ensure reliable and efficient operation over time. However, a significant challenge arises from the use of multifuel sources, as many conventional and alternative fuels, such as natural gas, diesel, and biogas, contain impurities. Contaminants like phosphine, sulphur, and siloxanes predominantly affect the fuel electrode, while chromium deposition is a major issue for the air electrode. These impurities not only reduce performance but also cause irreversible structural damage, threatening the stability of the cells. Preventing electrode poisoning through contaminant-free fuels is vital for maintaining SOEL functionality and extending their operational lifespan. [130]

#### 2.3.4.1 Silica poisoning

Silicon-based impurities are a notable challenge for SOEL systems, affecting both fuel and air electrodes. Among these, siloxanes-common in biogas and digester gas are significant contaminants. While their impact on SOFCs is relatively limited, their presence in SOE systems can be more

GA No. 101137802

detrimental. Additionally, silicon and silica, often introduced through glass sealing materials or water used during electrolysis, can contribute to system degradation. These impurities can cause electrode passivation and other adverse effects, emphasizing the need for effective strategies to minimize their impact on SOEL performance.

Silica originating from glass sealing materials or water used during electrolysis can negatively affect the performance of SOE systems. In conditions of high steam partial pressure,  $\text{SiO}_2$  tends to deposit at the interface between the fuel electrode and the electrolyte. This deposition disrupts electrochemical reactions and leads to electrode passivation. The primary issue is the accumulation of  $\text{SiO}_2$  rather than elemental silicon. Research, including findings by Schefold et al. [131], highlights how silica evaporation from glass sealing materials contributes to the deactivation of electrolysis processes and significant performance deterioration. Further studies reveal that  $\text{SiO}_2$  reacts with nickel, creating inclusions that compromise the integrity of the electrode structure, ultimately reducing the system's efficiency and stability. [130]

#### 2.3.4.2 Chlorine poisoning

The integrity of the fuel electrode in solid oxide cells (SOCs) is severely impacted by chlorine poisoning, a phenomenon reported across several studies, primarily in SOFC systems. Research by Jeanmonod et al. [258] extended these findings to co-electrolysis (SOE) operation. The study revealed distinct effects based on operating conditions:

- At Open Circuit Voltage (OCV): Exposure of the Ni/YSZ fuel electrode to biogas containing 10 ppm of HCl did not affect SOEL performance.
- Under Polarization: Exposure to biogas with 5 ppm HCl led to significant and irreversible performance degradation. The extent of these losses increased proportionally with the operating current.

Durability tests at  $0.5 \text{ A/cm}^2$  in biogas containing 1 ppmv of chlorine showed a steady rise in voltage, indicating a high degradation rate. Chlorine was found to reduce the electrochemical activity and catalytic performance of nickel, potentially leading to Ni depletion. This highlights the critical need to address chlorine contamination to ensure the longevity and performance of SOEL systems.

#### 2.3.4.3 Sulphur poisoning

In the world of SOEL one of the most insidious challenges comes from sulphur impurities, silent saboteurs that lurk in the fuels used to power these advanced systems. Sulphur is pervasive, finding its way into  $\text{CO}_2$  rich fuels used for co-electrolysis. Even after rigorous desulfurization processes, trace amounts often remain—just a few parts per million—but even this can wreak havoc on the delicate balance required for efficient SOEL operation.

The trouble begins the moment sulphurous species enter the system. Their presence catalyses the deposition of carbon and accelerates changes in the structure of critical materials like nickel, which is a key component of the fuel electrode. As these changes unfold, the performance of the SOE begins to degrade. The initial stage of sulphur poisoning is abrupt—a sharp drop in efficiency that can often be startling. If the exposure continues, the system might stabilize temporarily, degrade at a slower pace, or, in the worst-case scenario, continue to deteriorate steadily.

Researchers have uncovered both the threats and the possibilities for recovery. In some cases, when sulphurous impurities are removed from the fuel, the SOEL can bounce back, regaining its original performance levels. However, this recovery isn't guaranteed. Factors like the operating temperature,

GA No. 101137802

the duration of sulphur exposure, and the concentration of sulphur all play crucial roles. At higher temperatures, the damage is often reversible, but at lower temperatures, the degradation becomes more permanent and irreversible.

The interplay between sulphur and the materials within the SOEL reveals a complex and delicate relationship. For instance, sulphur doesn't just inhibit electrochemical reactions—it reshapes the environment where these reactions occur. It accelerates carbon deposits in unexpected places, sometimes well outside the regions predicted by theoretical calculations. This ability to disrupt the system's equilibrium makes sulphur a particularly dangerous adversary in co-electrolysis modes, where even the tiniest concentrations can have outsized effects.

To combat this persistent threat, engineers and scientists have devised an arsenal of sulphur removal technologies. From biofiltration systems to advanced adsorption methods, and from hydro-desulfurization beds to innovative metal-organic frameworks (MOFs), these solutions strive to purify the fuel to the highest possible standard. While sulphur cannot always be completely eradicated, the goal remains the same: to protect the delicate inner workings of the SOEL and ensure its continued performance in a world filled with challenges.

Sulphur, while small and seemingly insignificant, is a reminder of the intricacies and vulnerabilities of even the most advanced technologies—a force to be reckoned with and, ultimately, overcome [222]

#### 2.3.4.4 Chromium poisoning

Chromium poisoning is a significant contributor to air electrode degradation in SOEL systems, primarily due to the evaporation of chromium species from Fe-Cr alloy interconnects. The presence of steam in the air accelerates chromium volatilization and subsequent deposition onto the air electrode, leading to undesired degradation mechanisms [259–262]. Chromium species such as  $\text{Cr}_2\text{O}_3$  and  $\text{SrCrO}_4$  form secondary phases, which interfere with the electrochemical processes critical to SOE performance. [222]

During SOEL operation, chromium oxides and strontium chromate ( $\text{SrCrO}_4$ ) have been reported to deposit on both the electrode's inner surface and the electrolyte [263]. Chromium deposition has been identified as a chemical process that leads to the formation of secondary phases, such as  $\text{SrCrO}_4$ ,  $\text{Cr}_2\text{O}_3$ , and  $\text{CrO}_{2.5}$ , on the electrode and electrolyte surfaces. Focusing on the LSCF electrode, Wei et al. [264] observed that these phases are closely associated with SrO segregation under air electrode polarization conditions, which inhibits the oxygen evolution reaction (OER) and reduces system performance.

The effects of chromium poisoning appear to be independent of the operation mode. In addition to chromium, boron and sulfur—originating from interconnects, air streams, or glass sealing—have also been reported to negatively impact the activity and stability of the air electrode in both SOFC and SOEL systems.

#### 2.3.5 PCCEL

Readers are referred to “Catalyst instability” and “Instability due to contaminants” sections for the description of relevant degradation mechanisms in the gas diffusion electrodes.



## 2.4 Degradation mechanisms related to the instability of the bipolar or monopolar plates

### 2.4.1 AEL

The bipolar plates can be considered as a significant repetitive component of the AEL welded by a main plate and pole frame. The frame constitute sealing lines, lye and gas–liquid flow passages[265]. Among various mesh structures (concave-convex plate, machined flow plate), expanded mesh structure is favoured accounting to its rich shape and easy processing. Parallely, the design considerations for the end plates are vital for the effective operation of bipolar plates for large scale applications accounting to limiting leakages and deviations during long term operations. The end plate constitutes of specific support frame along with specific passage holes for the gas-liquid, and electrolyte (lye) flow. Gaskets and separators (such as Zirfon, detailed in previous section) are also critical components. Each bipolar plate except that the endplate is used as both cathode and anode, and all the bipolar plates are coupled in series. In a electrolyser, the sequence of component in closer arrangements are in the order of endplate, membrane, gasket, woven mesh, expanded mesh, bipolar plate. Both bipolar and monopolar plates configurations are used in AEL systems where the materials used are expected to be corrosion resistant (stainless steel, titanium), light weight (aluminium, carbon composites), conductive and mechanically strong. The anode and cathode associated with each bipolar plate are electrically connected through the metallic structure of the bipolar plate and ionically connected through the electrolyte in the manifold. Overall, a closed circuit between the anode and cathode on either side of each bipolar plate is established. Gaskets are vital for AEL as they ensure the efficient sealing of components, mechanical support, minimize mechanical strain caused due to the electrolyser operation, vibrational damping, thermal insulation, chemical resistant etc. Polytetrafluoroethylene (PTFE) gaskets are the commonly known gaskets employed for studies.106 Some other examples of gaskets include ethylene propylene diene monomer, nitrile rubber, silicone rubber etc. Some of the possible degradation phenomena among this set of components associated with bipolar plates are detailed below. As these plates are also charged and in contact with the electrolyte, the degradation mechanism is similar as the ones discussed for anode and cathode. Hence, most significant issue is associated with bipolar plates that are in intermittent conditions and will be detailed in the following sub-section.

- a. **Hydrogen embrittlement and Corrosion:** This is known to affect the metal components, accounting to the hydrogen adsorption into the metal structure of bipolar plates. This can aid in cracks or fractures under mechanical stress, making the components brittle and eventually lowering the lifespan of the electrolyser systems. Interestingly, the concerns to embrittlement are minimal in AEL systems unlike PEM system, due to the alkaline conditions. Employing stainless steel and Ni alloy are often recommended by the experts, although the low likelihood of this phenomena in AEL, it cannot be ruled out entirely. The risk associated with this phenomenon can aid to diffusion of metal ions from the bipolar plate to electrolyte under extreme conditions, aiding towards efficiency loss or electrolyser failure. Corrosion of metallic components could be a threat to metallic bipolar plates. This could be accounted to the high alkaline environment, and high pH and OH<sup>-</sup> ions can enhance the degradation of metallic components. Despite the use of stainless steel or Ni based alloys, pitting or localized corrosion are evident in bipolar plates.

- b. **Gaskets Degradations:** Mechanical degradation of gaskets are reported to occur when subjected to pressure cycling experiments resulting in gas leakages[266]. Monitoring gas leakages via leak test apparatus are crucial as well, to evaluate the effectiveness of employed gaskets. Metallic impurities are also known to affect the gasket materials, causing their leaching. For instance, KOH are reported to constitute low amount of  $Zn^{2+}$  ions, that can aid in leaching of gasket materials[267]. In an interesting study conducted by Barwe et al., the use of Viton<sup>®</sup> gaskets (fluoropolymer elastomer), in mitigating the deactivation of cathodes caused by electrolyte impurities in electrolysers (Ni//Ni) was studied[268]. Post experiment analysis of cathode showed traces of Zn that might has arisen due to the degradation via leaching of Zn components. The soft and flexible gasket turned out to be hardened and brittle post exposure to harsh operating conditions. Continuous use of such gaskets may not be ideal as they can lead to improper sealing and malfunctioning of the electrolyser. In a recent study on lab scale electrolyser fabrication for AST protocol formulation, the use polydimethylsiloxane (PDMS) gaskets were reported[71].
- c. **Degradation of Tubing, and Peristaltic Pump:** Contamination from various sources can enhance the degradation to components such as silicone tubing, pumps and/or electrolyte reservoirs. For instance, the silicone tubing from previous experiments can result in corrosion related contamination and eventual degradation[71].<sup>71</sup> New tubing's are recommended for use, and cleaning the tubing with nitric acid post experiment, flushing with deionized water, initial preconditioning with electrolyte and discarding would be an ideal practice to eliminate residues and contamination. Chemical exposure and physical stress could enhance the degradation and contamination of peristaltic pumps, calling for routinely replacing pump tubing's with materials like Norprene, following assessments and identified variations. Glass containers are subjected to etching upon its use as electrolyte reservoirs, under extreme conditions, such as high temperatures or strong alkaline solutions[71,269]. The use of PTFE containers could be an alternative to prevent etching-induced degradation.
- d. **Reverse Current:** The reverse current phenomena experienced during the shutdown are known to severely affect the bipolar plates, especially central ones, when compared to other bipolar plates. During shutdown the potential of the middle bipolar plate changes. They are known to get significantly affected during the shutdown conditions[70]. Possible solution to mitigate the issues involve, rapid cooling of electrolyte post shut off condition, to enhance the catalysts durability. Electrolyte circulation should be stopped immediately after shutting off to prevent potential issues. The reverse current is found to be in dependent of dissolved gases and is dependent only on the electrode potential.

## 2.4.2 AEMEL

Bipolar and monopolar plates are the backbone of AEMEL systems, playing crucial roles in current collection, structural stability, and the effective distribution of reactants and products. However, the aggressive operating conditions—marked by high alkalinity, reactive oxygen species, and exposure to hydrogen—pose significant challenges to their stability and performance. Various degradation pathways undermine these plates, often beginning with corrosion[270], where the alkaline electrolyte and oxygen at the anode cause oxidative damage. Metals like stainless steel or nickel alloys, while

GA No. 101137802

commonly used, can suffer from the leaching of ions, which may contaminate the electrolyte and degrade the membrane or catalyst[271].

Over time, passivation layers[272], such as oxides or hydroxides, can form on the plate surfaces. While initially protective, these layers increase electrical resistance, reducing the system's overall efficiency. Furthermore, the structural integrity of the plates is tested by repeated thermal and pressure cycling[273], which may cause physical defects like cracks or delamination, jeopardizing the cell's tight sealing and uniform current distribution.

Another critical issue is hydrogen embrittlement[274], where hydrogen atoms diffuse into the metal lattice, weakening the material and causing brittle fractures. This is particularly problematic under high-pressure operating conditions. At the same time, the highly alkaline environment can degrade protective coatings or lead to direct chemical reactions with the plate material, resulting in chemical instability.

In addition, contaminants—either from impurities in the feedwater or degradation products of the plates themselves—can deposit on critical areas such as gas channels and catalyst surfaces, impeding their functionality. These issues are further exacerbated by thermal and electrochemical stresses, where hotspots and uneven current distribution accelerate material degradation.

### 2.4.3 PEMEL

Mono- and bipolar plates fulfil various functions in the assembly and operation of a PEMEL stack. Positioned at either stack terminal (monopolar plates) or as an intermediary that separates and connects cells in series (bipolar plates), these components[112,217,275]:

- Conduct and distribute current evenly across all cells,
- Guide and contain fluid through flow channels with impermeable walls for proper mass transport of both reactant and products,
- Maintain product gas separation between adjacent cells to prevent cross-leakage, and
- Provide mechanical support for the MEA to keep it in place and withstand clamping forces in stack assembly.

Typically made from stainless steel (SS) or titanium, these plates can account for up to 53% of the total stack cost, making them a key factor in PEMEL system economics[217]. As bipolar plates (BPPs) are constructed from similar materials as PTLs, they are subject to comparable degradation mechanisms. However, their reduced surface area leads to slower degradation rates in comparison, making stainless steel-based plates a promising area of research. As a cost-saving approach, carbon-based or SS plates with corrosion-resistant coatings (precious metals, nitrides, carbide layers) are continually being explored, but continue to face challenges in performance, stability, and longevity [217,275]. These metrics are generally compromised by key degradation mechanisms, discussed below.

Passivation: Similar to phenomena observed in titanium-based PTLs, high potentials experienced at the anode side introduce oxidative stresses and form oxide layers, such as titanium dioxide (TiO<sub>2</sub>), which render the surface film electrically insulating and act as a barrier to current distribution and current flow. Throughout the PEM stack's lifetime, the growth of this passive layer degrades the plate's electrical conductivity. This increases the voltage required to overcome the rising contact resistance and to maintain desired current densities, which ultimately reduces system efficiency. The

GA No. 101137802

development and implementation of protective coatings, such as the use of platinum, are essential to mitigate these degradation modes, ensuring durability of the stack[111,112,217,276].

**Corrosion:** Operational environmental factors, such as the acidic medium, elevated temperatures, and high running voltages of the PEMEL, promote the electrochemical corrosion of metal-based plates causing surface degradation. As these effects are particularly pronounced in the anodic chamber, proximity to the OER catalyst layer, where conditions are harshest due to high electrochemical activity, becomes a hotspot for corrosion-driven degradation (Fig. 8)[217].

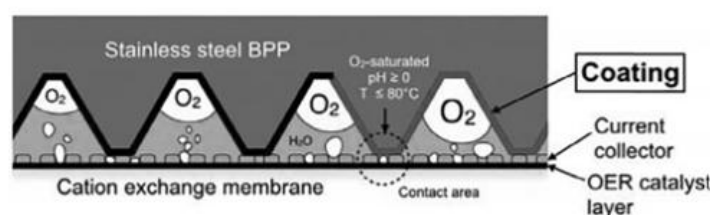


Figure 8. Cross-sectional view of PEM electrolyzer anode, depicting the flow channels of the stainless steel bipolar plate (BPP) and the interactions at the catalyst layer interface. The corrosion prone area is highlighted by the dashed circle, adapted from [217]

As this deterioration progresses, microscopic changes in the material surface topography of the plate occur, leading to non-uniform gaps, cracks and flakes. These surface defects create uneven contact points between stack components, reducing the effective contact area and thereby increasing ohmic resistance, the Interfacial Contact Resistance (ICR). Further material degradation becomes a primary concern as its cumulative effects lead to increased porosity and thinning of the plate, compromising its mechanical integrity and long-term stability[112,217,275,276].

While titanium plates benefit from an additional, naturally forming passivation layer to limit corrosion, much like the mechanisms observed in Ti-based PTLs (section 2.3), stainless steel plates depend more on surface modifications via applied protective coatings to resist low-pH environments. Under constant exposure, however, both types of protective barriers gradually erode, leaving the underlying bulk material vulnerable to rapid degradation. Once compromised, stainless steel undergoes more aggressive corrosion than its titanium counterpart, underscoring the challenge and need of balancing its initial cost-effectiveness with the requirements for durable, often expensive coatings – a critical consideration for system economics and ongoing research[217,276].

**Hydrogen Embrittlement:** A further BPP degradation mechanism, largely observed at the cathode, is hydrogen embrittlement. According to Teuku et al., during a 500-hour long-term durability test, titanium plates can exhibit an absorbed hydrogen concentration over 1000 ppm[217]. Hydrogen embrittlement can be traced to two prevalent pathways: (i) *internal* hydrogen embrittlement (IHE), and (ii) hydride formation.

**Internal hydrogen embrittlement (IHE).** Due to its relatively small size and high diffusivity, hydrogen atoms tend to flow into the metal structures of titanium-based or stainless steel BPPs, occupying their *interstitial* sites and becoming confined at defects such as dislocations and areas under higher strain (*stress fields*), like grain boundaries (Figure 9). As more hydrogen accumulates over time, it not only hinders the metal's ability to deform but also exerts a localized pressure in these regions, making the material increasingly brittle and prone to fractures. Under external stress, cracks initiate and propagate through the metal, growing as the localized hydrogen buildup continues to weaken the structure[83].

**Hydride formation.** Once a critical concentration is reached in these stress-prone regions (under a given temperature and pressure), the presence of hydrogen within the metal lattice can lead to the formation of metal hydrides, arising as a cascading effect and consequence to IHE. These hydrides further weaken the metal structure, reduce its ductility, decrease its tensile strength, and promote crack propagation[83,112,217].

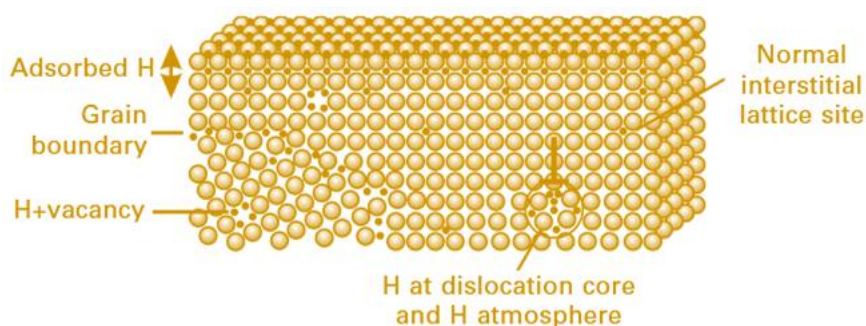


Figure 9. Schematic visualisation of hydrogen trap sites in a metallic lattice on an atomic scale, showcasing interstitial sites, grain boundaries, and dislocations, adapted from [83].

According to Lynch, high temperatures and elevated partial pressure of  $H_2$  promote its diffusion into the BPP's metal lattice, whereas lower temperatures favor its accumulation[83]. It can, therefore, be inferred that this process may be exacerbated by temperature cycling and pressure spikes, fluctuations that are typically observed during startup or shutdown of PEMEL. This suggests that hydrogen embrittlement may be stimulated and worsened under dynamic operating conditions, highlighting the need for further research to better understand its long-term impacts and develop more suitable mitigation strategies. Both pathways compromise the BPPs' structural integrity, causing layer separation and eventual mechanical failure, the implications of which point to a loss of containment (gas crossover or leakage), increased contact resistances, and a decrease in overall system efficiency[83,112,217,276].

**Mechanical Degradation:** Recurring mechanical stress also drives the degradation of mono- and bipolar plates, primarily through thermal and pressure cycling, which cumulatively lead to material fatigue in titanium- and stainless-steel-based plates. This results in the formation and spread of micro-cracks, compromising their structural integrity. Additionally, surface defects emerge similar to those observed under corrosion mechanisms, further increasing the interfacial contact resistance (ICR) and reducing system efficiency[112,217,275].

*Implications* - Overall, each degradation phenomenon undermines the structural integrity of the BPPSs, which cumulatively can accelerate the entire process, posing a serious safety risk and a potential system-wide shut down. As the plates weaken, the probability of containment loss increases, which, depending on the severity and region, may result in sealing failure, gas leakage, cross-contamination and unwanted product mixing. This not only diminishes stack efficiency, but also introduces a severe fire or explosion hazard given the highly flammable nature of hydrogen in the presence of oxygen. Long-term durability studies are needed to better quantify these risks and develop effective maintenance and mitigation strategies to prevent catastrophic failures.

#### 2.4.4 SOEL

The interconnect in a SOEL stack serves multiple essential functions. It provides electrical contact between individual cells while also physically separating the fuel side (cathode) and oxygen side (anode) gases. Additionally, it facilitates gas distribution across both cells, which is achieved through channels integrated into its surface design. These channels ensure efficient and uniform delivery of gases, supporting optimal cell performance and system operation.

The degradation of interconnectors in SOELs primarily results from the oxidation of stainless steel, which forms a protective chromium-based oxide scale at high temperatures. This oxide layer is essential for electronic conductivity and gas separation but is susceptible to degradation due to chromium depletion. The oxidation rate is influenced by oxygen partial pressure, steam content, and operating temperature, with higher steam levels and temperatures accelerating the process.

Material composition and interconnector thickness also play critical roles. Stainless steels with 17–22 wt.% chromium support scale formation, but prolonged operation depletes chromium, reducing protection. Thicker interconnectors exhibit slower degradation due to greater material reserves. Protective coatings can mitigate oxidation by shielding the base material from reactive gases. [277,278]

While coatings on interconnectors (ICs) are essential for reducing oxidation rates and chromium evaporation, they can also introduce specific degradation mechanisms under certain conditions:

- **High-Temperature Oxidation During Sintering:**  
 Perovskite oxide coatings, such as  $\text{La}_{1-x}\text{Sr}_x\text{MnO}_3$  (LSM) and  $\text{La}_{0.6}\text{Sr}_{0.4}\text{Co}_{0.2}\text{Fe}_{0.8}\text{O}_3$  (LSCF48), require sintering at temperatures above 1000°C to achieve sufficient density. However, at these temperatures, undesirable oxidation can occur between the coating and the underlying steel plate, potentially altering the interfacial properties and affecting long-term performance. Lower-temperature sintering results in increased porosity, reducing the protective efficacy of the coating.
- **Pre-Oxidation Effects from Heat Treatments:**  
 For coatings applied as oxide powders via methods like Wet Powder Spraying (WPS), heat treatments are necessary for adhesion. These treatments can lead to pre-oxidation of the stainless steel, which in turn influences the subsequent oxidation kinetics during operation in oxygen-rich environments.
- **Carburization in Carbon-Rich Atmospheres:**  
 In  $\text{CO}_2$  or CO-containing atmospheres, dense oxide coatings are critical to preventing carburization. However, inadequate coating performance can allow carbon penetration, leading to the formation of chromium carbides and metal dusting. For example, the application

of a Ni-layer as a contact enhancement can promote carbide formation, especially with thicker coatings, lower chromium content in the steel, and higher operational temperatures.

- **Breakaway Oxidation:**

If chromium evaporation outpaces the formation of protective  $\text{Cr}_2\text{O}_3$  scales, or if the Cr content in the steel falls below critical levels, breakaway oxidation can occur. This process often involves the formation of less protective iron oxides or the penetration of  $\text{CO}_2$  through the oxide scale, resulting in severe degradation.

### 2.4.5 PCCEL

In a PCC stack, as in SOCs, the interconnector serves as a critical connecting element between cells. It provides an electrical pathway between the air electrode of one cell and the fuel electrode of the adjacent cell. To fulfill this role, the interconnector must possess high electrical conductivity. Additionally, it features channels on either side to facilitate gas flow. Its structure must be dense and impermeable to molecular diffusion, as it acts as a physical barrier protecting the air electrode from the reducing environment of the fuel electrode and vice versa[279].

Protonic ceramic fuel and electrolysis cells (PCFCs/PCCELS) have yet to be demonstrated in a stack configuration. Consequently, experimental investigations into the oxidation behavior of metallic interconnectors under relevant operating conditions are limited.

The suitability of a material for use as an interconnector depends on specific operational conditions and design requirements. For proton-conductive ceramic stacks, the interconnector material must exhibit excellent chemical and thermo-mechanical stability at 500–600°C, good thermal conductivity, and a coefficient of thermal expansion (CTE) that is compatible with the electrolyte and electrodes to minimize thermal stresses. Ni-, Cr-, and Fe-based oxidation-resistant alloys are considered potential candidates due to their ability to meet these requirements[280]. Among these, ferritic stainless steels (FSSs) containing Fe and Cr stand out as the most promising materials. They offer excellent formability, low cost, and CTE compatibility with other PCC stack components[281]. Specifically, FSSs have a CTE range of  $11.5\text{--}12 \times 10^{-6} \text{ K}^{-1}$ , closely aligning with that of BZCY in dehydrated conditions ( $10\text{--}14 \times 10^{-6} \text{ K}^{-1}$ )[282].

Bare FSSs can endure high temperatures only if they form and maintain protective chromium-rich oxide scales. If this passivation fails, rapid "breakaway" oxidation occurs, leading to the formation of iron-rich oxides, surface degradation, and eventual interconnector failure[283].

The passivation process depends on the temperature, gas atmosphere, and the alloy's composition, particularly its chromium content. At lower oxidation temperatures (450–700°C) in static air, FSSs tend to form non-protective iron oxides (e.g.,  $\alpha\text{-Fe}_2\text{O}_3$  and  $\text{Fe}_3\text{O}_4$ ) due to insufficient chromium diffusion from the bulk to the surface[280]. However, as temperatures rise above 700°C, chromium diffusion improves, facilitating the formation of protective  $\text{Cr}_2\text{O}_3$  oxide layers. Alloys with chromium content exceeding 20 wt.% are more likely to form these protective layers even at lower temperatures.

Exposure to humidified environments, such as the air- $\text{H}_2\text{O}$  mixtures typical in PCCELS, accelerates the formation of non-protective iron oxides[284]. Additionally, oxide scale growth, whether protective or non-protective, increases the area-specific resistance (ASR) of the interconnector, degrading the stack's electrical performance over time. Another challenge is "Cr poisoning," where volatile Cr species from chromia-rich scales deposit on electrodes or at the electrode/electrolyte interface, reducing

electrochemical activity and cell performance. While Cr poisoning has been extensively studied in SOCs, its effects in PCCs remain largely unexplored and require careful control.

To mitigate breakaway oxidation and control oxide scale growth and chromium evaporation, various strategies have been explored, including surface treatments, bulk composition modifications, and protective coatings[285].

In the study by Wang et al.[280], protective coatings such as  $Y_2O_3$ ,  $Ce_{0.02}Mn_{1.49}Co_{1.49}O_4$ ,  $CuMn_{1.8}O_4$ , and Ce/Co were applied to stainless steel sheets to enhance oxidation resistance. Dual-atmosphere testing validated the effectiveness of these coatings under realistic PCFC/PCCEL operating conditions, with hydrogen gradients across the interconnect. Several combinations of metals and coatings were found to be viable for interconnect applications in PCFC/PCCEL stacks

## 2.5 Degradation mechanisms related to the instability of components due to contaminants.

### 2.5.1 AEL

Contaminant involves any foreign entity that has the potential to alter the dynamic of a specific reaction. This could be electrolyte impurity, water impurity, catalyst leaching, external contamination etc, and it is vital to keep the experiments contaminant free in order to prevent the degradation of components and electrolysers lifetime. Contaminants can often alter or introduce new electronic states affecting both the electrotonic structures of active sites and charge transfer dynamics in electrocatalysts[267–269,286].

- Impurities:** Among cationic impurities  $Fe^{2+}$  is reported to positively enhance the OER activity in AEL electrolysers through adsorption and deposition mechanisms[267] wherein in some cases the impurities were part of reagent grade KOH[287], while in few other cases they were added deliberately[288], and sometimes part of electrolyte in nanomolar level[289]. For instance, reports on Fe deposited over nickel oxide are available, where it led to formation of NiFe layered double hydroxides, one of the most active non-precious metal OER catalysts[290]. Interestingly, the presence of Fe was also found to result in preventing the adverse effects caused in Ni catalysts due to Ni-H formation. Conflicting results on the role of Ni as promoter and inhibitor are reported. Ni-H was also detected on a RANEY® Ni–Al anode, post its operation at  $300 \text{ mA cm}^{-2}$  in 10% potassium hydroxide[291]. The catalysts showcased an increased overpotential values and hydride was confirmed from the XRD analysis. The catalysts were restored upon employing a high temperature treatment for 120 min in 1000 C. Sometimes the coated Fe particles could detach from catalyst surface resulting  $HFeO_2^-$  via corrosion, but are reducible back to metallic Fe under specific electrochemical conditions[292]. Further, with increasing Fe content (90 wt%) in Fe-Ni cathodes, the HER activity was enhanced. This enhancement was due to the enhanced active surface area resulting from the reduction of  $Ni^{2+}$  and  $Fe^{2+}$  ions during cathodic sweeps. Parallely, the negative impact of cathodic impurities such as  $Zn^{2+}$  are available in literature. The sources could be from KOH electrolyte, while there are chances for them to leach from plastic components such as gaskets as well and cause significant degradation effects. In order to confirm its negative impact  $Zn(NO_3)_2 \cdot 6H_2O$  at  $0.067 \text{ mg mL}^{-1}$ , was added to the catholyte of a nickel/nickel electrolyser operated at 50



$\text{mA cm}^{-2}$ . [268] Observations were made that the cell voltage was increased during its operation and zinc dendrites were found on electrodes. Also, it is known that cations such as  $\text{Zn}^{2+}$ ,  $\text{Cd}^{2+}$ , or  $\text{Pb}^{2+}$ , that are not active OER or HER catalysts and would decrease the performance upon adsorption [267]. All are known to prime sources of catalyst poisoning and among them  $\text{Zn}^{2+}$ , are known to form dendrites at negative potentials at cathodes, significantly affecting the electrocatalyst durability.  $\text{Mg}^{2+}$  ions as impurities, are known to deposit as  $\text{Mg}(\text{OH})_2$  at high pH, resulting in severe mass transport issues in electrocatalysts [67].  $\text{Ca}^{2+}$ , and  $\text{Mg}^{2+}$ , cations can also deposit at high pH and may block reactant access to catalyst sites. Inert impurities can majorly lead to precipitation issues at high pH levels due to the minimal/low solubility of certain metallic ions and carbonates [267]. Such impurities can result in mass transport issues causing clogging of porous layers of electrode, separators etc. Catalyst poisoning of anode and cathode via organic impurities is also reported in literature.

Impurities in electrolyte are seen to have both positive and negative effects on the components in AEL. For instance, incorporation of Fe impurities in KOH electrolyte was found to enhance the OER activity, while presence of  $\text{Zn}^{2+}$ ,  $\text{Cd}^{2+}$ , or  $\text{Pb}^{2+}$  is known to have set back on both anode and cathode materials. In a study report by Trotochaud et al. rise in the OER reaction with aging of KOH was reported to be from the Fe impurities in KOH electrolyte, which prevent the conversion of  $\gamma\text{-NiOOH}$  to  $\beta\text{-NiOOH}$  [293]. Nearly 25 % of codeposited Fe was found to form a Ni-Fe layered double hydroxide, leading to overall increase in the OER activity. Later, in another work by Klaus et al., effects of Fe incorporation on structure-activity relationships in Ni-(oxy)hydroxide were evaluated using various techniques. Several interesting insights were brought in to light of which critical ones accounts to the successful demonstration of in situ catalysts structure modifications wherein Fe electrolyte impurity incorporation on the Ni-(oxy)hydroxide catalyst structure to be the reason for enhanced OER activity [290].

Water employed for the experimentation are also crucial as tap water constituting cations and anions ( $\text{Na}^+$ ,  $\text{Ca}^{2+}$ ,  $\text{Mg}^{2+}$ ,  $\text{Al}^{3+}$ ,  $\text{Cl}^-$ ,  $\text{HCO}_3^-$ ,  $\text{SO}_4^{2-}$ ,  $\text{NO}_3^-$ ) serve as impurities and significantly hamper the HER reaction and rise in anode potential.

- Corrosion:** The effect of  $\text{Cl}^-$  anionic impurities are not very dominant in case of AEL electrolyzers, and is a concern only with experiments with direct seawater electrolysis. For instance, a nickel electrode was operated at saturated sodium chloride plus 30 wt% sodium hydroxides at  $467 \text{ mA cm}^{-2}$  [177]. Post nine days, the system failed due to short circuiting of electrode. Further analysis showed that the nickel electrode was corroded to NiO (black particles), due to the high saline electrolyte. Basically, the  $\text{Cl}^-$  ions were known to attack the passive layer on nickel surface aiding to corrosion as well. ASTs experiments on catalysts NiFe and NiFe/NiS<sub>x</sub>, showed that the catalysts showed ideal performance and higher durability [294]. Beyond corrosion,  $\text{Cl}^-$  ions can lower conductivity of electrolyte, substituting  $\text{OH}^-$ , leading to eventual degradation of the catalysts. Overall, certain nickel catalysts are resistant to saline conditions while some degrade.

## 2.5.2 AEMEL

In the field of anion exchange membrane electrolysis (AEMEL), contaminants play a pivotal role in the degradation mechanisms of system components, posing significant challenges to performance and

GA No. 101137802

durability. These contaminants, originating from feedwater impurities, atmospheric CO<sub>2</sub>, or material degradation by-products, instigate chemical, mechanical, and electrochemical instabilities in critical cell components such as membranes, ionomers, catalysts, and gas diffusion layers (GDLs).

### **Chemical Instabilities of Anion Exchange Membranes and Ionomers**

The core of AEMEL systems, the anion exchange membrane, relies on quaternary ammonium (QA) functional groups to conduct hydroxide ions. However, these QA groups are highly susceptible to chemical attack by contaminants. Transition metal ions, such as Fe<sup>3+</sup> and Cu<sup>2+</sup>, catalyze the breakdown of these groups through nucleophilic substitution and Hofmann elimination reactions. These processes lead to irreversible losses in ionic conductivity and mechanical strength. For instance, demonstrated that Fe<sup>3+</sup> accelerates QA group degradation, forming insoluble precipitates that damage the polymer matrix and significantly shorten the membrane's lifespan. Similarly, chloride ions, often introduced via impurities in feedwater, can initiate polymer chain scission, further compromising membrane integrity[295–297].

### **Catalyst Poisoning by Contaminants**

The electrocatalysts employed for the oxygen evolution reaction (OER) and hydrogen evolution reaction (HER) are also vulnerable to contaminants. Sulfate ions (SO<sub>4</sub><sup>2-</sup>) from feedwater and atmospheric CO<sub>2</sub> are particularly detrimental. Sulfur species adsorb onto the catalyst surface, blocking active sites and impairing catalytic efficiency. Additionally, CO<sub>2</sub> reacts with hydroxide ions to form carbonate species, reducing the local concentration of hydroxide ions and subsequently lowering the ionic conductivity of the membrane. Several authors[298,299] highlighted the impact of sulfate ions on metal-based catalysts, showing a dramatic decrease in OER activity, while [300–303] documented the negative influence of carbonate formation on the overall ionic transport.

### **Mechanical Degradation Due to Precipitation**

Hard water impurities, especially calcium (Ca<sup>2+</sup>) and magnesium (Mg<sup>2+</sup>) ions, can precipitate as insoluble hydroxides or carbonates within the membrane structure. These precipitates block membrane pores, increasing ionic resistance and inducing mechanical stress. Over time, these stresses can lead to membrane cracking or rupture. Shahid et al[304] observed that calcium carbonate deposits within AEMs not only reduced cell efficiency but also caused irreversible mechanical damage, emphasizing the importance of water quality management.

### **Gas Diffusion Layer Fouling**

The gas diffusion layers, essential for effective gas transport, are also affected by contaminants. Organic substances and heavy metals can adsorb onto GDL surfaces, altering their wettability and structural properties. This fouling increases polarization resistance and disrupts uniform catalyst utilization. Miller et al[305]. reported significant performance losses in AEM electrolyzers due to organic contamination in GDLs, which led to uneven gas distribution and heightened energy losses.

### **Mitigating Contamination Effects**

To address these challenges, multiple mitigation strategies have been explored. The use of high-purity deionized water minimizes the introduction of metal ions and organic impurities. Pre-treatment systems, such as ion-exchange filters and CO<sub>2</sub> scrubbers, are effective in reducing contaminant loads. Material innovation also plays a role; researchers are developing chemically robust QA groups and

GA No. 101137802

alternative functional groups to resist degradation. Periodic cleaning protocols, including acid/base flushing, help dissolve precipitates and restore membrane performance. These approaches, combined with vigilant operational monitoring, are essential for maintaining the longevity and efficiency of AEMEL systems.

### 2.5.3 PEMEL

PEMEL rely on a pure DI water supply. Cationic contaminants majorly impact the conductivity of the ionomer and membrane as discussed earlier. Upon cation exchange, protons from the PFSA can recombine with the anionic partner of the impurity and can therefore decrease the pH of the water leaving the cell[306], which can further trigger corrosion of BOP components. At the same time, cations drawn to the cathode can lower the proton activity there, which was discussed in some studies to lead to an alkaline HER mechanism, releasing hydroxide ions[210,307] that could also lead to corrosion effects at the cathode. It should be noted here that even simple cationic contamination of the PFSA will not just lead to an increase in Ohmic resistance but can also change the ECSA due to loss of ionically well-connected active sites of both electrodes.

Due to the low potential of the cathode and high potential at the anode, cationic impurities as transition metals can deposit on the catalyst, leading to additional kinetic losses. Due to the shift in pH upon proton exchange by such ions, deposits can form in various structures, which further hinders coherent predictions of deposit severity[308].

One special type of cationic contaminant is ion that are known to catalyse radical formation out of chemically formed hydrogen peroxide, as  $\text{Fe}^{2+}$ . Those radicals can chemically decompose the ionomer phase as discussed earlier.

Anionic contaminants on the other hand are expected to decrease the catalytic activity of the PGM catalysts due to competing adsorption with the net reaction intermediates. Whether such a competing mechanism is actually decreasing the OER or HER conversion rate depends on the exact anion in question. Net electrochemical conversion of halogen ions, i.e., the chlorine evolution reaction upon Cl-contamination of the feed water are expected to occur at high anodic potentials[309]. Adsorption of halides on the cathode can further enhance hydrogen peroxide production[310,311], which is the source for radicals decomposing the ionomer and membrane (see chapter 2.2)[312]. Anionic impurities play a special role in the stability of the titanium based porous transport layer and bipolar plates as discussed earlier.

Other impurities as organic compounds dragged into the stack in the feed water are expected to be oxidized at the anode due to the high potentials necessary for the OER. Oxidation products of such contaminants might further impact the catalytic activity of the Ir-based anode catalyst. They could also aggravate PGM dissolution, though the exact mechanisms and severities will largely depend on the impurity type, which has not been studied yet to the best of our knowledge.

A special attention might have to be place on the production of CO and CO<sub>2</sub> at the anode upon organic impurity oxidation. If sufficient amount of CO/CO<sub>2</sub> were to cross over to the cathode, the strong adsorption as CO<sub>ads</sub> on the platinum-based catalyst at the low operation voltages, the ECSA available for the HER will be significantly reduced[313].

In general, we distinguish between two types of contaminants based on their origin; endogenous impurities and exogenous impurities.

#### Source of Contaminants:

D2.1 – < Degradation phenomena compendium > (PU)

- **Endogenous Impurities:** Contaminants such as  $\text{Fe}^{3+}$ ,  $\text{Cu}^{2+}$ , and  $\text{Ti}^{2+}$  are released from within the system and can be traced to the corrosion of system components like the porous transport layers (PTLs), the bipolar plates (BPPs), and/or other auxiliary, balance-of-plant equipment. These impurities are released due to the harsh acidic conditions and high operating potentials of the system and act as inherent system contaminants[112,217,275,276].
- **Exogenous Impurities:** Trace ions like  $\text{Na}^+$ ,  $\text{Ca}^{2+}$ ,  $\text{Cl}^-$  can accumulate in the system over time. These contaminants originate from external sources, including insufficiently purified feedwater and water recirculation loops, and residues left on auxiliary component during manufacturing and assembly. These ions disrupt system efficiency by triggering unwanted, localized electrochemical reactions and chemical degradation pathways, leading to gradual deterioration of performance-critical components and overall system efficiency[112,114,125].

### Impact on Catalyst Layers:

- **Active Site Poisoning:** Sulfur and chloride ions adsorb onto catalyst surfaces, forming stable complexes that inhibit effective reaction activity. In particular, deterioration of sulfur-based PEM components such as gaskets, seals, etc., can lead to the formation of sulfur-platinum complexes at the cathode, which poison active catalytic sites for the hydrogen evolution reaction (HER). Degradation of the cathodic catalyst has been observed to be irreversible below 0.9 V, reducing catalytic activity and leading to long-term performance decline[112,114,125].
- **Metal Ion Deposition:** Metal ions (e.g.,  $\text{Fe}^{2+}$ ,  $\text{Ti}^{2+}$ ), released from PTL or BPP corrosion, deposit on catalyst surfaces, physically blocking active sites and interfering with effective mass and charge transport steps key to HER and OER. This leads to catalyst surface fouling and diminished electrochemical performance over time[112,114,124].
- **Oxidation of Organics (1):** Other impurities such as organic compounds dragged into the stack in the feed water are expected to be oxidized at the anode due to the high potentials necessary for the OER. Oxidation products of such contaminants might further impact the catalytic activity of the Ir-based anode catalyst. They could also aggravate PGM dissolution, though the exact mechanisms and severities will largely depend on the impurity type, which has not been studied yet to the best of our knowledge.
- **Oxidation of Organics (2):** A special attention might have to be placed on the production of CO and  $\text{CO}_2$  at the anode upon organic impurity oxidation. If sufficient amount of CO/ $\text{CO}_2$  were to cross over to the cathode, the strong adsorption as COads on the platinum based catalyst at the low operation voltages, the ECSA available for the HER will be significantly reduced [313].
- **Kinetic Losses & Deposits:** Due to the low potential of the cathode and high potential at the anode, cationic impurities such as transition metals can deposit on the catalyst, leading to additional kinetic losses. Due to the shift in pH upon proton exchange by such ions, deposits can form in various structures, which further hinders coherent predictions of deposit severity [210].
- **Anionic Contaminants:** These are expected to decrease the catalytic activity of the PGM catalysts due to competing adsorption with the net reaction intermediates. Whether such a competing mechanism is actually decreasing the OER or HER conversion rate depends on the exact anion in question. Net electrochemical conversion of halogen ions, i.e., the chlorine evolution reaction upon  $\text{Cl}^-$  contamination of the feed water are expected to occur at high anodic potentials[309].
- **Adsorption of halides on the cathode** can further enhance hydrogen peroxide production[310,311], which is the source for radicals decomposing the ionomer and membrane (see chapter 2.2)[128].

### Impact on the Membrane and Ionomer:

- **Chemical Attack via ROS:** The presence of iron and copper ion contaminants catalyzes Fenton-like reactions, contributing to the formation of reactive oxygen species (ROS) like hydroxyl radicals (OH•) that attack the PFSA structure of the membrane (as addressed in Section 2.2). ROS damage the polymer backbone of the membrane structure, releasing fluoride species in the process – an indicator of membrane degradation. Elevated temperatures can accelerate this process, doubling the fluoride release rate (FRR) with every 10°C increase observed[111,112,125,129]. Membrane thinning, structural failure and increased gas crossover can all be tied to this degradation pathway.
- **Cationic Ionomer Contamination:** Cations such as Na<sup>+</sup> and Ca<sup>2+</sup> (common tap water impurities) exchange with Brønsted acid sites in the ionomer and, in the process, deactivate these proton-conducting sites, thereby, decreasing the ionomer's ability to support the Grotthuss mechanism. These ions become lodged in the ionomer and accumulate over time, forming water-cation-complexes, which affect the membrane's characteristics, increasing its charge transfer resistance, disrupting its ability to absorb water, and diminishing overall system efficiency[112,129]. Padgett et al. demonstrated that these cation contaminants can be removed again upon subsequent rinsing cycles using clean DI water supply. This makes the use of a pure DI water supply imperative for long-term PEMEL operation[210].
- **Secondary effects of Cationic Ionomer Contamination:** Upon cation exchange, protons from the PFSA can recombine with the anionic partner of the impurity and can therefore decrease the pH of the water leaving the cell[307], which can further trigger corrosion of BOP components. At the same time, cations drawn to the cathode can lower the proton activity there, which, as discussed in some studies, lead to an alkaline HER mechanism, releasing hydroxide ions[307] that could also lead to corrosion effects at the cathode. It should be noted here that even simple cationic contamination of the PFSA will not just lead to an increase in Ohmic resistance but can also change the ECSA due to loss of ionically well connected active sites of both electrodes.
- **Transition Metal Cations:** Contaminants like Fe<sup>3+</sup> are known to lead to irreversible ionomer and PEM degradation, i.e., rinsing cycles are only able to recover a small portion of the original PEM conductivity. Such contaminations commonly originate from corrosion processes, but they could also form in the cell upon contamination with debris (and subsequent "in-situ" corrosion caused by the environment at the anode) from pumps or e.g. scratched passive BOP components. Impacts on proton conductivity of cations has been observed for contamination levels of the feedwater of <10 ppm [211].

### Impact on PTLs and BPPs:

- **Pitting Corrosion & Dissolution of Protective Layers:** Chloride and fluoride ions from impurities in water sources or ionomer degradation corrode PTL and BPP materials by destabilizing and dissolving protective passive layers (see Section 2.4). This exposes the base material, creating localized sites for electrochemical reactions. At these sites, contaminant ions promote pitting corrosion, where confined, ion-rich environments within the pits accelerate material dissolution and cause the pits to deepen over time. The resulting roughened surfaces increase interfacial contact resistances (ICR) and disrupt current distribution. Over time, the materials become weakened and more susceptible to mechanical failure under operational stresses. Low pH and high temperatures further exacerbate these effects[112,125,275,276]
- **Anionic impurities play a special role in the stability of the titanium based porous transport layer and bipolar plates** (see earlier Sections on PTL and BPP).

- Corrosion of the PTL will be aggravated by anionic contaminants in the water such as fluoride ions, which can be formed upon membrane and ionomer decomposition via hydroxyl radicals.

## 2.5.4 SOEL

In section 2.3.4, we thoroughly analysed potential contaminants that may arise during SOEL operation. These contaminants were discussed in the second chapter as they play a critical role in the degradation mechanisms of our electrodes, directly influencing their performance and long-term stability. Understanding their effects is essential for developing strategies to mitigate degradation and enhance the overall durability of the system.

## 2.5.5 PCCEL

As for the solid oxide cells, also the performance and longevity of proton conductive ceramic cells heavily depend on the integrity of their electrodes, which play a critical role in the electrochemical processes. Protonic ceramic fuel or electrolysis cells (PCFC/PCCEL) have not yet been demonstrated in a stack, hence the stack behavior under contaminants has never been investigated yet. The impact of contaminants can be expected by comparison with the behavior of SOEC, as the two technologies share similar materials and operating conditions. As the fuel electrode of proton conductive ceramic cells is made by similar materials as SOCs, the same contaminants, such as chlorine, sulfur, and siloxanes could predominantly affect the fuel electrode, while chromium deposition would remain a potential issue for the air electrode.

### 1) Silica poisoning

Silicon-based impurities could originate from water or glass sealing materials. For SOECs, it is reported that in conditions of high steam partial pressure, SiO<sub>2</sub> accumulates at the interface between the fuel electrode and the electrolyte, and also reacts with Nickel. In PCCELs this type of poisoning is expected to be less relevant than in SOECs, as the fuel electrode is not exposed to steam, but remains in a reducing atmosphere. Silica poisoning could be expected to have an impact on the air electrode where steam is provided, but currently there is no evidence from literature to corroborate this possible degradation mechanism.

### 2) Chlorine and Sulfur poisoning

The presence of chlorine and sulfur could occur in the case of co-electrolysis. Due to proton-conducting electrolyte of PCCEL, co-electrolysis is possible only if CO<sub>2</sub> is provided to the fuel electrode, while H<sub>2</sub>O at the air electrode. Moreover, the co-electrolysis requires a mixed proton-oxygen conduction in the electrolyte, to allow the co-ionic movement of charges (i.e. protons to fuel electrode and oxygen to air electrode). This type of process is in an early stage of investigation in the EU project ECOLEFINS (<https://ecolefinsproject.eu/>). Alternatively to co-electrolysis, in the work of Danilov et al. CO<sub>2</sub> is sent to the fuel electrode to reduce the hydrogen partial pressure, promoting the overall hydrogen production in a protonic cell[314].

In the case contaminated streams of CO<sub>2</sub> are sent to the fuel electrode (for co-electrolysis or alternative applications), the chlorine and sulfur poisoning mechanisms could be similar to those reported for Ni-based electrodes of SOECs (readers are referred to SOEC section). However, no evidence from literature has been reported in PCCEL, to the authors' knowledge.

### 3) Chromium poisoning

Chromium poisoning is primarily due to the evaporation of chromium species from Fe-Cr alloy interconnects. The presence of steam in the air accelerates chromium volatilization and subsequent

deposition onto the air electrode. The mechanism of chromium poisoning has been presented in the section dedicated to SOE. In PCCEL operation it is expected that the operating conditions of the air electrode could be favorable for chromium poisoning. Readers are referred to the section dedicated to interconnect degradation of PCCEL for the discussion of the literature.

## 2.6 Degradation mechanisms related to electrolyte variables: including composition, concentration and flow configuration

### 2.6.1 AEL

The concentration, composition, conductivity, compatibility with chosen catalysts, cost etc of electrolyte are vital for efficient functioning of electrolysers, as corrosive nature of electrolyte accounts to the events such as metal dissolution, pH variation etc can degrade the electrolyser components. Electrolyte with a concentration of about 40 wt% KOH are employed for the experimentation and corrosivity of electrolyte will be in one of the main challenges in AELs.

Overall, employing the electrolyte subject to the components employed in the electrolyser would be subject to components, wherein the researchers or engineers has to play a key role in understanding and customizing them subject to the need.

#### a. Composition and concentration

Electrolyte composition is vital as variation can cause degradation of components, especially during long term applications. Variation to composition and concentration are expected when subject to prolonged experimental conditions can lead to multiple other events such as, corrosion, dissolution, leaching etc. Also, impurities in electrolyte can also alter the electrolyser functioning and is well detailed in the above section (Section 2.5, A). Variation of pH can influence the electrolyte make them corrosive in nature. In a study by Manabe et al., durability of Ni base electrode was evaluated against the pH of solution employed[294]. The experiments were conducted in room temperature at different pH levels with electrolyte constituting pure water, 2 wt% and 30 wt% NaOH and the rest potential measurements were conducted to assess electrochemical stability. The Pourbaix's pH-potential diagram confirmed that the Ni dissolves differently based on the solution's pH level. Thus, pH plays a vital role in AEL and, the experiments concluded that maintaining the electrolyte in alkaline conditions would be ideal for enhanced durability, when compared to acidic or neutral medium. In another study, Man et al., chemical stability of martensitic AM355 stainless steel in a chloride-containing electrolyte was conducted using the Fe-Cr-H<sub>2</sub>O Pourbaix diagram[315]. The results revealed the catalysts are not ideal for use in acidic or basic pH levels due to its inability to retain the passive surface layer, which is crucial for corrosion resistance. Meanwhile, in another study, on investigating cathodic reactions on SS304L in high pH environments within a pH range of 13.6 to 16.5, (referencing Pourbaix diagrams)[316]. Observations were made that at pH levels below 16.5, the oxygen reduction reaction predominates at the cathode while at pH 16.5, oxide reduction becomes the primary mechanism responsible for cathodic corrosion. In another report in Al-Zn alloy, cathodic polarization at pH at 10.1 resulted in the Al leaching resulting in catalyst modification[317]. Thus, variation to electrolyte pH can aid in degradation of associated components. With KOH and NaOH being common **electrolytes** employed for AEL,[173,318] the former is mainly used accounting to its high ionic conductivity and corrosion to resistance.

Researchers have also focused in evaluating other electrolytes such as LiOH and Ba(OH)<sub>2</sub>[173,319]. Concentration also plays a vital role in the AEL; as the elevated concentration of ion such as OH<sup>-</sup>, facilitate faster electrochemical reaction at electrode surface and thereby aid in higher hydrogen production. Employment of high concentration electrolyte solution can also aid a decline in cell voltage, increased solution resistance inhibiting the smooth flows of ions and electrons, evaporation concerns etc. Thus, the researchers have found the technical advantage of using dil. KOH solutions (20 to 30 wt%), accounting to its low **corrosive** nature over conc 40 wt% KOH. The coming of gel electrolytes in AEL has also showcased some interesting results[178]. Saline electrolyte are known to cause severe corrosion and is detailed well in the above section (**Section 2.5**). Several material and strategies have been suggested in order to mitigate the degradation associated with the electrolyte[71]. For instance, maintain the composition of electrolyte is crucial to confirm the variations as part of experimentation are from actual tested variable and not due to deviation in electrolyte composition. Use of same electrolyte salt from supplier are recommended, as purity could vary between suppliers and could affect the analysis. Anodized 3D printed martensitic steel abbreviated as AerMet100; delivered some interesting observation as well. This bifunctional electrocatalyst showed high HER and OER activity along with long term stability at high current density and low corrosion rate. 3D printing and anodization are the preparatory method employed in the fabrication of catalysts with conditions such as 3.5 wt% NaCl, 800 mA cm<sup>-2</sup>, 3 min. The catalyst showed a corrosion layer thickness of 33.94-29.03 μm (HER catalyst) and 32.83-29.03 μm (OER catalyst) after the overall water splitting for 140 h at 570 mA cm<sup>-2</sup>. Overall, low corrosion rate for both HER and OER at high current density confirm its excellent stability of catalyst. Other corrosion resistant materials are carbon steel, alloy 400, 800, passivated Ni, PTFE, PFA, PPS and nickel-based catalysts with passivation layer, etc.

b. **Flow configuration**

Induced electrolyte flow could be considered as an effective method for the consistent supply of reactants at the electrode surface. Further, it helps in eliminating gas bubbles, and increasing reaction rates. The optimal flow rate depends on electrode dimensions, electrolyte composition, and applied current density. Thus, only very indirectly influence on the degradation and stability can be drawn. In an interesting study by Emam et al.,[320] effect of two different induced flow configuration was evaluated :

1. Configuration-x: flows from anode to cathode, aligning with the water-splitting process;
2. Configuration-z: directs flow to sweep hydrogen bubbles from the cathode surface.

The Configuration-z effectively was shown to drives hydrogen bubbles upward, enhancing overall cell efficiency making it slightly crucial over another configuration. The flow rate of water in AEL is reported to be 0.5–5 L/min and the optimum found to be in the order of 2–3 L/min[173].

## 2.6.2 AEMEL

There is significant motivation to reduce the concentration of the electrolyte since shunt currents (electrical shorts)[175] develop within an electrolyser stack, requiring careful optimization of the flow channels and manifolds to increase electrical resistances without introducing other losses, such as increased energy for pumping, into the BOP[176].



### 2.6.3 PEMEL

PEMEL generally run on pure DI water supply. With contaminations having been discussed in the preceding chapter, the only remaining “electrolyte” variable is the flow configuration. Depending on the cell or stack design, the flow configuration could impact the temperature distribution and therefore increase local degradation phenomena, which are generally temperature dependent. Scientific data trying to understand such influences on PEMEL remain limited and this is an area of ongoing research.

#### Flow configuration

The flow-field plate is a vital component in the function of the electrolyzer: i) It supplies the electrolyte to the active sites of the MEA, removes the produced gases, distributes the applied current and provides structural support for the MEA[321]. At the anode, the water flows from the channel in the flow-field plate through the PTL to the core electrode by diffusion and convective transfer.

Increasing operational current density ( $>2 \text{ A cm}^{-2}$ ) of PEMEL could result in severe mass transport issues, as the increased gas production forms a veil reducing water access to the electrocatalyst surface of the MEA. Therefore, the shape and dimension of the channels in the flow-field plate become crucial. Unoptimized design of the flow-field could result in mass transport hindrance, and therefore, degrades performance. Thus, well-designed and optimized flow-field plates are required for efficient and cost-effective PEMEL stacks, especially at high current densities.

Dedigama et al. studied the influence of a wide range for the channels depth and observed a negligible effect of the different depths at low operational currents ( $< 1 \text{ A cm}^{-2}$ )[322]. They report that at higher current densities ( $> 1 \text{ A cm}^{-2}$ ), an impact on the cell efficiency within different depths was observed, which was attributed to the opposing impact of flow velocity and mass transfer characteristics. Although, a point to highlight is how the different flow channel conditions may lead to physical degradation on the PEMEL, creating high hydraulic pressure originated from an excessive flow rate of circulating water that further may cause catalyst leaching, mechanical stressing on the membrane[323]. The inhomogeneous water distribution inside the flow channel of bipolar plates, causes inhomogeneous distribution of electric current that, in turn, may generate hot spots and membrane swelling[324,325].

### 2.6.4 SOEL

Refer to 2.3.4.

### 2.6.5 PCCEL

#### *Impact of Humidification*

Humidification has an impact both on the electrolyte conductivity of PCCEL and on degradation. In general, the increase in water partial pressure decreases electrolyte conductivity mechanisms. For example, the measured protonic, oxygen ionic, and electron- hole transport numbers of a typical BZCY72 proton conductor are dependent on  $p\text{O}_2$  and  $p\text{H}_2\text{O}$  at intermediate temperature (600 and 700°C)[158]. The protonic conductivity is dominant under higher humid and lower oxygen partial pressure conditions at the lower temperature, while the oxygen ion conductivity under the dry and

GA No. 101137802

reducing conditions, and the hole conductivity under the conditions of a dry and oxidizing atmosphere at a higher temperature.

Su and Hu[228] reviewed various experiments examining the effects of steam concentration supplied to the air electrode at a laboratory scale, with investigations spanning a range of 3% to 50%. In general, elevated water partial pressures accelerate material degradation and promote microstructural changes. For electrolytes or air electrodes containing alkaline-earth elements, the presence of water vapor can significantly influence strain effects and chemical expansion due to variations in water vapor partial pressure.

Additionally, water vapor can catalyze the breakdown of perovskite oxides into base oxides, increase the formation of surface hydroxides, and enhance impurity mobility[326]. As a result, PCCEs operating under highly humidified conditions exhibit accelerated degradation rates[154,163].

For instance, air electrodes such as PBSCF and  $\text{NdBa}_{0.5}\text{Sr}_{0.5}\text{Co}_{1.5}\text{Fe}_{0.5}\text{O}_{5+\delta}$  demonstrated stable polarization resistance when exposed to 20%  $\text{H}_2\text{O}$ -humidified air under cyclic currents ( $\pm 1 \text{ A cm}^{-2}$  for 36 hours per cycle). However, a significant increase in polarization resistance was observed at 30%  $\text{H}_2\text{O}$ , attributed to intensified Ba and Sr segregation under higher  $\text{H}_2\text{O}$  concentrations[163].

#### *Impact of Oxygen Partial Pressure*

The oxygen partial pressure ( $p\text{O}_2$ ) plays a critical role in influencing reaction kinetics, chemical stability, and the ionic and electronic conductivities of air electrode and electrolyte materials. At the triple-phase boundary (TPB), higher  $p\text{O}_2$  levels hinder proton or oxygen ion transport but increase hole concentration due to parasitic oxidation reactions[228]. Under oxidizing conditions, this p-type electronic conductivity contributes to the electronic leakage of proton-conducting electrolytes, thereby reducing the Faradaic efficiency of PCCEs[154].

Recent findings indicate that Ce-rich BZCYb1711 exhibits a significantly lower electronic charge carrier transference number compared to BZY20, as the former promotes hydration reactions and mitigates parasitic oxidation[327,328]. Changes in  $p\text{O}_2$  can also induce chemical strain in many air electrode materials, such as BCFZY and PBSCF, leading to dimensional shrinkage or expansion[158]. The resulting mechanical stress can cause delamination at the electrode/electrolyte interface, ultimately compromising the stability of PCCEs.

## 2.7 Summary of all technologies

Technology	Catalyst layer degradation	Separator, Membranes, and Ionomers degradation	Porous Transport Layer degradation	Bipolar or Monopolar Plates degradation	Components degradation Due to Contaminants	Degradation due to Electrolyte Variables including composition, concentration and flow configuration
<b>AEL</b>	Corrosion, Dissolution, Deactivation, Passivation, Surface Reconstruction. Mechanical Wear: Gas bubble dynamics and stress cause structural degradation	Thermal and Chemical Degradation, Mechanical Stress and Gas Crossover, Leaching of zirconia particles (for Zirfon components)	Corrosion, structural changes under alkaline conditions	Hydrogen Embrittlement and Corrosion, Reverse Current Effects	Electrolyte and water impurities (Cationic Impurities, Anionic Impurities), Catalyst Poisoning, Corrosion-Induced Degradation, Precipitation and Clogging, Radical Formation	Corrosion and leaching, pH-induced degradation, High concentration effects, Gas bubble accumulation, Saline electrolyte corrosion
Relevance in terms of literature /papers	+++	++	++	+	++	++
<b>AEMEL</b>	Dissolution, Agglomeration, Delamination, Poison of Actives sites.	Chemical Degradation: Hofmann Elimination, Hydrolytic Cleavage, cationic Group Oxidation. Mechanical Degradation: Swelling and Dimensional Changes, Adhesion Failure. Thermal Degradation: AEI degradation under OER conditions	Mechanical Degradation, Gas Bubble-Related Degradation, Corrosion, Surface Property Degradation	Corrosion, Passivation Layer Formation, Mechanical Degradation, Hydrogen Embrittlement, Chemical Instability, Contaminant Deposition, Thermal and Electrochemical Stresses	Chemical Instabilities of Membranes and Ionomers, Catalyst Poisoning, Mechanical Degradation Due to Precipitation, Gas Diffusion Layer (GDL) Fouling	Membrane: Hotspots and localized thinning; Electrode: Catalyst degradation; Gaskets: Deformation and leaks; Manifolds: Wear at stress points
Relevance in terms of literature /papers	+++	+++	++	+	++	++
<b>PEMEL</b>	Dissolution, Phase Transformation, Agglomeration, Support Degradation, Poison of Actives sites.	Membrane: Mechanical and Chemical Degradation, Ionic Contamination; Ionomer: Mechanical and Chemical Degradation	Corrosion (Ti and carbon GDL), Oxide Layer Growth	Corrosion, Passivation, Slower Degradation Compared to PTLs	Cationic: Ion Exchange, Radical Formation; Anionic: Competing Adsorption; Organic: Oxidation Effects	Membrane: Localized thinning and cracking; Catalyst: Uneven distribution; Bipolar Plates: Mechanical stress; Seals: Loss of integrity
Relevance in terms of literature /papers	+++	+++	++	+	++	+++
<b>SOEL</b>	Ni Reoxidation, Agglomeration, Sintering	Structural Degradation, Thermal Expansion Mismatch, Oxygen Clustering	PTL weakening due to high temperatures	High-Temperature Oxidation, Coating Degradation, Chromium Evaporation	Silica, Chlorine, Sulfur: Deposition and structural changes; Chromium Oxide Formation	Steam flow rate and partial pressure critical
Relevance in terms of literature /papers	+++	+++	+	++	++	++
<b>PCCCL</b>	Agglomeration, sintering	High temperature and chemical stability challenges	Porosity and flow-related degradation	Compatibility with ceramic-based systems	Limited data on specific contaminants	Stability under thermal and chemical conditions
Relevance in terms of literature /papers	+++	+++	+	-	-	++

Table 3. Summary of all technologies

Summary of all technologies analysis employs a symbolic rating system to indicate the relative significance or impact of each operational mode or degradation factor on electrolyser performance and reliability. The symbols are defined as follows:

- **+++**: Represents a high impact, indicating a critical influence on performance or reliability.
- **++**: Denotes a moderate impact, where the factor has a significant but not dominant effect.
- **+**: Indicates a low impact, with minor effects on performance or reliability.
- **-**: Reflects minimal or negligible impact, with little to no observable effect.
- **0**: Signifies no observable impact or relevance under typical operational conditions.

### 3 Relation between Operational Modes and Degradation

The operational modes of electrolyser, and in general the degradation factors (including also operating conditions and external/manufacturing/BoP factors), depending on their frequency and intensity, will activate specific degradation mechanisms (chemical, physical/mechanical), and will result in degradation effects, related to electrolyser performance, reliability and safety.

A scheme of main degradation factors, mechanisms and effects is provided in Figure 10. The scheme provides a structured representation of the degradation process in electrolysis technologies, showing the interconnection between degradation factors, degradation mechanisms, and their ultimate effects on electrolyser operation.

The top section (degradation factors, yellow box) outlines the primary stressors and conditions that initiate degradation in electrolysers. These factors are categorized into operational modes, operating conditions/parameters, and external/manufacturing/ BoP influences, which serve as precursors to degradation mechanisms.

The middle section (degradation mechanisms, green box) identifies how the stressors translate into specific degradation mechanisms that affect the electrolyser’s components. Each mechanism stems from one or more factors and results in tangible changes in the material properties of critical parts like bipolar plates, porous transport layers, membranes, separators, interconnectors, ionomers, catalysts, or electrodes.

The bottom section (degradation effects, red box) illustrates the real-world consequences of these degradation mechanisms. It connects the microscopic changes occurring at the component level to broader impacts on the system's safety, performance, reliability, and economic viability.

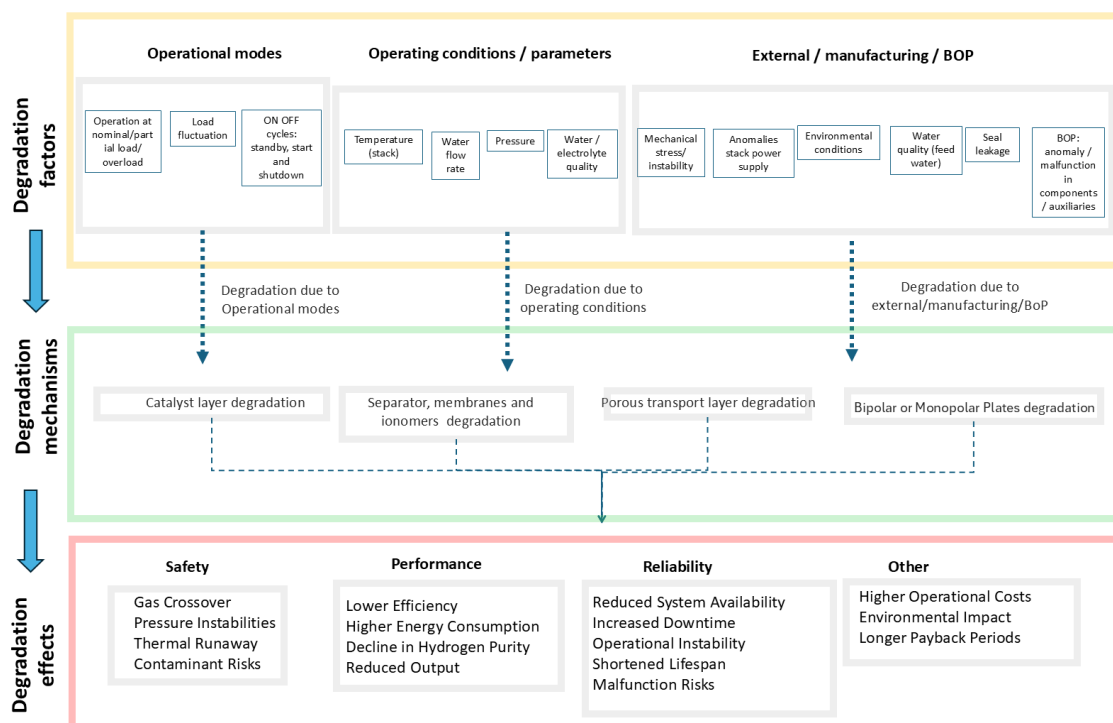


Figure 10. Degradation factors, degradation mechanisms and degradation effects

GA No. 101137802

Each electrolyser type has unique operational vulnerabilities that affect its efficiency and lifespan, particularly when exposed to the dynamic power fluctuations typical of renewable energy sources. In AEL, steady, continuous operation is preferred to minimize electrode passivation and resistive losses caused by exposure to caustic electrolytes and high temperatures. In contrast, AEMEL systems are especially sensitive to chemical degradation of their anion exchange membranes, with high temperatures and fluctuating load conditions accelerating structural weakening and reducing ion conductivity. PEMEL systems face degradation from both membrane thinning and catalyst layer deactivation under high-frequency cycling and elevated temperatures, which amplify membrane and ionomer wear.

For high-temperature electrolysis, SOEL systems present distinct challenges. These systems are susceptible to thermal stress due to frequent temperature fluctuations, which can lead to mechanical cracking of ceramic components, delamination of electrode layers, and degradation of electrolyte materials. Furthermore, impurities in the feed gas and dynamic load conditions can exacerbate the reduction-oxidation (redox) cycling, resulting in electrode performance loss and increased maintenance requirements.

In PCCEL systems, which operate with proton-conducting ceramic electrolytes, the primary vulnerabilities are related to protonic defect mobility and material stability under variable humidity and temperature conditions. PCCEL systems are particularly sensitive to changes in operational humidity levels, which can compromise proton conductivity and cause structural fatigue in ceramic layers. Additionally, exposure to contaminants such as CO<sub>2</sub> can lead to the formation of undesirable carbonate phases, further reducing efficiency and durability.

These differences underscore the need for optimized operational strategies tailored to the specific degradation mechanisms of each electrolyser type. Such strategies are critical for ensuring improved durability and performance, especially in settings powered by intermittent renewable energy sources. In the following section, we explore the durability of both low- and high-temperature electrolysis by examining key studies in this field. This analysis aims to uncover critical insights and recent advancements that have improved the durability of AEL, AEMEL, PEMEL, SOEL, and PCCEL systems. Emphasis is placed on best practices, innovative materials, and emerging technologies that enhance the operational lifespan of these electrolysers. Key operational factors influencing durability, such as load fluctuation, partial load conditions, and on/off cycling, are discussed to highlight their impacts on system stability. Power quality, along with temperature and pressure conditions, is also addressed, as these variables can accelerate or mitigate degradation processes. Additionally, the roles of water flow rate, shunt currents, and reverse currents are examined to provide a comprehensive understanding of how these aspects influence electrolyser durability and performance under real-world conditions.

Key operational modes impacting durability across these electrolyser types include[329]: operational modes, operating conditions/parameters and external/manufacturing/BoP. The durability of electrolysers is influenced by a complex interplay of factors, categorized into operational modes, operating conditions/parameters, and external/manufacturing/Balance of Plant (BoP) considerations. Each category addresses distinct aspects of system behavior and external influences, collectively determining the longevity and reliability of the technology.

- **Operational modes/Partial Load Operation:**
  - Hydrogen production at **nominal load**: Operating at the design load where the system achieves optimal efficiency and durability.

- Hydrogen production at **Partial Load/minimum**: Operating at partial loads can introduce imbalances in gas production, potentially leading to inefficiencies and localized degradation over time.
- Hydrogen production at **Overload**: Operating above nominal capacity increases stress on the membrane, catalysts, and cell structure, causing accelerated wear, overheating, and a higher risk of mechanical failure.
- **Load Fluctuations**: Regular changes in load can lead to mechanical and chemical stress on the membrane and catalyst layers, affecting the long-term stability of the electrolyser.
- **Start-Stop Cycles (ON OFF)**: Repeated start-stop cycles, especially common in intermittent renewable energy applications, can cause rapid changes in operating conditions, leading to both reversible and irreversible degradation, particularly for catalysts and membrane materials.
- **Reverse Currents**: Reverse Currents: Occurs when voltage polarity reverses, often during power interruptions or imbalances in stack operation. Reverse currents can cause localized overheating, damage ionomer structures, and accelerate membrane degradation. This phenomena can be attributed into External/manufacturing/BoP as well.
- **Emergency shutdown**: Sudden shutdowns can create extreme conditions (thermal, mechanical, and chemical) that increase the risk of permanent damage to the stack and auxiliary components.
- **Hot standby**: The system is maintained at operating temperature without producing hydrogen. While it minimizes thermal cycling, prolonged hot standby can lead to gradual catalyst degradation and gas diffusion issues.
- **Cold standby**: The system is cooled to ambient temperature, reducing energy consumption but increasing the risk of thermal shock and startup-related stress upon resumption.
- **Operating conditions/parameters:**
  - **Temperature**: Consistent operating temperature is critical. Fluctuations can degrade membranes, especially in AEMEL and PEMEL, where ionomer stability is highly sensitive to thermal changes. High-temperature systems (SOEL) and (PCCEL) suffer from thermal cycling-induced stress and cracking
  - **Water Flow Rate**: Uniform water or electrolyte distribution avoids dry spots and ensures cooling. Inconsistent flow leads to hot spots, increasing degradation rates and reducing efficiency.
  - **Pressure**: Hydrogen pressure levels, especially at high operating pressures, affect both membrane durability and electrode stability.
  - **Water / electrolyte quality**: Impurities in water or electrolyte can cause fouling, scaling, or corrosion, reducing membrane conductivity and catalyst effectiveness.
- **External/manufacturing/BoP:**
  - **Mechanical stress/ instability**: Mechanical vibrations or poor stack assembly can lead to uneven stress distribution, causing physical damage to membranes and electrodes over time.
  - **Anomalies stack power supply**: Variations in power quality (e.g., transient spikes or dips) affect voltage stability and increase stress on components.
  - **Shunt Currents**: In multi-cell stacks, shunt currents cause uneven current distribution, localized overheating, and increased ion transport stress on the membrane.
  - **Environmental conditions**: Factors such as ambient temperature, humidity, and contaminants in the surrounding air can affect electrolyser operation, especially in systems with exposed seals or sensitive components.

- **Water quality (feed water):** Water quality is crucial for electrolyser performance and durability. Impurities like ions (e.g., calcium, magnesium, and chloride) can cause scaling, fouling, and corrosion, reducing efficiency and lifespan.
- **Seal leakage:** Leakage in seals can compromise gas separation, leading to cross-contamination and reduced efficiency, as well as potential safety hazards.
- **BoP:** anomaly / malfunction in components / auxiliaries: Malfunctions in auxiliary systems (e.g., pumps, compressors, heat exchangers, piping) can disrupt water flow, cooling, or pressure control, indirectly accelerating stack degradation.

## 3.1 Load Fluctuation

### 3.1.1 AEL

The study by Senan F. Amireh et al. [330] investigates the impact of power supply fluctuations and partial-load operations on the efficiency of alkaline water electrolysis (AEL) systems, particularly when powered by variable renewable energy sources. The researchers combined a six-pulse thyristor rectifier model with a dynamic electrolysis model to simulate the effects of residual current ripples on system efficiency. Their findings indicate that, without filtering, efficiency losses range from 1.2–2.5% at full load to 5.6–10.6% at 20% load. Implementing an optimized L-filter significantly reduces these losses, limiting ripple-induced efficiency drops to 0.5–0.8% at full load and 0.8–1.2% at low loads. This research highlights the challenges that thyristor-based rectifiers face in maintaining efficiency during partial-load operations, which are common in renewable energy applications. While thyristor rectifiers are cost-effective, their inefficiencies under fluctuating loads suggest that transistor-based rectifiers, which inherently produce fewer ripples, may be more suitable for dynamic operations despite their higher costs.

The study by S. Hu et al. [331] focuses on optimizing the load range and electrolysis efficiency of a 250-kW AEL system under high-dynamic operation conditions, such as those driven by wind or photovoltaic (PV) power. The authors develop a synergistic regulation strategy, adjusting pressure and lye flow rate to balance hydrogen-to-oxygen impurity content (HTO) and electrolysis efficiency. At high loads, the system maximizes pressure and lye flow to ensure efficiency, while at low loads, it minimizes these parameters to broaden the operational range safely. Key findings reveal that this strategy extends the minimum load boundary significantly, from 42.0% in traditional setups to 15.6%, without compromising safety. In dynamic power scenarios, wind and PV energy utilization reached up to 98.3% and 95.6%, respectively, with the system maintaining high electrolysis efficiency. This approach demonstrates the feasibility of AEL systems in fluctuating renewable energy environments, providing a model for enhancing efficiency and safety in large-scale hydrogen production directly coupled with renewable sources.

The study by L. Cammann et al. [332] examines the optimal design and operational strategies for an AEL plant powered by wind energy, focusing on maximizing hydrogen production efficiency. Using a detailed mathematical model, the authors evaluate different configurations within the plant's Balance of Plant (BoP), analysing factors like pressurization, heat exchanger size, and independent power supplies for each electrolyser stack. By modelling gas purity and temperature constraints, they identify the operational boundaries for safety and efficiency under varying wind power inputs.

Key findings indicate that flexible pressure operation and individual power supplies improve operational flexibility and efficiency, allowing the plant to operate safely at a lower load range, with production increases of up to 9% for degraded plants and 4.5% for novel configurations. The study

GA No. 101137802

concludes that, while flexible pressure and independent power supplies offer the most production gains, the best design depends on specific power availability and cost constraints in wind-powered hydrogen production scenarios.

The study by D. Huang et al.[333] explores a size design strategy for scaling up AEL stacks integrated with renewable energy sources. The research focuses on the effects of bubble coverage and shunt currents that occur when electrode areas are expanded, or additional electrodes are added in larger AEL systems. A multiphysics model was developed to describe the electrochemical and two-phase flow processes in an industrial AEL stack, validated with an experimental error within 4% for current-voltage predictions. The study finds that using smaller cell designs in an on-grid system can boost hydrogen production rates by over 6%, promoting a trend towards miniaturized cell areas. Off-grid systems show that hydrogen production can vary by more than 4% across different stack designs due to load distribution.

This approach suggests that AEL systems require specific optimizations to handle renewable power fluctuations, with strategic design adjustments enhancing both hydrogen output and efficiency. The model provides a basis for optimizing stack configurations in green hydrogen production facilities connected to renewable sources.

The study by S.Ding et al[334]. investigates a multi-power-level configuration scheme and scheduling strategy for a multi-stack alkaline water electrolysis (AEL) system connected to off-grid wind power. The research leverages mixed integer linear programming (MILP) to optimize hydrogen production by configuring electrolysers of different power levels. The study compares several configurations, finding that a mixed configuration ( $2 \times 5$  MW and  $2 \times 2.5$  MW) delivers the highest income and improved operational flexibility, with a minimum load set to 3.33% of the rated capacity. This approach distributes the load across low-power electrolysers to handle fluctuating power, reducing maintenance costs and prolonging equipment life, as high-power electrolysers remain in more stable states.

This configuration improves income by up to 6.8% over single-power schemes, making the multi-stack AEL system a more efficient and flexible solution for renewable hydrogen production.

### 3.1.2 AEMEL

The study by M. Ranz et al[335], investigates the dynamics of loss mechanisms in anion exchange membrane electrolysis (AEMEL) using advanced methods such as electrochemical impedance spectroscopy (EIS) and distribution of relaxation times (DRT) analysis. This research reveals detailed insights into AEMEL behaviour, identifying five primary loss mechanisms, including the hydrogen and oxygen evolution reactions and ionic transport losses within the catalyst layers. Through EIS and DRT analysis, the study correlates specific frequencies with each loss mechanism, aiding in pinpointing the physicochemical origins of inefficiencies.

Notably, the study identifies the membrane and ionomer as the components most prone to degradation. Exposed to alkaline media, these materials undergo structural and chemical stresses, leading to diminished ion conductivity and water diffusivity, which impact the overall efficiency and lifespan of the electrolysis cell. These findings emphasize the importance of enhancing membrane and ionomer stability, thus providing critical insights for improving membrane electrode assemblies and optimizing AEMEL systems for more durable and efficient renewable hydrogen production.



### 3.1.3 PEMEL

The study by Yingyu Ding et al.[336] investigates how fluctuating voltage conditions affects platinum-coated titanium bipolar plates in proton exchange membrane electrolysis (PEMEL). Voltage fluctuations, common with renewable energy sources, impact the efficiency, corrosion resistance, and stability of PEMEL components. Using simulated triangular and square voltage waveforms, the research evaluates the effects of different voltage ranges and fluctuation frequencies on bipolar plates. Results indicate that platinum-coated titanium plates exhibit higher current densities compared to uncoated titanium due to platinum's catalytic effect. The current response varies with waveform type: triangular waves lead to sharp peaks in current density near the water decomposition voltage (1.23 V), while square waves show delayed stabilization, suggesting differing corrosion impacts. Higher triangular wave frequencies reduce current response stability, while square waves mainly impact the range of current response without destabilizing it. Electrochemical impedance spectroscopy (EIS) shows that triangular fluctuations decrease corrosion resistance more than square waves. Lower fluctuation frequencies also reduce resistance, indicating increased corrosion susceptibility. Surface analysis via X-ray photoelectron spectroscopy (XPS) reveals that fluctuating voltage conditions alter the oxidation state of platinum on the bipolar plates. Lower frequencies lead to greater platinum oxidation under square wave conditions, likely due to extended exposure to high potentials. In summary, both waveform and frequency significantly influence the electrochemical stability of platinum-coated titanium bipolar plates in PEMEL. Triangular fluctuations promote corrosion more than square waves, and platinum oxidation varies depending on the waveform and fluctuation frequency. These findings are crucial for improving PEMEL systems integrated with renewable energy, where voltage stability may be inconsistent.

The study by Yanhui Xu et al.[337], explores how fluctuating power from renewable sources impacts proton exchange membrane electrolysis (PEMEL) systems, with a focus on material degradation and efficiency under varied power conditions. The team analyzes typical fluctuation patterns from wind and photovoltaic (PV) sources, simulating conditions that PEMEL systems may experience in real-world applications, such as grid peak shaving and off-grid hydrogen production.

The findings indicate that PEMEL systems experience accelerated degradation of both the membrane and catalyst layers due to power fluctuations. Membrane degradation is primarily driven by mechanical stress and the chemical attack of free radicals, while the catalyst layer deteriorates due to high current densities and frequent potential shifts. Simulations show different degradation behaviors across fluctuating conditions: high-load, low-fluctuation conditions produce moderate membrane wear, whereas high-fluctuation, low-output conditions significantly impact both the membrane and catalyst.

Under PV scenarios, sunny days with consistent power lead to a stable yet gradual decline in PEMEL efficiency, whereas cloudy conditions with high power variability lead to more rapid performance loss, with the catalyst layer especially susceptible. The study suggests that understanding and optimizing operating conditions could extend PEMEL lifespans, crucial for integrating green hydrogen production with renewable sources.

The study by D. Niblett et al.[338] reviews the potential of proton exchange membrane electrolysis (PEMEL) for hydrogen production powered by offshore wind energy, particularly under the fluctuating power conditions typical of this renewable source. The research highlights that fluctuating offshore wind energy can impact PEMEL efficiency, hydrogen purity, and system durability due to frequent load changes, which can accelerate material degradation. The authors compare PEMEL with alkaline and

GA No. 101137802

membraneless electrolyzers, considering factors like cost, scalability, and resilience to the offshore environment.

The study identifies specific challenges for PEMEL, including the high costs of precious metal catalysts like platinum and iridium, which are necessary for high efficiency but can limit scalability. Additionally, PEMEL's rapid response time and high current density make it ideal for integration with variable wind power, although its lifespan can be shorter than alkaline systems due to load-induced degradation of membranes and catalyst layers. This review suggests optimizing PEMEL for offshore wind applications may involve reducing reliance on rare metals, enhancing materials durability, and developing configurations to handle variable loads efficiently.

The study by E.Crespi et al[339]. investigates the performance and flexibility of a 60-kW PEMEL system for dynamic operation under varying loads, reflecting conditions similar to renewable energy inputs. Utilizing both experimental testing and dynamic modelling, the study evaluates the response of PEMEL components to load changes, highlighting key insights on efficiency and durability at partial loads. The research confirms that PEMEL systems maintain stable temperature and pressure under partial load conditions, although specific energy consumption increases significantly as load decreases—from 67 kWh/kg at high loads (1 A/cm<sup>2</sup>) to 140 kWh/kg at low loads (0.3 A/cm<sup>2</sup>). The study proposes improvements like regulating water flow and hydrogen dryer regeneration to lower specific energy consumption, enhancing the system's adaptability to fluctuating renewable energy.

The study by B.Xu et al[340]. evaluates the dynamic behaviour of proton exchange membrane electrolysis (PEMEL) under fluctuating current conditions, which are typical in renewable energy applications. Using a comprehensive three-dimensional multi-physics model, the authors simulate and analyse parameters like mass transfer, fluid flow, temperature, and hydrogen crossover under variable current loads. Findings show that temperature takes approximately 15 seconds to stabilize after a load change, while oxygen concentration and voltage experience transient overshoots. Notably, hydrogen crossover increases sharply when the current density drops, with peak values reaching twice the steady-state concentration. These insights highlight critical behaviours that could inform the optimization of PEMEL systems for renewable integration.

The study by S. Siracusano et al[341]. examines the degradation mechanisms in proton exchange membrane electrolysis (PEMEL) cells under steady-state and load-thermal cycling conditions. Using a 90 μm short-side-chain Aquivion™ membrane with low catalyst loadings (0.4 mg<sub>IrRuOx</sub>/cm<sup>2</sup> at the anode and 0.1 mg<sub>Pt</sub>/cm<sup>2</sup> at the cathode), the study compares performance loss under continuous and dynamic operations at high current density (3 A/cm<sup>2</sup>). Findings reveal that load cycling accelerates catalyst degradation, particularly the loss of ruthenium at the anode, while continuous operation leads to membrane thinning and larger reversible losses due to gas supersaturation in catalyst micropores. Impedance and post-operation analyses indicate that steady-state conditions cause higher reversible mass transfer losses, while load cycling results in greater catalyst degradation, specifically sub-stoichiometric Ir-Ru oxide formation. These insights suggest different degradation mechanisms depending on operation mode, informing design choices for durable PEMEL.

The study by S.Kim et al.[342] investigates the degradation of iridium-based catalysts in PEMEL under various voltage stress conditions. Focusing on how different voltage cycling affects the crystal structure of iridium (Ir), the researchers conducted tests at constant high voltage, cyclic voltage between 1.7 and 1.9 V, and with open circuit voltage (OCV) cycling. They found that high-frequency voltage cycles caused the crystalline structure of Ir to irreversibly transform into a metallic form, significantly lowering the oxygen evolution reaction (OER) activity and thus the performance of the PEMEL cells. This transformation to metallic Ir under OCV conditions, in particular, led to pronounced degradation,

GA No. 101137802

highlighting the need for operational protocols that avoid such stress conditions to preserve catalyst stability.

The study by A.J. McLeod et al.[343] explores degradation mechanisms in PEMEL cells under accelerated stress testing, focusing on anode and cathode overpotentials. Using a specially designed in-situ reference electrode, the researchers monitored degradation rates over 1000 hours, with an average full-cell degradation rate of 77  $\mu\text{V}/\text{h}$ . Key findings indicate that an increase in anode ohmic resistance is the primary driver of efficiency loss, while microscopic changes in the cathode catalyst layer contribute to increased activation overpotential. These results suggest that optimizing the anode to reduce ohmic losses and enhancing cathode stability could significantly improve PEMEL durability. The study by A. Sandoval-Amor et al[344]. examines membrane degradation in PEMEL cells under different operating conditions by measuring the fluoride concentration in water output at both the anode and cathode of a 4-cell PEMEL stack. The operating conditions tested include temperatures of 25°C and 40°C, water flow rates of 20, 25, and 30 mL/min with a nominal water consumption of 2 mL/min, and three load levels ranging from a nominal load of 8 V and 0.26 A/cm<sup>2</sup> to a lower load of 6.8 V and 0.05 A/cm<sup>2</sup>. The results indicate a linear correlation between fluoride concentration and conductivity in the water output, confirming that conductivity measurements can provide a real-time assessment of membrane degradation across varying temperatures, flow rates, and load conditions. Notably, the degradation of the membrane was identified as the most significant component impacted under these conditions, as fluoride release indicated progressive chemical wear. This real-time diagnostic tool is beneficial for monitoring the health of PEMEL membranes, especially under dynamic load conditions.

The study by S.H.Frensch et al[345]. investigates the influence of different operation modes on degradation in PEMEL cells. The research examines seven operation modes, including constant current, constant voltage, and dynamic cycling, to evaluate their effects on membrane durability and overall cell performance. High-frequency cycling (10 seconds dwell time) and solar profile cycling resulted in reduced voltage degradation rates due to decreased total ohmic resistance. However, these dynamic modes led to elevated fluoride emissions, indicating membrane and ionomer degradation, especially on the cathode side. Additionally, higher operating temperatures exacerbated membrane thinning and fluoride loss, suggesting that while elevated temperatures improve efficiency, they reduce the membrane's lifespan due to increased gas crossover and enhanced Ti-PTL passivation.

The study by G.Bender et al[346]. investigates the degradation mechanisms in PEMEL systems under different operational conditions, including temperature, current density, and cycling frequency. The study reports that under high-temperature conditions (up to 80°C) and dynamic cycling, the PEMEL system shows accelerated degradation rates, with fluoride emission rates reaching approximately 14  $\mu\text{g}/\text{cm}^2/\text{h}$ , indicating significant membrane wear. The membrane's thinning rate was observed to be around 0.2  $\mu\text{m}/1000$  hours at elevated temperatures, especially under high current densities and intermittent load cycling. Voltage degradation rates were reported at 3.0 mV/h under standard load conditions, increasing with higher temperature and fluctuating power, which accelerates catalyst dissolution and ionomer loss.

These findings underscore the sensitivity of PEMEL systems to operational conditions and highlight the need for optimized temperature and load management to reduce degradation, particularly in renewable energy applications with variable power inputs.

The study by M. Möckl et al[347]. investigates degradation mechanisms in PEMEL systems with a focus on iridium utilization and operational efficiency in low-iridium-load membrane electrode assemblies (MEAs). This research highlights how load cycling between 0.2 and 2.0 A/cm<sup>2</sup> affects MEA durability,

GA No. 101137802

particularly observing that iridium-based oxygen evolution reaction (OER) catalysts exhibit significant performance alteration over 3,700 hours of operation. The PEMEL system tested with a conventional iridium catalyst at high loadings ( $2 \text{ mg/cm}^2$ ) showed a continuous improvement at  $2 \text{ A/cm}^2$  of  $-18 \mu\text{V/h}$ , which could be mainly ascribed to an improved ohmic resistance over time. The novel catalyst with a low loading of  $0.25 \text{ mg/cm}^2$  had a degradation rate of roughly  $1 \mu\text{V/h}$  though also here the ohmic resistance improvement of the membrane led to a cell performance increase of  $-8 \mu\text{V/h}$ . Though the mass activity for both systems decreased over cycling (and therewith the kinetic overpotential increased), the beneficial effect of the reduced high frequency overcompensated for this degradation effect, leading to an overall cell performance improve over the course of the study.

The study by Alia et al [348]. compares how different potential profiles affect catalyst layer degradation. They show that the upper potential limit significantly affects performance when exceeding  $1.8 \text{ V}$ , especially at low anode loadings. Additionally, the potential profile shape changes the degradation extent with the most detrimental being a slow cathodic scan and a fast anodic step in the potential range of  $1.4\text{-}2 \text{ V}$ . They further showed that the number of transients is more important for degradation than the holding time at the upper or lower potential limit

### 3.1.4 SOEL

The study, along with findings by D.M. A Duenas et al. [349], highlights the durability of the SOEL module through its consistent performance and robust design. Homogeneous temperature profiles and stable voltage outputs across the four-stack configuration indicate effective thermal management and reduced thermomechanical stress, key factors in ensuring long-term reliability. The system's ability to handle load fluctuations during transitions between SOEL and SOFC modes, while maintaining operational stability, further underscores its potential for sustained industrial use in hydrogen production and power generation.

### 3.1.5 PCCEL

Polarization-dependent degradation is a concern for PCCELS, as current density plays a pivotal role in the structural degradation of cells, as it directly influences the overpotential at the electrodes. For instance, a reversible protonic ceramic cell with a  $\text{CaZr}_{0.9}\text{In}_{0.1}\text{O}_{3-\delta}$  electrolyte exhibited a high degradation rate of 18% under an applied voltage of  $1.2 \text{ V}$ , whereas its performance remained stable during operation in fuel cell mode at  $0.8 \text{ V}$  [350]. The observed differences in degradation behavior were attributed to variations in elementary reactions under different bias potentials.

Dailly et al. investigated the long-term durability of a  $\text{BaZr}_{0.1}\text{Ce}_{0.8}\text{Y}_{0.1}\text{O}_{3-\delta}$ -based protonic ceramic cell and reported a degradation rate of only 1.2% per 1000 hours in fuel cell mode. However, this rate increased to 5–8% per 1000 hours during reversible operation in fuel cell/electrolysis modes [351]. Interestingly, the ohmic resistance of PCCELS was found to decrease with increasing applied potentials, likely due to enhanced electronic conductivity [352]. This behavior has been attributed to n-type electronic conduction at the electrolyte–fuel electrode interface and p-type electronic conduction at the electrolyte–air electrode interface [352]. As a result, operating PCCELS at high cell voltages may reduce Faradaic efficiency, posing a potential challenge [149].

## 3.2 Partial Load

### 3.2.1 AEL

The study by F. Brissaud et al[353]. examines the durability and operational performance of both alkaline electrolysis (AEL) and proton exchange membrane electrolysis (PEMEL) in the context of the industrial-scale Jupiter 1000 Power-to-Gas project. Jupiter 1000, which integrates AEL and PEMEL systems, provides insights into the challenges of efficiency, flexibility, and startup dynamics for both electrolyser types when used with renewable energy sources. The AEL system demonstrated steady performance but required extended startup times and exhibited energy efficiency around 66%, while the PEMEL system, though more flexible and quicker to start, showed efficiency limits with increased power consumption in auxiliary systems. Degradation phenomena differed between the systems, with AEL systems experiencing electrode passivation over time and PEMEL systems facing membrane and catalyst layer degradation due to load cycling. These insights emphasize the operational strategies needed for optimized durability and efficiency of AEL and PEMEL in dynamic environments.

### 3.2.2 AEMEL

The study by M. Moreno-Gonzalez et al[193]. explores the long-term durability and performance of an anion exchange membrane electrolysis (AEMEL) cell using a reinforced Aemion+<sup>®</sup> membrane under alkaline conditions. Operating over a period of up to 8900 hours at 70°C with a 1 M KOH electrolyte, the study demonstrates minimal degradation, with hydrogen crossover rates well below industrial safety limits. Key findings show that the AEMEL system maintained high efficiency, attributed to the robust nature of the Aemion+<sup>®</sup> membrane, which exhibited negligible change in ionic conductivity over the extended operation. These results suggest that AEMEL systems with stable and chemically resistant membranes like Aemion+<sup>®</sup> have the potential to achieve efficiency and durability standards comparable to those of PEMEL systems, while surpassing the traditional performance of AEL systems in high-demand environments.

### 3.2.3 PEMEL

The study by B.Sanchez Batalla et al.[354] explores degradation in proton exchange membrane electrolysis (PEMEL) cells using electrochemical impedance spectroscopy (EIS) combined with distribution of relaxation times (DRT) analysis. This approach allowed the authors to precisely identify and monitor degradation processes over extended operational periods. The study focuses on a PEMEL cell with low iridium catalyst loading to assess degradation mechanisms under constant current conditions. Key findings indicate that charge transfer resistance at the anode, particularly related to the oxygen evolution reaction, represents the most significant contributor to performance decline. Additionally, the DRT analysis revealed increased ionic resistance in the catalyst layer over time, likely due to catalyst dissolution and membrane contamination.

### 3.2.4 SOEL

See section 3.4.2

### 3.2.5 PCCEL

Not relevant data was found.

### 3.3 Start-Stop Cycles (On/Off cycles)

The paragraph refers to operational modes related to ON/OFF cycles, such as: cold/hot/warm standby, cold/hot start, shutdown, emergency shutdown, and also pressure variation and phenomena of shunt current (which is discussed in section 3.8).

#### 3.3.1 AEL

In a recent work by Raul et al., two stability protocols were developed wherein in the first stability test, low (60 mA for 10 min) and high (480 mA for 20 min) current steps were altered with each cycle lasting 30 min, and then repeated 120 times for a total of 60 hours. Further, the second stability test combined both fluctuating current and shutdown steps, incorporating an open-circuit potential (OCP) step for 2 min between high and low currents[86]. Overall, exposure to such variations can also impact electrolyzer components. For example, it can lead to catalyst degradation (including mechanical wear, passivation, and corrosion) [355], alterations in electrode structures (such as changes to the oxide layer that increase overpotential), mass transport limitations due to inconsistent gas bubble formation and removal, and electrolyte imbalances.

#### 3.3.2 AEMEL

Anion Exchange Membrane Electrolysers (AEMELs) experience several degradation mechanisms when subjected to on-off cycling, which affects their overall performance and operational lifespan. These mechanisms include catalyst degradation, membrane degradation, and the formation of deleterious species, all of which interact in complex ways to impair the system.

- Catalyst Degradation

Repeated on-off cycling imposes thermal and electrochemical stresses on the catalyst layer, causing structural and compositional changes that degrade its performance. Catalyst nanoparticles, particularly those supported on carbon, are prone to detachment, migration, and agglomeration during cycling. This results in a reduced active surface area, compromising catalytic activity and efficiency[356]. Additionally, during the off-state, residual hydrogen crossover to the oxygen electrode can chemically interact with oxygen evolution reaction (OER) catalysts such as nickel or iridium oxides. These interactions can lead to temporary improvements in catalytic activity through the formation of hydrous oxides, but over time, they result in increased contact resistance with the porous transport layer (PTL). This eventually diminishes performance and accelerates the degradation of the catalyst[356].

- Membrane Degradation

The anion exchange membrane (AEM), a critical component of AEMELs, is highly susceptible to chemical and mechanical degradation under on-off cycling. Chemical degradation occurs due to the alkaline environment and exposure to reactive oxygen species (ROS), which attack the functional groups of the membrane. For instance, membranes with aryl ether backbones can undergo cleavage, leading to structural damage and ionic conductivity loss[357]. Mechanical degradation is exacerbated by pressure and temperature fluctuations during on-off cycling, leading to membrane thinning, pinhole formation, and eventual gas crossover[358].

- Formation of Carbonate and Reactive Species

On-off cycles facilitate the formation of carbonate species in AEMELs, particularly when atmospheric CO<sub>2</sub> dissolves into the electrolyte during idle periods. These carbonates can accumulate on the membrane and electrodes, acting as poisons that reduce ionic conductivity and catalyst effectiveness[359]. During startup, these species decompose, releasing adsorbed CO<sub>2</sub> that initially improves performance but subsequently leads to voltage instability and rapid degradation. Hydrogen crossover during the off-state exacerbates degradation by introducing unwanted chemical reactions at the anode, such as the reduction of metal oxides and the creation of hydrous species. These reactions increase internal resistance and lead to catalyst dissolution, further contaminating the membrane[360].

### 3.4 Synergistic Effects

These degradation mechanisms are often interdependent. For instance, the dissolution of catalyst materials can introduce metal ions into the membrane, which, in turn, accelerate its chemical breakdown. Simultaneously, increased gas crossover due to membrane degradation exposes the catalyst layer to harsher conditions, exacerbating its wear. Such synergies underline the need for integrated approaches to mitigate degradation.

#### 3.4.1 PEMEL

The study by Xu Boschi et al[361]. focuses on predicting degradation in proton exchange membrane electrolysis (PEMEL) cells under constant and start-stop load conditions using a data-driven convolutional neural network-long short-term memory (CNN-LSTM) model. The researchers collected data from PEMEL systems operating under steady loads for 1140 hours and start-stop loads for 660 hours. The model was trained to predict voltage variations over time, achieving a high accuracy with an R<sup>2</sup> value above 0.98. Results show that constant load operation led to a degradation rate of 4.5% over 1000 hours, while start-stop loads exhibited a slower degradation rate of 2.5%. This difference suggests that start-stop conditions partially allow for voltage recovery, thereby slowing degradation. The CNN-LSTM model proved effective in long-term prediction, offering potential for real-time PEMEL system monitoring.

In the study by Weiss et al.[362], the effect of pure load cycling (1 A/cm<sup>2</sup>, 3 A/cm<sup>2</sup>, 1.3 V hold; 10 min each) vs on-off-cycles (1 A/cm<sup>2</sup>, 3 A/cm<sup>2</sup>, 1.3 V hold; 10 min each) were compared directly. It could be shown that over the course of 500 cycles, the performance kept improving if the potential was kept at 1.3 V in the idle times. The improvement can be directly correlated to a steady improve in High-frequency resistance (HFR). On the other hand, letting the cell relax to OCV within each cycle lead firstly to an improvement in performance, but after 10 cycles, the performance kept decreasing significantly. Crossover hydrogen was shown to change the IrO<sub>2</sub> catalyst during the idle times leading first to an improved performance due to transformation into a more OER active hydrous iridium oxide. However, due to an increased contact resistance of the hydrous oxide toward the PTL, the overall performance degraded over time. Additionally, iridium deposits upon dissolution of the hydrous iridium oxide catalyst have been found in the membrane.

#### 3.4.2 SOEL

The study by Y. Fan et al. [363] explores a novel approach to improving the durability and performance of solid oxide electrolysis cells (SOELs) through the infiltration of SrFe<sub>2</sub>O<sub>4-δ</sub> into La<sub>0.8</sub>Sr<sub>0.2</sub>MnO<sub>3</sub>/yttria-stabilized zirconia (LSM/YSZ) air electrodes. This strategy specifically targets the prevention of air

GA No. 101137802

electrode delamination, a critical failure mode that undermines long-term SOEL operation. In conventional SOELs, the LSM/YSZ air electrode is prone to delamination due to the buildup of oxygen pressure at the electrode/electrolyte interface and the material's low ionic conductivity. The baseline cells in this study exhibited catastrophic delamination after only 350 hours of operation at 800°C. In contrast, cells treated with SrFe<sub>2</sub>O<sub>4-δ</sub> infiltration sustained over 900 hours of continuous operation without signs of delamination. This demonstrates the efficacy of the infiltration process in mitigating structural degradation. The SrFe<sub>2</sub>O<sub>4-δ</sub> infiltration enhanced the durability of the air electrode by introducing Fe-doped LSM nanoparticles onto the electrode surface. These nanoparticles played a critical role in increasing ionic conductivity and extending the triple-phase boundary (TPB), where electrochemical reactions occur. The study observed that the infiltrated nanoparticles maintained their small grain size (~20 nm) and intact morphology even after 900 hours of operation, ensuring sustained performance. A key aspect of this durability approach is the cation exchange facilitated by the infiltrate. Sr and Fe ions from the SrFe<sub>2</sub>O<sub>4-δ</sub> solution diffused into the LSM backbone, transforming it into a mixed ionic and electronic conductor. This process increased the electrode's ionic conductivity, reduced polarization resistance, and enhanced the overall electrocatalytic activity for oxygen evolution reactions. By addressing both structural stability and electrochemical performance, this study presents infiltration as a viable method for enhancing SOEL durability. The findings underscore the potential of surface modification techniques to prevent degradation, improve efficiency, and extend the operational lifespan of SOEL systems, paving the way for more robust and reliable hydrogen production technologies.

The study by Chengqiao Xi et al. [364] explores the performance and durability of flat-tube solid oxide electrolysis cells (SOELs) for H<sub>2</sub>O/CO<sub>2</sub> co-electrolysis, presenting a promising solution that merges the mechanical robustness of tubular designs with the high-power density advantages of planar configurations. This innovative approach aims to address the challenges of scaling SOEL technology for industrial applications.

Over 1000 hours of continuous operation at 750°C with a constant current density of 300 mA/cm<sup>2</sup> demonstrated the durability of the flat-tube SOEL. The observed degradation rate of 10.69%/kh (122 mV/kh) aligns with performance metrics of planar SOELs, solidifying the flat-tube cell's potential for long-term use. The researchers found that increasing the temperature and water vapor content in the fuel electrode significantly enhanced electrochemical performance, achieving a current density of 674 mA/cm<sup>2</sup> at 800°C.

Using advanced electrochemical impedance spectroscopy (EIS) and distribution of relaxation time (DRT) analysis, the study identified five distinct polarization processes influencing cell performance. Among these, the primary degradation mechanism was traced to the fuel electrode, specifically the three-phase boundary of Ni-YSZ. Structural analysis revealed the sintering and loss of nickel particles near the electrolyte, driven by high steam concentrations at the fuel electrode inlet. This reduction in active reaction sites contributed significantly to the observed performance decline.

Microstructural analysis further highlighted the stability of the oxygen electrode, which exhibited no significant structural changes over the testing period, emphasizing its resilience compared to the fuel electrode. The flat-tube design not only retained robust mechanical integrity but also offered superior resistance to gas leakage, a common issue in conventional planar cells.

This study demonstrates the potential of flat-tube SOELs as a scalable and efficient solution for H<sub>2</sub>O/CO<sub>2</sub> co-electrolysis. By addressing the challenges of nickel particle sintering and enhancing the stability of the fuel electrode, this design offers a viable pathway for large-scale syngas production, aligning with carbon-neutral energy goals.



### 3.4.3 PCCEL

Not relevant data was found.

## 3.5 Temperature

### 3.5.1 AEL

With temperature playing a crucial role in AEL, performance of electrodes was evaluated at various temperature in a study reported by the Raul A. Marquez et al[86]. Typically, high temperatures can enhance electrode kinetics, electrolyte conductivity, and gas removal, making them ideal for industrial conditions. Fluctuations in current can also aid in corrosion and/or modify reaction rates. With increase in temperature from 20 to 80 °C at 150 mA cm<sup>-2</sup> cell potential reduced by 200 mV as reported in [266]. Further in another interesting work on low temperature electrolysers detailed temperature settings for the TIPs for AEL single cell and short stack testing are detailed[266].

### 3.5.2 AEMEL

Temperature is a critical operational parameter for Anion Exchange Membrane Electrolysers (AEMELs), directly influencing their performance and durability. While elevated temperatures often enhance reaction kinetics and ionic conductivity, they also accelerate degradation processes in key components such as membranes, catalysts, and electrode structures. Understanding these mechanisms and their mitigation is essential for improving AEMEL durability.

#### **Membrane Degradation**

The anion exchange membrane (AEM) is central to the electrolyser's function, facilitating ion transport while maintaining separation between the anode and cathode gases. However, at elevated temperatures, the chemical stability of AEMs can degrade significantly. Studies have shown that high temperatures exacerbate the breakdown of polymer backbones and ion-exchange groups, particularly in AEMs with aryl ether bonds, which are prone to alkaline hydrolysis and oxidation[365].

For instance, it has been observed that temperatures above 60°C lead to a marked decline in ionic conductivity due to the structural degradation of the membrane. Novel membranes with enhanced thermal stability, such as those with cross-linked polymer structures or stable aromatic backbones, are being developed to combat this issue[366].

#### **Catalyst Layer Degradation**

The catalyst layer in AEMELs is also significantly affected by temperature. At high temperatures, catalyst particles, especially those supported on carbon, are susceptible to sintering, which reduces their active surface area and compromises catalytic efficiency. Furthermore, elevated temperatures can intensify the interaction between the catalyst and membrane or binder materials, leading to the formation of inactive phases[367]. This is particularly problematic for oxygen evolution reaction (OER) catalysts like nickel-based oxides, which may undergo phase transitions or dissolution at higher temperatures, further diminishing their long-term activity[367].

#### **Electrode and Gas Diffusion Layer (GDL) Degradation**

Electrodes and gas diffusion layers (GDLs) also face degradation challenges at elevated temperatures. The binders used to fabricate electrodes can lose their structural integrity, leading to delamination and

GA No. 101137802

increased interfacial resistance. Similarly, GDLs can experience changes in their porosity and hydrophobicity due to thermal stresses, which hinder effective gas transport and reduce electrolyzer efficiency[368].

### Formation of Carbonate Species

In addition to structural degradation, elevated temperatures can accelerate chemical interactions that produce carbonate species, especially in the presence of dissolved CO<sub>2</sub>. These carbonates can block active sites on the membrane and electrodes, further reducing ionic conductivity and catalytic performance[369].

### Mitigation Strategies

- **Material Advancements:** Developing thermally stable membranes with robust backbones and cross-linked structures is essential. Research into aromatic and fluorinated polymers has shown promise for retaining mechanical integrity and ionic conductivity at higher temperatures[370].
- **Temperature Control:** Maintaining optimal operating temperatures that balance reaction kinetics and material stability is critical. Operating protocols can be tailored to minimize thermal stresses and degradation rates[371].
- **Optimized Catalysts:** Utilizing thermally stable catalysts, such as those with strong metal-support interactions or high-temperature sintering resistance, can improve durability. For example, cobalt-doped nickel catalysts have demonstrated enhanced stability under elevated temperatures[372].
  - **Protective Coatings:** Applying protective coatings to components like the GDL can shield them from thermal degradation, preserving their structural and functional properties[373]

## 3.5.3 PEMEL

The study by S.Siracusano et al[341]. focuses on the effects of thermal load cycling on the degradation of proton exchange membrane electrolysis (PEMEL) cells, particularly examining how temperature variations combined with load cycling impact efficiency and component longevity. Results indicate that thermal cycling induces changes in the membrane-electrode assembly (MEA), with membrane thinning and increased mass transfer resistance observed over prolonged cycles. The temperature shifts accelerate degradation by promoting reversible losses associated with gas supersaturation in the catalyst micropores, affecting gas escape efficiency. Additionally, thermal cycles exacerbate the formation of sub-stoichiometric oxides on the anode catalyst, leading to gradual performance declines and heightened catalyst degradation. These findings highlight the need for thermal management in PEMEL systems to enhance durability under fluctuating renewable energy input.

## 3.5.4 SOEL

The study by P. Khajavi et al. [374] delves into the pressing issue of high-temperature degradation (HTD) in 3 mol% yttria-stabilized zirconia (3YSZ), a key material used in solid oxide fuel and electrolysis cells (SOELs). The research identifies HTD as a significant barrier to the long-term durability of these systems, particularly when operated for extended periods exceeding 8,500 hours at temperatures between 700 and 800 °C. This degradation manifests as a transformation of the 3YSZ structure from the tetragonal to the monoclinic phase, resulting in embrittlement and reduced mechanical strength that can lead to cell failure. A central finding of the study is the critical role of grain size in determining the material's resistance to degradation. Fine-grained 3YSZ supports, with grain sizes below 200 nm, demonstrated exceptional durability, showing negligible phase transformation even under prolonged

GA No. 101137802

exposure to harsh conditions. Conversely, larger-grained supports, with grain sizes exceeding 239 nm, were far more susceptible to degradation. This discovery underscores the importance of microstructural optimization in extending the operational lifespan of SOELs. The study also highlights the influence of the operating environment, particularly the presence of water vapor. Higher concentrations of H<sub>2</sub>O in the atmosphere were found to accelerate phase transformation, presenting a challenge for SOELs that require high steam levels for efficient performance. This environmental sensitivity adds another layer of complexity to the durability of these systems. In addressing these challenges, the research points to the development and use of fine-grained 3YSZ as a promising solution. By leveraging materials with optimized microstructures, the durability and performance of SOELs can be significantly improved, paving the way for more robust and reliable systems in industrial applications. The study's findings provide a roadmap for overcoming degradation challenges and enhancing the longevity of SOC technology

### 3.5.5 PCCEL

Not relevant data was found.

## 3.6 Pressure

### 3.6.1 AEL

Operating pressure is a pivotal parameter in alkaline electrolyser (AEL) systems, significantly influencing their performance and degradation mechanisms. While higher pressures improve gas production rates and efficiency, they also exacerbate challenges such as gas solubility, electrode wear, and system stability.

#### **Gas Solubility and Crossover**

Increased pressure enhances the solubility of hydrogen and oxygen in the electrolyte, leading to greater gas crossover rates. This phenomenon reduces gas purity and increases the risk of forming explosive mixtures. F. Allebrond al. demonstrated that elevated pressures significantly amplify gas crossover, necessitating robust gas separation and management strategies [375].

#### **Electrode Degradation**

Elevated pressures intensify bubble formation on electrode surfaces, reducing active surface area and accelerating mechanical wear. Md S. Opu. [376] found that increased pressure results in larger and more frequent gas bubbles, which degrade electrode performance over time.

#### **Electrolyte and Material Challenges**

Higher pressures alter electrolyte properties and impose mechanical stresses on components such as diaphragms and seals, potentially leading to system failure. Jang D et al. [377] highlighted that robust material design is necessary to counteract the effects of pressure-induced degradation and maintain system integrity.

#### **System Efficiency vs. Degradation Trade-Off**

While high pressure improves volumetric gas production and facilitates downstream compression, it necessitates stronger system components and careful pressure optimization to avoid accelerated

degradation. This trade-off underscores the need for advanced materials and system designs that balance efficiency and durability.

### 3.6.2 AEMEL

Operating pressure is a key parameter in Anion Exchange Membrane Electrolysers (AEMELs), directly impacting their efficiency and durability. While higher pressures often enhance reaction kinetics and gas production rates, they also contribute to material degradation and operational challenges.

#### Membrane Degradation

Parrondo et al. (2014) [378] highlighted that elevated pressures exacerbate the chemical degradation of anion exchange membranes (AEMs). This degradation is particularly pronounced in membranes with aryl ether bonds, which are susceptible to alkaline hydrolysis and oxidation under pressure. These processes lead to a reduction in ionic conductivity and mechanical strength, thereby affecting the long-term performance of AEMELs.

#### Catalyst Layer Degradation

Lei et al. (2024) [379] observed that increased operating pressures intensify gas solubility in the electrolyte, resulting in higher gas crossover rates and bubble formation on catalyst surfaces. These phenomena diminish the active surface area available for catalytic reactions and cause physical damage to the catalyst layer over time. This insight underscores the need for catalysts that can withstand the physical and chemical stresses induced by high-pressure operation.

#### Electrode and GDL Degradation

Vinodh et al. (2023) [380] discussed how elevated pressures impact the structural integrity of electrodes and gas diffusion layers (GDLs). They noted that gas bubbles formed under high pressure can lead to delamination of electrode materials, increasing interfacial resistance. Similarly, GDLs experience changes in porosity and hydrophobicity, reducing effective gas transport and compromising the overall efficiency of the system.

### 3.6.3 PEMEL

Operating pressure is a crucial parameter in Proton Exchange Membrane Electrolysers (PEMELs), directly impacting their efficiency and long-term durability. While elevated pressures can enhance hydrogen production rates and volumetric efficiency, they also contribute to material degradation and operational challenges.

#### Membrane Degradation

Van Dijk et al. (2013)[381] emphasized that high operating pressures increase the permeation of hydrogen and oxygen through the proton exchange membrane (PEM), leading to the formation of reactive oxygen species. These species attack the polymer structure, causing chemical degradation and reducing the ionic conductivity and mechanical strength of the membrane. This degradation compromises the overall efficiency and durability of the electrolyser.

#### Catalyst Layer Degradation

GA No. 101137802

According to Fateev et al. (2013)[382], increased operating pressures amplify gas solubility in the electrolyte, leading to higher rates of gas crossover and bubble formation on catalyst surfaces. These bubbles reduce the active surface area for catalytic reactions and cause physical damage to the catalyst layer, leading to diminished catalytic efficiency over time. The study highlighted the need for robust catalyst designs to withstand such stresses.

### **Electrode and GDL Degradation**

Shiva Kumar et al. (2019)[383] discussed the effects of high pressure on the structural integrity of electrodes and gas diffusion layers (GDLs). Gas bubbles formed under elevated pressures can lead to delamination of electrode materials and increased interfacial resistance. Furthermore, the GDL may experience changes in porosity and hydrophobicity, which hinder effective gas transport and reduce overall cell performance.

## **3.6.4 SOEL**

Operating pressure is a critical parameter influencing the performance and durability of Solid Oxide Electrolysis Cells (SOECs). While elevated pressures can enhance reaction kinetics and gas production rates, they also introduce challenges related to material degradation and operational stability.

### **Electrode Delamination**

High operating pressures can lead to increased oxygen partial pressures at the electrode–electrolyte interface, which may cause mechanical stress and eventual delamination of the oxygen electrode. This delamination results in increased cell resistance and reduced efficiency. Virkar (2010)[384] developed a model to calculate the internal oxygen partial pressure, highlighting that elevated pressures exacerbate this issue, leading to accelerated degradation of the SOEL.

### **Electrolyte Degradation**

Elevated pressures can also impact the stability of the electrolyte material. Yttria-stabilized zirconia (YSZ), commonly used as an electrolyte in SOECs, may undergo phase decomposition under high-pressure conditions, leading to reduced ionic conductivity and mechanical integrity. Butz et al. (2009)[385] observed that such degradation is influenced by operating conditions, including pressure, which can accelerate the decomposition process.

## **3.6.5 PCCEL**

Operating pressure is a significant parameter in Protonic Ceramic Electrolysis Cells (PCCELs), directly affecting their efficiency, performance, and longevity. While elevated pressures enhance hydrogen production rates and overall system efficiency, they can also accelerate degradation processes and mechanical failures.

### **Electrode Degradation**

Ghezal-Ayagh et al. (2021)[386] reported that high pressures can lead to increased mechanical stress on electrode materials, causing microstructural damage and performance degradation over time. In their study, they highlighted the importance of optimizing the air electrode composition and structure to mitigate these effects, especially under elevated pressure conditions.

### **Electrolyte Stability**

Hernandez Rodriguez (2019)[387] explored the degradation mechanisms of proton-conducting ceramic electrolytes under high-pressure and high-temperature environments. The study found that pressures beyond the material's mechanical and chemical stability thresholds led to a reduction in ionic conductivity and structural degradation. This underscores the necessity of employing advanced materials to enhance electrolyte stability in pressurized systems.

### **Mechanical Integrity**

Pirou et al. (2022)[388] examined the mechanical effects of elevated pressures on PCCEs and identified cracking and delamination of cell components as critical issues. They demonstrated that mechanical failures often arise from non-uniform stress distributions and emphasized the importance of robust cell designs to counteract these pressures. Their findings suggest that optimizing the mechanical properties of cell components is essential for maintaining long-term reliability.

## **3.7 Water Flow rate and water quality**

The study by H.Becker et al[389]. investigates the degradation mechanisms in low-temperature electrolysis technologies, specifically AEL, AEMEL, and PEMEL, with a focus on the impact of impurities. This review examines how various impurities in the water supply—such as metal ions, chlorides, and organic compounds—affect each electrolyser type's performance, durability, and efficiency. In PEMEL systems, impurities like iron and copper accelerate membrane degradation through fluoride release and membrane thinning, with reported degradation rates in voltage around 0.1–0.12% per 1000 hours. AEMEL systems are particularly sensitive to degradation due to hydroxide ion reactions with the membrane's polymer structure, while AEL systems experience issues with electrode passivation under high pH and temperature conditions.

These findings underline the critical need for high water purity to maintain system longevity across all electrolyser types. Strategies for minimizing impurity impacts include advanced water purification systems and impurity-tolerant materials.

## **3.8 Anomalies stack power supply**

In industrial-scale alkaline electrolysers (AELs), used extensively for hydrogen production, efficiency losses due to unintended electrical phenomena pose significant challenges. One critical issue is AC ripple—a form of electrical interference that arises from the superposition of alternating current (AC) components on the direct current (DC) power supplied to the electrolyser. AC ripple affects the stability of the electrochemical reactions and can exacerbate efficiency losses, particularly in systems powered by renewable energy sources characterized by fluctuating power supply.

### **3.8.1 AEL: Shunt currents**

The study of Georgios Sakas et al[390]. examines the impact of shunt currents on the energy efficiency of industrial-scale alkaline electrolysers (AELs) used in hydrogen production. Shunt currents are unintended electrical flows that bypass the main electrolytic path, leading to significant efficiency losses, especially during partial-load operations. In a 3 MW AEL model, shunt currents account for

GA No. 101137802

approximately 16.8% of input power at full load, but this figure escalates to about 75.4% at 30% load, increasing the specific energy consumption (SEC) from 61 to 182 kWh per kilogram of hydrogen. This efficiency decline poses a substantial challenge for AELs powered by intermittent renewable energy sources.

The study suggests that distributing power equally across multiple AEL lines can minimize SEC when more than one line is required to meet hydrogen demand, resulting in up to a 10% improvement in efficiency. Additionally, reducing shunt currents to a scaling factor of 0.2 or lower mitigates efficiency losses at reduced loads, indicating that controlling shunt currents could enhance performance during partial operations. Safety considerations impose a minimum load limit to prevent hazardous gas mixing, ensuring hydrogen concentrations remain below explosive thresholds. Optimizing load distribution with equal power across lines, combined with strategies to reduce shunt currents, improves both efficiency and safety in hydrogen production. This research underscores the importance of careful design and operation to make AELs more energy-efficient and adaptable for renewable-powered hydrogen production.

### 3.8.2 AEMEL: Reverse currents

The study by J. Naveen Guruprasad et al [391]. examines the degradation rates of various electrode materials in anion exchange membrane electrolysis (AEMEL) under reverse current conditions, which are common in renewable energy-driven applications with intermittent power. Using a dual platinum-wire reference electrode setup, the researchers quantified degradation rates across different cathode materials. The study found that NiMo/C exhibited the highest degradation rate, with a decline in activity by approximately 15% over 500 hours, followed by PtRu/C with a 10% decline, and Pt/C with a lower degradation rate of about 5% over the same period. The anode material, NiFe-LDH, demonstrated high stability, showing minimal degradation. These results highlight the varying susceptibility of non-noble metal catalysts to reverse currents, emphasizing the importance of developing more resilient materials for long-term AEMEL stability.

## 3.9 Environmental conditions, Mechanical stress, seal leakage; BOP

Environmental conditions, mechanical stress, seal integrity, and the balance of plant (BOP) components are critical factors influencing the performance and durability of various electrolysis technologies, including Alkaline Electrolysers (AEL), Anion Exchange Membrane Electrolysers (AEMEL), Proton Exchange Membrane Electrolysers (PEMEL), Solid Oxide Electrolysers (SOEL), and Protonic Ceramic Electrolysers (PCCEL).

### 3.9.1 AEL

Environmental conditions such as temperature and humidity significantly impact AEL performance. Zeng et al. (2010)[392] highlighted that temperature fluctuations affect electrolyte conductivity and electrode kinetics, leading to efficiency losses. Humidity levels influence the evaporation rate of the electrolyte, potentially altering its concentration and conductivity.

Mechanical stress from pressure variations can cause structural fatigue in components like electrodes and diaphragms. Brauns et al. (2003)[393] reported that mechanical degradation of diaphragms due to stress leads to decreased cell efficiency and reduced lifespan

GA No. 101137802

Seal leakage poses risks of electrolyte loss and gas cross-contamination, compromising both efficiency and safety. Carmo et al. (2013)[394] emphasized the importance of seal integrity to prevent hydrogen and oxygen mixing, which could lead to explosive hazards.

The BOP components, including pumps and gas separators, must be robust to handle corrosive electrolytes and maintain system integrity. Ursúa et al. (2012)[395] discussed the necessity of corrosion-resistant materials and precise control systems in the BOP to ensure reliable long-term operation

### 3.9.2 AEMEL

AEMELs are sensitive to environmental conditions that affect membrane stability and ionic conductivity. Dekel (2018)[396] noted that humidity levels impact membrane hydration, directly influencing ionic conductivity and overall cell performance.

Mechanical stress can lead to membrane deformation or rupture, especially under varying pressure conditions. Varcoe et al. (2014)[397] observed that the mechanical integrity of the AEM is crucial for long-term operation, as mechanical failure can lead to gas crossover and efficiency loss.

Seal integrity is essential to prevent gas crossover and maintain safe operation. Wang et al. (2015)[398] emphasized the importance of robust sealing materials that can withstand the alkaline environment and mechanical stresses.

The BOP must ensure precise water management and gas handling to optimize performance and longevity. Jeong and Park (2024)[399] discussed design considerations for BOP components in AEMEL systems, highlighting the need for materials compatible with alkaline conditions.

### 3.9.3 PEMEL

PEMELs are particularly vulnerable to environmental factors that cause membrane degradation. Carmo et al. (2013)[400] reported that impurities in water and temperature variations can lead to membrane deterioration, affecting cell performance.

Mechanical stresses, such as those from thermal cycling, can induce cracks in the membrane electrode assembly (MEA), leading to performance loss. Babic et al. (2017)[401] investigated the effects of mechanical stress on MEA durability, finding that repeated stress significantly reduces lifespan.

Seal leakage can result in hazardous gas mixing. Moreno et al. (2011)[402] emphasized the need for durable sealing materials that maintain integrity over a wide range of operating conditions.

The BOP requires careful design to manage water purity and thermal conditions effectively. Caparros et al. (2020)[403] discussed the importance of BOP components in maintaining optimal operating conditions for PEMELs.

### 3.9.4 SOEL

SOELs operate at high temperatures, making them susceptible to thermal stresses that can cause mechanical failure in ceramic components. Wang et al. (2012)[404] observed that thermal cycling leads to cracking and delamination in SOELs, reducing operational lifespan.

Seal integrity is challenging due to thermal expansion mismatches, leading to potential gas leaks. Singh et al. (2007)[405] studied the development of compliant seal materials to accommodate thermal expansion and maintain seal integrity at high temperatures.



GA No. 101137802

The BOP must accommodate high-temperature operations and ensure material compatibility to prevent degradation. Stoots et al. (2009)[406] highlighted the need for high-temperature-compatible components in the BOP to ensure efficient heat management and system reliability.

### 3.9.5 PCCEL

PCCELS, like SOELs, operate at elevated temperatures, which can induce mechanical stress and affect seal materials. Haile (2003)[407] investigated the mechanical properties of proton-conducting ceramics and noted that thermal expansion and mechanical stress can lead to cracking.

Environmental conditions such as humidity impact protonic conductivity. Kreuer (2003)[408] discussed the influence of water vapor on the conductivity of protonic ceramics, emphasizing the need for controlled humidity conditions.

Seal leakage can lead to efficiency losses and safety hazards. Iwahara et al. (1981)[409] highlighted the importance of developing seal materials compatible with protonic ceramics to maintain system integrity.

The BOP must manage thermal and humidity conditions to maintain optimal performance. Ferguson et al. (2021)[410] emphasized the need for precise control of environmental conditions in the BOP design for PCCEL systems.

## 3.10 Stressors or degradation factors

The following tables provides a concise overview of the main stressors and their impacts on each type of electrolyser system, highlighting specific degradation mechanisms that influence their durability[411].

Electrolyser technologies are subject to various stressors that influence their performance and longevity, with each type exhibiting specific vulnerabilities due to its materials and operational design. Low-temperature systems, such as Alkaline Electrolysers (AEL), Anion Exchange Membrane Electrolysers (AEMEL), and Proton Exchange Membrane Electrolysers (PEMEL), face degradation mechanisms stemming from high current densities, dynamic electrical operations, and elevated temperatures. For instance, AEL systems experience catalyst erosion under high current densities, while PEMEL systems suffer from catalyst dissolution. AEMEL, particularly sensitive to cycling-induced stresses, sees reduced membrane durability during on/off operations. These stressors, coupled with fluctuations in water/electrolyte flow and pressure cycling, contribute to wear and inefficiencies across all low-temperature technologies.

High-temperature systems, such as Solid Oxide Electrolysers (SOEL) and Proton-Conducting Ceramic Electrolysers (PCCEL), face distinct challenges related to their ceramic components. SOEL systems, for example, are prone to thermal stress and mechanical cracking during dynamic operations, while PCCEL systems encounter similar issues at the ceramic-electrode interface due to phase transitions. Elevated operating temperatures, although essential for these systems, can exacerbate material degradation, including catalyst sintering and electrolyte instability. Pressure cycling and uneven steam or water distribution further amplify mechanical stress and reduce operational reliability.

The following tables summarize the interactions between stressors and their impacts on these electrolyser technologies, emphasizing the need for tailored strategies to mitigate these effects and enhance system durability:

### 3.10.1 AEL, AEMEL, PEMEL

Degradation factors	Impact on AEL	Impact on AEMEL	Impact on PEMEL
Overload	Catalyst erosion and efficiency reduction	Membrane degradation and catalyst loss	Catalyst dissolution
Start-Stop Cycles (On/Off cycles)	Performance drops and structural stress	Reduced membrane durability due to cycling stress	Increased membrane and electrode wear; catalyst dissolution; PTL corrosion
Load Fluctuations (i.e: AC Ripple)	Electrode degradation	Membrane and electrode degradation	Membrane and catalyst layer degradation
Elevated Stack Operating Temperature	Increased gas crossover and membrane wear	Accelerated chemical breakdown of membrane	Accelerated ionomer degradation
Pressure Cycling	Stack component fatigue	Pressure-induced stress on membrane	Pressure-related membrane stress; catalyst dissolution
Water/Electrolyte Flow Rate Variations	Reduced ionic conductivity and efficiency	Flow inconsistencies causing membrane wear	Water supply variations affecting performance

Table 4. Stressors for AEL, AEMEL and PEMEL

### 3.10.2 SOEL, PCCEL

Degradation factors	Impact on SOEL	Impact on PCCEL
Overload	Accelerated electrode sintering, increased ohmic resistance, thermal stress on ceramic components.	Accelerated electrode degradation, proton conductivity reduction, increased thermal stress.
Start-Stop Cycles (On/Off cycles)	Thermal cycling stress, electrode delamination, reduction-oxidation cycling leading to degradation.	Fatigue of ceramic-electrode interface, phase transitions leading to mechanical instability.
Load Fluctuations (i.e: AC Ripple)	Increased thermal stress on electrolyte, localized overpotential, degradation of interconnects.	Potential destabilization of ceramic proton conductor, localized degradation in electrode layers.
Elevated Stack Operating Temperature	Catalyst sintering, electrodes and IC, phase instability in electrolyte, mechanical failure of sealing components.	Proton conductor chemical degradation, sintering of electrode materials, mechanical stress in seals.

Pressure Cycling	Stress-induced microcracks in ceramic layers, interconnect fatigue, and sealing failure.	Mechanical stress on ceramic layers, fatigue cracks in electrolyte or electrode structures.
Water/Electrolyte Flow Rate Variations	Inefficient steam distribution causing localized overheating, underperformance or ni-reoxidation effects.	Reduced proton conductivity, uneven cooling/heating cycles leading to material fatigue.

Table 5. Stressors for SOEL and PCCEL

### 3.11 Impact of Degradation factors on Performance and Reliability

Electrolysers operate under diverse conditions that can significantly affect their performance, durability, and reliability. Each technology—Alkaline Electrolysis (AEL), Anion Exchange Membrane Electrolysis (AEMEL), Proton Exchange Membrane Electrolysis (PEMEL), Solid Oxide Electrolysis (SOEL), and Proton-Conducting Ceramic Electrolysis (PCCEL)—is uniquely influenced by operational modes and degradation factors due to differences in materials, design, and operating principles. The table provides a comprehensive evaluation of these influences, rating the impact of various factors on each technology.

Load fluctuations and partial load operation, for instance, impose stress on components such as membranes, electrodes, and current collectors, with AEL and PEMEL being particularly affected. Similarly, start-stop cycles, common in dynamic energy systems, exacerbate wear and tear, especially in PEMEL systems where membrane integrity is a critical concern.

Temperature plays a central role in degradation, with SOEL systems—operating at extreme temperatures—facing significant challenges related to thermal stress, while low-temperature systems like AEMEL and PEMEL encounter different thermal management issues. The quality of water and electrolyte, crucial for ionic conductivity, affects all systems but varies in severity based on the electrolyte type and operational conditions.

Mechanical stress and instability are critical concerns for systems operating at high pressures or under fluctuating loads, with SOEL particularly vulnerable due to the brittle nature of its materials at elevated temperatures. Seal integrity and anomalies in stack power supply are additional factors that can disrupt operation and accelerate degradation.

Each factor is rated to reflect its significance, with higher ratings indicating a greater impact on performance and reliability. This structured evaluation provides insights into the challenges faced by different electrolyser technologies and highlights areas requiring targeted mitigation strategies. By understanding these vulnerabilities, researchers and engineers can develop solutions to enhance system resilience and ensure the long-term viability of electrolyser operations in diverse applications.

Operational Mode / Degradation Factor	Relevance in terms of degradation entity / impact on performance / reliability				
	AEL	AEMEL	PEMEL	SOEL	PCCEL
Load Fluctuations	+++	+++	+++	++	++
Partial Load	++	++	++	-	-
Overload	+++	+++	+++	+	+
Start-Stop Cycles (On/Off cycles)	+++	+++	+++	++	++
Temperature	++	++	++	+++	-
Water Flow Rate	++	++	++	+	+
Pressure	+++	++	+++	++	+
Water (recirculation)/ electrolyte quality	++	++	++	++	+
Mechanical Stress/Instability	++	++	++	++	++
Anomalies stack power supply	++	++	++	++	++
Reverse Currents	++	++	-	-	-
Shunt Currents	++	++	-	-	-
Environmental Conditions	+	+	+	++	++
Water quality (feed water)	++	++	++	+++	+++
Seal Leakage	+	+	+	++	++
BOP: anomaly / malfunction in components / auxiliaries	++	++	+++	++	++

Table 6. Impact of Operational Modes and Degradation Factors on Electrolyser Technologies

The Table 5 employs a symbolic rating system to indicate the relative significance or impact of each operational mode or degradation factor on electrolyser performance and reliability. The symbols are defined as follows:

- **+++**: Represents a high impact, indicating a critical influence on performance or reliability.
- **++**: Denotes a moderate impact, where the factor has a significant but not dominant effect.
- **+**: Indicates a low impact, with minor effects on performance or reliability.
- **-**: Reflects minimal or negligible impact, with little to no observable effect.
- **0**: Signifies no observable impact or relevance under typical operational conditions.

This rating system provides a clear and concise way to compare the influence of different factors across various electrolyser technologies.

## 4 Industrial and partners experience of this topic

This section presents a comprehensive overview of the degradation mechanisms encountered across various electrolyser technologies under specific testing conditions, as identified by ELECTROLIFE industrial partners. The data is organized by partner name, technology type, and specific degradation mechanisms affecting key components. It also includes current mitigation strategies employed to address these challenges.

The insights gathered represent collaborative efforts to enhance the durability and efficiency of electrolyser systems, with contributions from key industrial partners, including Stargate, Pietro Fiorentini/Hyter, 1s1Energy, SolydEra and Kerionics. The summary covers a range of technologies, such as Alkaline Electrolysis (AEL), Anion Exchange Membrane Electrolysis (AEMEL), Proton exchange membrane electrolysis (PEMEL), Solid Oxide Electrolysis (SOEL), and Proton Ceramic Conductivity Electrolysis (PCCEL), reflecting a wide spectrum of operating conditions and material challenges.

Each partner has contributed detailed observations on degradation phenomena, including corrosion, contamination, mechanical damage, and chemical deterioration. In parallel, mitigation strategies—ranging from optimized design adaptations to advanced material selection—are provided to support improved system reliability and performance.

Partner name	Technology	Testing conditions	Degradation mechanism-components	Current mitigation strategies
Stargate	AEL	Any	Corrosion of metallic components	Nickel coatings
Stargate	AEL	Stainless steel BOP	Iron contamination of electrodes	Iron tolerant electrodes
Stargate	AEL	Any	Membrane clogging	Avoid particles in lye stream. Optimized electrode activation procedure (if required).
Stargate	AEL	Unwelded electrode <-> BPP	Loss of contact	Design adaption
Stargate	AEL	Any	Electrode coating loss	Avoiding certain third party electrode suppliers
Stargate	AEL	Any	Catalyst delamination	Developing new coating techniques
Stargate	AEL	Any	Corrosion of metallic components	Nickel coatings

Stargate	AEL	Stainless steel BOP	Iron contamination of electrodes	Iron tolerant electrodes
Pietro Fiorentini/Hyter	AEMEL	High flow rate	Anode catalyst delamination	Keep flow rate slow (1-2 ml/min/cm <sup>2</sup> )
Pietro Fiorentini/Hyter	AEMEL	On/off Cycles	Increases degradation rate	Keep slow current ramps. When shutting down, inertize with N <sub>2</sub>
Pietro Fiorentini/Hyter	AEMEL	Pressure cycling	Membrane mechanical degradation	Increase and decrease pressure slowly
Pietro Fiorentini/Hyter	AEMEL	Rise of current density (>0.5A/cm <sup>2</sup> )	Faster rate of degradation	For the moment keep current density @ 0.4A/cm <sup>2</sup>
Pietro Fiorentini/Hyter	AEMEL	Black out of bench test	Degradation, not identified	Avoid it
Pietro Fiorentini/Hyter	AEMEL	High Temperature	Membrane chemical degradation	Keep T @ 45°C
1s1 Energy	PEMEL	Repeated compression cycles under varying pressure	Membrane mechanical extrusion	Improve membrane resilience through reinforcement layers and optimized compression protocols.
1s1 Energy	PEMEL	High-temperature operation (80–120°C), extended operation in humidified environments	Gasket leaching	Develop temperature-resistant gasket materials with reduced susceptibility to chemical leaching.
1s1 Energy	PEMEL	Combined compression cycling and high-temperature operation	Gasket mechanical failure	Optimize gasket material and design to withstand thermal and mechanical stresses.
1s1 Energy	PEMEL	Repeated on/off cycles with rapid	Membrane pinhole formation	Utilize membranes with

		current and temperature changes		higher durability and enhanced chemical stability for transient operations.
SolydEra	SOEL	Operation at high current density	Delamination of the air electrode	Work at lower current density
SolydEra	SOEL	High temperature, High current density	Ni migration	Work at lower current density and reduce the temperature
SolydEra	SOEL	Low quality of steam, occurrence of impurities	Steam Electrode contamination	Use high purity steam (e.g. ISO 3696:1987 Grade 1)
Kerionics	PCCEL	High-temperature operation (600–800°C), cyclic heating/cooling, humidified hydrogen environment	Electrolyte chemical degradation (proton conductivity loss)	Optimize electrolyte composition (e.g., doping levels)
Kerionics	PCCEL	Thermal cycling, variable load operation, exposure to rapid temperature changes	Cracking of ceramic components due to TEC mismatch	Implement gradual heating/cooling protocols. Selection of compatible TEC ceramic and metallic materials.
Kerionics	PCCEL	Long-term exposure to high humidity, high temperature, and oxygen-rich environments	Metal interconnect oxidation or corrosion, increased resistances	Use protective coatings (e.g., chromia-forming alloys)
Kerionics	PCCEL	High-pressure testing, mechanical stress during assembly or operation	Short circuits due to undesired contact between components	Improve requirements for flatness and manufacturing tolerances

Table 7. Electrolife partners degradation phenomena observed

A collection of information and suggestions from commercial electrolysers manufacturers (that are kept anonymous for confidentiality reasons), regarding operational modes and influence on degradation, is provided in the following. The information coming from the different manufacturers is

GA No. 101137802

sometimes conflicting, indicating that some degradation mechanisms are closely related to the specific electrolyser and operative conditions/parameters.

#### **PEMEL**

- Manufacturer A reports to be witnessing, from currently operating systems, that frequent starts and stops (given by the RES supply) do not affect to the lifetime.
- Manufacturer B on the other hand, states that “degradation is affected by frequent start and stops, especially by frequent cold starts”. The manufacturer also provides a formula useful to assess the impact of different events in the residual life of the electrolyser. In this formula “Equivalent Operating Hours of operation” are calculated considering operating hours and (with weights) other events, such as the “number of external triggered emergency shutdowns”, “cold starts” and “standby starts”.
- Manufacturer C reports that pressure highly influence degradation of stack, because high pressure enhances diffusion of H<sub>2</sub> molecules towards the oxygen side, that react and produce in part water, and in part another chemical product (H<sub>2</sub>O<sub>2</sub>) which causes rapid degradation of membrane. The same manufacturer: in the datasheet declares the life of electrolyser in terms of “number of pressure cycles” (instead of “number of operating hours”); recommends to reduce/avoid the operation at minimum load, in order to reduce degradation.

#### **AEL**

- Manufacturer A states that the degradation of its electrolyser system depends mainly on the presence of the KOH inside the system, for its corrosive action. Indeed, the degradation value they guarantee (1%/year), is independent of the system operating hours.
- Manufacturer B recommends to limit/avoid running the plant at over-load (110%) (maximum 30 min per day).



## 5 EU funded project analysis

Extensive knowledge on durability has been generated by previous EU supported projects on fuel cell, e.g. SOFC-LIFE, STAYERS, DEMMEA, CAMELOT, FURTHER-FC, DOLPHIN, ID-FAST, ROBANODE, HEALTH-CODE, ADASTRA, SOCTESQA, which should be used by the project to further generate in-depth understanding of superimposed mechanisms underpinning the degradation of electrolyser stacks over long term operation. All this information is obtained from public deliverables available on Projects & Results (<https://cordis.europa.eu/projects>).

Name of project	Consortium	Technology	TRL	Degradation mechanism studied	Results
SOFC-LIFE	Forschungszentrum Jülich GmbH, Hexis AG, HTceramix / SOFCPower, Topsøe Fuel Cell A/S	Solid Oxide Fuel Cells (SOFC), including Stack Modules and Anode Supported Cells	5-7	Anode morphological changes, nickel-steel corrosion, stability of cathode materials (LSM and LSCF), processes at the cathode-interconnect interface, anode Ni-network degradation, and contact resistance in interconnect-cathode layers	Minor degradation in the anode cermet and some issues with nickel-steel interfaces; slight degradation observed in cathodes (LSM and LSCF). Notable degradation at cathode-interconnect interfaces was a significant factor. Models developed to predict single degradation phenomena were validated with tests: Hexis AG's SOFC stack tests confirmed model predictions, with interconnect steel showing significant impact on degradation; HTceramix short stacks showed accurate prediction of initial degradation and long-term rates, and Topsøe's model captured degradation mainly due to Ni coarsening. Quantitative and empirical models for degradation mechanisms were developed and validated across these partner entities.

STAYERS	Nedstack Fuel Cell Technology B.V., Solvay Specialty Polymers, Solvicore GmbH & Co., SINTEF, JRC	Stationary PEM Fuel Cells	5-7	Membrane durability, MEA degradation (especially cathode), seal and stack housing stability, contamination effects (e.g., CO, NO <sub>2</sub> , SO <sub>2</sub> ), and flow field improvements	Developed a robust PEM fuel cell system with components achieving over 40,000 hours of continuous operation. Improvements in membranes (IMP1 and IMP2) and MEAs led to extended lifetimes. The ASTs revealed the dominant degradation in cathode surface area. Specific degradation and contaminant protocols were established, enabling lifetime prediction and resilience to contaminants. Final field tests demonstrated operational durability, leading to commercial interest for large-scale stationary PEM applications.
CAMELOT	SINTEF, PowerCell, Johnson Matthey Fuel Cells, BMW, FAST Simulations, Chemnitz University of Technology, IMTEK, PRETEXO	PEM Fuel Cells for Transport Applications	5-6	Limitations in MEA performance due to water transport, charge, and heat transfer in ultra-thin, low-catalyst-loaded MEA layers. Evaluated catalyst layer degradation and performance under varying conditions	Developed an updated open-source FAST-FC model with improved water and ion transport simulations, validated with experimental data. Achieved production of ultra-thin reinforced membranes (<10 μm) and characterized MEAs using advanced techniques. Model publicly available on GitHub for community use, enabling predictions of performance limits in next-generation MEAs for automotive applications. Identified optimal catalyst gradients to enhance performance while reducing costs through lower catalyst loading

FURTHER-FC	CEA, DLR, Imperial College London, Toyota Motor Europe, Institut National Polytechnique de Toulouse, University of Montpellier, Paul Scherrer Institute, Hochschule Esslingen, Chemours, University of Calgary	PEM Fuel Cells for High-Current Automotive Applications	5-6	Performance limitations in the Cathode Catalyst Layer (CCL), including oxygen transport, proton conductivity, catalyst distribution, and water management.	Established multiscale models (DNS, PNM, LBM) to study the CCL at different scales. Enhanced CCL designs to optimize oxygen and proton transport, with advanced characterization tools like SANS, AFM, and operando thermography. New catalyst layer designs with tailored porosity and ionomer distributions show promise in improving oxygen transport efficiency and reducing Pt content. The project provides insights into MEA performance limits, supporting future durable and high-performing low-Pt PEMFCs for automotive use
DOLPHIN	CEA, SYMBIO, HEXCEL, CHEMOURS, ZSW, University of Manchester, DMG Mori Additive	Disruptive PEM Fuel Cell Stack with Novel Components and Architecture	5-6	Hydrogen crossover, performance limitations due to rib-channel dimensions, GDL thinning, membrane durability, heat, and mass transfer	Developed 5kW PEMFC stack with lightweight composite terminal plates, Single Layer Graphene (SLG) membrane coating to reduce H <sub>2</sub> permeation, ultra-thin GDL, and new bipolar plate designs. Achieved SLG coatings compatible up to 120°C, with increased durability (6000 hours), reduced cost per kW, and power density improvements meeting KPIs. Key innovations include advanced flow-field designs and coating processes for durability and cost efficiency, promising scalable PEMFC solutions for automotive
ID-FAST	CEA, DLR, ZSW, Politecnico di Milano, FPM, BMW	PEM Fuel Cells for Automotive Applications	5-7	Real-world PEMFC degradation under automotive conditions, cathode catalyst layer (CCL) degradation, GDL degradation, platinum dissolution, carbon	Developed realistic ID-FAST driving cycles based on automotive data to identify degradation mechanisms under operational conditions. Created validated Accelerated Stress Test (AST) protocols for components like MEAs, catalysts, and membranes. ASTs demonstrated acceleration factors of up to 7-10,

				corrosion, Ostwald ripening.	showing degradation profiles close to real-world ageing. Model simulations confirmed temperature and voltage effects on degradation, providing a foundation for standardized AST protocols supporting the automotive sector
ROBANO DE	Foundation for Research and Technology Hellas (FORTH), Technische Universität Clausthal, National Technical University of Athens, Ecole Polytechnique Federale de Lausanne, Consejo Superior de Investigaciones Científicas, Centre National de la Recherche Scientifique, MIRTEC S.A., Saint-Gobain	SOFC Anode Modification	5-7	Anode degradation in hydrogen and natural gas-fueled SOFCs, focusing on microstructural changes, carbon deposition, sulfur poisoning, oxidation/reduction effects, and thermal/electrochemical sintering.	Developed Ni-based cermet anodes modified with Au, Mo, and Re to improve carbon and sulfur tolerance. The modified anodes showed enhanced catalytic activity, carbon tolerance, and electrochemical performance. Au and Mo modifications specifically improved carbon tolerance and catalytic performance, with Mo strengthening Ni-O bonds, albeit reducing CH <sub>4</sub> reforming performance. Two mathematical models were created to predict degradation rates, linking polarization to metal particle size and three-phase boundary length, aiding in durable anode design.
HEALTH-CODE	Università degli Studi di Salerno (UNISA), EIFER, UFC, AAU, BPSE	PEM Fuel Cells with EIS-based Diagnostic Tool	5-6	Fuel and oxidant starvation, drying, flooding, CO and sulfur contamination, fuel composition changes	Developed an embedded EIS-based diagnostic tool that achieved 100% detection of faults and over 90% isolation of incipient faults in $\mu$ -CHP and backup systems. It enables real-time fault detection and classification to support maintenance and reliability improvements. The

					diagnostic tool identified faults early to avoid irreversible stack damage, with seamless integration and a minimal cost impact on the total system cost. This tool allows for remote monitoring, enhancing operational reliability, and optimizing maintenance scheduling.
ADASTR A	ENEA, EPFL, IEES, CEA, DTU, UNIGE, SolidPower , Sunfire, EIFER, UNISA	Solid Oxide Cells (SOC) for CHP and P2X Application s	5-7	Degradation mechanisms including redox cycling, thermal and load cycling, fuel/oxidant starvation, sulfur poisoning, steam starvation, high-temperature exposure, overpotential aging, interconnect corrosion, and electrode microstructural evolution.	Developed 12 Accelerated Stress Test (AST) protocols, segmented into in-situ and ex-situ tests, allowing early detection and quantification of SOC degradation. Testing methods included electrochemical impedance spectroscopy, THD analysis, and post-operation characterization. Results yielded protocols with accelerated factors up to 10, reducing qualification time and enhancing SOC durability predictions. Key outcomes included tools for predictive maintenance, extended durability, and improved resource efficiency for SOC manufacturing
SOCTES QA	DTU Energy, DLR, CEA, ENEA, JRC, EIFER, NTU	Solid Oxide Fuel Cells (SOFC) and Electrolysis Cells (SOEC) for micro-CHP, APU, electrolysis , and reversible energy storage systems	5-7	Degradation from thermal cycling, start-up/shut-down cycles, constant current operation, variable current, gas composition changes, and reactant utilization. Addressed both steady state and dynamic degradation modes.	Developed and validated 11 test modules, including start-up, impedance spectroscopy, and shut-down protocols, integrated into 5 application-specific test programs. Protocols achieved high reproducibility and relevance for industrial application and are being implemented in IEC standards. The project advanced standardized testing for SOFC/SOEC performance, enhancing reliability and market readiness of SOC systems

Table 8. Summary of EU project funded related to degradation studies

The following summary provides insights into various projects focused on advancing fuel cell and electrolysis technologies. This information, sourced from CORDIS (<https://cordis.europa.eu/>), highlights the collaborative efforts of different consortiums addressing specific degradation mechanisms to improve resilience, operational life, and scalability across diverse industrial applications.

#### SOFC-LIFE

- Tech: SOFC (Solid Oxide Fuel Cells)
- Degradation: Anode and cathode interface degradation, nickel-steel corrosion

## GA No. 101137802

- Results: Minor degradation was observed, with validated models accurately predicting degradation patterns, supporting improved stack durability in SOFC systems.

## STAYERS

- Tech: Stationary PEM Fuel Cells
- Degradation: Membrane, MEA, and contamination effects
- Results: Developed a PEM fuel cell system with 40,000+ hours of continuous operation, with enhanced membranes and MEAs contributing to extended lifetimes and resilience in stationary applications.

## CAMELOT

- Tech: PEM Fuel Cells for Transport
- Degradation: Catalyst layer degradation and MEA performance limitations due to water, charge, and heat transfer
- Results: Created the improved FAST-FC model and produced ultra-thin membranes, advancing MEA performance predictions for automotive applications.

## FURTHER-FC

- Tech: High-Current PEM Fuel Cells for Automotive
- Degradation: Cathode catalyst layer limitations
- Results: Optimized oxygen transport and lowered Pt usage, using advanced modeling to enhance automotive MEA designs.

## DOLPHIN

- Tech: Disruptive PEM Stack Architecture
- Degradation: Hydrogen crossover, rib-channel, and GDL limitations
- Results: New PEMFC stack design with improved power density and durability, providing scalable solutions for automotive applications.

## ID-FAST

- Tech: PEM Fuel Cells for Automotive
- Degradation: CCL, GDL degradation, Pt dissolution, and carbon corrosion
- Results: Developed AST protocols that replicate real-world degradation, enhancing durability standards for automotive PEMFCs.

## ROBANODE

- Tech: SOFC Anode Modification
- Degradation: Anode degradation from fuel composition and conditions
- Results: Modified Ni-based anodes with improved carbon and sulfur tolerance, reducing degradation in SOFCs fueled by hydrogen and natural gas.

## HEALTH-CODE

- Tech: PEM Fuel Cells with Diagnostic Tool
- Degradation: Starvation, contamination, and fuel composition issues
- Results: EIS-based diagnostic tool developed for fault detection, enhancing reliability and reducing maintenance in  $\mu$ -CHP and backup systems.

## ADASTRA

- Tech: SOEL for CHP and Power-to-X Applications

GA No. 101137802

- Degradation: Redox cycling, thermal/load cycling, sulfur poisoning
- Results: 12 AST protocols were developed to study SOC degradation, improving predictive maintenance and supporting efficient SOC manufacturing.

#### SOCTESQA

- Tech: SOFC and SOEC for micro-CHP, APU, electrolysis, and energy storage
- Degradation: Thermal cycling, start-up/shut-down cycles, variable current operation
- Results: Developed 11 standardized testing modules for SOFC/SOEC systems, increasing reliability and industrial readiness for these technologies.

#### Other relevant projects:

**INSIDE** (In-situ Diagnostics in Water Electrolysers) Grant agreement ID: 621237

Consortium: Coordinator: DEUTSCHES ZENTRUM FÜR LUFT - UND RAUMFAHRT EV (Germany)

- Tech: Diagnostic tools for AEL, AEMEL, and PEMEL electrolysers, integrating real-time sensors.
- Challenges: Corrosion from 30% KOH, PCB damage, and connector leakage during ASTs; limited testing due to time constraints.
- Results: Modular PEEK sensor housing tested in "dry" conditions; 10-cell stack tested for performance, but AST protocols remained undefined due to persistent leakage issues.

**RESELYSER** (Hydrogen from RES: pressurized alkaline electrolyser with high efficiency and wide operating range); Grant agreement ID: 278732

Consortium: Coordinator: German Aerospace Center (DLR)

- Tech: High-pressure AWE with innovative separator membrane and internal electrolyte circulation, targeting renewable energy integration.
- Performance: Achieved 76% HHV efficiency at 0.75 A/cm<sup>2</sup>; stable operation up to 90°C; >90% efficiency retention over 1,100 on/off cycles.
- Materials: NiAlMo-coated cathodes and NiAl-coated anodes; cathode stability up to 2,930 hours; anode stability for 497 days.
- Results: E-bypass-separator reduced gas impurities and improved mass transfer; stack costs of €2,300/(Nm<sup>3</sup>/h) at 65 bar; degradation limited cell efficiency to 72% after extended cycling tests.

## 6 Characterization techniques

This section outlines the comprehensive characterization techniques employed for assessing the performance, durability, and degradation of electrolyser systems. The techniques are categorized based on the type of electrolyser technology: Alkaline Electrolysis (AEL), Anion Exchange Membrane Electrolysis (AEMEL), Proton Exchange Membrane Electrolysis (PEMEL), Solid Oxide Electrolysis (SOEL), and Proton Ceramic Conductivity Electrolysis (PCCEL).

For each technology, the table identifies specific characterization techniques, their purposes, and the focus areas of analysis. These methodologies are vital for understanding the underlying mechanisms of degradation, identifying material and structural weaknesses, and guiding improvements in design and material selection.

### 6.1.1 AEL

Characterization Techniques	Purpose	Focus Areas
Electrochemical Impedance Spectroscopy (EIS)	Assess resistance changes in electrodes and electrolytes due to degradation	Catalyst layer integrity, gas diffusion resistance
Distribution of Relaxation Times (DRT)	Decompose impedance data for specific degradation	Separator/electrode interface characteristics
Scanning Electron Microscopy (SEM)	Visualize electrode surface morphology and detect degradation	Electrode surface roughness, oxide layer formation
Energy-Dispersive X-ray Spectroscopy (EDX)	Elemental analysis and mapping can aid information on the catalysts composition	Electrodes degradation
Transmission electron microscopy (TEM)	Active site distribution and structural changes	Catalyst stability
Atomic Force Microscopy (AFM)	Surface topography/ morphology and changes in surface roughness	Electrodes degradation
UV-Vis spectroscopy (UV-Vis)	Detect the dissolution of metal, alloys and passive layers at very low concentration levels.	Catalyst stability
X-ray Photoelectron Spectroscopy (XPS)	Analyze chemical composition and oxidation states	Catalyst stability, corrosion
X-ray Diffraction (XRD)	Identify crystalline phases and structural changes	Phase stability, electrode degradation
Hydrogen and Oxygen Crossover Testing	Assess gas separation efficiency and safety	Membrane porosity, gas purity
Mass Spectrometry (MS)	Quantify trace contaminants in product gases	Purity of H <sub>2</sub> /O <sub>2</sub> , detection of degradation products

Table 9. Characterization techniques for AEL



### 6.1.2 AEMEL

Characterization Techniques	Purpose	Focus Areas
Electrochemical Impedance Spectroscopy (EIS)	Measure internal resistance	Ionic/electronic resistance, degradation tracking
Distribution of Relaxation Times (DRT)	Decompose impedance data for specific degradation	Membrane/electrode interface characteristics
Scanning Electron Microscopy (SEM)	Visualize electrode surface morphology and detect degradation	Electrode surface roughness, oxide layer formation
X-ray Photoelectron Spectroscopy (XPS)	Analyze chemical composition and oxidation states	Catalyst stability, corrosion
X-ray Diffraction (XRD)	Identify crystalline phases and structural changes	Phase stability, electrode degradation
Transmission electron microscopy (TEM)	Active site distribution and structural changes	Catalyst stability
Ultraviolet-visible spectro-photometry (UV-Vis)	Detect the dissolution of metal, alloys and passive layers at very low concentration levels.	Catalyst stability
Fourier Transform Infrared Spectroscopy (FTIR)	Identify chemical bonds, detect degradation	Chemical stability, functional group analysis
Thermogravimetric Analysis (TGA)	Assess thermal stability	Component durability under cycling
Ion Chromatography (IC)	Measure ion leaching/composition in electrolyte	Alkaline resistance, chemical stability
Hydrogen and Oxygen Crossover Testing	Measure gas crossover rates for membrane degradation	Membrane durability, contaminant buildup
Mass Spectrometry (MS)	Quantify trace contaminants in product gases	Purity of H <sub>2</sub> /O <sub>2</sub> , detection of degradation products

Table 10. Characterization techniques for AEMEL

### 6.1.3 PEMEL

Characterization Techniques	Purpose	Focus Areas
Electrochemical Impedance Spectroscopy (EIS)	Track membrane/electrode resistance changes	Ionic resistance, , electrical resistance,, catalyst layer stability
Distribution of Relaxation Times (DRT)	Decompose impedance data for specific degradation	Membrane/electrode interface characteristics
X-ray Photoelectron Spectroscopy (XPS)	Analyze catalyst surface chemistry	Catalyst oxidation, contamination
Cross-sectional Scanning Electron Microscopy (SEM)	Examine MEA layers and degradation	Membrane thinning, structural changes; membrane intrusion into PTL

GA No. 101137802

Inductively Coupled Plasma Mass Spectrometry (ICP-MS)	Quantify catalyst metal dissolution	Catalyst stability, contamination
Transmission electron microscopy (TEM)	Active site distribution and structural changes	Catalyst stability
X-ray Diffraction (XRD)	Identify crystalline phases and structural changes	Phase stability, electrode degradation
Hydrogen and Oxygen Crossover Testing	Assess membrane gas crossover	Membrane integrity, durability under load; ; catalyst layer structure
Fluoride Emission Rate (FER) Testing	Measure fluoride release for membrane degradation	Membrane longevity, load cycling impact
Mass Spectrometry (MS)	Quantify trace contaminants in product gases	Purity of H <sub>2</sub> /O <sub>2</sub> , detection of degradation products

Table 11. Characterization techniques for PEMEL

### 6.1.4 SOEL

Characterization Techniques	Purpose	Focus Areas
Electrochemical Impedance Spectroscopy (EIS)	Measure internal resistance	Ionic/electronic resistance, degradation tracking
Distribution of Relaxation Times (DRT)	Decompose impedance data for specific degradation	Electrode/membrane interface, oxygen electrode degradation
Raman Spectroscopy	Analyze structural changes in materials	High-temperature phase transitions, catalyst degradation
Thermogravimetric Analysis (TGA)	Assess thermal stability	Durability under high-temperature cycling
Scanning Electron Microscopy (SEM)	Morphological analysis of electrodes	Surface roughness, structural degradation
X-ray Diffraction (XRD)	Analyze crystalline structure	Catalyst sintering, phase identification
Transmission electron microscopy (TEM)	Active site distribution and structural changes	Catalyst stability
X-ray Diffraction (XRD)	Identify crystalline phases and structural changes	Phase stability, electrode degradation
Mass Spectrometry (MS)	Quantify trace contaminants in product gases	Purity of H <sub>2</sub> /O <sub>2</sub> , detection of degradation products

Table 12. Characterization techniques for SOEL

### 6.1.5 PCCEL

Characterization Techniques	Purpose	Focus Areas
Electrochemical Impedance Spectroscopy (EIS)	Measure internal resistance	Proton conductivity, degradation tracking
Distribution of Relaxation Times (DRT)	Decompose impedance data for specific degradation	Electrode/membrane interface, proton transport losses
Fourier Transform Infrared Spectroscopy (FTIR)	Identify chemical bonds, detect degradation	Chemical stability, functional group identification

GA No. 101137802

Ion Chromatography (IC)	Measure ion leaching/composition in electrolyte	Alkaline or acidic stability, ionic contamination
Thermogravimetric Analysis (TGA)	Assess thermal stability	Durability under thermal cycling
Scanning Electron Microscopy (SEM)	Morphological analysis of electrodes	Microstructure, structural degradation
X-ray Diffraction (XRD)	Analyze crystalline structure	Catalyst sintering, phase identification
Transmission electron microscopy (TEM)	Active site distribution and structural changes	Catalyst stability
Hydrogen and Oxygen Crossover Testing	Measure gas crossover rates for membrane degradation	Membrane integrity, contaminant buildup
Mass Spectrometry (MS)	Quantify trace contaminants in product gases	H <sub>2</sub> /O <sub>2</sub> purity, detection of degradation products

Table 13. Characterization techniques for PCCEL

## 7 Exploring Interconnections between Technologies

Electrolysis technologies, both low-temperature (AEL, AEMEL, PEMEL) and high-temperature (SOEL, PCCEL), encounter degradation mechanisms that impact the efficiency and durability of their components. While the operating principles and environmental conditions of these systems differ, several degradation phenomena reveal overlapping challenges.

### Common Features in Degradation Mechanisms

#### Material Corrosion and Dissolution:

- **Low-Temperature Electrolysis:** Corrosion and dissolution of electrode materials are prevalent, particularly in alkaline and acidic environments. In PEMEL, the dissolution of iridium at the anode under high potential accelerates degradation, while in AEL and AEMEL, cathodic corrosion due to hydroxide ions is significant
- **High-Temperature Electrolysis:** Similar issues arise in SOEL and PCCEL, where metal oxides used in electrodes degrade under oxidative conditions. The combination of high temperatures and reactive species (e.g., oxygen ions) destabilizes electrode materials, leading to dissolution.

#### Gas Bubble Formation:

- **Low-Temperature Electrolysis:** Gas bubbles formed during the hydrogen and oxygen evolution reactions obstruct catalyst surfaces, hinder mass transfer, and increase local mechanical stress, leading to detachment of catalyst layers
- **High-Temperature Electrolysis:** Although operating in a different regime, SOEL and PCCEL encounter bubble-induced issues, particularly at high current densities, where gas phase buildup at the electrodes disrupts ionic conductivity and thermal stability

#### Electrode Delamination and Structural Instability:

- **Low-Temperature Electrolysis:** Electrodes can delaminate due to differential stresses, chemical reactions, and repeated cycling of operational conditions. In PEMEL, catalyst layer detachment is exacerbated by water management challenges and ionomer degradation
- **High-Temperature Electrolysis:** Thermal cycling in SOEL leads to mechanical stress and delamination of ceramic electrodes. Similar to low-temperature systems, material incompatibilities between the electrolyte and electrode can exacerbate this issue

#### Deactivation of Catalytic Sites

- **Low-Temperature Electrolysis:** Catalyst deactivation in PEMEL, AEL, and AEMEL occurs due to poisoning (e.g., CO, sulfur species), surface oxidation, and sintering of nanoparticles under high potential and prolonged operation.
- **High-Temperature Electrolysis:** Catalyst deactivation in SOEL and PCCEL is driven by sintering and agglomeration of active sites under extreme temperatures. Poisoning by contaminants (e.g., silica) further reduces catalytic activity

GA No. 101137802

#### Membrane or Electrolyte Instability:

- Low-Temperature Electrolysis: Chemical degradation of membranes in PEMEL (fluoropolymer-based) and AEMEL (quaternary ammonium-based) due to attack by reactive intermediates such as hydroxyl radicals or nucleophilic ions is common.
- High-Temperature Electrolysis: In SOEL and PCCEL, the stability of ceramic electrolytes (e.g., YSZ in SOEL) is compromised by chemical interactions with electrode materials and high thermal stress. For the purpose of which barrier layers are used.

#### Operational Overlaps

##### Thermal and Mechanical Stress:

- Both technologies experience material degradation due to temperature-induced stresses. Low-temperature systems face mechanical stresses from differential expansion during thermal cycling, while high-temperature systems endure similar stresses but at higher magnitudes due to extreme operating temperatures

##### Contaminant-Induced Instabilities

- Contaminants such as sulfur compounds, and metal ions disrupt ionic transport and poison catalysts across both low- and high-temperature systems, necessitating effective purification of feedstocks

##### Intermittent Operation Challenges:

- Coupling with renewable energy sources introduces intermittent operations, creating transient stresses that affect both technologies. Shutdown and startup cycles exacerbate mechanical and chemical degradation

By understanding these commonalities, cross-technology strategies can be developed, such as robust material design, advanced coatings, and optimized operational protocols. This alignment not only improves individual system lifetimes but also enables more effective integration into diverse energy systems.

## 8 Conclusions

The ELECTROLIFE D2.1 report, titled Degradation Phenomena Compendium, is a pivotal contribution to understanding the complex interplay of mechanisms that influence the performance and longevity of electrolysis technologies. As a cornerstone of the EU-funded ELECTROLIFE project, this document provides a comprehensive, multidisciplinary analysis that bridges fundamental research and industrial applicability. Below are the key conclusions drawn from the report:

1. **Understanding Degradation Mechanisms:** The report thoroughly examines degradation phenomena across five primary electrolysis technologies—Alkaline Electrolysis (AEL), Anion Exchange Membrane Electrolysis (AEMEL), Proton Exchange Membrane Electrolysis (PEMEL), Solid Oxide Electrolysis (SOEL), and Proton-Conducting Ceramic Electrolysis (PCCEL). Each technology's unique components, such as catalysts, membranes, and interconnectors, exhibit distinct degradation behaviors influenced by chemical, mechanical, and environmental stressors.

### 2. Critical Components and Stressors:

**Catalysts:** Challenges include corrosion, dissolution, and deactivation, which affect electrochemical performance. **Membranes and Ionomers:** These are vulnerable to operational stressors, including temperature variations, contaminants, and mechanical fatigue. **Porous Transport Layers and Bipolar Plates:** These components face wear from contamination, flow-induced stresses, and operational conditions. **Contaminants:** External impurities exacerbate material degradation, reducing system efficiency and reliability.

3. **Operational Impacts:** The report highlights how operational modes, such as load fluctuations, partial loads, and on/off cycles, significantly impact degradation. High-temperature operations (SOEL and PCCEL) and load dynamics in low-temperature systems (AEL, AEMEL, PEMEL) reveal the need for advanced control strategies to mitigate adverse effects.

4. **Interconnections and Synergies:** By comparing degradation across different technologies, the compendium identifies commonalities and unique vulnerabilities. These insights pave the way for cross-technology improvements and the development of shared mitigation strategies.

5. **Advancing Characterization Techniques:** Detailed characterization of material stress responses is critical to advancing electrolyser design. The use of advanced methods, such as electrochemical impedance spectroscopy (EIS) and accelerated durability tests (ADT), provides valuable data for modeling and predicting degradation.

6. **Industrial and EU Project Integration:** Drawing on experiences from industrial stakeholders and other EU-funded projects, the report emphasizes the importance of practical data integration to ensure theoretical models align with real-world applications.

### 7. Recommendations for Future Research:

GA No. 101137802

Emphasizing self-healing materials and robust catalyst designs to enhance durability.  
Developing advanced protective coatings and membranes tailored to specific stressors.  
Leveraging digital twins to simulate degradation and predict long-term performance.

8.Call to Action: The report serves as both a technical guide and a strategic blueprint for advancing hydrogen production technologies. It underscores the need for continued innovation and collaboration to achieve scalable, cost-effective, and durable solutions.

In essence, the D2.1 deliverable is a vital resource for both researchers and industry professionals. By addressing the intricate challenges of electrolyser degradation, it lays the foundation for future advancements, driving the hydrogen economy forward and supporting the transition to a sustainable energy landscape.

## 9 Risks and interconnections

### 9.1 Risks/problems encountered

If applicable (consider using table below to report risks – and solutions ! – encountered for the activities/tasks related to this deliverable)

Risk No.	What is the risk	Probability of risk occurrence <sup>1</sup>	Effect of risk <sup>1</sup>	Solutions to overcome the risk
WP2-1	Insufficient availability of PCCEL degradation data due to resource constraints or long test durations.	2 (Medium)	Limits the availability of comprehensive data needed for experimental campaigns.	Address through design of experimental campaigns under Task 2.2 of WP2 to systematically generate and structure the required data.
WP2-2	Insufficient availability of SOEL degradation data due to resource constraints or long test durations.	2 (Medium)	Limits the robustness of degradation databases.	Mitigate by leveraging the experimental campaigns planned in Task 2.2 of WP2 to optimize data collection and improve availability.

<sup>1)</sup> Probability risk will occur: 1 = high, 2 = medium, 3 = Low

### 9.2 Interconnections with other deliverables

This deliverable is closely connected to the activities detailed in Deliverable 4.1, “Specification, Terminology, and Harmonized Protocols for LTEL,” which defines the tests and stressors to be addressed in the subsequent phases of the Electrolife project. Furthermore, it serves as a foundational pillar for WP3: Degradation Modelling and Lifetime Prediction and WP5: Testing and Diagnostic Tools.



## 10 Reference

- [1] A.. Pilenga, G.. Tsotridis, EU harmonised terminology for low temperature water electrolysis for energy storage applications, Publications Office of the European Union, 2018.
- [2] IEC TS 62282-1:2013, 2017.
- [3] Y. Zuo, S. Bellani, M. Ferri, G. Saleh, D. V Shinde, M.I. Zappia, R. Brescia, M. Prato, L. De Trizio, I. Infante, F. Bonaccorso, L. Manna, High-Performance Alkaline Water Electrolyzers Based on Ru-Perturbed Cu Nanoplatelets Cathode, *Nat Commun* 14 (2023) 4680.  
<https://doi.org/10.1038/s41467-023-40319-5>.
- [4] H. Tüysüz, Alkaline Water Electrolysis for Green Hydrogen Production, *Acc Chem Res* 57 (2024) 558–567. <https://doi.org/10.1021/acs.accounts.3c00709>.
- [5] N. Guillet, P. Millet, Alkaline Water Electrolysis, in: *Hydrogen Production*, John Wiley & Sons, Ltd, 2015: pp. 117–166. <https://doi.org/10.1002/9783527676507.ch4>.
- [6] N.A. Gladkikh, M.A. Maleeva, L.B. Maksaeva, M.A. Petrunin, A.A. Rybkina, T.A. Yurasova, A.I. Marshakov, R.K. Zalavutdinov, Localized Dissolution of Carbon Steel Used for Pipelines under Constant Cathodic Polarization Conditions, *International Journal of Corrosion and Scale Inhibition* 7 (2018).
- [7] S. Choudhary, K. Ogle, O. Gharbi, S. Thomas, N. Birbilis, Recent Insights in Corrosion Science from Atomic Spectroelectrochemistry, *Electrochemical Science Advances* 2 (2022) e2100196. <https://doi.org/10.1002/elsa.202100196>.
- [8] T.J.P. Hersbach, M.T.M. Koper, Cathodic Corrosion: 21st Century Insights into a 19th Century Phenomenon, *Curr Opin Electrochem* 26 (2021) 100653. <https://doi.org/10.1016/j.coelec.2020.100653>.
- [9] M.M. Elnagar, L.A. Kibler, T. Jacob, Metal deposition and electrocatalysis for elucidating structural changes of gold electrodes during cathodic corrosion, *Green Chemistry* 25 (2023) 6238–6252. <https://doi.org/10.1039/D3GC01614E>.
- [10] N. Esfandiari, M. Aliofkhazraei, A.N. Colli, F.C. Walsh, S. Cherevko, L.A. Kibler, M.M. Elnagar, P.D. Lund, D. Zhang, S. Omanovic, J. Lee, Metal-based cathodes for hydrogen production by alkaline water electrolysis: Review of materials, degradation mechanism, and durability tests, *Prog Mater Sci* 144 (2024) 101254. <https://doi.org/10.1016/j.pmatsci.2024.101254>.
- [11] I. Flis-Kabulska, J. Flis, Electroactivity of Ni–Fe cathodes in alkaline water electrolysis and effect of corrosion, *Corros Sci* 112 (2016) 255–263. <https://doi.org/10.1016/j.corsci.2016.07.017>.
- [12] J.T. Kraakman, Gas Crossover in Alkaline Water Electrolysis, n.d.
- [13] M.M. Bakker, D.A. Vermaas, Gas bubble removal in alkaline water electrolysis with utilization of pressure swings, *Electrochim Acta* 319 (2019) 148–157. <https://doi.org/10.1016/j.electacta.2019.06.049>.
- [14] S. Holmin, L.-Å. Näslund, Á.S. Ingason, J. Rosen, E. Zimmermann, Corrosion of ruthenium dioxide based cathodes in alkaline medium caused by reverse currents, *Electrochim Acta* 146 (2014) 30–36. <https://doi.org/10.1016/j.electacta.2014.09.024>.
- [15] B. El Ibrahimy, J.V. Nardeli, L. Guo, An Overview of Corrosion, in: 2021: pp. 1–19. <https://doi.org/10.1021/bk-2021-1403.ch001>.

- [16] J. Ćwiek, Prevention methods against hydrogen degradation of steel, 2010. [www.journalamme.org](http://www.journalamme.org).
- [17] P. Jemmelly, S. Mischler, D. Landolt, Tribocorrosion behaviour of Fe–17Cr stainless steel in acid and alkaline solutions, *Tribol Int* 32 (1999) 295–303. [https://doi.org/10.1016/S0301-679X\(99\)00051-1](https://doi.org/10.1016/S0301-679X(99)00051-1).
- [18] S. Sebbahi, A. Assila, A. Alaoui Belghiti, S. Laasri, S. Kaya, E.K. Hlil, S. Rachidi, A. Hajjaji, A comprehensive review of recent advances in alkaline water electrolysis for hydrogen production, *Int J Hydrogen Energy* 82 (2024) 583–599. <https://doi.org/10.1016/j.ijhydene.2024.07.428>.
- [19] C. Li, J.-B. Baek, Recent Advances in Noble Metal (Pt, Ru, and Ir)-Based Electrocatalysts for Efficient Hydrogen Evolution Reaction, *ACS Omega* 5 (2020) 31–40. <https://doi.org/10.1021/acsomega.9b03550>.
- [20] G. Gao, G. Zhao, G. Zhu, B. Sun, Z. Sun, S. Li, Y.-Q. Lan, Recent advancements in noble-metal electrocatalysts for alkaline hydrogen evolution reaction, *Chinese Chemical Letters* 36 (2025) 109557. <https://doi.org/10.1016/j.ccllet.2024.109557>.
- [21] M. Chatenet, B.G. Pollet, D.R. Dekel, F. Dionigi, J. Deseure, P. Millet, R.D. Braatz, M.Z. Bazant, M. Eikerling, I. Staffell, P. Balcombe, Y. Shao-Horn, H. Schäfer, Water electrolysis: from textbook knowledge to the latest scientific strategies and industrial developments, *Chem Soc Rev* 51 (2022) 4583–4762. <https://doi.org/10.1039/D0CS01079K>.
- [22] M.N. Lakhan, A. Hanan, A. Hussain, I. Ali Soomro, Y. Wang, M. Ahmed, U. Aftab, H. Sun, H. Arandiyani, Transition metal-based electrocatalysts for alkaline overall water splitting: advancements, challenges, and perspectives, *Chemical Communications* 60 (2024) 5104–5135. <https://doi.org/10.1039/D3CC06015B>.
- [23] S. Barua, A. Balčiūnaitė, D. Upskuvienė, J. Vaičiūnienė, L. Tamašauskaitė-Tamašiūnaitė, E. Norkus, 3D Nickel–Manganese bimetallic electrocatalysts for an enhanced hydrogen evolution reaction performance in simulated seawater/alkaline natural seawater, *Int J Hydrogen Energy* 79 (2024) 1490–1500. <https://doi.org/10.1016/j.ijhydene.2024.07.131>.
- [24] X. Wang, J. Zhou, W. Cui, F. Gao, Y. Gao, F. Qi, Y. Liu, X. Yang, K. Wang, Z. Li, Y. Yang, J. Chen, W. Sun, L. Sun, H. Pan, Electron Manipulation and Surface Reconstruction of Bimetallic Iron–Nickel Phosphide Nanotubes for Enhanced Alkaline Water Electrolysis, *Advanced Science* 11 (2024). <https://doi.org/10.1002/advs.202401207>.
- [25] L. Xu, W. Li, J. Luo, L. Chen, K. He, D. Ma, S. Lv, D. Xing, Carbon-based materials as highly efficient catalysts for the hydrogen evolution reaction in microbial electrolysis cells: Mechanisms, methods, and perspectives, *Chemical Engineering Journal* 471 (2023) 144670. <https://doi.org/10.1016/j.cej.2023.144670>.
- [26] H. Fei, J. Dong, M.J. Arellano-Jiménez, G. Ye, N. Dong Kim, E.L.G. Samuel, Z. Peng, Z. Zhu, F. Qin, J. Bao, M.J. Yacamán, P.M. Ajayan, D. Chen, J.M. Tour, Atomic cobalt on nitrogen-doped graphene for hydrogen generation, *Nat Commun* 6 (2015) 8668. <https://doi.org/10.1038/ncomms9668>.
- [27] E. Zhang, W. Song, Review—Self-Supporting Electrocatalysts for HER in Alkaline Water Electrolysis, *J Electrochem Soc* 171 (2024) 052503. <https://doi.org/10.1149/1945-7111/ad4c0d>.

- [28] A. Goswami, D. Ghosh, D. Pradhan, K. Biradha, *In Situ* Grown Mn(II) MOF upon Nickel Foam Acts as a Robust Self-Supporting Bifunctional Electrode for Overall Water Splitting: A Bimetallic Synergistic Collaboration Strategy, *ACS Appl Mater Interfaces* 14 (2022) 29722–29734. <https://doi.org/10.1021/acsami.2c04304>.
- [29] M.S.S. Danish, Exploring metal oxides for the hydrogen evolution reaction (HER) in the field of nanotechnology, *RSC Sustainability* 1 (2023) 2180–2196. <https://doi.org/10.1039/D3SU00179B>.
- [30] Z. Morgan Chan, D.A. Kitchaev, J. Nelson Weker, C. Schnedermann, K. Lim, G. Ceder, W. Tumas, M.F. Toney, D.G. Nocera, Electrochemical trapping of metastable Mn<sup>3+</sup> ions for activation of MnO<sub>2</sub> oxygen evolution catalysts, *Proceedings of the National Academy of Sciences* 115 (2018). <https://doi.org/10.1073/pnas.1722235115>.
- [31] S. Díaz-Coello, D. Winkler, C. Griesser, T. Moser, J.L. Rodríguez, J. Kunze-Liebhäuser, G. García, E. Pastor, Highly Active W<sub>2</sub>C-Based Composites for the HER in Alkaline Solution: the Role of Surface Oxide Species, *ACS Appl Mater Interfaces* 16 (2024) 21877–21884. <https://doi.org/10.1021/acsami.4c01612>.
- [32] V.N. Kuleshov, N. V. Kuleshov, S.A. Dovbysh, E.Ya. Udris, Yu.A. Slavnov, S.A. Grigoriev, N.A. Yashtulov, High-performance composite cathodes for Alkaline electrolysis of water, *Russian Journal of Applied Chemistry* 90 (2017) 389–392. <https://doi.org/10.1134/S1070427217020107>.
- [33] Cathode alkaline water electrolysis electrode (PGM-free), <https://www.fuelcellstore.com/cathode-alkaline-water-electrolysis-electrode> (n.d.).
- [34] Electrochemical Basis of Corrosion, [https://www.gamry.com/framework%20help/html5%20-%20tripane%20-%20audience%20a/content/dc/introduction\\_to\\_dc\\_corrosion/electrochemical%20basis%20of%20corrosion.htm](https://www.gamry.com/framework%20help/html5%20-%20tripane%20-%20audience%20a/content/dc/introduction_to_dc_corrosion/electrochemical%20basis%20of%20corrosion.htm) (n.d.).
- [35] N. Sato, Basics of Corrosion Chemistry, in: *Green Corrosion Chemistry and Engineering*, Wiley, 2011: pp. 1–32. <https://doi.org/10.1002/9783527641789.ch1>.
- [36] F. Safizadeh, G. Houlachi, E. Ghali, Electrocatalytic activity and corrosion behavior of Fe Mo and Fe Mo P coatings employed as cathode material for alkaline water electrolysis, *Int J Hydrogen Energy* 43 (2018) 7938–7945. <https://doi.org/10.1016/j.ijhydene.2018.03.071>.
- [37] L. Öjefors, Self-discharge of the alkaline iron electrode, *Electrochim Acta* 21 (1976) 263–266. [https://doi.org/10.1016/0013-4686\(76\)80016-3](https://doi.org/10.1016/0013-4686(76)80016-3).
- [38] T.J.P. Hersbach, I.T. McCrum, D. Anastasiadou, R. Wever, F. Calle-Vallejo, M.T.M. Koper, Alkali Metal Cation Effects in Structuring Pt, Rh, and Au Surfaces through Cathodic Corrosion, *ACS Appl Mater Interfaces* 10 (2018) 39363–39379. <https://doi.org/10.1021/acsami.8b13883>.
- [39] P. Li, M. Du, Effect of chloride ion content on pitting corrosion of dispersion-strengthened-high-strength steel, *Corrosion Communications* 7 (2022) 23–34. <https://doi.org/10.1016/j.corcom.2022.03.005>.
- [40] A.I. Yanson, P. Rodriguez, N. Garcia-Araez, R. V. Mom, F.D. Tichelaar, M.T.M. Koper, Cathodic Corrosion: A Quick, Clean, and Versatile Method for the Synthesis of Metallic Nanoparticles, *Angewandte Chemie International Edition* 50 (2011) 6346–6350. <https://doi.org/10.1002/anie.201100471>.

- [41] H.J. Chuang, S.Y. Chen, S. I. i. Chan, Corrosion and hydrogen damage resistance of stainlesssteels in Ni / MHx batteries, *Corros Sci* 41 (1999) 1347–1358. [https://doi.org/10.1016/S0010-938X\(98\)00189-9](https://doi.org/10.1016/S0010-938X(98)00189-9).
- [42] I. Flis-Kabulska, J. Flis, Hydrogen evolution and corrosion products on iron cathodes in hot alkaline solution, *Int J Hydrogen Energy* 39 (2014) 3597–3605. <https://doi.org/10.1016/j.ijhydene.2013.12.158>.
- [43] D.E. Williams, R.C. Newman, Q. Song, R.G. Kelly, Passivity breakdown and pitting corrosion of binary alloys, *Nature* 350 (1991) 216–219. <https://doi.org/10.1038/350216a0>.
- [44] , J. Jankowski, Electrochemical Methods for Corrosion Rate Determination Under Cathodic Polarisation Conditions - A Review Part I - DC Methods, *Corrosion Reviews* 20 (2002) 159–178. <https://doi.org/10.1515/CORRREV.2002.20.3.159>.
- [45] M.G.R. Mahlobo, T.W.P. Seadira, M.M. Mabuza, P.A. Olubambi, Application of voltammetry as a technique to monitor cathodic protection performance of steel in simulated soil solution, *Electrochem Commun* 166 (2024) 107777. <https://doi.org/10.1016/j.elecom.2024.107777>.
- [46] T.A. Hemkemeier, F.C.R. Almeida, A. Sales, A.J. Klemm, Corrosion monitoring by open circuit potential in steel reinforcements embedded in cementitious composites with industrial wastes, *Case Studies in Construction Materials* 16 (2022) e01042. <https://doi.org/10.1016/j.cscm.2022.e01042>.
- [47] C. Wang, Y. Yu, P. He, J. Zhang, X. Ma, H. Zhang, H. Li, M. Shao, Electrochemical Corrosion Behavior of CrFeCoNi and CrMnFeCoNi Coatings in Salt Solution, *Metals (Basel)* 12 (2022) 1752. <https://doi.org/10.3390/met12101752>.
- [48] M. Prazák, The Polarization Resistance Method for Corrosion Testing, *Materials and Corrosion* 25 (1974) 104–112. <https://doi.org/10.1002/maco.19740250207>.
- [49] D. Drazic, J. Popic, Anomalous dissolution of metals and chemical corrosion, *Journal of the Serbian Chemical Society* 70 (2005) 489–511. <https://doi.org/10.2298/JSC0503489D>.
- [50] L.f. Vorkapić, D.M. Dražić, The dissolution of iron under cathodic polarization, *Corros Sci* 19 (1979) 643–651. [https://doi.org/10.1016/S0010-938X\(79\)80134-1](https://doi.org/10.1016/S0010-938X(79)80134-1).
- [51] A. Pismenny, STRAY CURRENT CORROSION OF CARBON STEEL, ELECTROPLATED NICKEL, AND ELECTROLESS NICKEL IN AN ALKALINE ENVIRONMENT, 2001.
- [52] G. Gao, A.P. O’Mullane, A. Du, 2D MXenes: A New Family of Promising Catalysts for the Hydrogen Evolution Reaction, *ACS Catal* 7 (2017) 494–500. <https://doi.org/10.1021/acscatal.6b02754>.
- [53] W. Stichel, Corrosion control in the chemical process industries. Von C. P. Dillon; 420 Seiten, Herausg. für das Materials Technology Institute of the Chemical Process Industries, Inc. von NACE International, Houston, Texas, 2. Auflage 1994, MIT Publication Nr. 45, \$ 93.00, \$ 65.00 (NACE Member), ISBN 1-877914-58-4, *Materials and Corrosion* 46 (1995) 250–251. <https://doi.org/https://doi.org/10.1002/maco.19950460416>.
- [54] R. Solmaz, A. Döner, G. Kardaş, The stability of hydrogen evolution activity and corrosion behavior of NiCu coatings with long-term electrolysis in alkaline solution, *Int J Hydrogen Energy* 34 (2009) 2089–2094. <https://doi.org/10.1016/j.ijhydene.2009.01.007>.
- [55] H.E.G. Rommal, P.J. Morgan, The Role of Absorbed Hydrogen on the Voltage-Time Behavior of Nickel Cathodes in Hydrogen Evolution, *J Electrochem Soc* 135 (1988) 343–346. <https://doi.org/10.1149/1.2095612>.

- [56] J.F. Monteiro, Yu.A. Ivanova, A.V. Kovalevsky, D.K. Ivanou, J.R. Frade, Reduction of magnetite to metallic iron in strong alkaline medium, *Electrochim Acta* 193 (2016) 284–292. <https://doi.org/10.1016/j.electacta.2016.02.058>.
- [57] S. Liu, Y. Li, D. Wang, S. Xi, H. Xu, Y. Wang, X. Li, W. Zang, W. Liu, M. Su, K. Yan, A.C. Nielanders, A.B. Wong, J. Lu, T.F. Jaramillo, L. Wang, P. Canepa, Q. He, Alkali cation-induced cathodic corrosion in Cu electrocatalysts, *Nat Commun* 15 (2024) 5080. <https://doi.org/10.1038/s41467-024-49492-7>.
- [58] M. Schalenbach, A.R. Zeradjanin, O. Kasian, S. Cherevko, K.J.J. Mayrhofer, A Perspective on Low-Temperature Water Electrolysis – Challenges in Alkaline and Acidic Technology, *Int J Electrochem Sci* 13 (2018) 1173–1226. <https://doi.org/10.20964/2018.02.26>.
- [59] R. Parsons, Atlas of electrochemical equilibria in aqueous solutions, *J Electroanal Chem Interfacial Electrochem* 13 (1967) 471. [https://doi.org/10.1016/0022-0728\(67\)80059-7](https://doi.org/10.1016/0022-0728(67)80059-7).
- [60] M. Schalenbach, F.D. Speck, M. Ledendecker, O. Kasian, D. Goehl, A.M. Mingers, B. Breitbach, H. Springer, S. Cherevko, K.J.J. Mayrhofer, Nickel-molybdenum alloy catalysts for the hydrogen evolution reaction: Activity and stability revised, *Electrochim Acta* 259 (2018) 1154–1161. <https://doi.org/10.1016/j.electacta.2017.11.069>.
- [61] A.R. Despić, V.D. Jović, Electrochemical Deposition and Dissolution of Alloys and Metal Composites—Fundamental Aspects, in: 1995: pp. 143–232. [https://doi.org/10.1007/978-1-4899-1724-9\\_2](https://doi.org/10.1007/978-1-4899-1724-9_2).
- [62] H. Nady, M.M. El-Rabiei, M. Samy, M.A. Deyab, G.M. Abd El-Hafez, Novel Ni–Cr-based alloys as hydrogen fuel sources through alkaline water electrolytes, *Int J Hydrogen Energy* 46 (2021) 34749–34766. <https://doi.org/10.1016/j.ijhydene.2021.08.056>.
- [63] S. Cherevko, S. Geiger, O. Kasian, N. Kulyk, J.-P. Grote, A. Savan, B.R. Shrestha, S. Merzlikin, B. Breitbach, A. Ludwig, K.J.J. Mayrhofer, Oxygen and hydrogen evolution reactions on Ru, RuO<sub>2</sub>, Ir, and IrO<sub>2</sub> thin film electrodes in acidic and alkaline electrolytes: A comparative study on activity and stability, *Catal Today* 262 (2016) 170–180. <https://doi.org/10.1016/j.cattod.2015.08.014>.
- [64] D.S. Hall, C. Bock, B.R. MacDougall, The Electrochemistry of Metallic Nickel: Oxides, Hydroxides, Hydrides and Alkaline Hydrogen Evolution, *J Electrochem Soc* 160 (2013) F235–F243. <https://doi.org/10.1149/2.026303jes>.
- [65] A. Delvaux, G. Lumbeeck, H. Idrissi, J. Proost, Effect of microstructure and internal stress on hydrogen absorption into Ni thin film electrodes during alkaline water electrolysis, *Electrochim Acta* 340 (2020) 135970. <https://doi.org/10.1016/j.electacta.2020.135970>.
- [66] D.W. Kirk, S. Thorpe, Nickel Cathode Passivation in Alkaline Water Electrolysis, *ECS Trans* 2 (2007) 71–76. <https://doi.org/10.1149/1.2408970>.
- [67] S. Barwe, B. Mei, J. Masa, W. Schuhmann, E. Ventosa, Overcoming cathode poisoning from electrolyte impurities in alkaline electrolysis by means of self-healing electrocatalyst films, *Nano Energy* 53 (2018) 763–768. <https://doi.org/10.1016/j.nanoen.2018.09.045>.
- [68] T. Dickinson, A.F. Povey, P.M.A. Sherwood, Dissolution and passivation of nickel. An X-ray photoelectron spectroscopic study, *Journal of the Chemical Society, Faraday Transactions 1: Physical Chemistry in Condensed Phases* 73 (1977) 327. <https://doi.org/10.1039/f19777300327>.

- [69] D.S. Hall, D.J. Lockwood, C. Bock, B.R. MacDougall, Nickel hydroxides and related materials: a review of their structures, synthesis and properties, *Proceedings of the Royal Society A: Mathematical, Physical and Engineering Sciences* 471 (2015) 20140792. <https://doi.org/10.1098/rspa.2014.0792>.
- [70] Y. Kim, S.-M. Jung, K.-S. Kim, H.-Y. Kim, J. Kwon, J. Lee, H.-S. Cho, Y.-T. Kim, Cathodic Protection System against a Reverse-Current after Shut-Down in Zero-Gap Alkaline Water Electrolysis, *JACS Au* 2 (2022) 2491–2500. <https://doi.org/10.1021/jacsau.2c00314>.
- [71] C. Xu, W. Gao, Pilling-Bedworth ratio for oxidation of alloys, *Materials Research Innovations* 3 (2000) 231–235. <https://doi.org/10.1007/s100190050008>.
- [72] Q. Jiang, D. Lu, C. Liu, N. Liu, B. Hou, The Pilling-Bedworth Ratio of Oxides Formed From the Precipitated Phases in Magnesium Alloys, *Front Mater* 8 (2021). <https://doi.org/10.3389/fmats.2021.761052>.
- [73] Y. UCHINO, T. KOBAYASHI, S. HASEGAWA, I. NAGASHIMA, Y. SUNADA, A. MANABE, Y. NISHIKI, S. MITSUSHIMA, Dependence of the Reverse Current on the Surface of Electrode Placed on a Bipolar Plate in an Alkaline Water Electrolyzer, *Electrochemistry* 86 (2018) 138–144. <https://doi.org/10.5796/electrochemistry.17-00102>.
- [74] Y. Uchino, T. Kobayashi, S. Hasegawa, I. Nagashima, Y. Sunada, A. Manabe, Y. Nishiki, S. Mitsushima, Relationship Between the Redox Reactions on a Bipolar Plate and Reverse Current After Alkaline Water Electrolysis, *Electrocatalysis* 9 (2018) 67–74. <https://doi.org/10.1007/s12678-017-0423-5>.
- [75] H. Bode, K. Dehmelt, J. Witte, Zur kenntnis der nickelhydroxidelektrode—I.Über das nickel (II)-hydroxidhydrat, *Electrochim Acta* 11 (1966) 1079–1087. [https://doi.org/10.1016/0013-4686\(66\)80045-2](https://doi.org/10.1016/0013-4686(66)80045-2).
- [76] G.B. Darband, M. Aliofkhaezai, S. Shanmugam, Recent advances in methods and technologies for enhancing bubble detachment during electrochemical water splitting, *Renewable and Sustainable Energy Reviews* 114 (2019) 109300. <https://doi.org/10.1016/j.rser.2019.109300>.
- [77] Q. Liu, A. Atrens, A critical review of the influence of hydrogen on the mechanical properties of medium-strength steels, *Corrosion Reviews* 31 (2013) 85–103. <https://doi.org/10.1515/corrrev-2013-0023>.
- [78] Y. Sui, X. Ji, Anticatalytic Strategies to Suppress Water Electrolysis in Aqueous Batteries, *Chem Rev* 121 (2021) 6654–6695. <https://doi.org/10.1021/acs.chemrev.1c00191>.
- [79] E.G. Dafft, K. Bohnenkamp, H.J. Engell, Investigations of the hydrogen evolution kinetics and hydrogen absorption by iron electrodes during cathodic polarization, *Corros Sci* 19 (1979) 591–612. [https://doi.org/10.1016/S0010-938X\(79\)80130-4](https://doi.org/10.1016/S0010-938X(79)80130-4).
- [80] J. Flis, Changes in hydrogen entry rate and in surface of iron during cathodic polarisation in alkaline solutions, *Electrochim Acta* 44 (1999) 3989–3997. [https://doi.org/10.1016/S0013-4686\(99\)00168-1](https://doi.org/10.1016/S0013-4686(99)00168-1).
- [81] S.K. Dwivedi, M. Vishwakarma, Hydrogen embrittlement in different materials: A review, *Int J Hydrogen Energy* 43 (2018) 21603–21616. <https://doi.org/10.1016/j.ijhydene.2018.09.201>.
- [82] C.D. Beachem, A new model for hydrogen-assisted cracking (hydrogen “embrittlement”), *Metallurgical Transactions* 3 (1972) 441–455. <https://doi.org/10.1007/BF02642048>.
- [83] S.P. Lynch, Hydrogen embrittlement (HE) phenomena and mechanisms, in: *Stress Corrosion Cracking*, Elsevier, 2011: pp. 90–130. <https://doi.org/10.1533/9780857093769.1.90>.

- [84] C. Sequeira, D. Cardoso, L. Amaral, B. Sljukic, D. Santos, Corrosion-resistant materials for alkaline water electrolyzers, *CORROSION* (2020) 3289. <https://doi.org/10.5006/3289>.
- [85] A. Abdel Haleem, J. Huyan, K. Nagasawa, Y. Kuroda, Y. Nishiki, A. Kato, T. Nakai, T. Araki, S. Mitsushima, Effects of operation and shutdown parameters and electrode materials on the reverse current phenomenon in alkaline water analyzers, *J Power Sources* 535 (2022) 231454. <https://doi.org/10.1016/j.jpowsour.2022.231454>.
- [86] R.A. Marquez, M. Espinosa, E. Kalokowski, Y.J. Son, K. Kawashima, T.V. Le, C.E. Chukwuneke, C.B. Mullins, A Guide to Electrocatalyst Stability Using Lab-Scale Alkaline Water Electrolyzers, *ACS Energy Lett* 9 (2024) 547–555. <https://doi.org/10.1021/acsenergylett.3c02758>.
- [87] N. KRSTAJIC, V. JOVIC, L. GAJICKRSTAJIC, B. JOVIC, A. ANTOZZI, G. MARTELLI, Electrodeposition of Ni–Mo alloy coatings and their characterization as cathodes for hydrogen evolution in sodium hydroxide solution, *Int J Hydrogen Energy* 33 (2008) 3676–3687. <https://doi.org/10.1016/j.ijhydene.2008.04.039>.
- [88] E.B. Ferreira, S. Tahmasebi, G. Jerkiewicz, On the Catalytic Activity and Corrosion Behavior of Polycrystalline Nickel in Alkaline Media in the Presence of Neutral and Reactive Gases, *Electrocatalysis* 12 (2021) 146–164. <https://doi.org/10.1007/s12678-020-00637-4>.
- [89] M. Alsabet, M. Grdeń, G. Jerkiewicz, Electrochemical Growth of Surface Oxides on Nickel. Part 3: Formation of  $\beta$ -NiOOH in Relation to the Polarization Potential, Polarization Time, and Temperature, *Electrocatalysis* 6 (2015) 60–71. <https://doi.org/10.1007/s12678-014-0214-1>.
- [90] D. Cubicciotti, Potential-pH diagrams for alloy-water systems under LWR conditions, *Journal of Nuclear Materials* 201 (1993) 176–183. [https://doi.org/10.1016/0022-3115\(93\)90173-V](https://doi.org/10.1016/0022-3115(93)90173-V).
- [91] B. Beverskog, I. Puigdomenech, Revised pourbaix diagrams for iron at 25–300 °C, *Corros Sci* 38 (1996) 2121–2135. [https://doi.org/10.1016/S0010-938X\(96\)00067-4](https://doi.org/10.1016/S0010-938X(96)00067-4).
- [92] F. Safizadeh, E. Ghali, G. Houlachi, Electrocatalysis developments for hydrogen evolution reaction in alkaline solutions – A Review, *Int J Hydrogen Energy* 40 (2015) 256–274. <https://doi.org/10.1016/j.ijhydene.2014.10.109>.
- [93] J. Divisek, H. Schmitz, B. Steffen, Electrocatalyst materials for hydrogen evolution, *Electrochim Acta* 39 (1994) 1723–1731. [https://doi.org/10.1016/0013-4686\(94\)85157-3](https://doi.org/10.1016/0013-4686(94)85157-3).
- [94] J. DIVISEK, J. MERGEL, H. SCHMITZ, Advanced water electrolysis and catalyst stability under discontinuous operation, *Int J Hydrogen Energy* 15 (1990) 105–114. [https://doi.org/10.1016/0360-3199\(90\)90032-T](https://doi.org/10.1016/0360-3199(90)90032-T).
- [95] H. Wendt, G. Kreysa, *Electrochemical Engineering*, Springer Berlin Heidelberg, Berlin, Heidelberg, 1999. <https://doi.org/10.1007/978-3-662-03851-2>.
- [96] M. JANJUA, R. LEROY, Electrocatalyst performance in industrial water electrolyzers, *Int J Hydrogen Energy* 10 (1985) 11–19. [https://doi.org/10.1016/0360-3199\(85\)90130-2](https://doi.org/10.1016/0360-3199(85)90130-2).
- [97] S. Ruck, A. Körner, A. Hutzler, M. Bierling, J. Gonzalez, W. Qu, C. Bock, S. Thiele, R. Peach, C. V Pham, Carbon supported NiRu nanoparticles as effective hydrogen evolution catalysts for anion exchange membrane water electrolyzers, *Journal of Physics: Energy* 4 (2022) 044007. <https://doi.org/10.1088/2515-7655/ac95cd>.
- [98] H.-Y. Jung, J.W. Kim, Role of the glass transition temperature of Nafion 117 membrane in the preparation of the membrane electrode assembly in a direct methanol fuel cell (DMFC), *Int J Hydrogen Energy* 37 (2012) 12580–12585. <https://doi.org/10.1016/j.ijhydene.2012.05.121>.

GA No. 101137802

- [99] J.E. Park, S.Y. Kang, S.-H. Oh, J.K. Kim, M.S. Lim, C.-Y. Ahn, Y.-H. Cho, Y.-E. Sung, High-performance anion-exchange membrane water electrolysis, *Electrochim Acta* 295 (2019) 99–106. <https://doi.org/10.1016/j.electacta.2018.10.143>.
- [100] P. Mardle, B. Chen, S. Holdcroft, Opportunities of Ionomer Development for Anion-Exchange Membrane Water Electrolysis, *ACS Energy Lett* 8 (2023) 3330–3342. <https://doi.org/10.1021/acseenergylett.3c01040>.
- [101] M. Bierling, D. McLaughlin, B. Mayerhöfer, S. Thiele, Toward Understanding Catalyst Layer Deposition Processes and Distribution in Anodic Porous Transport Electrodes in Proton Exchange Membrane Water Electrolyzers, *Adv Energy Mater* 13 (2023). <https://doi.org/10.1002/aenm.202203636>.
- [102] S. Koch, P.A. Heizmann, S.K. Kilian, B. Britton, S. Holdcroft, M. Breitwieser, S. Vierrath, The effect of ionomer content in catalyst layers in anion-exchange membrane water electrolyzers prepared with reinforced membranes (Aemion<sup>TM</sup>), *J Mater Chem A Mater* 9 (2021) 15744–15754. <https://doi.org/10.1039/D1TA01861B>.
- [103] J.E. Park, H.E. Bae, M. Karuppanan, K.M. Oh, O.J. Kwon, Y.-H. Cho, Y.-E. Sung, Effect of catalyst layer designs for high-performance and durable anion-exchange membrane water electrolysis, *Journal of Industrial and Engineering Chemistry* 109 (2022) 453–460. <https://doi.org/10.1016/j.jiec.2022.02.033>.
- [104] B. Chen, A.L.G. Biancolli, C.L. Radford, S. Holdcroft, Stainless Steel Felt as a Combined OER Electrocatalyst/Porous Transport Layer for Investigating Anion-Exchange Membranes in Water Electrolysis, *ACS Energy Lett* 8 (2023) 2661–2667. <https://doi.org/10.1021/acsenergylett.3c00878>.
- [105] M.K. Bates, Q. Jia, N. Ramaswamy, R.J. Allen, S. Mukerjee, Composite Ni/NiO-Cr<sub>2</sub>O<sub>3</sub> Catalyst for Alkaline Hydrogen Evolution Reaction, *The Journal of Physical Chemistry C* 119 (2015) 5467–5477. <https://doi.org/10.1021/jp512311c>.
- [106] E. Cossar, F. Murphy, J. Walia, A. Weck, E.A. Baranova, Role of Ionomers in Anion Exchange Membrane Water Electrolysis: Is Aemion the Answer for Nickel-Based Anodes?, *ACS Appl Energy Mater* 5 (2022) 9938–9951. <https://doi.org/10.1021/acsaem.2c01604>.
- [107] D. Li, I. Matanovic, A.S. Lee, E.J. Park, C. Fujimoto, H.T. Chung, Y.S. Kim, Phenyl Oxidation Impacts the Durability of Alkaline Membrane Water Electrolyzer, *ACS Appl Mater Interfaces* 11 (2019) 9696–9701. <https://doi.org/10.1021/acsami.9b00711>.
- [108] G.A. Lindquist, S.Z. Oener, R. Krivina, A.R. Motz, A. Keane, C. Capuano, K.E. Ayers, S.W. Boettcher, Performance and Durability of Pure-Water-Fed Anion Exchange Membrane Electrolyzers Using Baseline Materials and Operation, *ACS Appl Mater Interfaces* 13 (2021) 51917–51924. <https://doi.org/10.1021/acsami.1c06053>.
- [109] R.A. Krivina, G.A. Lindquist, M.C. Yang, A.K. Cook, C.H. Hendon, A.R. Motz, C. Capuano, K.E. Ayers, J.E. Hutchison, S.W. Boettcher, Three-Electrode Study of Electrochemical Ionomer Degradation Relevant to Anion-Exchange-Membrane Water Electrolyzers, *ACS Appl Mater Interfaces* 14 (2022) 18261–18274. <https://doi.org/10.1021/acsami.1c22472>.
- [110] R.A. Krivina, G.A. Lindquist, S.R. Beaudoin, T.N. Stovall, W.L. Thompson, L.P. Twight, D. Marsh, J. Grzyb, K. Fabrizio, J.E. Hutchison, S.W. Boettcher, Anode Catalysts in Anion-Exchange-Membrane Electrolysis without Supporting Electrolyte: Conductivity, Dynamics, and Ionomer Degradation, *Advanced Materials* 34 (2022). <https://doi.org/10.1002/adma.202203033>.



- [111] G. Papakonstantinou, G. Algara-Siller, D. Teschner, T. Vidaković-Koch, R. Schlögl, K. Sundmacher, Degradation study of a proton exchange membrane water electrolyzer under dynamic operation conditions, *Appl Energy* 280 (2020) 115911. <https://doi.org/10.1016/j.apenergy.2020.115911>.
- [112] E. Wallnöfer-Ogris, I. Grimmer, M. Ranz, M. Höglinger, S. Kartusch, J. Rauh, M.-G. Macherhammer, B. Grabner, A. Trattner, A review on understanding and identifying degradation mechanisms in PEM water electrolysis cells: Insights for stack application, development, and research, *Int J Hydrogen Energy* 65 (2024) 381–397. <https://doi.org/10.1016/j.ijhydene.2024.04.017>.
- [113] H. Yu, L. Bonville, J. Jankovic, R. Maric, Microscopic insights on the degradation of a PEM water electrolyzer with ultra-low catalyst loading, *Appl Catal B* 260 (2020) 118194. <https://doi.org/10.1016/j.apcatb.2019.118194>.
- [114] H. Becker, J. Murawski, D. V. Shinde, I.E.L. Stephens, G. Hinds, G. Smith, Impact of impurities on water electrolysis: a review, *Sustain Energy Fuels* 7 (2023) 1565–1603. <https://doi.org/10.1039/d2se01517j>.
- [115] O. Kasian, J. Grote, S. Geiger, S. Cherevko, K.J.J. Mayrhofer, The Common Intermediates of Oxygen Evolution and Dissolution Reactions during Water Electrolysis on Iridium, *Angewandte Chemie International Edition* 57 (2018) 2488–2491. <https://doi.org/10.1002/anie.201709652>.
- [116] S.A. Grigoriev, K.A. Dzhus, D.G. Bessarabov, P. Millet, Failure of PEM water electrolysis cells: Case study involving anode dissolution and membrane thinning, *Int J Hydrogen Energy* 39 (2014) 20440–20446. <https://doi.org/10.1016/j.ijhydene.2014.05.043>.
- [117] C. Rakousky, U. Reimer, K. Wippermann, S. Kuhri, M. Carmo, W. Lueke, D. Stolten, Polymer electrolyte membrane water electrolysis: Restraining degradation in the presence of fluctuating power, *J Power Sources* 342 (2017) 38–47. <https://doi.org/10.1016/j.jpowsour.2016.11.118>.
- [118] P. Millet, A. Ranjbari, F. de Guglielmo, S.A. Grigoriev, F. Auprêtre, Cell failure mechanisms in PEM water electrolyzers, *Int J Hydrogen Energy* 37 (2012) 17478–17487. <https://doi.org/10.1016/j.ijhydene.2012.06.017>.
- [119] S. Siracusano, N. Van Dijk, R. Backhouse, L. Merlo, V. Baglio, A.S. Aricò, Degradation issues of PEM electrolysis MEAs, *Renew Energy* 123 (2018) 52–57. <https://doi.org/10.1016/j.renene.2018.02.024>.
- [120] C. Rozain, P. Millet, Electrochemical characterization of Polymer Electrolyte Membrane Water Electrolysis Cells, *Electrochim Acta* 131 (2014) 160–167. <https://doi.org/10.1016/j.electacta.2014.01.099>.
- [121] H. Becker, J. Murawski, D. V. Shinde, I.E.L. Stephens, G. Hinds, G. Smith, Impact of impurities on water electrolysis: a review, *Sustain Energy Fuels* 7 (2023) 1565–1603. <https://doi.org/10.1039/D2SE01517J>.
- [122] T. Audichon, B. Guenot, S. Baranton, M. Cretin, C. Lamy, C. Coutanceau, Preparation and characterization of supported RuIr(1-x)O<sub>2</sub> nano-oxides using a modified polyol synthesis assisted by microwave activation for energy storage applications, *Appl Catal B* 200 (2017) 493–502. <https://doi.org/10.1016/j.apcatb.2016.07.048>.

- [123] H. Yu, L. Bonville, J. Jankovic, R. Maric, Microscopic insights on the degradation of a PEM water electrolyzer with ultra-low catalyst loading, *Appl Catal B* 260 (2020) 118194. <https://doi.org/10.1016/j.apcatb.2019.118194>.
- [124] Z. Zhang, A. Baudy, A. Testino, L. Gubler, Cathode Catalyst Layer Design in PEM Water Electrolysis toward Reduced Pt Loading and Hydrogen Crossover, *ACS Appl Mater Interfaces* (2024). <https://doi.org/10.1021/acsami.4c01827>.
- [125] Y. Xing, H. Li, G. Avgouropoulos, Research Progress of Proton Exchange Membrane Failure and Mitigation Strategies, *Materials* 14 (2021) 2591. <https://doi.org/10.3390/ma14102591>.
- [126] E. Kuhnert, V. Hacker, M. Bodner, A Review of Accelerated Stress Tests for Enhancing MEA Durability in PEM Water Electrolysis Cells, *Int J Energy Res* 2023 (2023) 1–23. <https://doi.org/10.1155/2023/3183108>.
- [127] U. Babic, T.J. Schmidt, L. Gubler, Communication—Contribution of Catalyst Layer Proton Transport Resistance to Voltage Loss in Polymer Electrolyte Water Electrolyzers, *J Electrochem Soc* 165 (2018) J3016–J3018. <https://doi.org/10.1149/2.0031815jes>.
- [128] E. Kuhnert, O. Kiziltan, V. Hacker, M. Bodner, Investigation of the Impact of Chloride Contamination on Degradation in PEM Water Electrolyzer Cells, *ECS Trans* 112 (2023) 485–494. <https://doi.org/10.1149/11204.0485ecst>.
- [129] Z. Rui, K. Hua, Z. Dou, A. Tan, C. Zhang, X. Shi, R. Ding, X. Li, X. Duan, Y. Wu, Y. Zhang, X. Wang, J. Li, J. Liu, A new insight into the chemical degradation of proton exchange membranes in water electrolyzers, *J Mater Chem A Mater* 12 (2024) 9563–9573. <https://doi.org/10.1039/D3TA05224A>.
- [130] V. Subotić, C. Hochenauer, Analysis of solid oxide fuel and electrolysis cells operated in a real-system environment: State-of-the-health diagnostic, failure modes, degradation mitigation and performance regeneration, *Prog Energy Combust Sci* 93 (2022) 101011. <https://doi.org/10.1016/J.PECS.2022.101011>.
- [131] J. Schefold, A. Brisse, H. Poepke, 23,000 h steam electrolysis with an electrolyte supported solid oxide cell, *Int J Hydrogen Energy* 42 (2017) 13415–13426. <https://doi.org/10.1016/j.ijhydene.2017.01.072>.
- [132] J. Schefold, A. Brisse, H. Poepke, 23,000 h steam electrolysis with an electrolyte supported solid oxide cell, *Int J Hydrogen Energy* 42 (2017) 13415–13426. <https://doi.org/10.1016/j.ijhydene.2017.01.072>.
- [133] V. Subotić, S. Futamura, G.F. Harrington, J. Matsuda, K. Natsukoshi, K. Sasaki, Towards understanding of oxygen electrode processes during solid oxide electrolysis operation to improve simultaneous fuel and oxygen generation, *J Power Sources* 492 (2021). <https://doi.org/10.1016/j.jpowsour.2021.229600>.
- [134] B. Königshofer, G. Pongratz, G. Nusev, P. Boškosi, M. Höber, Đ. Juričić, M. Kusnezoff, N. Trofimenko, H. Schröttner, C. Hochenauer, V. Subotić, Development of test protocols for solid oxide electrolysis cells operated under accelerated degradation conditions, *J Power Sources* 497 (2021). <https://doi.org/10.1016/j.jpowsour.2021.229875>.
- [135] J. Sehested, J.A.P. Gelten, I.N. Remediakis, H. Bengaard, J.K. Nørskov, Sintering of nickel steam-reforming catalysts: Effects of temperature and steam and hydrogen pressures, *J Catal* 223 (2004) 432–443. <https://doi.org/10.1016/j.jcat.2004.01.026>.

- [136] A. Faes, A. Hessler-Wyser, A. Zryd, J. Van Herle, A review of RedOx cycling of solid oxide fuel cells anode, *Membranes (Basel)* 2 (2012) 585–664. <https://doi.org/10.3390/membranes2030585>.
- [137] M. Hubert, J. Laurencin, P. Cloetens, B. Morel, D. Montinaro, F. Lefebvre-Joud, Impact of Nickel agglomeration on Solid Oxide Cell operated in fuel cell and electrolysis modes, *J Power Sources* 397 (2018) 240–251. <https://doi.org/10.1016/j.jpowsour.2018.06.097>.
- [138] T. Sakai, K. Arakawa, M. Ogushi, T. Ishihara, H. Matsumoto, Y. Okuyama, Atmosphere dependence of anode reaction of intermediate temperature steam electrolysis using perovskite type proton conductor, *Journal of Solid State Electrochemistry* 19 (2015) 1793–1798. <https://doi.org/10.1007/s10008-015-2808-9>.
- [139] P.S. Jørgensen, J.R. Bowen, Determination of Three Dimensional Microstructure Parameters from a Solid Oxide Ni/YSZ Electrode after Electrolysis Operation, *ECS Trans* 35 (2011) 1655–1660. <https://doi.org/10.1149/1.3570152>.
- [140] G. Rinaldi, S. Diethelm, E. Oveisi, P. Burdet, J. Van herle, D. Montinaro, Q. Fu, A. Brisse, Post-test Analysis on a Solid Oxide Cell Stack Operated for 10,700 Hours in Steam Electrolysis Mode, *Fuel Cells* 17 (2017) 541–549. <https://doi.org/10.1002/fuce.201600194>.
- [141] Y. Zou, T. Lin, Y. Sun, Z. Chen, C. Guan, Y. Li, S.P. Jiang, N. Ai, K. Chen, Anodic polarization creates an electrocatalytically active Ni anode/electrolyte interface and mitigates the coarsening of Ni phase in SOFC, *Electrochim Acta* 391 (2021). <https://doi.org/10.1016/j.electacta.2021.138912>.
- [142] B. Song, E. Ruiz-Trejo, N.P. Brandon, Enhanced mechanical stability of Ni-YSZ scaffold demonstrated by nanoindentation and Electrochemical Impedance Spectroscopy, *J Power Sources* 395 (2018) 205–211. <https://doi.org/10.1016/j.jpowsour.2018.05.075>.
- [143] L. Holzer, B. Iwanschitz, T. Hocker, B. Münch, M. Prestat, D. Wiedenmann, U. Vogt, P. Holtappels, J. Sfeir, A. Mai, T. Graule, Microstructure degradation of cermet anodes for solid oxide fuel cells: Quantification of nickel grain growth in dry and in humid atmospheres, *J Power Sources* 196 (2011) 1279–1294. <https://doi.org/10.1016/j.jpowsour.2010.08.017>.
- [144] M.P. Hoerlein, M. Riegraf, R. Costa, G. Schiller, K.A. Friedrich, A parameter study of solid oxide electrolysis cell degradation: Microstructural changes of the fuel electrode, *Electrochim Acta* 276 (2018) 162–175. <https://doi.org/10.1016/j.electacta.2018.04.170>.
- [145] C.E. Frey, Q. Fang, D. Sebold, L. Blum, N.H. Menzler, A Detailed Post Mortem Analysis of Solid Oxide Electrolyzer Cells after Long-Term Stack Operation, *J Electrochem Soc* 165 (2018) F357–F364. <https://doi.org/10.1149/2.0961805jes>.
- [146] D. The, S. Grieshammer, M. Schroeder, M. Martin, M. Al Daroukh, F. Tietz, J. Schefold, A. Brisse, Microstructural comparison of solid oxide electrolyser cells operated for 6100 h and 9000 h, *J Power Sources* 275 (2015) 901–911. <https://doi.org/10.1016/j.jpowsour.2014.10.188>.
- [147] L. Bi, S. Boulfrad, E. Traversa, Steam electrolysis by solid oxide electrolysis cells (SOECs) with proton-conducting oxides, *Chem. Soc. Rev.* 43 (2014) 8255–8270. <https://doi.org/10.1039/C4CS00194J>.
- [148] L. Lei, J. Zhang, Z. Yuan, J. Liu, M. Ni, F. Chen, Progress Report on Proton Conducting Solid Oxide Electrolysis Cells, *Adv Funct Mater* 29 (2019). <https://doi.org/10.1002/adfm.201903805>.

GA No. 101137802

- [149] C. Duan, J. Huang, N. Sullivan, R. O'Hayre, Proton-conducting oxides for energy conversion and storage, *Appl Phys Rev* 7 (2020). <https://doi.org/10.1063/1.5135319>.
- [150] F. He, D. Song, R. Peng, G. Meng, S. Yang, Electrode performance and analysis of reversible solid oxide fuel cells with proton conducting electrolyte of BaCe<sub>0.5</sub>Zr<sub>0.3</sub>Y<sub>0.2</sub>O<sub>3-δ</sub>, *J Power Sources* 195 (2010) 3359–3364. <https://doi.org/10.1016/j.jpowsour.2009.12.079>.
- [151] H. Tian, W. Li, L. Ma, T. Yang, B. Guan, W. Shi, T.L. Kalapos, X. Liu, Deconvolution of Water-Splitting on the Triple-Conducting Ruddlesden–Popper-Phase Anode for Protonic Ceramic Electrolysis Cells, *ACS Appl Mater Interfaces* 12 (2020) 49574–49585. <https://doi.org/10.1021/acsami.0c12987>.
- [152] M. Papac, V. Stevanović, A. Zakutayev, R. O'Hayre, Triple ionic–electronic conducting oxides for next-generation electrochemical devices, *Nat Mater* 20 (2021) 301–313. <https://doi.org/10.1038/s41563-020-00854-8>.
- [153] D. Medvedev, Trends in research and development of protonic ceramic electrolysis cells, *Int J Hydrogen Energy* 44 (2019) 26711–26740. <https://doi.org/10.1016/j.ijhydene.2019.08.130>.
- [154] C. Duan, R. Kee, H. Zhu, N. Sullivan, L. Zhu, L. Bian, D. Jennings, R. O'Hayre, Highly efficient reversible protonic ceramic electrochemical cells for power generation and fuel production, *Nat Energy* 4 (2019) 230–240. <https://doi.org/10.1038/s41560-019-0333-2>.
- [155] S. Choi, T.C. Davenport, S.M. Haile, Protonic ceramic electrochemical cells for hydrogen production and electricity generation: exceptional reversibility, stability, and demonstrated faradaic efficiency, *Energy Environ Sci* 12 (2019) 206–215. <https://doi.org/10.1039/C8EE02865F>.
- [156] C. Sun, S. Yang, Y. Lu, J. Wen, X. Ye, Z. Wen, Tailoring a micro-nanostructured electrolyte-oxygen electrode interface for proton-conducting reversible solid oxide cells, *J Power Sources* 449 (2020) 227498. <https://doi.org/10.1016/j.jpowsour.2019.227498>.
- [157] A.P. Tarutin, J.G. Lyagaeva, D.A. Medvedev, L. Bi, A.A. Yaremchenko, Recent advances in layered Ln<sub>2</sub>NiO<sub>4+δ</sub> nickelates: fundamentals and prospects of their applications in protonic ceramic fuel and electrolysis cells, *J Mater Chem A Mater* 9 (2021) 154–195. <https://doi.org/10.1039/D0TA08132A>.
- [158] W. Wang, D. Medvedev, Z. Shao, Gas Humidification Impact on the Properties and Performance of Perovskite-Type Functional Materials in Proton-Conducting Solid Oxide Cells, *Adv Funct Mater* 28 (2018). <https://doi.org/10.1002/adfm.201802592>.
- [159] E. Vøllestad, R. Strandbakke, M. Tarach, D. Catalán-Martínez, M.-L. Fontaine, D. Beeaff, D.R. Clark, J.M. Serra, T. Norby, Mixed proton and electron conducting double perovskite anodes for stable and efficient tubular proton ceramic electrolyzers, *Nat Mater* 18 (2019) 752–759. <https://doi.org/10.1038/s41563-019-0388-2>.
- [160] F. Giannici, A. Chiara, G. Canu, A. Longo, A. Martorana, Interface Solid-State Reactions in La<sub>0.8</sub>Sr<sub>0.2</sub>MnO<sub>3</sub>/Ce<sub>0.8</sub>Sm<sub>0.2</sub>O<sub>2</sub> and La<sub>0.8</sub>Sr<sub>0.2</sub>MnO<sub>3</sub>/BaCe<sub>0.9</sub>Y<sub>0.1</sub>O<sub>3</sub> Disclosed by X-ray Microspectroscopy, *ACS Appl Energy Mater* 2 (2019) 3204–3210. <https://doi.org/10.1021/acsaem.9b00037>.
- [161] J.C. De Vero, H. Yokokawa, K. Develos-Bagarinao, S.-S. Liu, H. Kishimoto, T. Ishiyama, K. Yamaji, T. Horita, Influence of electrolyte substrates on the Sr-segregation and SrSO<sub>4</sub> formation in La<sub>0.6</sub>Sr<sub>0.4</sub>Co<sub>0.2</sub>Fe<sub>0.8</sub>O<sub>3-δ</sub> thin films, *MRS Commun* 9 (2019) 236–244. <https://doi.org/10.1557/mrc.2018.208>.

- [162] H. Li, X. Chen, S. Chen, Y. Wu, K. Xie, Composite manganate oxygen electrode enhanced with iron oxide nanocatalyst for high temperature steam electrolysis in a proton-conducting solid oxide electrolyzer, *Int J Hydrogen Energy* 40 (2015) 7920–7931. <https://doi.org/10.1016/j.ijhydene.2015.04.067>.
- [163] Y. Zhou, E. Liu, Y. Chen, Y. Liu, L. Zhang, W. Zhang, Z. Luo, N. Kane, B. Zhao, L. Soule, Y. Niu, Y. Ding, H. Ding, D. Ding, M. Liu, An Active and Robust Air Electrode for Reversible Protonic Ceramic Electrochemical Cells, *ACS Energy Lett* (2021) 1511–1520. <https://doi.org/10.1021/acsenergylett.1c00432>.
- [164] A.P. Tarutin, G.K. Vdovin, D.A. Medvedev, A.A. Yaremchenko, Fluorine-containing oxygen electrodes of the nickelate family for proton-conducting electrochemical cells, *Electrochim Acta* 337 (2020) 135808. <https://doi.org/10.1016/j.electacta.2020.135808>.
- [165] H. Ding, W. Wu, C. Jiang, Y. Ding, W. Bian, B. Hu, P. Singh, C.J. Orme, L. Wang, Y. Zhang, D. Ding, Self-sustainable protonic ceramic electrochemical cells using a triple conducting electrode for hydrogen and power production, *Nat Commun* 11 (2020) 1907. <https://doi.org/10.1038/s41467-020-15677-z>.
- [166] H. Shimada, T. Yamaguchi, H. Sumi, Y. Yamaguchi, K. Nomura, Y. Fujishiro, Effect of Ni diffusion into BaZr<sub>0.1</sub>Ce<sub>0.7</sub>Y<sub>0.1</sub>Yb<sub>0.1</sub>O<sub>3</sub>– electrolyte during high temperature co-sintering in anode-supported solid oxide fuel cells, *Ceram Int* 44 (2018) 3134–3140. <https://doi.org/10.1016/j.ceramint.2017.11.081>.
- [167] C. Sun, Y. Li, X. Ye, Z. Wen, A robust air electrode supported proton-conducting reversible solid oxide cells prepared by low temperature co-sintering, *J Power Sources* 492 (2021) 229602. <https://doi.org/10.1016/j.jpowsour.2021.229602>.
- [168] M.C. Tucker, Progress in metal-supported solid oxide electrolysis cells: A review, *Int J Hydrogen Energy* 45 (2020) 24203–24218. <https://doi.org/10.1016/j.ijhydene.2020.06.300>.
- [169] R.S. Jupudi, G. Zappi, R. Bourgeois, Prediction of shunt currents in a bipolar electrolyzer stack by difference calculus, *J Appl Electrochem* 37 (2007) 921–931. <https://doi.org/10.1007/s10800-007-9330-4>.
- [170] A.N. Colli, H.H. Girault, Compact and General Strategy for Solving Current and Potential Distribution in Electrochemical Cells Composed of Massive Monopolar and Bipolar Electrodes, *J Electrochem Soc* 164 (2017) E3465–E3472. <https://doi.org/10.1149/2.0471711jes>.
- [171] M.-Z. Yang, H. Wu, J.R. Selman, A model for bipolar current leakage in cell stacks with separate electrolyte loops, *J Appl Electrochem* 19 (1989) 247–254. <https://doi.org/10.1007/BF01062308>.
- [172] T. ul Haq, Y. Haik, A roadmap towards sustainable anode design for alkaline water electrolysis, *Appl Catal B* 334 (2023) 122853. <https://doi.org/10.1016/j.apcatb.2023.122853>.
- [173] T. Liu, X. Wang, X. Jiang, C. Deng, S. Niu, J. Mao, W. Zeng, M. Liu, H. Liao, Mechanism of corrosion and sedimentation of nickel electrodes for alkaline water electrolysis, *Mater Chem Phys* 303 (2023) 127806. <https://doi.org/10.1016/j.matchemphys.2023.127806>.
- [174] S. Cherevko, A.R. Zeradjanin, A.A. Topalov, N. Kulyk, I. Katsounaros, K.J.J. Mayrhofer, Dissolution of Noble Metals during Oxygen Evolution in Acidic Media, *ChemCatChem* 6 (2014) 2219–2223. <https://doi.org/10.1002/cctc.201402194>.
- [175] W. Liu, X. Ding, J. Cheng, J. Jing, T. Li, X. Huang, P. Xie, X. Lin, H. Ding, Y. Kuang, D. Zhou, X. Sun, Inhibiting Dissolution of Active Sites in 80 °C Alkaline Water Electrolysis by Oxyanion

- Engineering, *Angewandte Chemie International Edition* 63 (2024).  
<https://doi.org/10.1002/anie.202406082>.
- [176] A.E. Thorarinsdottir, S.S. Veroneau, D.G. Nocera, Self-healing oxygen evolution catalysts, *Nat Commun* 13 (2022) 1243. <https://doi.org/10.1038/s41467-022-28723-9>.
- [177] J. Brauns, J. Schönebeck, M.R. Kraglund, D. Aili, J. Hnát, J. Žitka, W. Mues, J.O. Jensen, K. Bouzek, T. Turek, Evaluation of Diaphragms and Membranes as Separators for Alkaline Water Electrolysis, *J Electrochem Soc* 168 (2021) 014510. <https://doi.org/10.1149/1945-7111/abda57>.
- [178] J. Hnát, M. Plevová, J. Žitka, M. Paidar, K. Bouzek, Anion-selective materials with 1,4-diazabicyclo[2.2.2]octane functional groups for advanced alkaline water electrolysis, *Electrochim Acta* 248 (2017) 547–555. <https://doi.org/10.1016/j.electacta.2017.07.165>.
- [179] D. Aili, M.R. Kraglund, J. Tavacoli, C. Chatzichristodoulou, J.O. Jensen, Polysulfone-polyvinylpyrrolidone blend membranes as electrolytes in alkaline water electrolysis, *J Memb Sci* 598 (2020) 117674. <https://doi.org/10.1016/j.memsci.2019.117674>.
- [180] F. Le Formal, L. Yerly, E. Potapova Mensi, X. Pereira Da Costa, F. Boudoire, N. Guijarro, M. Spodaryk, A. Züttel, K. Sivula, Influence of Composition on Performance in Metallic Iron–Nickel–Cobalt Ternary Anodes for Alkaline Water Electrolysis, *ACS Catal* 10 (2020) 12139–12147. <https://doi.org/10.1021/acscatal.0c03523>.
- [181] C. Hu, L. Zhang, J. Gong, Recent progress made in the mechanism comprehension and design of electrocatalysts for alkaline water splitting, *Energy Environ Sci* 12 (2019) 2620–2645. <https://doi.org/10.1039/C9EE01202H>.
- [182] K. Kneifel, K. Hattenbach, Properties and long-term behavior of ion exchange membranes, *Desalination* 34 (1980) 77–95. [https://doi.org/10.1016/S0011-9164\(00\)88582-3](https://doi.org/10.1016/S0011-9164(00)88582-3).
- [183] M.G. Marino, K.D. Kreuer, Alkaline Stability of Quaternary Ammonium Cations for Alkaline Fuel Cell Membranes and Ionic Liquids, *ChemSusChem* 8 (2015) 513–523. <https://doi.org/10.1002/cssc.201403022>.
- [184] B. Bauer, H. Strathmann, F. Effenberger, Anion-exchange membranes with improved alkaline stability, *Desalination* 79 (1990) 125–144. [https://doi.org/10.1016/0011-9164\(90\)85002-R](https://doi.org/10.1016/0011-9164(90)85002-R).
- [185] S.A. Nuñez, M.A. Hickner, Quantitative <sup>1</sup>H NMR Analysis of Chemical Stabilities in Anion-Exchange Membranes, *ACS Macro Lett* 2 (2013) 49–52. <https://doi.org/10.1021/mz300486h>.
- [186] D. Henkensmeier, M. Najibah, C. Harms, J. Žitka, J. Hnát, K. Bouzek, Overview: State-of-the Art Commercial Membranes for Anion Exchange Membrane Water Electrolysis, *Journal of Electrochemical Energy Conversion and Storage* 18 (2021). <https://doi.org/10.1115/1.4047963>.
- [187] D. Li, A.R. Motz, C. Bae, C. Fujimoto, G. Yang, F.-Y. Zhang, K.E. Ayers, Y.S. Kim, Durability of anion exchange membrane water electrolyzers, *Energy Environ Sci* 14 (2021) 3393–3419. <https://doi.org/10.1039/D0EE04086J>.
- [188] K.M. Beers, D.T. Hallinan, X. Wang, J.A. Pople, N.P. Balsara, Counterion Condensation in Nafion, *Macromolecules* 44 (2011) 8866–8870. <https://doi.org/10.1021/ma2015084>.
- [189] Q. Lei, K. Li, D. Bhattacharya, J. Xiao, S. Kole, Q. Zhang, J. Strzalka, J. Lawrence, R. Kumar, C.G. Arges, Counterion condensation or lack of solvation? Understanding the activity of ions in thin film block copolymer electrolytes, *J Mater Chem A Mater* 8 (2020) 15962–15975. <https://doi.org/10.1039/D0TA04266H>.

- [190] M. V. Ramos-Garcés, K. Li, Q. Lei, D. Bhattacharya, S. Kole, Q. Zhang, J. Strzalka, P.P. Angelopoulou, G. Sakellariou, R. Kumar, C.G. Arges, Understanding the ionic activity and conductivity value differences between random copolymer electrolytes and block copolymer electrolytes of the same chemistry, *RSC Adv* 11 (2021) 15078–15084. <https://doi.org/10.1039/D1RA02519H>.
- [191] B. Chen, P. Mardle, S. Holdcroft, Probing the effect of ionomer swelling on the stability of anion exchange membrane water electrolyzers, *J Power Sources* 550 (2022) 232134. <https://doi.org/10.1016/j.jpowsour.2022.232134>.
- [192] K.-D. Kreuer, The role of internal pressure for the hydration and transport properties of ionomers and polyelectrolytes, *Solid State Ion* 252 (2013) 93–101. <https://doi.org/10.1016/j.ssi.2013.04.018>.
- [193] M. Moreno-González, P. Mardle, S. Zhu, B. Gholamkhash, S. Jones, N. Chen, B. Britton, S. Holdcroft, One year operation of an anion exchange membrane water electrolyzer utilizing Aemion+® membrane: Minimal degradation, low H<sub>2</sub> crossover and high efficiency, *Journal of Power Sources Advances* 19 (2023). <https://doi.org/10.1016/j.powera.2023.100109>.
- [194] M. Mandal, G. Huang, P.A. Kohl, Highly Conductive Anion-Exchange Membranes Based on Cross-Linked Poly(norbornene): Vinyl Addition Polymerization, *ACS Appl Energy Mater* 2 (2019) 2447–2457. <https://doi.org/10.1021/acsaem.8b02051>.
- [195] W. Chen, M. Mandal, G. Huang, X. Wu, G. He, P.A. Kohl, Highly Conducting Anion-Exchange Membranes Based on Cross-Linked Poly(norbornene): Ring Opening Metathesis Polymerization, *ACS Appl Energy Mater* 2 (2019) 2458–2468. <https://doi.org/10.1021/acsaem.8b02052>.
- [196] T. Weissbach, A.G. Wright, T.J. Peckham, A. Sadeghi Alavijeh, V. Pan, E. Kjeang, S. Holdcroft, Simultaneous, Synergistic Control of Ion Exchange Capacity and Cross-Linking of Sterically-Protected Poly(benzimidazolium)s, *Chemistry of Materials* 28 (2016) 8060–8070. <https://doi.org/10.1021/acs.chemmater.6b03902>.
- [197] M. Chen, M. Mandal, K. Groenhout, G. McCool, H.M. Tee, B. Zulevi, P.A. Kohl, Self-adhesive ionomers for durable low-temperature anion exchange membrane electrolysis, *J Power Sources* 536 (2022) 231495. <https://doi.org/10.1016/j.jpowsour.2022.231495>.
- [198] H.M. Tee, H. Park, P.N. Shah, J.A. Trindell, J.D. Sugar, P.A. Kohl, Self-Adhesive Ionomers for Alkaline Electrolysis: Optimized Hydrogen Evolution Electrode, *J Electrochem Soc* 169 (2022) 124515. <https://doi.org/10.1149/1945-7111/acab8a>.
- [199] H. Park, P.N. Shah, H.M. Tee, P.A. Kohl, Self-adhesive ionomers for alkaline electrolysis: Optimized oxygen evolution electrode, *J Power Sources* 564 (2023) 232811. <https://doi.org/10.1016/j.jpowsour.2023.232811>.
- [200] B. Mayerhöfer, F.D. Speck, M. Hegelheimer, M. Bierling, D. Abbas, D. McLaughlin, S. Cherevko, S. Thiele, R. Peach, Electrochemical- and mechanical stability of catalyst layers in anion exchange membrane water electrolysis, *Int J Hydrogen Energy* 47 (2022) 4304–4314. <https://doi.org/10.1016/j.ijhydene.2021.11.083>.
- [201] G.F. Swiegers, R.N.L. Terrett, G. Tsekouras, T. Tsuzuki, R.J. Pace, R. Stranger, The prospects of developing a highly energy-efficient water electrolyser by eliminating or mitigating bubble effects, *Sustain Energy Fuels* 5 (2021) 1280–1310. <https://doi.org/10.1039/D0SE01886D>.

- [202] Z. Zakaria, S.K. Kamarudin, A review of alkaline solid polymer membrane in the application of AEM electrolyzer: Materials and characterization, *Int J Energy Res* 45 (2021) 18337–18354. <https://doi.org/10.1002/er.6983>.
- [203] B. Mayerhöfer, K. Ehelebe, F.D. Speck, M. Bierling, J. Bender, J.A. Kerres, K.J.J. Mayrhofer, S. Cherevko, R. Peach, S. Thiele, On the effect of anion exchange ionomer binders in bipolar electrode membrane interface water electrolysis, *J Mater Chem A Mater* 9 (2021) 14285–14295. <https://doi.org/10.1039/D1TA00747E>.
- [204] P. Fortin, T. Khoza, X. Cao, S.Y. Martinsen, A. Oyarce Barnett, S. Holdcroft, High-performance alkaline water electrolysis using Aemion™ anion exchange membranes, *J Power Sources* 451 (2020) 227814. <https://doi.org/10.1016/j.jpowsour.2020.227814>.
- [205] C. Kim, J.C. Bui, X. Luo, J.K. Cooper, A. Kusoglu, A.Z. Weber, A.T. Bell, Tailored catalyst microenvironments for CO<sub>2</sub> electroreduction to multicarbon products on copper using bilayer ionomer coatings, *Nat Energy* 6 (2021) 1026–1034. <https://doi.org/10.1038/s41560-021-00920-8>.
- [206] A.Y. Faid, L. Xie, A.O. Barnett, F. Seland, D. Kirk, S. Sunde, Effect of anion exchange ionomer content on electrode performance in AEM water electrolysis, *Int J Hydrogen Energy* 45 (2020) 28272–28284. <https://doi.org/10.1016/j.ijhydene.2020.07.202>.
- [207] M.F. Ernst, V. Meier, M. Kornherr, H.A. Gasteiger, Preparation and Performance Evaluation of Microporous Transport Layers for Proton Exchange Membrane (PEM) Water Electrolyzer Anodes, *J Electrochem Soc* 171 (2024) 074511. <https://doi.org/10.1149/1945-7111/ad63cf>.
- [208] F. Fouda-Onana, M. Chandesris, V. Médeau, S. Chelghoum, D. Thoby, N. Guillet, Investigation on the degradation of MEAs for PEM water electrolyzers part I: Effects of testing conditions on MEA performances and membrane properties, *Int J Hydrogen Energy* 41 (2016) 16627–16636. <https://doi.org/10.1016/j.ijhydene.2016.07.125>.
- [209] Z. Zhang, Z. Han, A. Testino, L. Gubler, Platinum and Cerium-Zirconium Oxide Co-Doped Membrane for Mitigated H<sub>2</sub> Crossover and Ionomer Degradation in PEWE, *J Electrochem Soc* 169 (2022) 104501. <https://doi.org/10.1149/1945-7111/ac94a3>.
- [210] E. Padgett, A. Adesso, H. Yu, J. Wrubel, G. Bender, B. Pivovar, S.M. Alia, Performance Losses and Current-Driven Recovery from Cation Contaminants in PEM Water Electrolysis, *J Electrochem Soc* 171 (2024) 064510. <https://doi.org/10.1149/1945-7111/ad576b>.
- [211] M. KELLY, B. EGGER, G. FAFLEK, J. BESENHARD, H. KRONBERGER, G. NAUER, Conductivity of polymer electrolyte membranes by impedance spectroscopy with microelectrodes, *Solid State Ion* 176 (2005) 2111–2114. <https://doi.org/10.1016/j.ssi.2004.07.071>.
- [212] A. Kusoglu, A.Z. Weber, New Insights into Perfluorinated Sulfonic-Acid Ionomers, *Chem Rev* 117 (2017) 987–1104. <https://doi.org/10.1021/acs.chemrev.6b00159>.
- [213] M. Zatoń, J. Rozière, D.J. Jones, Current understanding of chemical degradation mechanisms of perfluorosulfonic acid membranes and their mitigation strategies: a review, *Sustain Energy Fuels* 1 (2017) 409–438. <https://doi.org/10.1039/C7SE00038C>.
- [214] L. Ghassemzadeh, S. Holdcroft, Quantifying the Structural Changes of Perfluorosulfonated Acid Ionomer upon Reaction with Hydroxyl Radicals, *J Am Chem Soc* 135 (2013) 8181–8184. <https://doi.org/10.1021/ja4037466>.
- [215] Z. Rui, K. Hua, Z. Dou, A. Tan, C. Zhang, X. Shi, R. Ding, X. Li, X. Duan, Y. Wu, Y. Zhang, X. Wang, J. Li, J. Liu, A new insight into the chemical degradation of proton exchange membranes in



- water electrolyzers, *J Mater Chem A Mater* 12 (2024) 9563–9573.  
<https://doi.org/10.1039/D3TA05224A>.
- [216] M. Zatoń, J. Rozière, D.J. Jones, Current understanding of chemical degradation mechanisms of perfluorosulfonic acid membranes and their mitigation strategies: a review, *Sustain Energy Fuels* 1 (2017) 409–438. <https://doi.org/10.1039/C7SE00038C>.
- [217] H. Teuku, I. Alshami, J. Goh, M.S. Masdar, K.S. Loh, Review on bipolar plates for low-temperature polymer electrolyte membrane water electrolyzer, *Int J Energy Res* 45 (2021) 20583–20600. <https://doi.org/10.1002/er.7182>.
- [218] A. Kumar, A. Ganguly, P. Papakonstantinou, Thermal stability study of nitrogen functionalities in a graphene network., *J Phys Condens Matter* 24 (2012) 235503.  
<https://doi.org/10.1088/0953-8984/24/23/235503>.
- [219] Y. Wang, W. Li, L. Ma, W. Li, X. Liu, Degradation of solid oxide electrolysis cells: Phenomena, mechanisms, and emerging mitigation strategies—A review, *J Mater Sci Technol* 55 (2020) 35–55. <https://doi.org/10.1016/j.jmst.2019.07.026>.
- [220] K. Chen, S.P. Jiang, Review—Materials Degradation of Solid Oxide Electrolysis Cells, *J Electrochem Soc* 163 (2016) F3070–F3083. <https://doi.org/10.1149/2.0101611jes>.
- [221] P. Moçoteguy, A. Brisse, A review and comprehensive analysis of degradation mechanisms of solid oxide electrolysis cells, *Int J Hydrogen Energy* 38 (2013) 15887–15902.  
<https://doi.org/10.1016/j.ijhydene.2013.09.045>.
- [222] V. Subotić, C. Hochenauer, Analysis of solid oxide fuel and electrolysis cells operated in a real-system environment: State-of-the-health diagnostic, failure modes, degradation mitigation and performance regeneration, *Prog Energy Combust Sci* 93 (2022) 101011.  
<https://doi.org/10.1016/J.PECS.2022.101011>.
- [223] K. Eguchi, T. Hatagishi, H. Arai, Power generation and steam electrolysis characteristics of an electrochemical cell with a zirconia-or ceria-based electrolyte, (n.d.).
- [224] F. Tietz, D. Sebold, A. Brisse, J. Schefold, Degradation phenomena in a solid oxide electrolysis cell after 9000 h of operation, *J Power Sources* 223 (2013) 129–135.  
<https://doi.org/10.1016/j.jpowsour.2012.09.061>.
- [225] R. Knibbe, M.L. Traulsen, A. Hauch, S.D. Ebbesen, M. Mogensen, Solid Oxide Electrolysis Cells: Degradation at High Current Densities, *J Electrochem Soc* 157 (2010) B1209.  
<https://doi.org/10.1149/1.3447752>.
- [226] M.A. Laguna-Bercero, R. Campana, A. Larrea, J.A. Kilner, V.M. Orera, Electrolyte degradation in anode supported microtubular yttria stabilized zirconia-based solid oxide steam electrolysis cells at high voltages of operation, *J Power Sources* 196 (2011) 8942–8947.  
<https://doi.org/10.1016/j.jpowsour.2011.01.015>.
- [227] M.A. Laguna-Bercero, R. Campana, A. Larrea, J.A. Kilner, V.M. Orera, Electrolyte degradation in anode supported microtubular yttria stabilized zirconia-based solid oxide steam electrolysis cells at high voltages of operation, *J Power Sources* 196 (2011) 8942–8947.  
<https://doi.org/10.1016/j.jpowsour.2011.01.015>.
- [228] H. Su, Y.H. Hu, Degradation issues and stabilization strategies of protonic ceramic electrolysis cells for steam electrolysis, *Energy Sci Eng* 10 (2022) 1706–1725.  
<https://doi.org/10.1002/ese3.1010>.

GA No. 101137802

- [229] E. Traversa, E. Fabbri, Proton conductors for solid oxide fuel cells (SOFCs), in: *Functional Materials for Sustainable Energy Applications*, Elsevier, 2012: pp. 515–537. <https://doi.org/10.1533/9780857096371.3.515>.
- [230] Z. Liu, M. Chen, M. Zhou, D. Cao, P. Liu, W. Wang, M. Liu, J. Huang, J. Shao, J. Liu, Multiple Effects of Iron and Nickel Additives on the Properties of Proton Conducting Yttrium-Doped Barium Cerate-Zirconate Electrolytes for High-Performance Solid Oxide Fuel Cells, *ACS Appl Mater Interfaces* 12 (2020) 50433–50445. <https://doi.org/10.1021/acsami.0c14523>.
- [231] S. Yang, Y. Wen, S. Zhang, S. Gu, Z. Wen, X. Ye, Performance and stability of BaCe<sub>0.8-x</sub>Zr<sub>0.2</sub>In<sub>x</sub>O<sub>3-δ</sub>-based materials and reversible solid oxide cells working at intermediate temperature, *Int J Hydrogen Energy* 42 (2017) 28549–28558. <https://doi.org/10.1016/j.ijhydene.2017.09.159>.
- [232] L. Bi, S.P. Shafi, E. Traversa, Y-doped BaZrO<sub>3</sub> as a chemically stable electrolyte for proton-conducting solid oxide electrolysis cells (SOECs), *J Mater Chem A Mater* 3 (2015) 5815–5819. <https://doi.org/10.1039/C4TA07202B>.
- [233] L. Bi, E. Traversa, Steam Electrolysis by Proton-Conducting Solid Oxide Electrolysis Cells (SOECs) with Chemically Stable BaZrO<sub>3</sub>-Based Electrolytes, *ECS Trans* 68 (2015) 3387–3393. <https://doi.org/10.1149/06801.3387ecst>.
- [234] J. Li, C. Wang, X. Wang, L. Bi, Sintering aids for proton-conducting oxides – A double-edged sword? A mini review, *Electrochem Commun* 112 (2020) 106672. <https://doi.org/10.1016/j.elecom.2020.106672>.
- [235] H. Su, Y.H. Hu, Degradation issues and stabilization strategies of protonic ceramic electrolysis cells for steam electrolysis, *Energy Sci Eng* 10 (2022) 1706–1725. <https://doi.org/10.1002/ese3.1010>.
- [236] S. Choi, T.C. Davenport, S.M. Haile, Protonic ceramic electrochemical cells for hydrogen production and electricity generation: exceptional reversibility, stability, and demonstrated faradaic efficiency, *Energy Environ Sci* 12 (2019) 206–215. <https://doi.org/10.1039/C8EE02865F>.
- [237] W. Tang, H. Ding, W. Bian, W. Wu, W. Li, X. Liu, J.Y. Gomez, C.Y. Regalado Vera, M. Zhou, D. Ding, Understanding of A-site deficiency in layered perovskites: promotion of dual reaction kinetics for water oxidation and oxygen reduction in protonic ceramic electrochemical cells, *J Mater Chem A Mater* 8 (2020) 14600–14608. <https://doi.org/10.1039/D0TA05137C>.
- [238] R. Murphy, Y. Zhou, L. Zhang, L. Soule, W. Zhang, Y. Chen, M. Liu, A New Family of Proton-Conducting Electrolytes for Reversible Solid Oxide Cells: BaHf<sub>x</sub>Ce<sub>0.8-x</sub>Y<sub>0.1</sub>Yb<sub>0.1</sub>O<sub>3-δ</sub>, *Adv Funct Mater* 30 (2020). <https://doi.org/10.1002/adfm.202002265>.
- [239] S. Rajendran, N.K. Thangavel, H. Ding, Y. Ding, D. Ding, L.M. Reddy Arava, Tri-Doped BaCeO<sub>3</sub> – BaZrO<sub>3</sub> as a Chemically Stable Electrolyte with High Proton-Conductivity for Intermediate Temperature Solid Oxide Electrolysis Cells (SOECs), *ACS Appl Mater Interfaces* 12 (2020) 38275–38284. <https://doi.org/10.1021/acsami.0c12532>.
- [240] S. Yang, S. Zhang, C. Sun, X. Ye, Z. Wen, Lattice Incorporation of Cu<sup>2+</sup> into the BaCe<sub>0.7</sub>Zr<sub>0.1</sub>Y<sub>0.1</sub>Yb<sub>0.1</sub>O<sub>3-δ</sub> Electrolyte on Boosting Its Sintering and Proton-Conducting Abilities for Reversible Solid Oxide Cells, *ACS Appl Mater Interfaces* 10 (2018) 42387–42396. <https://doi.org/10.1021/acsami.8b15402>.

- [241] Y. Guo, R. Ran, Z. Shao, S. Liu, Effect of Ba nonstoichiometry on the phase structure, sintering, electrical conductivity and phase stability of  $\text{Ba}_{1-x}\text{Ce}_{0.4}\text{Zr}_{0.4}\text{Y}_{0.2}\text{O}_{3-\delta}$  ( $0 \leq x \leq 0.20$ ) proton conductors, *Int J Hydrogen Energy* 36 (2011) 8450–8460. <https://doi.org/10.1016/j.ijhydene.2011.04.037>.
- [242] H.-S. Kim, H. Bin Bae, W. Jung, S.-Y. Chung, Manipulation of Nanoscale Intergranular Phases for High Proton Conduction and Decomposition Tolerance in  $\text{BaCeO}_3$  Polycrystals, *Nano Lett* 18 (2018) 1110–1117. <https://doi.org/10.1021/acs.nanolett.7b04655>.
- [243] N.U. Hassan, E. Motyka, J. Kweder, P. Ganesan, B. Brechin, B. Zulevi, H.R. Colón-Mercado, P.A. Kohl, W.E. Mustain, Effect of porous transport layer properties on the anode electrode in anion exchange membrane electrolyzers, *J Power Sources* 555 (2023) 232371. <https://doi.org/10.1016/j.jpowsour.2022.232371>.
- [244] R.R. Raja Sulaiman, W.Y. Wong, K.S. Loh, Recent developments on transition metal-based electrocatalysts for application in anion exchange membrane water electrolysis, *Int J Energy Res* 46 (2022) 2241–2276. <https://doi.org/10.1002/er.7380>.
- [245] M. Bernt, C. Schramm, J. Schröter, C. Gebauer, J. Byrknes, C. Eickes, H.A. Gasteiger, Effect of the  $\text{IrO}_x$  Conductivity on the Anode Electrode/Porous Transport Layer Interfacial Resistance in PEM Water Electrolyzers, *J Electrochem Soc* 168 (2021) 084513. <https://doi.org/10.1149/1945-7111/ac1eb4>.
- [246] P.M. Dmitri Bessarabov, *PEM Water Electrolysis*, Elsevier, 2018. <https://doi.org/10.1016/C2016-0-00574-0>.
- [247] C. Liu, M. Shviro, A.S. Gago, S.F. Zaccarine, G. Bender, P. Gazdzicki, T. Morawietz, I. Biswas, M. Rasinski, A. Everwand, R. Schierholz, J. Pfeilsticker, M. Müller, P.P. Lopes, R. Eichel, B. Pivovar, S. Pylypenko, K.A. Friedrich, W. Lehnert, M. Carmo, Exploring the Interface of Skin-Layered Titanium Fibers for Electrochemical Water Splitting, *Adv Energy Mater* 11 (2021). <https://doi.org/10.1002/aenm.202002926>.
- [248] Z. Kang, J. Mo, G. Yang, Y. Li, D.A. Talley, S.T. Retterer, D.A. Cullen, T.J. Toops, M.P. Brady, G. Bender, B.S. Pivovar, J.B. Green, F.-Y. Zhang, Thin film surface modifications of thin/tunable liquid/gas diffusion layers for high-efficiency proton exchange membrane electrolyzer cells, *Appl Energy* 206 (2017) 983–990. <https://doi.org/10.1016/j.apenergy.2017.09.004>.
- [249] M. Bernt, C. Schramm, J. Schröter, C. Gebauer, J. Byrknes, C. Eickes, H.A. Gasteiger, Effect of the  $\text{IrO}_x$  Conductivity on the Anode Electrode/Porous Transport Layer Interfacial Resistance in PEM Water Electrolyzers, *J Electrochem Soc* 168 (2021) 084513. <https://doi.org/10.1149/1945-7111/ac1eb4>.
- [250] C. Liu, M. Carmo, G. Bender, A. Everwand, T. Lickert, J.L. Young, T. Smolinka, D. Stolten, W. Lehnert, Performance enhancement of PEM electrolyzers through iridium-coated titanium porous transport layers, *Electrochem Commun* 97 (2018) 96–99. <https://doi.org/10.1016/j.elecom.2018.10.021>.
- [251] C. Liu, K. Wippermann, M. Rasinski, Y. Suo, M. Shviro, M. Carmo, W. Lehnert, Constructing a Multifunctional Interface between Membrane and Porous Transport Layer for Water Electrolyzers, *ACS Appl Mater Interfaces* 13 (2021) 16182–16196. <https://doi.org/10.1021/acsami.0c20690>.
- [252] T. Srour, K. Kumar, V. Martin, L. Dubau, F. Maillard, B. Gilles, J. Dillet, S. Didierjean, B. Amoury, T.D. Le, G. Maranzana, On the contact resistance between the anode and the porous

- transport layer in a proton exchange membrane water electrolyzer, *Int J Hydrogen Energy* 58 (2024) 351–361. <https://doi.org/10.1016/j.ijhydene.2024.01.134>.
- [253] C. Rakousky, U. Reimer, K. Wippermann, S. Kuhri, M. Carmo, W. Lueke, D. Stolten, Polymer electrolyte membrane water electrolysis: Restraining degradation in the presence of fluctuating power, *J Power Sources* 342 (2017) 38–47. <https://doi.org/10.1016/j.jpowsour.2016.11.118>.
- [254] C. Rakousky, U. Reimer, K. Wippermann, M. Carmo, W. Lueke, D. Stolten, An analysis of degradation phenomena in polymer electrolyte membrane water electrolysis, *J Power Sources* 326 (2016) 120–128. <https://doi.org/10.1016/j.jpowsour.2016.06.082>.
- [255] X.-Z. Yuan, N. Shaigan, C. Song, M. Aujla, V. Neburchilov, J.T.H. Kwan, D.P. Wilkinson, A. Bazylak, K. Fatih, The porous transport layer in proton exchange membrane water electrolysis: perspectives on a complex component, *Sustain Energy Fuels* 6 (2022) 1824–1853. <https://doi.org/10.1039/D2SE00260D>.
- [256] B. Zhao, C. Lee, J.K. Lee, K.F. Fahy, J.M. LaManna, E. Baltic, D.L. Jacobson, D.S. Hussey, A. Bazylak, Superhydrophilic porous transport layer enhances efficiency of polymer electrolyte membrane electrolyzers, *Cell Rep Phys Sci* 2 (2021) 100580. <https://doi.org/10.1016/j.xcrp.2021.100580>.
- [257] C. Rakousky, U. Reimer, K. Wippermann, M. Carmo, W. Lueke, D. Stolten, An analysis of degradation phenomena in polymer electrolyte membrane water electrolysis, *J Power Sources* 326 (2016) 120–128. <https://doi.org/10.1016/j.jpowsour.2016.06.082>.
- [258] G. Jeanmonod, S. Diethelm, J. Van herle, Poisoning effects of chlorine on a solid oxide cell operated in co-electrolysis, *J Power Sources* 506 (2021). <https://doi.org/10.1016/j.jpowsour.2021.230247>.
- [259] M. Stanislawski, J. Froitzheim, L. Niewolak, W.J. Quadackers, K. Hilpert, T. Markus, L. Singheiser, Reduction of chromium vaporization from SOFC interconnectors by highly effective coatings, *J Power Sources* 164 (2007) 578–589. <https://doi.org/10.1016/j.jpowsour.2006.08.013>.
- [260] E. Bucher, C. Gspan, T. Höschen, F. Hofer, W. Sitte, Oxygen exchange kinetics of La<sub>0.6</sub>Sr<sub>0.4</sub>CoO<sub>3-δ</sub> affected by changes of the surface composition due to chromium and silicon poisoning, *Solid State Ion* 299 (2017) 26–31. <https://doi.org/10.1016/j.ssi.2016.09.024>.
- [261] E. Bucher, M. Yang, W. Sitte, In Situ Investigations of the Chromium-Induced Degradation of the Oxygen Surface Exchange Kinetics of IT-SOFC Cathode Materials La<sub>0.6</sub>Sr<sub>0.4</sub>CoO<sub>3-δ</sub> and La<sub>0.58</sub>Sr<sub>0.4</sub>Co<sub>0.2</sub>Fe<sub>0.8</sub>O<sub>3-δ</sub>, *J Electrochem Soc* 159 (2012) B592–B596. <https://doi.org/10.1149/2.027206jes>.
- [262] E. Bucher, M. Yang, W. Sitte, In-situ Investigation of the Chromium Induced Degradation of the Oxygen Exchange Kinetics of the IT-SOFC Cathode Material La<sub>0.6</sub>Sr<sub>0.4</sub>CoO<sub>3-δ</sub>, *ECS Trans* 35 (2011) 2019–2025. <https://doi.org/10.1149/1.3570192>.
- [263] K. Chen, J. Hyodo, A. Dodd, N. Ai, T. Ishihara, L. Jian, S.P. Jiang, Chromium deposition and poisoning of La<sub>0.8</sub>Sr<sub>0.2</sub>MnO<sub>3</sub> oxygen electrodes of solid oxide electrolysis cells, *Faraday Discuss* 182 (2015) 457–476. <https://doi.org/10.1039/c5fd00010f>.
- [264] B. Wei, K. Chen, L. Zhao, Z. Lü, S.P. Jiang, Chromium deposition and poisoning at La<sub>0.6</sub>Sr<sub>0.4</sub>Co<sub>0.2</sub>Fe<sub>0.8</sub>O<sub>3-δ</sub> oxygen electrodes of solid oxide electrolysis cells, *Physical Chemistry Chemical Physics* 17 (2015) 1601–1609. <https://doi.org/10.1039/c4cp05110f>.

- [265] D. Cao, H. Xu, D. Cheng, Branch-leaf-shaped CuNi@NiFeCu nanodendrites as highly efficient electrocatalysts for overall water splitting, *Appl Catal B* 298 (2021) 120600. <https://doi.org/10.1016/j.apcatb.2021.120600>.
- [266] C. Spöri, J.T.H. Kwan, A. Bonakdarpour, D.P. Wilkinson, P. Strasser, The Stability Challenges of Oxygen Evolving Catalysts: Towards a Common Fundamental Understanding and Mitigation of Catalyst Degradation, *Angewandte Chemie International Edition* 56 (2017) 5994–6021. <https://doi.org/10.1002/anie.201608601>.
- [267] J. Shan, C. Ye, S. Chen, T. Sun, Y. Jiao, L. Liu, C. Zhu, L. Song, Y. Han, M. Jaroniec, Y. Zhu, Y. Zheng, S.-Z. Qiao, Short-Range Ordered Iridium Single Atoms Integrated into Cobalt Oxide Spinel Structure for Highly Efficient Electrocatalytic Water Oxidation, *J Am Chem Soc* 143 (2021) 5201–5211. <https://doi.org/10.1021/jacs.1c01525>.
- [268] X. Tang, S. Wang, L. Qian, M. Ren, P. Sun, Y. Li, J.Q. Yang, Corrosion Properties of Candidate Materials in Supercritical Water Oxidation Process, *Journal of Advanced Oxidation Technologies* 19 (2016). <https://doi.org/10.1515/jaots-2016-0119>.
- [269] D.Y. Chung, P.P. Lopes, P. Farinazzo Bergamo Dias Martins, H. He, T. Kawaguchi, P. Zapol, H. You, D. Tripkovic, D. Strmcnik, Y. Zhu, S. Seifert, S. Lee, V.R. Stamenkovic, N.M. Markovic, Dynamic stability of active sites in hydr(oxy)oxides for the oxygen evolution reaction, *Nat Energy* 5 (2020) 222–230. <https://doi.org/10.1038/s41560-020-0576-y>.
- [270] D. Li, A.R. Motz, C. Bae, C. Fujimoto, G. Yang, F.-Y. Zhang, K.E. Ayers, Y.S. Kim, Durability of anion exchange membrane water electrolyzers, *Energy Environ Sci* 14 (2021) 3393–3419. <https://doi.org/10.1039/D0EE04086J>.
- [271] E.K. Volk, M.E. Kreider, S. Kwon, S.M. Alia, Recent progress in understanding the catalyst layer in anion exchange membrane electrolyzers – durability, utilization, and integration, *EES Catalysis* 2 (2024) 109–137. <https://doi.org/10.1039/D3EY00193H>.
- [272] J. Zhang, X. Luo, Y. Ding, L. Chang, C. Dong, Effect of bipolar-plates design on corrosion, mass and heat transfer in proton-exchange membrane fuel cells and water electrolyzers: A review, *International Journal of Minerals, Metallurgy and Materials* 31 (2024) 1599–1616. <https://doi.org/10.1007/s12613-023-2803-6>.
- [273] H. Ito, N. Miyazaki, S. Sugiyama, M. Ishida, Y. Nakamura, S. Iwasaki, Y. Hasegawa, A. Nakano, Investigations on electrode configurations for anion exchange membrane electrolysis, *J Appl Electrochem* 48 (2018) 305–316. <https://doi.org/10.1007/s10800-018-1159-5>.
- [274] J. Lei, Z. Wang, Y. Zhang, M. Ju, H. Fei, S. Wang, C. Fu, X. Yuan, Q. Fu, M.U. Farid, H. Kong, A.K. An, R. Deng, F. Liu, J. Wang, Understanding and resolving the heterogeneous degradation of anion exchange membrane water electrolysis for large-scale hydrogen production, *Carbon Neutrality* 3 (2024) 25. <https://doi.org/10.1007/s43979-024-00101-y>.
- [275] L. Messing, K. Pellumbi, L. Hoof, N. Imming, S. Wilbers, L. Kopietz, M. Joemann, A. Grevé, K. Junge Puring, U. Apfel, Carbon Bipolar Plates in PEM Water Electrolysis: Bust or Must?, *Adv Energy Mater* 14 (2024). <https://doi.org/10.1002/aenm.202402308>.
- [276] P. Lettenmeier, R. Wang, R. Abouatallah, B. Saruhan, O. Freitag, P. Gazdzicki, T. Morawietz, R. Hiesgen, A.S. Gago, K.A. Friedrich, Low-Cost and Durable Bipolar Plates for Proton Exchange Membrane Electrolyzers, *Sci Rep* 7 (2017) 44035. <https://doi.org/10.1038/srep44035>.
- [277] W. Sitte, R. Merkle, eds., *High-Temperature Electrolysis*, IOP Publishing, 2023. <https://doi.org/10.1088/978-0-7503-3951-3>.

GA No. 101137802

- [278] M.C. Tucker, Progress in metal-supported solid oxide electrolysis cells: A review, *Int J Hydrogen Energy* 45 (2020) 24203–24218. <https://doi.org/10.1016/j.ijhydene.2020.06.300>.
- [279] W.Z. Zhu, S.C. Deevi, Development of interconnect materials for solid oxide fuel cells, *Materials Science and Engineering: A* 348 (2003) 227–243. [https://doi.org/10.1016/S0921-5093\(02\)00736-0](https://doi.org/10.1016/S0921-5093(02)00736-0).
- [280] R. Wang, Z. Sun, J.-P. Choi, S.N. Basu, J.W. Stevenson, M.C. Tucker, Ferritic stainless steel interconnects for protonic ceramic electrochemical cell stacks: Oxidation behavior and protective coatings, *Int J Hydrogen Energy* 44 (2019) 25297–25309. <https://doi.org/10.1016/j.ijhydene.2019.08.041>.
- [281] D.M.P.K.S.W.J.W.S. and P.S. Yang Z., *Materials Properties Database for Selection of High-Temperature Alloys and Concepts of Alloy Design for SOFC Applications*, 2002.
- [282] S. Anelli, A. Baggio, D. Ferrero, D. Schmider, J. Dailly, M. Santarelli, F. Smeacetto, Characterization and testing of glass-ceramic sealants for protonic ceramic electrolysis cells applications, *Ceram Int* 50 (2024) 17520–17531. <https://doi.org/10.1016/j.ceramint.2024.02.240>.
- [283] D.J. Young, J. Zurek, L. Singheiser, W.J. Quadackers, Temperature dependence of oxide scale formation on high-Cr ferritic steels in Ar–H<sub>2</sub>–H<sub>2</sub>O, *Corros Sci* 53 (2011) 2131–2141. <https://doi.org/10.1016/j.corsci.2011.02.031>.
- [284] A. Chyrkin, K.O. Gunduz, V. Asokan, J.-E. Svensson, J. Froitzheim, High temperature oxidation of AISI 441 in simulated solid oxide fuel cell anode side conditions, *Corros Sci* 203 (2022) 110338. <https://doi.org/10.1016/j.corsci.2022.110338>.
- [285] J.C.W. Mah, A. Muchtar, M.R. Somalu, M.J. Ghazali, Metallic interconnects for solid oxide fuel cell: A review on protective coating and deposition techniques, *Int J Hydrogen Energy* 42 (2017) 9219–9229. <https://doi.org/10.1016/j.ijhydene.2016.03.195>.
- [286] J.K. Lee, A. Bazylak, Bubbles: The Good, the Bad, and the Ugly, *Joule* 5 (2021) 19–21. <https://doi.org/10.1016/j.joule.2020.12.024>.
- [287] X. Zhao, H. Ren, L. Luo, Gas Bubbles in Electrochemical Gas Evolution Reactions, *Langmuir* 35 (2019) 5392–5408. <https://doi.org/10.1021/acs.langmuir.9b00119>.
- [288] J. Bleeker, C. van Kasteren, J.R. van Ommen, D.A. Vermaas, Gas bubble removal from a zero-gap alkaline electrolyser with a pressure swing and why foam electrodes might not be suitable at high current densities, *Int J Hydrogen Energy* 57 (2024) 1398–1407. <https://doi.org/10.1016/j.ijhydene.2024.01.147>.
- [289] L. Li, P.C.M. Laan, X. Yan, X. Cao, M.J. Mekkering, K. Zhao, L. Ke, X. Jiang, X. Wu, L. Li, L. Xue, Z. Wang, G. Rothenberg, N. Yan, High-Rate Alkaline Water Electrolysis at Industrially Relevant Conditions Enabled by Superaerophobic Electrode Assembly, *Advanced Science* 10 (2023). <https://doi.org/10.1002/adv.202206180>.
- [290] Y. Li, G. Zhang, W. Lu, F. Cao, Amorphous Ni–Fe–Mo Suboxides Coupled with Ni Network as Porous Nanoplate Array on Nickel Foam: A Highly Efficient and Durable Bifunctional Electrode for Overall Water Splitting, *Advanced Science* 7 (2020). <https://doi.org/10.1002/adv.201902034>.
- [291] X. Zhang, J. Hu, X. Cheng, K.A. Nartey, L. Zhang, Double metal–organic frameworks derived Fe–Co–Ni phosphides nanosheets as high-performance electrocatalyst for alkaline

- electrochemical water splitting, *Electrochim Acta* 367 (2021) 137536.  
<https://doi.org/10.1016/j.electacta.2020.137536>.
- [292] Y. Kuroda, T. Nishimoto, S. Mitsushima, Self-repairing hybrid nanosheet anode catalysts for alkaline water electrolysis connected with fluctuating renewable energy, *Electrochim Acta* 323 (2019) 134812. <https://doi.org/10.1016/j.electacta.2019.134812>.
- [293] Y. Kuroda, D. Mizukoshi, V. Yadav, T. Taniguchi, Y. Sasaki, Y. Nishiki, Z. Awaludin, A. Kato, S. Mitsushima, Integration of Multifunctionality in a Colloidal Self-Repairing Catalyst for Alkaline Water Electrolysis to Achieve High Activity and Durability, *Advanced Energy and Sustainability Research* 5 (2024). <https://doi.org/10.1002/aesr.202400196>.
- [294] H. Noelle, O. Pérol, M. Pérol, V. Avrillon, E. Belladame, J. Fayette, F. Fournié, A. Swalduz, J. Dessemon, J.-Y. Blay, E.-M. Neidhardt, P. Saintigny, M. Tabutin, M. Bousageon, D. Praud, B. Charbotel, B. Fervers, Occupational asbestos exposure and survival among lung cancer patients, *Lung Cancer* 179 (2023) 107182. <https://doi.org/10.1016/j.lungcan.2023.107182>.
- [295] D. Li, A.R. Motz, C. Bae, C. Fujimoto, G. Yang, F.-Y. Zhang, K.E. Ayers, Y.S. Kim, Durability of anion exchange membrane water electrolyzers, *Energy Environ Sci* 14 (2021) 3393–3419. <https://doi.org/10.1039/D0EE04086J>.
- [296] J. Lei, Z. Wang, Y. Zhang, M. Ju, H. Fei, S. Wang, C. Fu, X. Yuan, Q. Fu, M.U. Farid, H. Kong, A.K. An, R. Deng, F. Liu, J. Wang, Understanding and resolving the heterogeneous degradation of anion exchange membrane water electrolysis for large-scale hydrogen production, *Carbon Neutrality* 3 (2024) 25. <https://doi.org/10.1007/s43979-024-00101-y>.
- [297] W. Ng, W. Wong, N. Rosli, K. Loh, Commercial Anion Exchange Membranes (AEMs) for Fuel Cell and Water Electrolyzer Applications: Performance, Durability, and Materials Advancement, *Separations* 10 (2023) 424. <https://doi.org/10.3390/separations10080424>.
- [298] H. Becker, J. Murawski, D. V. Shinde, I.E.L. Stephens, G. Hinds, G. Smith, Impact of impurities on water electrolysis: a review, *Sustain Energy Fuels* 7 (2023) 1565–1603. <https://doi.org/10.1039/D2SE01517J>.
- [299] H.J. Kim, H.Y. Kim, J. Joo, S.H. Joo, J.S. Lim, J. Lee, H. Huang, M. Shao, J. Hu, J.Y. Kim, B.J. Min, S.W. Lee, M. Kang, K. Lee, S. Choi, Y. Park, Y. Wang, J. Li, Z. Zhang, J. Ma, S.-I. Choi, Recent advances in non-precious group metal-based catalysts for water electrolysis and beyond, *J Mater Chem A Mater* 10 (2022) 50–88. <https://doi.org/10.1039/D1TA06548C>.
- [300] S. Garg, C.A. Giron Rodriguez, T.E. Rufford, J.R. Varcoe, B. Seger, How membrane characteristics influence the performance of CO<sub>2</sub> and CO electrolysis, *Energy Environ Sci* 15 (2022) 4440–4469. <https://doi.org/10.1039/D2EE01818G>.
- [301] K. V. Petrov, J.C. Bui, L. Baumgartner, L.-C. Weng, S.M. Dischinger, D.M. Larson, D.J. Miller, A.Z. Weber, D.A. Vermaas, Anion-exchange membranes with internal microchannels for water control in CO<sub>2</sub> electrolysis, *Sustain Energy Fuels* 6 (2022) 5077–5088. <https://doi.org/10.1039/D2SE00858K>.
- [302] A. Zuber, I.M. Oikonomou, L. Gannon, I. Chudin, L. Reith, B. Can, M. Lounasvuori, T. Schultz, N. Koch, C. McGuinness, P.W. Menezes, V. Nicolosi, M.P. Browne, Effect of the Precursor Metal Salt on the Oxygen Evolution Reaction for NiFe Oxide Materials, *ChemElectroChem* 11 (2024). <https://doi.org/10.1002/celec.202400151>.
- [303] B.-R. Guo, M.-X. Chen, S.-W. Li, R.-H. Gao, B.-H. Sang, X.-Q. Ren, Z. Liu, X. Cao, J. Liu, Y.-N. Ding, P. Xu, Y. Xu, Construction of iron oxyhydroxide/nickel sulfate hydroxide hybrid electrocatalyst

- for efficient oxygen evolution, *Rare Metals* 43 (2024) 6394–6404.  
<https://doi.org/10.1007/s12598-024-02841-3>.
- [304] M.K. Shahid, Y. Choi, CO<sub>2</sub> as an Alternative to Traditional Antiscalants in Pressure-Driven Membrane Processes: An Experimental Study of Lab-Scale Operation and Cleaning Strategies, *Membranes (Basel)* 12 (2022) 918. <https://doi.org/10.3390/membranes12100918>.
- [305] H.A. Miller, K. Bouzek, J. Hnat, S. Loos, C.I. Bernäcker, T. Weißgärber, L. Röntzsch, J. Meier-Haack, Green hydrogen from anion exchange membrane water electrolysis: a review of recent developments in critical materials and operating conditions, *Sustain Energy Fuels* 4 (2020) 2114–2133. <https://doi.org/10.1039/C9SE01240K>.
- [306] R. Yoshimura, S. Wai, Y. Ota, K. Nishioka, Y. Suzuki, Effects of Artificial River Water on PEM Water Electrolysis Performance, *Catalysts* 12 (2022) 934.  
<https://doi.org/10.3390/catal12090934>.
- [307] L. Zhang, X. Jie, Z.-G. Shao, Z.-M. Zhou, G. Xiao, B. Yi, The influence of sodium ion on the solid polymer electrolyte water electrolysis, *Int J Hydrogen Energy* 37 (2012) 1321–1325.  
<https://doi.org/10.1016/j.ijhydene.2011.10.023>.
- [308] E. Padgett, A. Adesso, H. Yu, J. Wrubel, G. Bender, B. Pivovar, S.M. Alia, Performance Losses and Current-Driven Recovery from Cation Contaminants in PEM Water Electrolysis, *J Electrochem Soc* 171 (2024) 064510. <https://doi.org/10.1149/1945-7111/ad576b>.
- [309] J.G. Vos, M.T.M. Koper, Measurement of competition between oxygen evolution and chlorine evolution using rotating ring-disk electrode voltammetry, *Journal of Electroanalytical Chemistry* 819 (2018) 260–268. <https://doi.org/10.1016/j.jelechem.2017.10.058>.
- [310] T.J. Schmidt, U.A. Paulus, H.A. Gasteiger, R.J. Behm, The oxygen reduction reaction on a Pt/carbon fuel cell catalyst in the presence of chloride anions, *Journal of Electroanalytical Chemistry* 508 (2001) 41–47. [https://doi.org/10.1016/S0022-0728\(01\)00499-5](https://doi.org/10.1016/S0022-0728(01)00499-5).
- [311] I. Katsounaros, J.C. Meier, K.J.J. Mayrhofer, The impact of chloride ions and the catalyst loading on the reduction of H<sub>2</sub>O<sub>2</sub> on high-surface-area platinum catalysts, *Electrochim Acta* 110 (2013) 790–795. <https://doi.org/10.1016/j.electacta.2013.03.156>.
- [312] E. Padgett, A. Adesso, H. Yu, J. Wrubel, G. Bender, B. Pivovar, S.M. Alia, Performance Losses and Current-Driven Recovery from Cation Contaminants in PEM Water Electrolysis, *J Electrochem Soc* 171 (2024) 064510. <https://doi.org/10.1149/1945-7111/ad576b>.
- [313] T. Smolinka, M. Heinen, Y.X. Chen, Z. Jusys, W. Lehnert, R.J. Behm, CO<sub>2</sub> reduction on Pt electrocatalysts and its impact on H<sub>2</sub> oxidation in CO<sub>2</sub> containing fuel cell feed gas – A combined in situ infrared spectroscopy, mass spectrometry and fuel cell performance study, *Electrochim Acta* 50 (2005) 5189–5199. <https://doi.org/10.1016/j.electacta.2005.02.082>.
- [314] N. Danilov, A. Tarutin, J. Lyagaeva, G. Vdovin, D. Medvedev, CO<sub>2</sub>-promoted hydrogen production in a protonic ceramic electrolysis cell, *J Mater Chem A Mater* 6 (2018) 16341–16346. <https://doi.org/10.1039/C8TA05820B>.
- [315] X.X. Zheng, A.J. Böttger, K.M.B. Jansen, J. van Turnhout, J. van Kranendonk, Aging of Polyphenylene Sulfide-Glass Composite and Polysulfone in Highly Oxidative and Strong Alkaline Environments, *Front Mater* 7 (2020). <https://doi.org/10.3389/fmats.2020.610440>.
- [316] A.S. Emam, M.O. Hamdan, B.A. Abu-Nabah, E. Elnajjar, A review on recent trends, challenges, and innovations in alkaline water electrolysis, *Int J Hydrogen Energy* 64 (2024) 599–625.  
<https://doi.org/10.1016/j.ijhydene.2024.03.238>.



- [317] A. Abdel Haleem, H. Akutagawa, S. Nakayama, Y. Bao, Z. Awaludin, K. Nagasawa, Y. Kuroda, Y. Nishiki, S. Mitsushima, Innovative membrane with selective gas permeability for alkaline water electrolysis: Dependable cell performance under industrial conditions, *J Power Sources* 587 (2023) 233709. <https://doi.org/10.1016/j.jpowsour.2023.233709>.
- [318] F.P. Lohmann-Richters, S. Renz, W. Lehnert, M. Müller, M. Carmo, Review—Challenges and Opportunities for Increased Current Density in Alkaline Electrolysis by Increasing the Operating Temperature, *J Electrochem Soc* 168 (2021) 114501. <https://doi.org/10.1149/1945-7111/ac34cc>.
- [319] P. VERMEIREN, Evaluation of the ZirfonS separator for use in alkaline water electrolysis and Ni-H<sub>2</sub> batteries, *Int J Hydrogen Energy* 23 (1998) 321–324. [https://doi.org/10.1016/S0360-3199\(97\)00069-4](https://doi.org/10.1016/S0360-3199(97)00069-4).
- [320] P. VERMEIREN, ZirfonS: A new separator for Ni-H<sub>2</sub> batteries and alkaline fuel cells, *Int J Hydrogen Energy* 21 (1996) 679–684. [https://doi.org/10.1016/0360-3199\(95\)00132-8](https://doi.org/10.1016/0360-3199(95)00132-8).
- [321] J. Nie, Y. Chen, S. Cohen, B.D. Carter, R.F. Boehm, Numerical and experimental study of three-dimensional fluid flow in the bipolar plate of a PEM electrolysis cell, *International Journal of Thermal Sciences* 48 (2009) 1914–1922. <https://doi.org/10.1016/j.ijthermalsci.2009.02.017>.
- [322] J.O. Majasan, J.I.S. Cho, M. Maier, I. Dedigama, P.R. Shearing, D.J.L. Brett, Effect of Anode Flow Channel Depth on the Performance of Polymer Electrolyte Membrane Water Electrolyser, *ECS Trans* 85 (2018) 1593–1603. <https://doi.org/10.1149/08513.1593ecst>.
- [323] H. Ito, T. Maeda, A. Nakano, Y. Hasegawa, N. Yokoi, C.M. Hwang, M. Ishida, A. Kato, T. Yoshida, Effect of flow regime of circulating water on a proton exchange membrane electrolyzer, *Int J Hydrogen Energy* 35 (2010) 9550–9560. <https://doi.org/10.1016/j.ijhydene.2010.06.103>.
- [324] S. Sun, Y. Xiao, D. Liang, Z. Shao, H. Yu, M. Hou, B. Yi, Behaviors of a proton exchange membrane electrolyzer under water starvation, *RSC Adv* 5 (2015) 14506–14513. <https://doi.org/10.1039/C4RA14104K>.
- [325] Y. Kobayashi, K. Kosaka, T. Yamamoto, Y. Tachikawa, K. Ito, K. Sasaki, A solid polymer water electrolysis system utilizing natural circulation, *Int J Hydrogen Energy* 39 (2014) 16263–16274. <https://doi.org/10.1016/j.ijhydene.2014.07.153>.
- [326] C. Chatzichristodoulou, M. Chen, P. V Hendriksen, T. Jacobsen, M.B. Mogensen, *Electrochimica Acta* Understanding degradation of solid oxide electrolysis cells through modeling of electrochemical potential profiles, *Electrochim Acta* 189 (2016) 265–282. <https://doi.org/10.1016/j.electacta.2015.12.067>.
- [327] H. Zhu, S. Ricote, C. Duan, R.P. O’Hayre, D.S. Tsvetkov, R.J. Kee, Defect Incorporation and Transport within Dense BaZr<sub>0.8</sub>Y<sub>0.2</sub>O<sub>3-δ</sub> (BZY20) Proton-Conducting Membranes, *J Electrochem Soc* 165 (2018) F581–F588. <https://doi.org/10.1149/2.0161809jes>.
- [328] H. Zhu, S. Ricote, C. Duan, R.P. O’Hayre, R.J. Kee, Defect Chemistry and Transport within Dense BaCe<sub>0.7</sub>Zr<sub>0.1</sub>Y<sub>0.1</sub>Yb<sub>0.1</sub>O<sub>3-δ</sub> (BCZYYb) Proton-Conducting Membranes, *J Electrochem Soc* 165 (2018) F845–F853. <https://doi.org/10.1149/2.1091810jes>.
- [329] TSOTRIDIS Georgios, PILENGA Alberto, EU harmonised protocols for testing of low temperature water electrolyzers, 2021.
- [330] S.F. Amireh, N.N. Heineman, P. Vermeulen, R.L.G. Barros, D. Yang, J. van der Schaaf, M.T. de Groot, Impact of power supply fluctuation and part load operation on the efficiency of

- alkaline water electrolysis, *J Power Sources* 560 (2023) 232629.  
<https://doi.org/10.1016/j.jpowsour.2023.232629>.
- [331] S. Hu, B. Guo, S. Ding, Z. Tian, J. Gu, H. Yang, F. Yang, M. Ouyang, Study on the synergistic regulation strategy of load range and electrolysis efficiency of 250 kW alkaline electrolysis system under high-dynamic operation conditions, *ETransportation* 19 (2024) 100304.  
<https://doi.org/10.1016/j.etrans.2023.100304>.
- [332] L. Cammann, A. Perera, V. Alstad, J. Jäschke, Design and operational analysis of an alkaline water electrolysis plant powered by wind energy, *Int J Hydrogen Energy* 93 (2024) 963–974.  
<https://doi.org/10.1016/j.ijhydene.2024.10.176>.
- [333] D. Huang, Z. Zhong, X. Ai, K. Hu, B. Xiong, Q. Wen, J. Fang, S. Cheng, Size design strategy for scaling up alkaline water electrolysis stack integrated with renewable energy source: A multiphysics modeling approach, *Energy Convers Manag* 300 (2024) 117955.  
<https://doi.org/10.1016/j.enconman.2023.117955>.
- [334] S. Ding, Z. Tian, S. Hu, B. Guo, H. Yang, F. Yang, M. Ouyang, Study on multi-power-level configuration scheme and scheduling strategy for multi-stack alkaline water electrolysis system in off-grid wind power scenario, *Energy Convers Manag* 314 (2024) 118714.  
<https://doi.org/10.1016/j.enconman.2024.118714>.
- [335] M. Ranz, B. Grabner, B. Schweighofer, H. Wegleiter, A. Trattner, Dynamics of anion exchange membrane electrolysis: Unravelling loss mechanisms with electrochemical impedance spectroscopy, reference electrodes and distribution of relaxation times, *J Power Sources* 605 (2024) 234455. <https://doi.org/10.1016/j.jpowsour.2024.234455>.
- [336] Y. Ding, X. Luo, L. Chang, C. Dong, Response characteristics of platinum coated titanium bipolar plates for proton exchange membrane water electrolysis under fluctuating conditions, *Electrochem Commun* 168 (2024) 107819. <https://doi.org/10.1016/j.elecom.2024.107819>.
- [337] Y. Xu, M. Cheng, H. Chen, Y. Gui, Z. Deng, Y. Tong, G. Li, Power fluctuation of renewable energy source integrated system and its effect on proton exchange membrane water electrolysis, in: *PEM Water Electrolysis*, Elsevier, 2025: pp. 319–345.  
<https://doi.org/10.1016/B978-0-443-24062-1.00009-7>.
- [338] D. Niblett, M. Delpisheh, S. Ramakrishnan, M. Mamlouk, Review of next generation hydrogen production from offshore wind using water electrolysis, *J Power Sources* 592 (2024) 233904.  
<https://doi.org/10.1016/j.jpowsour.2023.233904>.
- [339] E. Crespi, G. Guandalini, L. Mastropasqua, S. Campanari, J. Brouwer, Experimental and theoretical evaluation of a 60 kW PEM electrolysis system for flexible dynamic operation, *Energy Convers Manag* 277 (2023) 116622.  
<https://doi.org/10.1016/j.enconman.2022.116622>.
- [340] B. Xu, Y. Yang, J. Li, Y. Wang, D. Ye, L. Zhang, X. Zhu, Q. Liao, Computational assessment of response to fluctuating load of renewable energy in proton exchange membrane water electrolyzer, *Renew Energy* 232 (2024) 121084.  
<https://doi.org/10.1016/j.renene.2024.121084>.
- [341] S. Siracusano, S. Trocino, N. Briguglio, F. Pantò, A.S. Aricò, Analysis of performance degradation during steady-state and load-thermal cycles of proton exchange membrane water electrolysis cells, *J Power Sources* 468 (2020) 228390.  
<https://doi.org/10.1016/j.jpowsour.2020.228390>.

- [342] S. Kim, K. Hyun, Y. Kwon, Effects of voltage stress conditions on degradation of iridium-based catalysts occurring during high-frequency operation of PEM water electrolysis, *Chemical Engineering Journal* 496 (2024) 154288. <https://doi.org/10.1016/j.cej.2024.154288>.
- [343] A.J. McLeod, L. V. Böhre, B. Bensmann, O.E. Herrera, W. Mérida, Anode and cathode overpotentials under accelerated stress testing of a PEM electrolysis cell, *J Power Sources* 589 (2024) 233750. <https://doi.org/10.1016/j.jpowsour.2023.233750>.
- [344] A. Sandoval-Amador, A. Egea-Corbacho, D. Engelhardt-Guerrero, D. Muñoz, M. Zurita-Gotor, Employment of online conductivity measurements as a diagnostic tool of perfluorosulfonic acid membrane degradation in PEMWE, *Int J Hydrogen Energy* 63 (2024) 510–516. <https://doi.org/10.1016/j.ijhydene.2024.03.198>.
- [345] S.H. Frensch, F. Fouda-Onana, G. Serre, D. Thoby, S.S. Araya, S.K. Kær, Influence of the operation mode on PEM water electrolysis degradation, *Int J Hydrogen Energy* 44 (2019) 29889–29898. <https://doi.org/10.1016/j.ijhydene.2019.09.169>.
- [346] G. Bender, M. Carmo, T. Smolinka, A. Gago, N. Danilovic, M. Mueller, F. Ganci, A. Fallisch, P. Lettenmeier, K.A. Friedrich, K. Ayers, B. Pivovar, J. Mergel, D. Stolten, Initial approaches in benchmarking and round robin testing for proton exchange membrane water electrolyzers, *Int J Hydrogen Energy* 44 (2019) 9174–9187. <https://doi.org/10.1016/j.ijhydene.2019.02.074>.
- [347] M. Möckl, M.F. Ernst, M. Kornherr, F. Allebrod, M. Bernt, J. Byrknes, C. Eickes, C. Gebauer, A. Moskovtseva, H.A. Gasteiger, Durability Testing of Low-Iridium PEM Water Electrolysis Membrane Electrode Assemblies, *J Electrochem Soc* 169 (2022) 064505. <https://doi.org/10.1149/1945-7111/ac6d14>.
- [348] S.M. Alia, S. Stariha, R.L. Borup, Electrolyzer Durability at Low Catalyst Loading and with Dynamic Operation, *J Electrochem Soc* 166 (2019) F1164–F1172. <https://doi.org/10.1149/2.0231915jes>.
- [349] D.M. Amaya Dueñas, D. Ullmer, M. Riedel, S.S. Ventura, M. Metten, M. Tomberg, M.P. Heddrich, S.A. Ansar, Performance assessment of a 25 kW solid oxide cell module for hydrogen production and power generation, *Int J Hydrogen Energy* 59 (2024) 570–581. <https://doi.org/10.1016/j.ijhydene.2024.01.346>.
- [350] X.-F. Ye, Y.B. Wen, S.J. Yang, Y. Lu, W.H. Luo, Z.Y. Wen, J.B. Meng, Study of CaZr<sub>0.9</sub>In<sub>0.1</sub>O<sub>3-δ</sub> based reversible solid oxide cells with tubular electrode supported structure, *Int J Hydrogen Energy* 42 (2017) 23189–23197. <https://doi.org/10.1016/j.ijhydene.2017.07.195>.
- [351] J. Dailly, M. Ancelin, M. Marrony, Long term testing of BCZY-based protonic ceramic fuel cell PCFC: Micro-generation profile and reversible production of hydrogen and electricity, *Solid State Ion* 306 (2017) 69–75. <https://doi.org/10.1016/j.ssi.2017.03.002>.
- [352] Y. Gan, J. Zhang, Y. Li, S. Li, K. Xie, J.T.S. Irvine, Composite Oxygen Electrode Based on LSCM for Steam Electrolysis in a Proton Conducting Solid Oxide Electrolyzer, *J Electrochem Soc* 159 (2012) F763–F767. <https://doi.org/10.1149/2.018212jes>.
- [353] F. Brissaud, A. Chaise, K. Gault, S. Soual, Lessons learned from Jupiter 1000, an industrial demonstrator of Power-to-Gas, *Int J Hydrogen Energy* 49 (2024) 925–932. <https://doi.org/10.1016/j.ijhydene.2023.10.003>.
- [354] B. Sánchez Batalla, J. Bachmann, C. Weidlich, Investigation of the degradation of proton exchange membrane water electrolysis cells using electrochemical impedance spectroscopy

- with distribution of relaxation times analysis, *Electrochim Acta* 473 (2024) 143492. <https://doi.org/10.1016/j.electacta.2023.143492>.
- [355] Tom Smolinka, *Electrochemical Power Sources: Fundamentals, Systems, and Applications*, 1st ed., Elsevier, 2021.
- [356] E.K. Volk, M.E. Kreider, S. Kwon, S.M. Alia, Recent progress in understanding the catalyst layer in anion exchange membrane electrolyzers – durability, utilization, and integration, *EES Catalysis* 2 (2024) 109–137. <https://doi.org/10.1039/D3EY00193H>.
- [357] T.H. Pham, A. Allushi, J.S. Olsson, P. Jannasch, Rational molecular design of anion exchange membranes functionalized with alicyclic quaternary ammonium cations, *Polym Chem* 11 (2020) 6953–6963. <https://doi.org/10.1039/D0PY01291B>.
- [358] J. Lei, Z. Wang, Y. Zhang, M. Ju, H. Fei, S. Wang, C. Fu, X. Yuan, Q. Fu, M.U. Farid, H. Kong, A.K. An, R. Deng, F. Liu, J. Wang, Understanding and resolving the heterogeneous degradation of anion exchange membrane water electrolysis for large-scale hydrogen production, *Carbon Neutrality* 3 (2024) 25. <https://doi.org/10.1007/s43979-024-00101-y>.
- [359] H.A. Miller, K. Bouzek, J. Hnat, S. Loos, C.I. Bernäcker, T. Weißgärber, L. Röntzsch, J. Meier-Haack, Green hydrogen from anion exchange membrane water electrolysis: a review of recent developments in critical materials and operating conditions, *Sustain Energy Fuels* 4 (2020) 2114–2133. <https://doi.org/10.1039/C9SE01240K>.
- [360] J. Lei, Z. Wang, Y. Zhang, M. Ju, H. Fei, S. Wang, C. Fu, X. Yuan, Q. Fu, M.U. Farid, H. Kong, A.K. An, R. Deng, F. Liu, J. Wang, Understanding and resolving the heterogeneous degradation of anion exchange membrane water electrolysis for large-scale hydrogen production, *Carbon Neutrality* 3 (2024) 25. <https://doi.org/10.1007/s43979-024-00101-y>.
- [361] B. Xu, W. Ma, W. Wu, Y. Wang, Y. Yang, J. Li, X. Zhu, Q. Liao, Degradation prediction of PEM water electrolyzer under constant and start-stop loads based on CNN-LSTM, *Energy and AI* 18 (2024) 100420. <https://doi.org/10.1016/j.egyai.2024.100420>.
- [362] A. Weiß, A. Siebel, M. Bernt, T.-H. Shen, V. Tileli, H.A. Gasteiger, Impact of Intermittent Operation on Lifetime and Performance of a PEM Water Electrolyzer, *J Electrochem Soc* 166 (2019) F487–F497. <https://doi.org/10.1149/2.0421908jes>.
- [363] J. Yang, J. Li, B. Liu, D. Yan, L. Jia, X. Han, K. Wu, J. Li, High and durable performance of an external-manifold designed reversible solid oxide cell stack, *J Power Sources* 580 (2023) 233390. <https://doi.org/10.1016/j.jpowsour.2023.233390>.
- [364] C. Xi, J. Sang, A. Wu, J. Yang, X. Qi, W. Guan, J. Wang, S.C. Singhal, Electrochemical performance and durability of flat-tube solid oxide electrolysis cells for H<sub>2</sub>O/CO<sub>2</sub> co-electrolysis, *Int J Hydrogen Energy* 47 (2022) 10166–10174. <https://doi.org/10.1016/j.ijhydene.2022.01.105>.
- [365] D. Li, A.R. Motz, C. Bae, C. Fujimoto, G. Yang, F.-Y. Zhang, K.E. Ayers, Y.S. Kim, Durability of anion exchange membrane water electrolyzers, *Energy Environ Sci* 14 (2021) 3393–3419. <https://doi.org/10.1039/D0EE04086J>.
- [366] L. Liu, H. Ma, M. Khan, B.S. Hsiao, Recent Advances and Challenges in Anion Exchange Membranes Development/Application for Water Electrolysis: A Review, *Membranes (Basel)* 14 (2024) 85. <https://doi.org/10.3390/membranes14040085>.

- [367] E.K. Volk, M.E. Kreider, S. Kwon, S.M. Alia, Recent progress in understanding the catalyst layer in anion exchange membrane electrolyzers – durability, utilization, and integration, *EES Catalysis 2* (2024) 109–137. <https://doi.org/10.1039/D3EY00193H>.
- [368] J. Lei, Z. Wang, Y. Zhang, M. Ju, H. Fei, S. Wang, C. Fu, X. Yuan, Q. Fu, M.U. Farid, H. Kong, A.K. An, R. Deng, F. Liu, J. Wang, Understanding and resolving the heterogeneous degradation of anion exchange membrane water electrolysis for large-scale hydrogen production, *Carbon Neutrality 3* (2024) 25. <https://doi.org/10.1007/s43979-024-00101-y>.
- [369] C.A. Giron Rodriguez, N.C. Kani, A.B. Moss, B.O. Joensen, S. Garg, W. Deng, T. Wilson, J.R. Varcoe, I. Chorkendorff, B. Seger, Insights into zero-gap CO<sub>2</sub> electrolysis at elevated temperatures, *EES Catalysis 2* (2024) 850–861. <https://doi.org/10.1039/D3EY00224A>.
- [370] S. Miyanishi, T. Yamaguchi, Highly conductive mechanically robust high  $M_w$  polyfluorene anion exchange membrane for alkaline fuel cell and water electrolysis application, *Polym Chem 11* (2020) 3812–3820. <https://doi.org/10.1039/D0PY00334D>.
- [371] Shaun Alia, HydroGEN: Low Temperature Electrolysis, in: DOE Hydrogen Program 2024 Annual Merit Review and Peer Evaluation Meeting, 2024: pp. 1–21.
- [372] E.K. Volk, M.E. Kreider, S. Kwon, S.M. Alia, Recent progress in understanding the catalyst layer in anion exchange membrane electrolyzers – durability, utilization, and integration, *EES Catalysis 2* (2024) 109–137. <https://doi.org/10.1039/D3EY00193H>.
- [373] G. Stelmacovich, S. Pylypenko, Characterization of Porous Transport Layers Towards the Development of Efficient Proton Exchange Membrane Water Electrolysis, *ChemElectroChem 11* (2024). <https://doi.org/10.1002/celec.202400377>.
- [374] P. Khajavi, P.V. Hendriksen, H.L. Frandsen, High-temperature degradation of tetragonal zirconia in solid oxide fuel and electrolysis cells: A critical challenge for long-term durability and a solution, *J Eur Ceram Soc 44* (2024) 6527–6539. <https://doi.org/10.1016/j.jeurceramsoc.2024.04.042>.
- [375] Frank Allebrod, The Effects of Pressure and Temperature on Alkaline Electrolysis, PhD Thesis, Technical University of Denmark., 2013.
- [376] Effect of Operating Parameters on Performance of Alkaline Water Electrolysis, *International Journal of Thermal and Environmental Engineering 09* (2015). <https://doi.org/10.5383/ijtee.09.02.001>.
- [377] D. Jang, H.-S. Cho, S. Kang, Numerical modeling and analysis of the effect of pressure on the performance of an alkaline water electrolysis system, *Appl Energy 287* (2021) 116554. <https://doi.org/10.1016/j.apenergy.2021.116554>.
- [378] J. Parrondo, C.G. Arges, M. Niedzwiecki, E.B. Anderson, K.E. Ayers, V. Ramani, Degradation of anion exchange membranes used for hydrogen production by ultrapure water electrolysis, *RSC Adv 4* (2014) 9875. <https://doi.org/10.1039/c3ra46630b>.
- [379] J. Lei, Z. Wang, Y. Zhang, M. Ju, H. Fei, S. Wang, C. Fu, X. Yuan, Q. Fu, M.U. Farid, H. Kong, A.K. An, R. Deng, F. Liu, J. Wang, Understanding and resolving the heterogeneous degradation of anion exchange membrane water electrolysis for large-scale hydrogen production, *Carbon Neutrality 3* (2024) 25. <https://doi.org/10.1007/s43979-024-00101-y>.
- [380] R. Vinodh, S.S. Kalanur, S.K. Natarajan, B.G. Pollet, Recent Advancements of Polymeric Membranes in Anion Exchange Membrane Water Electrolyzer (AEMWE): A Critical Review, *Polymers (Basel) 15* (2023) 2144. <https://doi.org/10.3390/polym15092144>.

GA No. 101137802

- [381] Nick VAN DIJK, PEM ELECTROLYSER DEGRADATION MECHANISMS AND PRACTICAL SOLUTIONS, [https://www.sintef.no/globalassets/project/novel/pdf/1-2\\_itm\\_vandijk\\_public.pdf](https://www.sintef.no/globalassets/project/novel/pdf/1-2_itm_vandijk_public.pdf) (2013).
- [382] V. Fateev, High pressure PEM electrolyzers: efficiency, life-time and safety issues, [https://www.sintef.no/globalassets/project/novel/pdf/2-4\\_nrckurchatov\\_fateev\\_public.pdf](https://www.sintef.no/globalassets/project/novel/pdf/2-4_nrckurchatov_fateev_public.pdf) (2013).
- [383] S. Shiva Kumar, V. Himabindu, Hydrogen production by PEM water electrolysis – A review, *Mater Sci Energy Technol* 2 (2019) 442–454. <https://doi.org/10.1016/j.mset.2019.03.002>.
- [384] A. V. Virkar, Mechanism of oxygen electrode delamination in solid oxide electrolyzer cells, *Int J Hydrogen Energy* 35 (2010) 9527–9543. <https://doi.org/10.1016/j.ijhydene.2010.06.058>.
- [385] B. Butz, R. Schneider, D. Gerthsen, M. Schowalter, A. Rosenauer, Decomposition of 8.5 mol.% Y<sub>2</sub>O<sub>3</sub>-doped zirconia and its contribution to the degradation of ionic conductivity, *Acta Mater* 57 (2009) 5480–5490. <https://doi.org/10.1016/j.actamat.2009.07.045>.
- [386] Hossein Ghezel-Ayagh, Proton-Conducting Ceramic Electrolyzers for High-Temperature Water Splitting, [https://www.hydrogen.energy.gov/docs/hydrogenprogramlibraries/pdfs/review21/p177\\_ghezel-ayagh\\_2021\\_p-pdf.pdf](https://www.hydrogen.energy.gov/docs/hydrogenprogramlibraries/pdfs/review21/p177_ghezel-ayagh_2021_p-pdf.pdf) (2021) 1–32.
- [387] Marcos Hernandez Rodriguez, PERFORMANCE DEGRADATION OF PROTON-CONDUCTING CERAMIC ELECTROLYZERS FOR HIGH-TEMPERATURE WATER SPLITTING, Colorado School of Mines, 2020.
- [388] S. Pirou, Q. Wang, P. Khajavi, X. Georgolamprou, S. Ricote, M. Chen, R. Kiebach, Planar proton-conducting ceramic cells for hydrogen extraction: Mechanical properties, electrochemical performance and up-scaling, *Int J Hydrogen Energy* 47 (2022) 6745–6754. <https://doi.org/10.1016/j.ijhydene.2021.12.041>.
- [389] H. Becker, J. Murawski, D. V. Shinde, I.E.L. Stephens, G. Hinds, G. Smith, Impact of impurities on water electrolysis: a review, *Sustain Energy Fuels* 7 (2023) 1565–1603. <https://doi.org/10.1039/D2SE01517J>.
- [390] G. Sakas, A. Ibáñez-Rioja, S. Pöyhönen, A. Kosonen, V. Ruuskanen, P. Kauranen, J. Ahola, Influence of shunt currents in industrial-scale alkaline water electrolyzer plants, *Renew Energy* 225 (2024) 120266. <https://doi.org/10.1016/j.renene.2024.120266>.
- [391] N. Guruprasad, J. van der Schaaf, M.T. de Groot, Unraveling the impact of reverse currents on electrode stability in anion exchange membrane water electrolysis, *J Power Sources* 613 (2024) 234877. <https://doi.org/10.1016/j.jpowsour.2024.234877>.
- [392] K. Zeng, D. Zhang, Recent progress in alkaline water electrolysis for hydrogen production and applications, *Prog Energy Combust Sci* 36 (2010) 307–326. <https://doi.org/10.1016/j.pecs.2009.11.002>.
- [393] J. Brauns, J. Schönebeck, M.R. Kraglund, D. Aili, J. Hnát, J. Žitka, W. Mues, J.O. Jensen, K. Bouzek, T. Turek, Evaluation of Diaphragms and Membranes as Separators for Alkaline Water Electrolysis, *J Electrochem Soc* 168 (2021) 014510. <https://doi.org/10.1149/1945-7111/abda57>.
- [394] M. Carmo, D.L. Fritz, J. Mergel, D. Stolten, A comprehensive review on PEM water electrolysis, *Int J Hydrogen Energy* 38 (2013) 4901–4934. <https://doi.org/10.1016/j.ijhydene.2013.01.151>.

- [395] A. Ursua, L.M. Gandia, P. Sanchis, Hydrogen Production From Water Electrolysis: Current Status and Future Trends, *Proceedings of the IEEE* 100 (2012) 410–426. <https://doi.org/10.1109/JPROC.2011.2156750>.
- [396] D.R. Dekel, Review of cell performance in anion exchange membrane fuel cells, *J Power Sources* 375 (2018) 158–169. <https://doi.org/10.1016/j.jpowsour.2017.07.117>.
- [397] J.R. Varcoe, P. Atanassov, D.R. Dekel, A.M. Herring, M.A. Hickner, Paul.A. Kohl, A.R. Kucernak, W.E. Mustain, K. Nijmeijer, K. Scott, T. Xu, L. Zhuang, Anion-exchange membranes in electrochemical energy systems, *Energy Environ. Sci.* 7 (2014) 3135–3191. <https://doi.org/10.1039/C4EE01303D>.
- [398] Y.-J. Wang, J. Qiao, R. Baker, J. Zhang, Alkaline polymer electrolyte membranes for fuel cell applications, *Chem Soc Rev* 42 (2013) 5768. <https://doi.org/10.1039/c3cs60053j>.
- [399] D. Jeong, J.-S. Park, Effect of Anion-Conducting Electrolytes in Pore-Filling Membranes on Performance and Durability in Water Electrolysis, *Membranes (Basel)* 14 (2024) 265. <https://doi.org/10.3390/membranes14120265>.
- [400] M. Carmo, D.L. Fritz, J. Mergel, D. Stolten, A comprehensive review on PEM water electrolysis, *Int J Hydrogen Energy* 38 (2013) 4901–4934. <https://doi.org/10.1016/j.ijhydene.2013.01.151>.
- [401] U. Babic, M. Suermann, F.N. Büchi, L. Gubler, T.J. Schmidt, Critical Review—Identifying Critical Gaps for Polymer Electrolyte Water Electrolysis Development, *J Electrochem Soc* 164 (2017) F387–F399. <https://doi.org/10.1149/2.1441704jes>.
- [402] R. Moreno Soriano, N. Rojas, E. Nieto, R. de Guadalupe González-Huerta, J.M. Sandoval-Pineda, Influence of the gasket materials on the clamping pressure distribution in a PEM water electrolyzer: Bolt torques and operation mode in pre-conditioning, *Int J Hydrogen Energy* 46 (2021) 25944–25953. <https://doi.org/10.1016/j.ijhydene.2021.03.076>.
- [403] J.J. Caparrós Mancera, F. Segura Manzano, J.M. Andújar, F.J. Vivas, A.J. Calderón, An Optimized Balance of Plant for a Medium-Size PEM Electrolyzer: Design, Control and Physical Implementation, *Electronics (Basel)* 9 (2020) 871. <https://doi.org/10.3390/electronics9050871>.
- [404] Y. Wang, W. Li, L. Ma, W. Li, X. Liu, Degradation of solid oxide electrolysis cells: Phenomena, mechanisms, and emerging mitigation strategies—A review, *J Mater Sci Technol* 55 (2020) 35–55. <https://doi.org/10.1016/j.jmst.2019.07.026>.
- [405] K. Singh, T. Walia, Review on silicate and borosilicate-based glass sealants and their interaction with components of solid oxide fuel cell, *Int J Energy Res* 45 (2021) 20559–20582. <https://doi.org/10.1002/er.7161>.
- [406] C.M. Stoots, J.E. O'Brien, J.S. Herring, J.J. Hartvigsen, Syngas Production via High-Temperature Coelectrolysis of Steam and Carbon Dioxide, *J Fuel Cell Sci Technol* 6 (2009). <https://doi.org/10.1115/1.2971061>.
- [407] S.M. Haile, Fuel cell materials and components☆☆☆The Golden Jubilee Issue—Selected topics in Materials Science and Engineering: Past, Present and Future, edited by S. Suresh., *Acta Mater* 51 (2003) 5981–6000. <https://doi.org/10.1016/j.actamat.2003.08.004>.
- [408] K.D. Kreuer, Proton-Conducting Oxides, *Annu Rev Mater Res* 33 (2003) 333–359. <https://doi.org/10.1146/annurev.matsci.33.022802.091825>.

GA No. 101137802

- [409] H. IWAHARA, T. ESAKA, H. UCHIDA, N. MAEDA, Proton conduction in sintered oxides and its application to steam electrolysis for hydrogen production, *Solid State Ion* 3–4 (1981) 359–363.  
[https://doi.org/10.1016/0167-2738\(81\)90113-2](https://doi.org/10.1016/0167-2738(81)90113-2).
- [410] K. Ferguson, A. Dubois, K. Albrecht, R.J. Braun, High performance protonic ceramic fuel cell systems for distributed power generation, *Energy Convers Manag* 248 (2021) 114763.  
<https://doi.org/10.1016/j.enconman.2021.114763>.
- [411] T. Malkow, A. Pilenga, EU harmonised accelerated stress testing protocols for low-temperature water electrolyser, 2024.



## 11 Acknowledgement

The author(s) would like to thank the partners in the project for their valuable comments on previous drafts and for performing the review.

### Project partners:

#	Partner short name	Partner Full Name
1	POLITO	Politecnico di Torino
2	UNR	Uniresearch B.V.
3	EGP	Enel Green Power SpA
4	FAU	Friedrich-Alexander-Universitaet Erlangen-Nuernberg
5	TUG	Graz University of Technology
6	KER	Kerionics s.l.
7	AAU	Aalborg University
8	FZJ	Forschungszentrum Jülich gmbh
9	ULille	University of Lille
10	STARGATE	Stargate Hydrogen Solutions OU
11	PF	Pietro Fiorentini s.p.a.
11.1	HYT	Hyter s.r.l. (Affiliated)
12	CNR	Consiglio Nazionale delle Ricerche
13	1s1	1s1 Energy Portugal Unipessoal Lda
14	AEA	AEA s.r.l.
15	VDX	Volytica diagnostics GmbH
16	SE	SolydEra SpA

### Disclaimer/ Acknowledgment



Copyright ©, all rights reserved. This document or any part thereof may not be made public or disclosed, copied or otherwise reproduced or used in any form or by any means, without prior permission in writing from the ELECTROLIFE Consortium. Neither the ELECTROLIFE Consortium nor any of its members, their officers, employees or agents shall be liable or responsible, in negligence or otherwise, for any

loss, damage or expense whatever sustained by any person as a result of the use, in any manner or form, of any knowledge, information or data contained in this document, or due to any inaccuracy, omission or error therein contained.

All Intellectual Property Rights, know-how and information provided by and/or arising from this document, such as designs, documentation, as well as preparatory material in that regard, is and shall remain the exclusive property of the ELECTROLIFE Consortium and any of its members or its licensors. Nothing contained in this document shall give, or shall be construed as giving, any right, title, ownership, interest, license or any other right in or to any IP, know-how and information.

The project is supported by the Clean Hydrogen Partnership and its members.

The project has received funding from Clean Hydrogen Partnership Joint Undertaking under Grant Agreement No 101137802. This Joint Undertaking receives support from the European Union's Horizon 2020 Research and Innovation programme, Hydrogen Europe and Hydrogen Europe Research.

Co-funded by the European Union. Views and opinions expressed are however those of the author(s) only and do not necessarily reflect those of the European Union or the Clean Hydrogen Partnership. Neither the European Union nor the granting authority can be held responsible for them.

GA No. 101137802

## 12 Appendix A - <<Appendix Title>>